Biomaterials from a Modular Peptide Scaffold

by

Wade Wang

B.S. Biochemistry
The University of Texas at Austin, 2013

SUBMITTED TO THE DEPARTMENT OF CHEMISTRY IN PARTIAL FULFILLMENT OF
THE REQUIREMENTS FOR THE DEGREE OF

DOCTOR OF PHILOSOPHY IN CHEMISTRY
AT THE
MASSACHUSETTS INSTITUTE OF TECHNOLOGY

June 2019

Signature redacted

Signature of Author: ___

Department of Chemistry
May 1, 2019

Signature redacted

Certified by: _____

Paula T. Hammond
David H. Koch Professor in Engineering
Thesis Supervisor

Signature redacted

Accepted by: _____

Robert W. Field
Haslam and Dewey Professor of Chemistry
Chair, Departmental Committee on Graduate Students
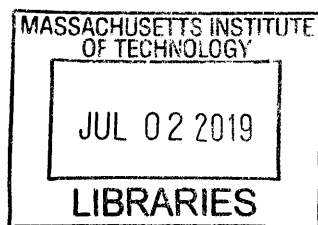
This doctoral thesis has been examined by a committee of the Department of Chemistry as follows:

Signature redacted

Professor Jeremiah A. Johnson...

Thesis Committee Chair
Associate Professor of Chemistry

Signature redacted

Professor Paula T. Hammond...........................

Thesis Supervisor
David H. Koch Professor in Engineering

Signature redacted

Professor Timothy M. Swager.............................

Thesis Committee Member
John D. MacArthur Professor of Chemistry

Biomaterials from a Modular Peptide Scaffold

By

Wade Wang

Submitted to the Department of Chemistry
on April 23rd, 2019 in Partial Fulfillment of the
Requirements for the Degree of Doctor of Philosophy

Abstract

Modular polymer scaffolds are an attractive solution to address the needs of biomaterial design
and engineering. Simple modification of the scaffold enables both screening an array of materials
as well as optimization of a single material. This thesis describes the development and applications
of two different polypeptide scaffolds that may be functionalized with click chemistry on both the
side chain and end group. We demonstrate the utility of these scaffolds with the synthesis of
biomaterials and biopolymers for drug delivery and tissue engineering applications.

One area of focus is the synthesis of a bioinspired polypeptide-hyaluronic acid conjugate.
Proteoglycans are an interesting class of biomacromolecules whose applications have been
limited by reproducible isolation from natural sources. Synthetic proteoglycans provide an
alternative as a reproducible and scalable solution, though many synthetic systems lack
biological activity. We have developed a method to synthesize polypeptide-hyaluronic acid
conjugates of various architectures that more closely mimic the composition of proteoglycans
found in nature. These conjugates exhibit biological activity distinct from native hyaluronic acid
of various sizes. The conjugates were also successfully employed in a three dimensional
vasculogenesis application. The synthesis of bulk hydrogels based off end to end linking of a
polypeptide scaffold was also investigated. This endeavor required optimization of the
polymerization conditions to achieve the desired end functionality. Ultimately, these polymers
may be end-linked to form a soft hydrogel. Finally, the effects of secondary structure on
polymer-drug conjugate efficacy are interrogated by grafting the anticancer drug doxorubicin
and poly(ethylene glycol) to polypeptide scaffolds that exhibit different degrees of α-helicity.
The drug release, toxicity, and conjugate association with cells was evaluated by *in vitro* assays.

Thesis Supervisor: Paula T. Hammond
David H. Koch Professor in Engineering

Acknowledgements

There have been many people that have helped me through the arduous journey of graduate school. First and foremost, I would like to thank my advisor Paula Hammond for her patience in guiding a chemist through an engineering lab heavily focused on biology applications. I've learned much in this interdisciplinary setting that has made me a well-rounded researcher. I would like to thank Jeremiah Johnson, my thesis chair, for being knowledgeable, relatable, and approachable and Tim Swager for his help in getting me oriented as a first year graduate student. I would not be in graduate school if it wasn't for my undergraduate advisor, Grant Willson. My tenure in his lab laid the foundation of research experience for me to build upon.

It has been great to be in the Hammond group inside and outside the lab. As the resident chemist, it was a pleasure to collaborate with most of the lab in some form. Jiahe has been a great colleague and friend. I will always remember our cycling trips together. Brett, Santi, Erik, and others never failed to keep things entertaining with their shenanigans. Most of my time was spent at the ISN, and I need to thank Bryan and Colin for their company. Donna and Marlisha do an amazing job maintaining the lab and office space. I've had the pleasure of mentoring two very talented MIT undergraduate students, Aofei Liu and Brian Zhong. Both were extraordinary in their aptitude and willingness to learn, and I know they will achieve greatness in their graduate studies at Stanford.

Justin Wolfe was my first friend at MIT. We even met during a visit weekend before MIT, became first year roommates, and have seen each other through many adventures. I'm lucky to have such an amazing friend group in my chemistry cohort: Kenny, Angela, Ethan, Alex, Dani, Kathleen, Jess, Sterling, Tim, Salima. I could fill volumes with the good times we've had in each other's company, especially during the early years. I joined the MIT cycling club team halfway through graduate school and my only regret is not starting sooner. There is no better group of people to ride, train, race, and party with. Instead of listing names, I will direct you to cycling.mit.edu. I even managed to convince the team to let me be treasurer. I look forward to reuniting with my friends wherever my career takes me.

Two people played a big part of my personal growth in graduate school, Cathy and Amanda. Thank you both for the lessons and adventures. Finally, I'd like to thank my family for their patience while I pursued a Ph.D. If you've read this far, there's a good chance you're looking for your name, and I apologize if you couldn't find it. Get in touch with me and let me make it up to you.

Preface

This thesis is comprised of material adapted from the publications below.

Peer reviewed:

Wang, W. and Hammond, P. T. Hydrolysis Resistant Functional Polypeptide Scaffold for Biomaterials. *Polym. Chem.* **2018**, *9* (3), 346–351.

In preparation:

Wang, W.; Brown A. T.; Griffith L. G.; Hammond, P.T. Synthesis and Biological Activity of Polypeptide-Hyaluronan Conjugates. *In preparation.*

Zhong, B.; Wang, W.; Hammond, P. T. Secondary Structure Influences Efficacy of Polymer-drug Conjugates Derived from "Clickable" Polypeptide Scaffolds. *Submitted.*

Relative Contributions

Chapters 1 and 3 are the sole work of the author. Chapter 2 is the sole work of the author with the exception of the 3D vasculogenesis application. Chapter 4 is a collaboration between the author and an undergraduate at MIT.

Table of contents

Chapter 1: Developing a peptide-based, hydrolysis-resistant polymer scaffold

1.1 Introduction

A biomaterial is defined by the International Union of Pure and Applied Chemistry (IUPAC) as "material exploited in contact with living tissues, organisms, or microorganisms".[1] These materials are commonly designed or engineered for healthcare, which is by far their most popular application. While biomaterials may be comprised of metals or composites, polymeric materials have proven to be among the most versatile with regard to chemical and physical properties.[2]

Polymeric biomaterials may be divided into two categories: natural and synthetic. Natural polymers are isolated from biological sources. Some well-known natural polymeric biomaterials include cellulose cotton (cellulose), wool/silk (keratin), and gelatin (collagen). Such polymers have been used for millennia in biomaterials applications ranging from wound healing to drug delivery to tissue culture because of their abundance and inherent biocompatibility or biological activity.[3] However, these polymers are commonly ill defined, difficult to isolate, difficult to modify, and susceptible to batch to batch variation.[4] On the other hand, synthetic biomaterials allow for precise control and modification of chemical structure and functionality through advances in living polymerization and click chemistry. While many simple polymers, such as poly(ethylene glycol), have been used to much success in biomaterial applications, it is difficult to endow biological activity to these polymers through chemical modification. Other synthetic polymers that are created by controlled polymerization but more easily modified are excellent candidates to replace simple synthetic polymers when complex functionality or biological activity are required.

Polypeptides produced by N-carboxyanhydride ring opening polymerization are an appealing material for the replacement of natural polymers in biological applications. The polymer backbone is inherently biocompatible and polymers with varying side chains can be synthesized to suit specific applications.[5] In particular, poly(γ-propargyl-L-glutamate) (PPLG) is an α-helical polypeptide that may be modified through copper-catalyzed azide-alkyne cycloaddition (CuAAC). The controlled polymerization and modification methods enable precise control of structure, making it a promising material for the replacement of natural polymers in biological applications.[6] [13] However, the limited lifetime of ester bonds on the side chain precludes PPLG from being used in long term applications or under harsh conditions where polymer degradation is undesirable such as polymeric platforms for organoids, hydrogels for long term 3D cultures, surface

functionalization for implant coatings, and scaffolds for tissue engineering. In addition, the increased lability of the ester bond under basic conditions or high temperatures limits the employment of otherwise useful post polymerization reactions or processing conditions.

One approach to synthesis of hydrolysis resistant functional polypeptides involves coupling of amines to poly(L-glutamate). This may be accomplished by displacement of a glutamic acid ester with an amine through nucleophilic acyl substitution. Despite being the most direct route to poly(L-glutamate) derivatives, this approach requires the use of excess amine and organic solvents. Commercially available poly(γ-benzyl-L-glutamate) (PBLG) reacts with amines, though achieving high conversion requires the use of catalysts or aggressive reaction conditions that may result in side reactions.[14] Poly(γ-trichloroethyl-L-glutamate) features a better leaving group as the ester, resulting in greater reactivity, but requires additional monomer synthesis and polymerization of the amino acid monomer. In addition, complete conversion without excess amine is still not guaranteed.[15,16] Alternatively, amines may be coupled to poly(L-glutamate) by reagents such as EDC or DMT-MM.[17,18] While this method has generated interesting materials, grafting density is limited. Literature examples of these couplings routinely report incomplete grafting, ranging from 50% to 90%, despite stoichiometric or excess amounts of amine. Synthesis of complex biomaterials often involves conjugation of high molecular weight components in low concentrations and aqueous medium, which would further reduce the grafting efficiency.

Thus, replacing amide bond coupling with a more robust chemistry, such CuAAC, would be beneficial in the synthesis of these materials. CuAAC, commonly referred to as click chemistry, has recently generated great attention due to its ease of execution, effectiveness, and tolerance of diverse functional groups. Previous examples of glutamic acid derivatives capable of post polymerization modification with CuACC have not demonstrated hydrolytic stability[9] or quantitative modification of every repeat unit with azides or alkynes.[17] To improve upon other approaches in synthesizing functional polypeptides, we have designed a hydrolysis resistant variant of PPLG through post polymerization modification of PBLG. Deprotection followed by amide bond coupling yields a polymer that retains α-helical structure, modular nature, and low dispersity of ester PPLG, but greatly improves hydrolytic stability by replacing the ester bond with an amide. Furthermore, we have found the synthetic route to be highly robust and scaleable. The

direct transformation of the poly(L-glutamate) backbone allows access to a broad molecular weight range.

1.2 Results and Discussion

A polypeptide with a functional group connected by an amide linkage on the side chain may be synthesized though either direct polymerization of a monomer containing an amide group or post polymerization modification of a polymer to install the functional group through amide bond coupling. A few examples of ring opening polymerization of NCA monomers containing an amide group on the side chain[5] encouraged attempts to synthesize the polymer through polymerization of a monomer bearing an amide linked alkyne group on the side chain. Propargyl groups were selectively installed on the ε-amine of lysine and γ-carboxylate of L-glutamate by blocking the α-amine and α-carboxylic acid with protecting groups or chelation with copper.[19] However, attempted synthesis of the NCA monomer by the Fuchs-Farthing method with triphosgene[20] did not yield the expected product. Alternative methods of NCA synthesis by protection of the α-carboxylic acid with *tert*-butyldimethylsilyl chloride followed by oxalyl chloride and DMF were also unsuccessful (Figure 1.7).[21]

Ultimately, a post polymerization modification strategy succeeded in the synthesis of amide linked PPLQ. Synthesis of PPLQ begins with the synthesis and subsequent polymerization of γ-Benzyl-L-glutamate N-carboxyanhydride to form poly(γ-benzyl-L-glutamate). The ester is saponified under basic conditions to produce the free carboxylic acid which is then coupled with propargylamine (Figure 1.1).

14
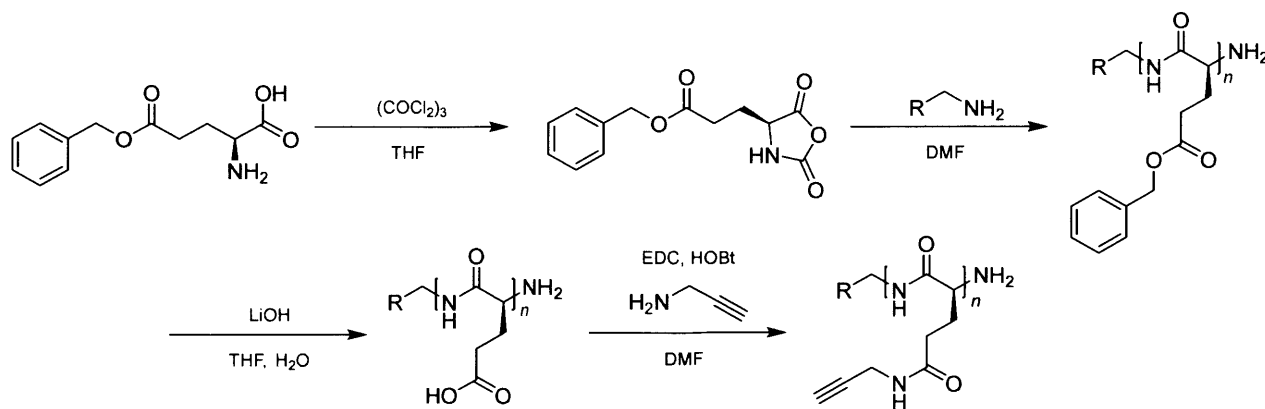
Figure 1.1 Synthesis of amide linked PPLQ by post polymerization modification.

The end of the PPLQ polymer chain may also be tuned by choice of amine initiator to give greater control over the final structure. The synthesis of end-functional polymers is prerequisite to forming end linked networks or attachment of targeting ligands. A norbornene group on the end of the polymer enables end functionalization after grafting by reactions with either a thiol or tetrazine. The norbornene group was installed on the end of PPLQ by initiating the polymerization of PBLG with a norbornene amine, and the subsequent post polymerization modifications are designed to preserve the norbornene group. Various conditions were screened for the deprotection of PBLG including hydrobromic acid in acetic acid, anisole in methanesulfonic acid[22], and trimethylsilyl iodide.[23,24] Only basic deprotection in lithium hydroxide preserved the norbornene end group while maintaining the α-helical structure of the polypeptide (Figure 1.8). Likewise, a few conditions were screened for the coupling of propargylamine to poly(L-glutamate). Uronium/aminium type coupling reagents as well as EDC alone or EDC with NHS were not successful. However, EDC with HOBt yielded the desired polymer (Figure 1.10).

The deprotection of benzyl esters on a polypeptide under basic conditions is not standard and does result in some racemization of the polypeptide when compared to known acidic deprotection methods that do not induce racemization. However, poly(L-glutamate) obtained by this deprotection method is still predominantly α-helical. Furthermore, the effect of racemization on secondary structure is diminished in both PPLQ and PPLQ-g-EO2 as determined by circular dichroism and FTIR (Figure 1.12-1.14). Because the secondary structure of PPLQ and PPLQ-EO2

is similar despite deprotection method, basic deprotection as described is suitable for when end group functionality is a priority. Otherwise, PPLQ may still be synthesized by acidic deprotection of PBLG with no subsequent changes to the procedure.

The synthesis of amide linked PPLQ has some notable advantages compared to the synthesis of ester linked PPLG. First, γ-benzyl glutamic acid is commercially available in both the L and D isomer. The convenient source of starting material, purification of the NCA by recrystallization, and quantitative post polymerization modification enables easy scale up of the synthesis to ten gram scale and larger. Moreover, the polymerization of the NCA monomer, γ-benzyl-L-glutamate NCA, is one of the most studied and characterized of all NCA polymerizations.[25] If desired, the NCA monomer as well as PBLG or poly(L-glutamate) are widely commercially available, enabling the synthesis of amide linked PPLQ in labs that may not be well equipped for organic chemistry.

Amide linked PPLQ retains all the positive characteristics of ester linked PPLG while bolstering the hydrolytic stability. NMR shows quantitative conversion of glutamic acid repeat units to γ-propargyl-L-glutamate (Figure 1.2) and GPC shows that the low dispersity characteristic of NCA polymerization is retained (Figure 1.3). In this regard, amide linked PPLQ synthesized by post polymerization modification is comparable to the hypothetical properties of amide linked PPLQ synthesized by polymerization of a NCA monomer bearing an alkyne. Furthermore, all alkyne groups on the polymer are accessible to modification by CuAAC with various azides. This suggests that the polymer forms a stable α-helix in solution, effectively displaying the alkynes on the side chains to enhance their reactivity[9]. The α-helical structure is further confirmed by CD spectroscopy (Figure 1.4). However, upon grafting, the secondary structure shifts to a random coil with some elements of a PPII helix (Figure 1.13). This structure may be favored by the possibility of side chain to backbone hydrogen bonding enabled by the amide bonds on the side chain.[26]
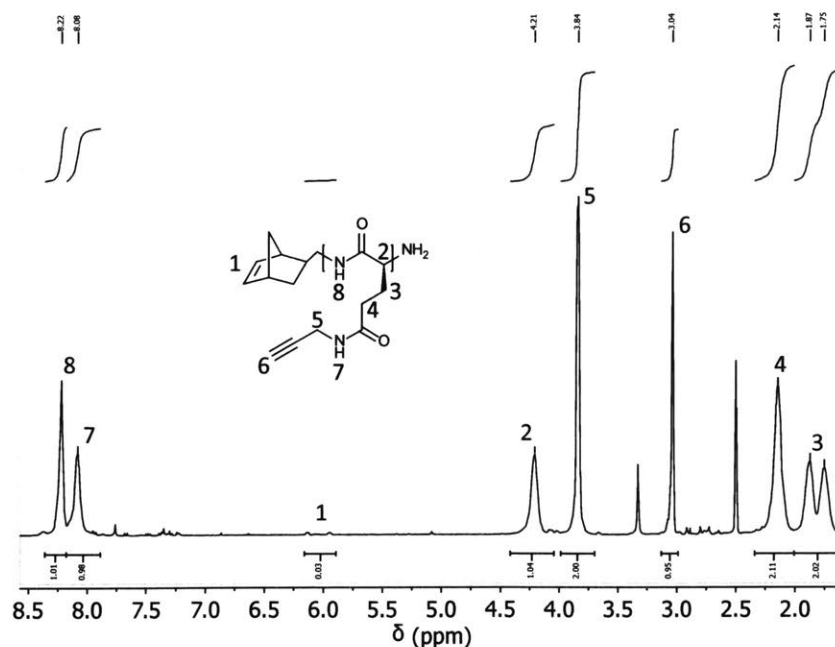
Figure 1.2. ^{1}H NMR of amide linked PPLG in DMSO-d_6. Additional peaks at δ 2.50 and 3.33 correspond to DMSO and water, respectively. Residual signals from HOBt, EDC, and DMF are from δ 7.0 – 8.0 and δ 2.5 – 3.0.
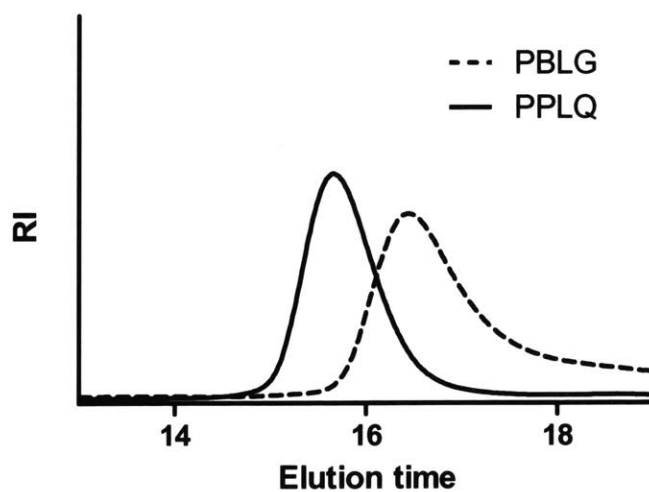

Figure 1.3. GPC trace of initial PBLG and derived PPLQ. For PPLQ, the calculated M_n is 11.6 kDa and PDI 1.11. For PBLG, the calculated M_n is 5.1 kDa and PDI 1.17. M_n and PDI were calculated based off PMMA standards.

17
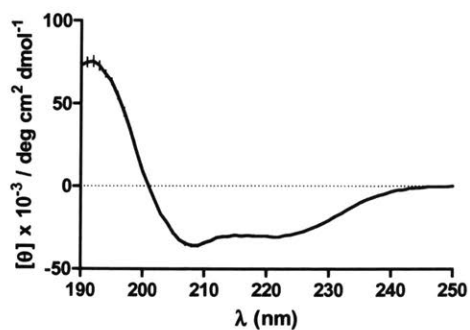
Figure 1.4. Circular dichroism spectrum of PPLQ in hexafluoroisopropanol (0.17 mg/mL).

To test the accessibility of the norbornene end group, PPLQ was first grafted with an azide modified diethylene glycol to render the polymer water soluble. The grafted product, PPLQ-g-EO2, was reacted with β-mercaptoethanol as a model thiol using LAP as a photoinitiator and illumination by a UV lamp. NMR confirmed the consumption of norbornene groups (Figure 1.5).
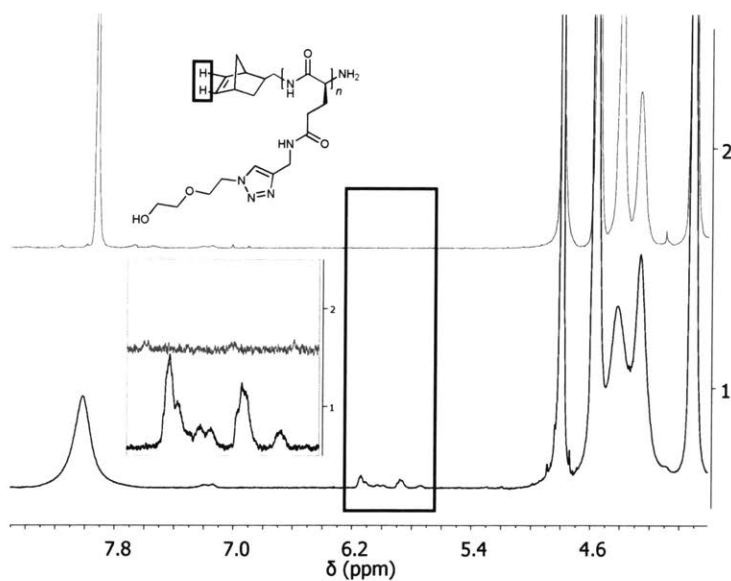

Figure 1.5. ^{1}H NMR analysis in D$_2$O detailing consumption of the norbornene end group of PPLQ in a model reaction with β-mercaptoethanol. The bottom spectrum is before illumination; the top spectrum is following illumination. The insert depicts the highlighted vinyl protons of norbornene on the end of PPLQ-g-EO2 prior to and after the photoreaction. The norbornene is and mix of *endo* and *exo* isomers. Thus, stereochemical complexity results in multiple peaks over the region.

18

The hydrolytic stability of amide PPLQ was evaluated over time by NMR spectroscopy. Various aqueous environments of pH 4.5, 8, 12, and 14 at room temperature were tested as well as a physiologically relevant environment of pH 7.4 at 37°C. Ester PPLG was quickly hydrolyzed in pH 12 and nearly instantly hydrolyzed at pH 14. The hydrolysis of ester PPLG at either slightly basic pH and physiological conditions was slower, but apparent. Amide PPLQ showed no detectable hydrolysis other than at pH 14. Even at extremely basic pH, the hydrolysis of amide PPLQ is slow. As hypothesized, converting the side chain linkage from ester to amide greatly improved hydrolytic stability (Figure 1.6).
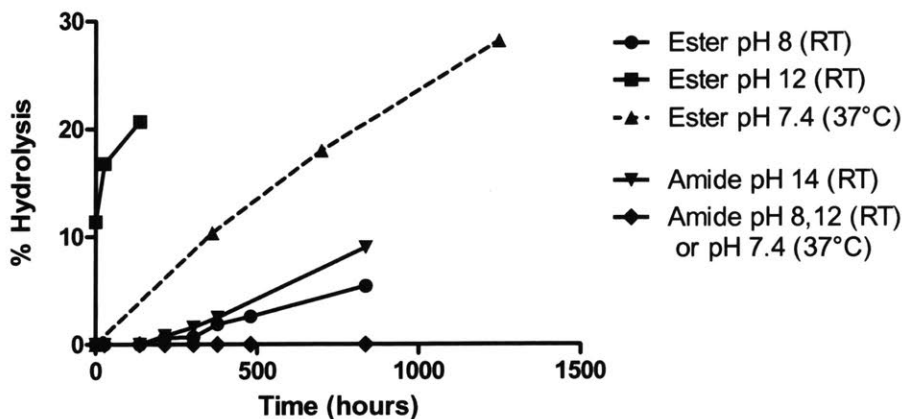

Figure 1.6. Hydrolysis over time for various functional groups of both ester and amide PPLG at different pH. Hydrolysis was undetectable for amide PPLQ at pH < 14 and both ester PPLG and amide PPLQ at acidic pH.

1.3 Conclusion

By converting the side chain linkage from an ester to an amide, the stability of PPLG in neutral and basic aqueous environments, especially at elevated temperatures, has been greatly improved. The improved stability makes amide PPLQ suitable for use in long term cell culture or other biological settings in addition to harsher pH environments. Although the propargyl group is installed after polymerization, the polymer shows complete modification comparable to polymerization of a propargyl containing monomer. In addition, other unique characteristics of ester PPLG such as the potential for quantitative grafting by CuAAC are retained. Amide PPLQ

exhibits many desirable properties for biomaterial applications such as facile functionalization and controlled synthesis. There is potential for modification to endow a diverse set of properties and mimic the structure and function of natural polymers. This new polymer, PPLQ, expands the already versatile nature of PPLG.

1.4 Experimental

Triphosgene, 3-(3-Dimethylaminopropyl)-1-ethyl-carbodiimide hydrochloride (EDC), 1-Hydroxybenzotriazole hydrate (HOBt), and γ-Benzyl-L-glutamate were obtained from Chem-Impex. 5-Norbornene-2-methylamine was obtained from TCI America. N,N-Dimethylformamide (DMF) was dried and stored over 3Å molecular sieves under an argon atmosphere prior to use. Lithium phenyl-2,4,6- trimethylbenzoylphosphinate (LAP)[27] and 2-(2-azidoethoxy)ethanol[28] were synthesized according to literature procedure. Regenerated cellulose 1 kDa molecular weight cutoff dialysis membrane was obtained from Spectrum Labs. All other reagents and materials were purchased from Sigma-Aldrich and used as received.

^{1}H and ^{13}C NMR spectra were obtained in CDCl$_3$, dimethyl sulfoxide-d$_6$ or deuterium oxide (Cambridge Isotope Laboratories) using a Bruker Avance 400 MHz NMR spectrometer at 25 °C. Circular dichroism (CD) spectroscopy was done on an Aviv model 202 CD spectrometer at 25 ± 0.1 °C, sampling every 1 nm with a 3 s averaging time over a range of 190−260 nm (bandwidth = 1.0 nm). Measurements were taken in a quartz cell of 1mm path length at a concentration between 0.1 − 0.5 mg/mL. Gel permeation chromatography (GPC) measurements in DMF with 10 mM LiBr were carried out using a Waters 1525 binary pump system equipped with two Polypore columns operated at 75 °C, series 2414 refractive index detector, and 717plus autosampler. Waters Breeze Chromatography Software Version 3.30 was used for data collection as well as data processing. The instrument was calibrated against narrow molecular weight poly(methyl methacrylate) standards. FT-IR was performed on a Thermo Nicolet Nexus 870 equipped with a KBr beamsplitter, DTGS-KBr detector, and DuraSamplIR II ATR accessory (SENSIR).
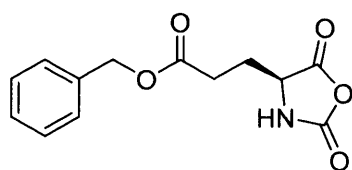
γ-Benzyl-L-glutamate N-carboxyanhydride

To a dispersion of γ-benzyl-L-glutamate (25.0 g, 112 mmol) in THF (200 mL) in a 1 L two neck round bottom flask equipped with a magnetic stir bar and rubber septum was added triphosgene (30.0 g, 100 mmol) in one portion. The mixture was stirred and sparged with a steady stream of argon under reflux for 2 h then cooled to RT. Hexanes (700 mL) were added and the mixture was allowed to sit for 7 h. The resulting precipitate was collected by vacuum filtration and washed 4 times with hexanes under a blanket of argon. The resulting solid was added to a flame dried 1 L flask, dissolved in anhydrous THF (300 mL), and recrystallized via solvent diffusion under a layer of hexanes (700 mL) in an argon atmosphere at RT. The solids were collected by vacuum filtration under a blanket of argon, washed 4 times with hexanes, and dried in $vacuo$ to give white crystals (25.7 g, 103 mmol, 92%). ^{1}H NMR (400 MHz, CDCl$_3$) δ: 7.46 – 7.31 (m, 5H), 6.49 (s, 1H), 5.37 – 5.01 (m, 2H), 4.40 (s, 1H), 2.63 (t, J = 6.3 Hz, 2H), 2.42 – 2.23 (m, 1H), 2.23 – 2.01 (m, 1H). ^{13}C NMR (100 MHz, CDCl$_3$) δ: 172.57, 169.46, 151.76, 135.28, 128.86, 128.77, 128.55, 67.30, 57.16, 30.11, 27.08.
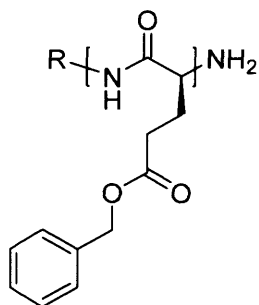

poly(γ-benzyl-L-glutamate) (PBLG)

A flame dried 100 mL Schlenk flask equipped with a magnetic stir bar and rubber septum was charged with NCA (3.28 g, 13.2 mmol) and DMF (30 mL). 5-Norbornene-2-methylamine (16.9 μL, 0.132 mmol) was added via micropipette with stirring and the reaction was sparged with a steady stream of argon at RT for 48 h. The reaction was added to water and the resulting precipitate was collected by centrifugation, washed 3 times with water, and dried in $vacuo$ to give a white powder (2.44 g, 11.9 mmol repeat units, 90%). ^{1}H NMR (400 MHz, DMSO) δ: 8.37 (s, 1H), 7.48 – 7.03 (m, 5H), 6.17 – 5.94 (m, 0.03H), 5.24 – 4.81 (m, 2H), 4.11 (s, 1H), 2.80 – 1.55 (m, 4H).
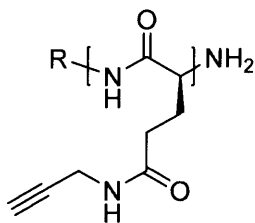
poly(γ-propargyl-L-glutamine) (PPLQ)

A round bottom flask equipped with a stir bar was charged with PBLG (6.00 g, 27.4 mmol repeat units) and THF (72 mL). The solution was cooled to 0 °C and a chilled solution of lithium hydroxide (1.70 g, 41.1 mmol) in water (24 mL) was added. The reaction was vigorously stirred at 4 °C for 12 h, diluted with water, and extracted 3 times with diethyl ether (3 x 100 mL). The organic layer was discarded and the pH of the aqueous layer was adjusted to 1-2 with 6M HCl. Residual ether was evaporated by sparging with compressed air and the solution was frozen and lyophilized to give a white solid. The solid was added to a round bottom flask equipped with a stir bar and DMF (25 mL), HOBt hydrate (ca. 20% water) (6.95 g, 41.1 mmol), and propargylamine (2.46 mL, 38.4 mmol) were added. EDC (6.83 g, 35.6 mmol) was added portionwise with stirring. After stirring for 24 h methanol (250 mL) was added. The precipitate was collected by centrifugation, washed with water, and dried *in vacuo* to give a white powder (2.63 g, 15.8 mmol repeat units, 58%). ^{1}H NMR (400 MHz, DMSO) δ: 8.22 (s, 1H), 8.09 (s, 1H), 6.16 – 5.93 (m, 0.02H), 4.21 (s, 1H), 3.85 (s, 2H), 3.07 (s, 1H), 2.15 (s, 2H), 1.82 (d, J = 48.3 Hz, 2H).
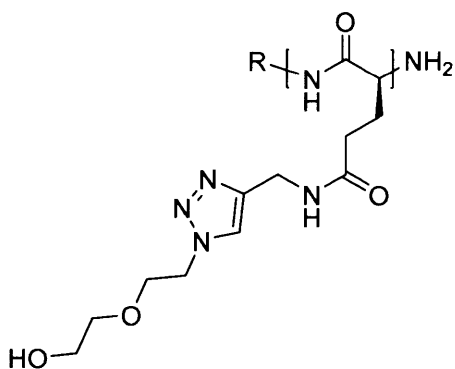
Poly(γ-((1-(2-(hydroxymethoxy)ethyl)-1H-1,2,3-triazol-4-yl)methyl)-L-glutamine) (PPLQ-g-EO2)

PPLQ (0.40 g, 2.4 mmol repeat units), DMF (10 mL), 2-(2-azidoethoxy)ethanol (0.34 mL, 2.9 mmol), and PMDETA (50 μL, 0.24 mmol) were added to a centrifuge tube. The tube was capped and vortexed to form a homogenous solution. The solution was sparged with a steady stream of argon for 20 minutes. Afterwards, copper (I) bromide (34 mg, 0.24 mmol) was added in one portion.

22

The tube was quickly capped, vortexed for 3 minutes, and allowed to sit for 12 h. Diethyl ether (40 mL) was added to the reaction and the resulting emulsion was separated by centrifugation. The diethyl ether was discarded and the remaining liquid was resuspended in DI water (5 mL). Dowex M4195 resin was added until the solution no longer appeared blue. The resin was removed by gravity filtration, the solution was dialyzed against water (MWCO 1000, RC), frozen, and lyophilized to give a white powder (0.65 g, 2.2 mmol repeat units, 91%). ^{1}H NMR (400 MHz, D$_2$O) δ: 8.02 (s, 1H), 6.19 – 5.81 (m, 1H), 4.56 (s, 2H), 4.41 (s, 1H), 4.26 (s, 1H), 3.91 (s, 2H), 3.61 (s, 2H), 3.53 (s, 2H), 2.36 (s, 2H), 2.16 – 1.80 (m, 2H).

Photochemical reaction

PPLQ-g-EO2 (35 mg), β-mercaptoethanol (0.28 µL), and LAP (0.44 mg) were added to 0.70 mL of deuterium oxide in a quartz cuvette. The solution was illuminated for 10 minutes by a 100 W long wave mercury UV lamp placed 7 cm above the sample.

Hydrolysis study

Hydrolysis of amide linked PPLQ and ester linked PPLG was determined by NMR. Polymer samples were rendered water soluble by grafting with an oligomeric ethylene glycol, dissolved in deuterium oxide (20 mg/mL), and the pH was adjusted by the addition of monosodium dihydrogen phosphate, sodium bicarbonate, or potassium carbonate to a final concentration of 10 mM. Sodium duteroxide was added to a final concentration of 150 mM. These additives gave solutions of pH 4.5, 8.0, 12, and 14, respectively, as determined by pH paper with pH increments of 0.5. A 23:77 ratio of monosodium dihydrogen phosphate to disodium monohydrogen phosphate was added to a final concentration of 250 mM for a solution of pH 7.4 at 37 °C. For PPLG and PPLQ, the peak corresponding to the aromatic proton on the triazole ring was used to determine extent of hydrolysis. Prior to hydrolysis, the peak is located at δ8.08 ppm. After hydrolysis, the peak is located at δ8.04 ppm. For determining PPLQ hydrolysis at pH 14, the triazole peak diminished over time, possibly due to proton exchange with the deuterated solvent. Instead, the peaks at δ3.90 ppm and δ3.85 ppm corresponding to protons on the oligomeric ethylene glycol were used to determine hydrolysis (see Fig. S4).

## Attempts at PPLQ synthesis by direct polymerization
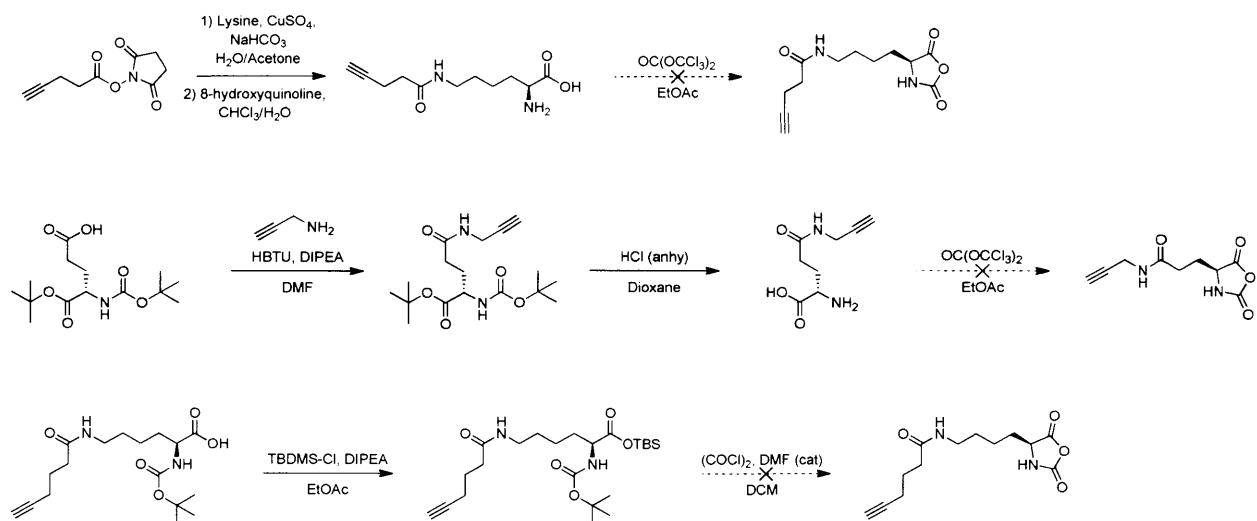
Figure 1.7. Strategies for synthesis of NCA monomer with an amide bond on the side chain. Formation of the amino acid was not an issue, but subsequent reactions proved unsuccessful. Synthesis of NCA by phosgene or triphosgene (Fuchs-Farthing method) begins by a dispersion of amino acid in organic solvent. Normally, the dispersion becomes a homogenous solution as the insoluble amino acid is converted to soluble NCA over the course of the reaction. For all conditions tested, the amino acid remained insoluble, indicating no conversion of amino acid to NCA. Various solvents (ethyl acetate, dichloroethane, dioxane, dichloromethane, tetrahydrofuran, acetonitrile) and additives (3 eq. pinene to amino acid, added prior to triphosgene) were screened by the same general procedure for NCA synthesis. A different amino acid structure resembling γ-propargyl-L-glutamine was also tested. None of the conditions described changed the outcome of the reaction. Changing the method of NCA formation by protection of the α-carboxylic acid by TBDMS followed by treatment with oxalyl chloride/DMF was also tested. TLC of the reaction did not show formation of product but rather reversion of the starting material to the unprotected carboxylic acid.

## Hydrolysis resistant alkyne containing polypeptides based off an ether linkage
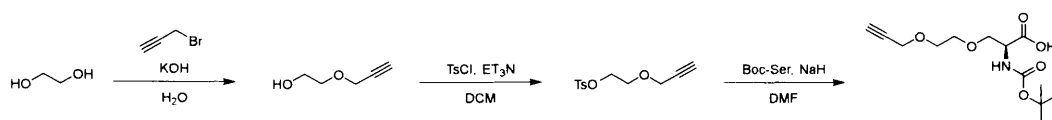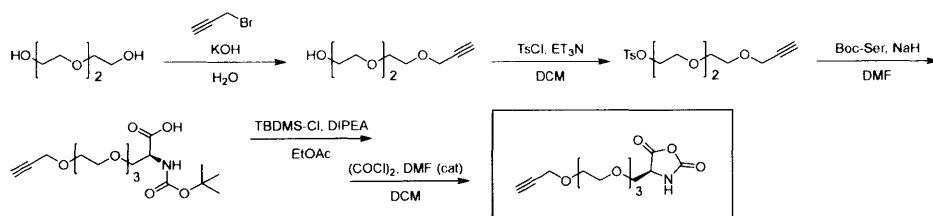
Figure 1.8. Synthesis of modified serines bearing an alkyne on the side chain attached by a hydrolysis resistant functional group. A modified amino acid based off an ether linkage was also investigated for the purpose of creating a water stable, α-helical polypeptide. This amino acid was synthesized by reacting an alkyne modified oligoethylene glycol and a N-Boc protected serine. Two variants of different spacer lengths were tested. While the N-carboxyanhydride was synthesized, the polymerization was not attempted. This route was deemed unsuitable due to the difficulty in preparation of large quantities of amino acid precursor in addition to purification of the N-carboxyanhydride monomer; high purity monomer is critical for success of N-carboxyanhydride polymerizations.
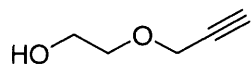

2-(prop-2-yn-1-yloxy)ethan-1-ol

To a chilled, stirring solution of potassium hydroxide (21.2 g) in water (33 mL) over an ice water bath was added ethylene glycol (52.7 mL, 0.943 mol) followed by dropwise propargyl bromide (80 wt% in toluene, 21.0 mL, 0.235 mol) over 30 minutes. The ice water bath was removed and the reaction was stirred at room temperature for 2 days, quenched with 1M HCl (150 mL), diluted with water (50 mL), and extracted three times with dichloromethane. The combined organic extracts were dried over sodium sulfate, and the solvent was removed *in vacuo*. Distillation under reduced pressure afforded a mix of the mono product with a small amount of disubstituted byproduct as a clear oil (7.65 g) which was used in subsequent steps without purification. ^{1}H NMR (400 MHz, Chloroform-d) δ 4.22 (d, J = 2.3 Hz, 3H), 3.81 − 3.74 (m, 2H), 3.73 (s, 1H), 3.70 − 3.63 (m, 2H), 2.46 (t, J = 2.4 Hz, 1H), 2.44 (t, J = 2.4 Hz, 0.3H), 2.10 (s, 1H).
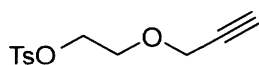

2-(prop-2-yn-1-yloxy)ethyl 4-methylbenzenesulfonate

To a chilled, stirring solution of 2-(prop-2-yn-1-yloxy)ethan-1-ol (7.5 g, 75 mmol) and triethylamine (31.5 mL, 226 mmol) in dichloromethane (250 mL) over an ice water bath was added portionwise tosyl chloride (21.4 g, 112 mmol) over 15 minutes. The ice water bath was removed and the reaction was stirred at room temperature for 26 hours, quenched with 200 mL 1M HCl, and extracted five times with dichloromethane. The combined organic extracts were died over magnesium sulfate and the solvent was removed *in vacuo*. Purification by flash chromatography with silica gel eluted by a 10% to 40% ethyl acetate:hexanes gradient afforded a yellow oil (10.3 g, 40.6 mmol, 54%).^{1}H NMR (400 MHz, Chloroform-*d*) δ 7.80 (d, *J* = 8.3 Hz, 2H), 7.35 (d, *J* = 7.9 Hz, 2H), 4.22 – 4.16 (m, 2H), 4.11 (d, *J* = 2.4 Hz, 3H), 3.76 – 3.66 (m, 2H), 2.45 (s, 4H). R_f 0.36 (40% EtOAc:Hex, visualized by UV)
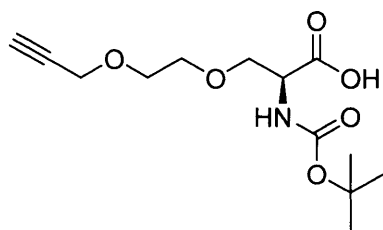

N-(*tert*-butoxycarbonyl)-O-(2-(prop-2-yn-1-yloxy)ethyl)-L-serine

A flame dried schlenk flask equipped with a magnetic stir bar was charged with N-Boc serine (0.672 g, 3.28 mmol) and N,N-dimethylformamide (15 mL). The solution was cooled to -20°C with a 10% ethanol:ethylene glycol bath over dry ice. Sodium hydride (60% dispersion in mineral oil, 0.302g, 7.53 mmol) was added portionwise with stirring under positive pressure of argon over 15 minutes. After addition, the cooling bath was removed and the reaction was stirred for 40 minutes. 2-(prop-2-yn-1-yloxy)ethyl 4-methylbenzenesulfonate (1.0 g, 3.9 mmol) was added dropwise over 2 minutes and the reaction was stirred for 24 hours. The reaction was then diluted with cold water and extracted with ethyl acetate. The organic phase was discarded, and the pH was adjusted to 1 by addition of cold 3M HCl. The aqueous solution was extracted three times with ethyl acetate. The combined organic extracts were rinsed with brine, dried over magnesium sulfate, and the solvent was removed *in vacuo*. Purification by flash chromatography with silica gel eluted by a 5% to 8% methanol:dichloromethane gradient afforded a yellow oil (482 mg, 1.68 mmol, 51%).^{1}H NMR (400 MHz, Chloroform-*d*) δ 5.54 (s, 1H), 4.38 (s, 1H), 4.22 (s, 2H), 3.95 (s, 1H), 3.71 (s, 5H), 2.46 (d, *J* = 2.5 Hz, 1H), 1.45 (s, 9H), 1.25 (s, 1H). R_f 0.36 (6% MeOH:DCM, visualized by anisaldehyde stain).
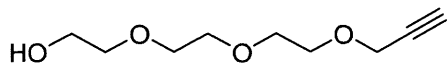
2-(2-(2-(prop-2-yn-1-yloxy)ethoxy)ethoxy)ethan-1-ol

To a chilled, stirring solution of triethylene glycol (33.5 mL, 250 mmol) and potassium hydroxide (5.61 g, 100 mmol) in water (10 mL) over an ice water bath was added dropwise propargyl bromide (80 wt% in toluene, 5.6 mL, 50 mmol) over 20 minutes. Upon completion, the cooling bath was removed and the reaction was stirred at room temperature for 3 days. The reaction was quenched with 50 mL of 1M HCl, diluted with 50 mL water, and extracted three times with dichloromethane. The combined organic extracts were dried over sodium sulfate and the solvent was removed *in vacuo* to give a yellow-orange oil (6.3 g, 33 mmol, 67%).^{1}H NMR (400 MHz, Chloroform-*d*) δ 4.21 (d, J = 2.4 Hz, 2H), 3.76 – 3.65 (m, 10H), 3.62 (q, J = 4.6 Hz, 2H), 2.53 (s, 1H), 2.44 (t, J = 2.4 Hz, 1H).
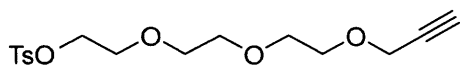

2-(2-(2-(prop-2-yn-1-yloxy)ethoxy)ethoxy)ethyl 4-methylbenzenesulfonate

To a chilled, stirring solution of 2-(2-(2-(prop-2-yn-1-yloxy)ethoxy)ethoxy)ethan-1-ol (5.98 g, 31.8 mmol) and triethylamine (13.5 mL, 95.6 mmol) in dichloromethane (100 mL) over an ice water bath was added portionwise tosyl chloride (9.12 g, 47.8 mmol) over 7 minutes. The ice water bath was removed and the reaction was stirred at room temperature for 28 hours, quenched with 100 mL 1M HCl, and extracted three times with dichloromethane. The combined organic extracts were died over magnesium sulfate and the solvent was removed *in vacuo*. Purification by flash chromatography with silica gel eluted by a 40% to 60% ethyl acetate:hexanes gradient afforded a yellow oil (6.95 g, 20.3 mmol, 64%).^{1}H NMR (400 MHz, Chloroform-*d*) δ 7.83 – 7.75 (m, 2H), 7.35 (d, J = 7.9 Hz, 2H), 4.23 – 4.09 (m, 4H), 3.74 – 3.60 (m, 6H), 3.59 (s, 3H), 3.52 (s, 1H), 2.45 (s, 3H), 2.44 – 2.41 (m, 1H). R$_f$ 0.16 (40% EtOAc:Hex, visualized by UV) 0.67 (4% MeOH:DCM, visualized by UV)
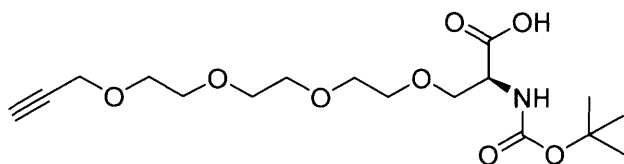
(S)-2-((*tert*-butoxycarbonyl)amino)-4,7,10,13-tetraoxahexadec-15-ynoic acid

A flame dried schlenk flask equipped with a magnetic stir bar was charged with N-Boc serine (0.672 g, 3.28 mmol) and N,N-dimethylformamide (15 mL). The solution was cooled to -20°C with a 10% ethanol:ethylene glycol bath over dry ice. Sodium hydride (60% dispersion in mineral oil, 0.302g, 7.53 mmol) was added portionwise with stirring under positive pressure of argon over 15 minutes. After addition, the cooling bath was removed and the reaction was stirred for 40 minutes. 2-(2-(2-(prop-2-yn-1-yloxy)ethoxy)ethoxy)ethyl 4-methylbenzenesulfonate (1.34 g, 3.9 mmol) was added dropwise over 2 minutes and the reaction was stirred for 21 hours. The reaction was then diluted with cold water and extracted with diethyl ether followed by extraction with ethyl acetate. The organic phase was discarded, and the pH was adjusted to 1 by addition of cold 3M HCl. The aqueous solution was extracted three times with ethyl acetate. The combined organic extracts were rinsed with brine, dried over magnesium sulfate, and the solvent was removed *in vacuo*. Purification by flash chromatography with silica gel eluted by a 5% to 10% methanol:dichloromethane gradient afforded a yellow oil (0.68 g, 1.8 mmol, 55%).^{1}H NMR (400 MHz, Chloroform-*d*) δ 5.62 (s, 1H), 4.38 (s, 1H), 4.24 (d, *J* = 1.5 Hz, 2H), 3.93 (dd, *J* = 9.6, 3.6 Hz, 1H), 3.82 – 3.56 (m, 14H), 2.45 (t, *J* = 2.4 Hz, 1H), 1.45 (s, 9H). R_f 0.25 (10% MeOH:DCM, visualized by anisaldehyde stain).
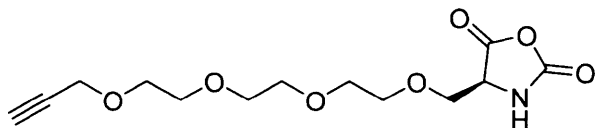
**(S)-4-(2,5,8,11-tetraoxatetradec-13-yn-1-yl)oxazolidine-2,5-dione**

To a chilled, stirring solution of (S)-2-((*tert*-butoxycarbonyl)amino)-4,7,10,13-tetraoxahexadec-15-ynoic acid (102 mg, 0.273 mmol) in ethyl acetate (2 mL) was added TBDMS-Cl (47 mg, 0.32 mmol) in one portion. The solution was stirred for two minutes and triethylamine (48 μL, 0.27 mmol) was added dropwise over 30 seconds. The reaction was stirred at 0°C for 1.5 hours. The crude reaction mix was filtered through a 0.45 μm PTFE syringe filter after which the solvent was removed *in vacuo*. Dichloromethane (2 mL) was added to dissolve the intermediate and the solution was cooled by an ice water bath. Oxalyl chloride (30 μL, 0.34 mmol) followed by DMF (10 μL) was added while stirring resulting in evolution of gas. The cooling bath was removed and the reaction was stirred at room temperature for 1 hour, the solvent was removed *in vacuo*, and

tetrahydrofuran was added, resulting a crystalline precipitate. The solution was filtered and the solids were washed with tetrahydrofuran to give a crystalline solid (16 mg, 0.053 mmol, 19%).^{1}H NMR (400 MHz, Chloroform-d) δ 7.51 (s, 1H), 4.41 (t, J = 3.4 Hz, 1H), 4.17 (d, J = 2.4 Hz, 2H), 4.08 – 3.89 (m, 2H), 3.89 – 3.45 (m, 12H), 2.45 (t, J = 2.4 Hz, 1H).
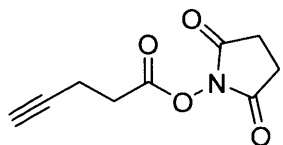
## 4-Pentynoic acid N-hydroxysuccinimide ester

To a stirring solution of 4-pentynoic acid (4.49 g, 45.7 mmol) and N-hydroxysuccinimide (5.54 g, 48.2 mmol) in DCM (185 mL) was added EDC HCl (9.24 g, 48.2 mmol) in one portion. The reaction was stirred overnight. Afterwards the solution was washed thrice with water (150 mL), rinsed with brine, and dried over $MgSO_4$. The solvent was removed *in vacuo* to yield a yellow-white solid (5.51 g, 28.2 mmol, 61%). ^{1}H NMR (400 MHz, $CDCl_3$) δ 2.94 – 2.86 (m, 2H), 2.84 (s, 4H), 2.67 – 2.57 (m, 2H), 2.06 (t, J = 2.7 Hz, 1H). ^{13}C NMR (101 MHz, Chloroform-d) δ 169.03, 167.14, 80.98, 70.16, 30.43, 25.70, 14.22.
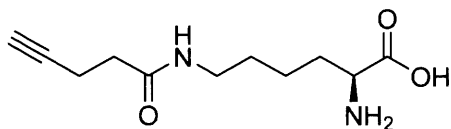

ε-6-Pentynoic-L-lysine[19]

To a stirring solution of L-lysine (0.47 g, 2.56 mmol) and sodium bicarbonate (0.90 g, 10.24 mmol) in water (7 mL) was added a solution of Cu(II) sulfate (0.32 g, 1.28 mmol) in water (3.5 mL) dropwise over 1 minute. The solution was stirred for 10 minutes after which a solution of 4-Pentynoic acid N-hydroxysuccinimide ester (0.50 g, 2.56 mmol) in acetone (3.5 mL) was added dropwise over 2 minutes. The reaction was stirred for 17 hours after which the precipitate was removed by filtration and washed with water followed by acetone. The isolated solid (0.66 g) was dissolved in a 1:1 mixture of chloroform and water (30 mL). 8-Hydroxyquinoline (0.55 g, 3.84 mmol) was added in one portion and the solution was stirred for 10 minutes. The precipitate was removed by filtration and the aqueous solution was washed four times with chloroform (30 mL). Residual chloroform was removed by sparging with N_2 and the aqueous solution was lyophilized

to give a white powder (0.46 g, 2.01 mmol, 79%).^{1}H NMR (400 MHz, D$_2$O) δ 3.73 (t, J = 6.1 Hz, 1H), 3.23 (t, J = 6.8 Hz, 2H), 2.56 – 2.39 (m, 4H), 1.98 – 1.79 (m, 2H), 1.65 – 1.50 (m, 2H), 1.50 – 1.30 (m, 2H).
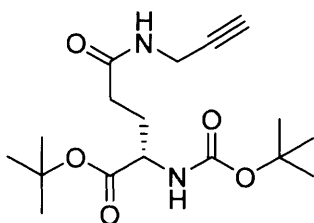

γ-Propargyl-Boc-L-Gln-OtBu

To a stirring solution of Boc-L-Glu-OtBu (3.00 g, 9.89 mmol) and DMF (90 mL) was added HBTU (4.50 g, 11.7 mmol) in one portion. Upon complete dissolution of the solids, propargylamine (0.665 mL, 10.4 mmol) followed by DIPEA (4.31 mL, 24.7 mmol) were added. The reaction was stirred for 3 hours after which EtOAc (360 mL) was added and the solution was washed with water (3 x 100 mL), rinsed with brine, and dried over MgSO$_4$. The solvent was removed *in vacuo* and the residue was purified by flash chromatography (10% followed by 30% EtOAc:DCM) yielding a white solid (2.47 g, 7.26 mmol, 73%).^{1}H NMR (400 MHz, CDCl$_3$) δ 6.53 (s, 1H), 5.25 (d, J = 7.5 Hz, 1H), 4.06 (dd, J = 5.2, 2.6 Hz, 2H), 2.35 – 2.25 (m, 2H), 2.23 (t, J = 2.6 Hz, 1H), 2.22 – 2.11 (m, 1H), 1.93 – 1.80 (m, 1H), 1.46 (s, 9H), 1.45 (s, 9H).^{13}C NMR (101 MHz, Chloroform-*d*) δ 171.95, 171.47, 82.52, 80.19, 79.71, 71.56, 60.52, 53.51, 32.61, 29.68, 29.37, 28.44, 28.11. R$_f$ 0.67 (20% EtOAc:DCM, visualized with CAM).
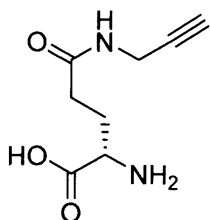
γ-Propargyl-L-glutamine

To a stirring solution of 4M HCl in dioxane (3.8 mL, 15.2 mmol) was added γ-propargyl-Boc-L-Gln-OtBu (0.496 g, 1.38 mmol) in one portion, and the reaction was stirred for 3 hours. EtOAc was added and the precipitate was collected by centrifugation and dried *in vacuo* yielding an off white powder (291 mg, 1.32 mmol, 96%). ^{1}H NMR (400 MHz, D$_2$O) δ 4.05 (t, J = 6.4 Hz, 1H),

3.97 (d, J = 2.2 Hz, 2H), 2.61 (s, 1H), 2.59 – 2.35 (m, 2H), 2.35 – 2.13 (m, 2H).^{13}C NMR (101 MHz, Deuterium Oxide) δ 174.07, 79.57, 71.73, 52.56, 31.00, 28.78, 27.02, 25.57.
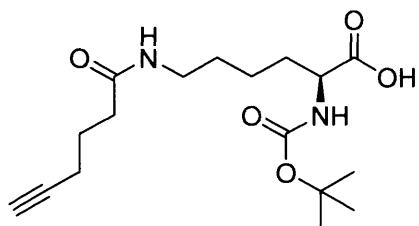
Nα-Boc-Nε-5-hexynoic-L-lysine

To a stirring solution of NHS (2.22 g, 19.0 mmol) and 5-hexynoic acid (2.03 g, 18.1 mmol) in DCM (76 mL) was added solid EDC (3.74 g, 19.5 mmol) over 30 seconds. The reaction was stirred overnight, after which consumption of the starting material was confirmed by TLC. The solution was washed three times with water, rinsed with brine, dried over MgSO₄, and the solvent was removed *in vacuo*. The resulting oil was used without further purification. ^{1}H NMR (400 MHz, Chloroform-*d*) δ 2.84 (s, 4H), 2.78 (t, J = 7.4 Hz, 2H), 2.35 (td, J = 6.9, 2.7 Hz, 2H), 2.02 (t, J = 2.6 Hz, 1H), 1.96 (q, J = 6.9 Hz, 2H).^{13}C NMR (101 MHz, Chloroform-*d*) δ 169.07, 168.17, 82.41, 69.83, 29.67, 25.59, 23.34, 17.60. R$_f$ 0.3 (30% EtOAc:Hexane, visualized with KMnO₄).

To a chilled, stirred solution of Boc-Lys-OH (4.46 g, 18.1 mmol) in saturated sodium bicarbonate (45 mL) was added the 5-hexynoic acid NHS ester in a solution of THF (45 mL) dropwise over 5 minutes. The reaction was stirred at room temperature for 24 hours. The THF was removed *in vacuo* and the resulting aqueous solution was cooled to 0°C by an external ice bath. The pH was adjusted to 2 by dropwise addition of 1N HCl with stirring. Afterwards, the aqueous solution was extracted by EtOAc (75 mL) and the organic extract was rinsed with brine and dried over MgSO₄. Removal of solvent *in vacuo* yielded a white solid (5.12 g, 15.0 mmol, 83% over 2 steps).^{1}H NMR (400 MHz, Chloroform-*d*) δ 10.07 (s, 1H), 5.88 (s, 1H), 5.27 (d, J = 7.7 Hz, 1H), 4.29 (d, J = 6.8 Hz, 1H), 3.26 (qd, J = 6.9, 2.7 Hz, 2H), 2.34 (t, J = 7.4 Hz, 2H), 2.25 (td, J = 6.8, 2.6 Hz, 2H), 1.99 (t, J = 2.6 Hz, 1H), 1.86 (p, J = 7.0 Hz, 3H), 1.80 – 1.65 (m, 1H), 1.65 – 1.49 (m, 2H), 1.45 (s, 9H), 1.44 – 1.36 (m, 2H).^{13}C NMR (101 MHz, Chloroform-*d*) δ 175.52, 173.45, 172.22, 83.57, 80.28, 69.49, 53.26, 39.38, 35.18, 32.14, 29.02, 28.48, 24.31, 22.50, 17.93.

Attempted formation of Nε-5-hexynoic-L-lysine NCA by oxalyl chloride[21]

31

To a chilled, stirring solution of N_α-Boc-N_ϵ-5-hexynoic-L-lysine (228 mg, 0.674 mmol) in EtOAc (4 mL) was added TBDMS-Cl (114 mg, 0.756 mmol) in one portion. The solution was stirred for two minutes and DIPEA (120 µL, 0.67 mmol) was added dropwise over 30 seconds. The reaction was stirred at 0°C for 1 hour, after which the starting material was completely consumed (TLC). R_f 0.69 (10% MeOH:DCM, visualized with $KMnO_4$). The salt was removed by filtration with a 0.45 µm PTFE syringe filter after which the solvent was removed *in vacuo*. DCM (2 mL) was added to dissolve the intermediate and the solution was cooled by an ice water bath. Oxalyl chloride (72 µL, 0.84 mmol) followed by DMF (10 µL) was added while stirring resulting in evolution of gas. TLC (10% MeOH:DCM, visualized with $KMnO_4$) showed presence of the starting amino acid.

The procedure was also performed with isolation of the intermediate TBDMS protected amino acid by flash chromatography (5% MeOH:DCM) prior to treatment with oxalyl chloride. The outcome of the reaction was the same.

Screening of deprotection conditions
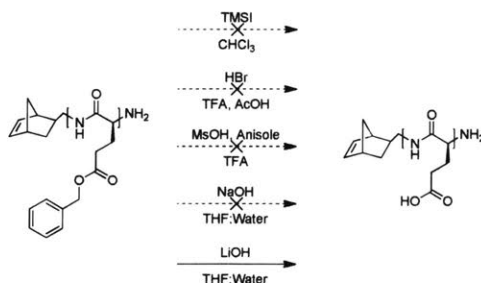
Figure 1.9. Screening of conditions for benzyl ester deprotection and preservation of norbornene end groups. All tested methods were adequate for the conversion of benzyl esters to the free carboxylic acid. However, only deprotection with LiOH demonstrated preservation of the norbornene end group as determined by NMR.

TMSI deprotection[23,24]

To a stirring solution of PBLG (0.50 g, 2.28 mmol repeat units) in chloroform (5 mL) was added TMS-I (0.39 mL, 2.73 mmol) dropwise over 1 minute. The reaction was stirred at 50°C for 2 hours

after which diethyl ether was added and the precipitate was collected by centrifugation, washed with water, and dried *in vacuo* to yield an off white powder (256 mg, 1.98 mmol repeat units, 87%).

HBr deprotection

To a stirring solution of PBLG (0.52 g, 2.37 mmol repeat units) in trifluoroacetic acid (3 mL) was added 33 wt% HBr in AcOH (1.1 mL). The reaction was stirred for 1 hour after which diethyl ether was added and the precipitate was collected by filtration, washed with diethyl ether, and dried *in vacuo* to yield an off white powder (0.27 g, 2.06 mmol repeat units, 87%).

MsOH, Anisole deprotection[22]

To a chilled stirring solution of PBLG (1.0 g, 4.56 mmol repeat units) in trifluoroacetic acid (10 mL) was added methanesulfonic acid (9.5 mL) dropwise over 1 minute followed by anisole (1.6 mL) dropwise over 1 minute. The reaction was stirred at 0°C for 20 minutes after which the cooling bath was removed and the reaction was stirred for an additional 20 minutes. Diethyl ether was added and the precipitate was collected by centrifugation, washed with diethyl ether, and dissolved in sat. NaHCO$_3$. The solution was exhaustively dialyzed against deionized water across a 2 kDa regenerated cellulose membrane. Afterwards the pH of the solution was adjusted to 2 by dropwise addition of 1M HCl and the precipitate was collected by centrifugation and dried *in vacuo* to yield a white powder (0.41 g, 3.19 mmol repeat units, 70%).

NaOH deprotection

To a chilled stirring solution of PBLG (1.0 g, 4.56 mmol repeat units) in THF (8 mL) was added a chilled solution of NaOH (0.37 mg, 9.1 mmol) in water (1 mL) dropwise over 2 minutes. The reaction was stirred for 20 hours at room temperature after which the solution was cooled to 0°C and the pH adjusted to 2 by dropwise addition of 1M HCl. The precipitate was collected by centrifugation and dried *in vacuo* yielding a white powder (88 mg, 0.68 mmol repeat units, 15%)

**Screening of amide bond coupling conditions**
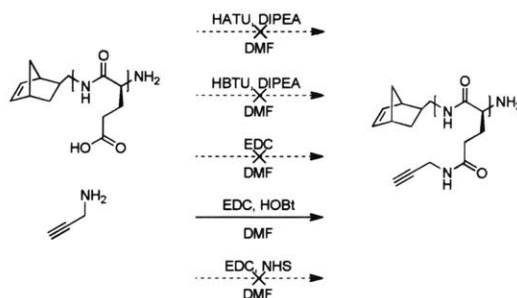
Figure 1.10. Screening of amide bond coupling conditions. Reactions were determined to be unsuccessful by spectroscopy or inability to isolate product by precipitation. In general, no reaction between the amine terminus of the polypeptide with carboxylic acid was observed. This reaction is likely suppressed by the use of excess propargylamine and the consumption of the amine terminus by side reactions during NCA polymerization.

Representative procedure for uronium/aminium coupling of propargylamine

To a stirring solution of poly(glutamate) (395 mg, 3.06 mmol repeat units) in DMF (10 mL) was added HBTU (1.53 g, 3.98 mmol) in one portion. Upon complete dissolution of the solid, DIPEA (1.6 mL, 9.2 mmol) was added and the solution stirred for 15 minutes. Afterwards, propargylamine (274 μL, 4.28 mmol) was added and the solution stirred 12 hours. The product was precipitated by addition of isopropanol, collected by centrifugation, and dried *in vacuo* to give a white powder (0.338 g) (see Fig. S3b).

Coupling by EDC

Coupling of poly(L-glutamate) and propargylamine by only EDC with no additives followed the same procedure as outlined in the main manuscript with exclusion of HOBt (see Fig. S3c). Coupling of poly(L-glutamate) and propargylamine by EDC and NHS followed the same procedure as outlined in the main manuscript with substitution of HOBt with NHS. No product was isolated from precipitation and the reaction was determined to be incomplete.
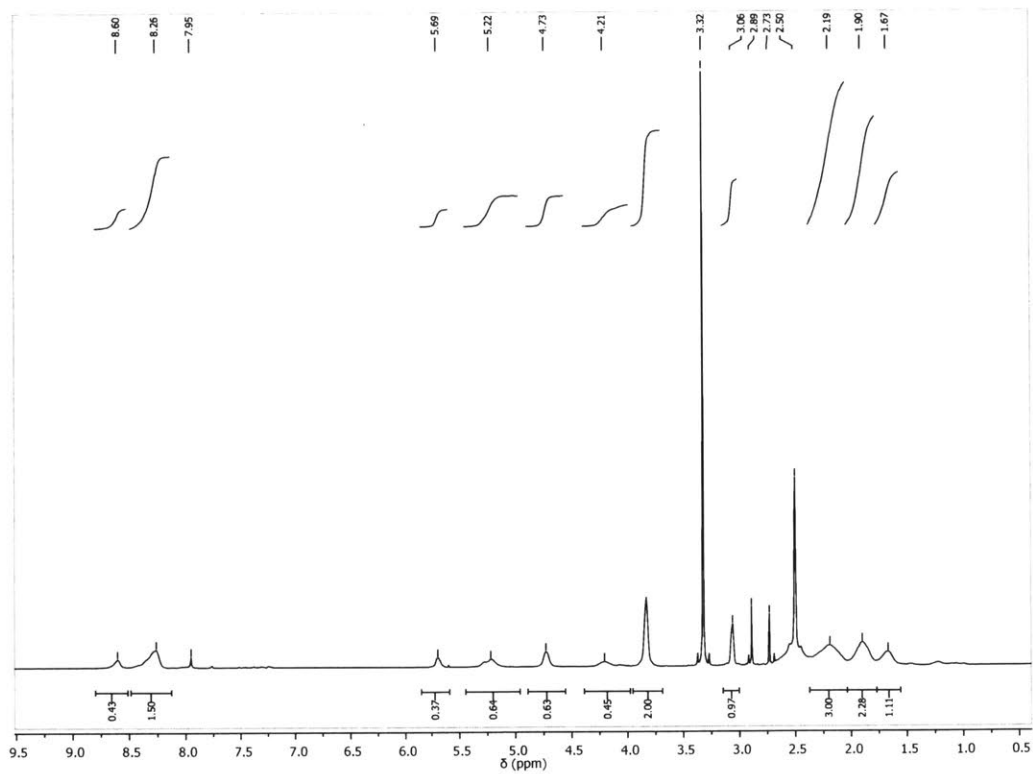
Figure 1.11. ^{1}H NMR spectrum of the product by HATU coupling in DMSO-d$_6$ exhibited extra peaks and incomplete integrations. Known solvents and impurities are located at δ 7.95, 2.89, 2.73 (DMF); δ 2.5 (DMSO); δ 3.32 (water)
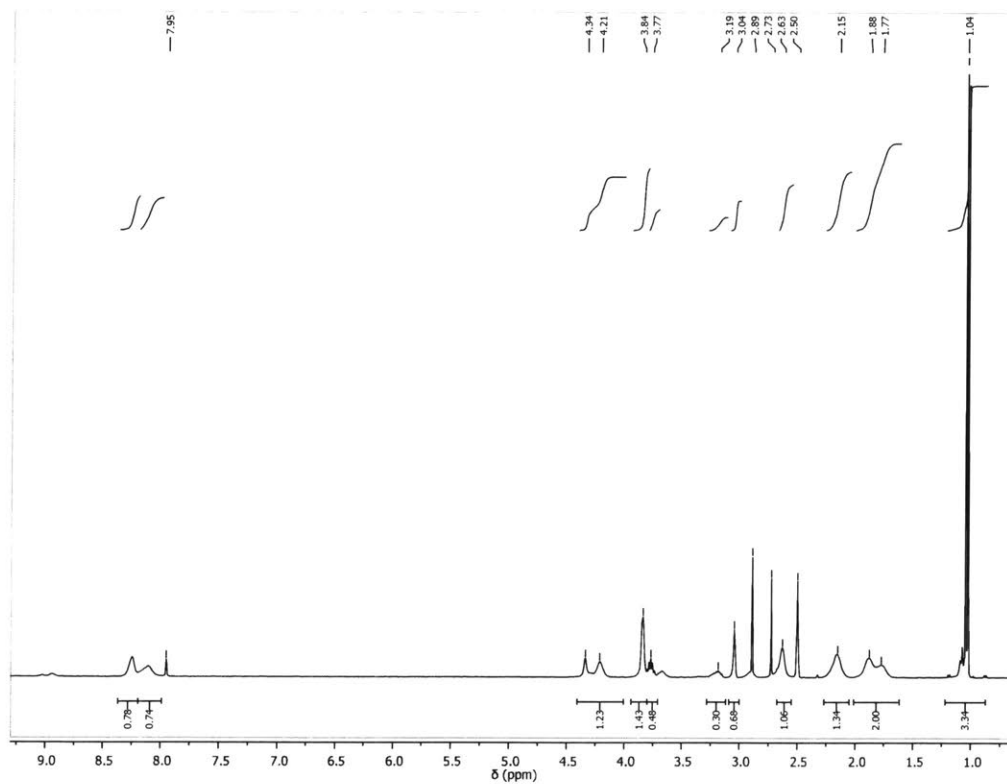
Figure 1.12. ^{1}H NMR spectrum of the product by EDC coupling with no additives in DMSO-d$_6$ exhibited extra peaks and incomplete integrations. Known solvents and impurities are located at δ 7.95, 2.89, 2.73 (DMF) and δ 2.5 (DMSO).
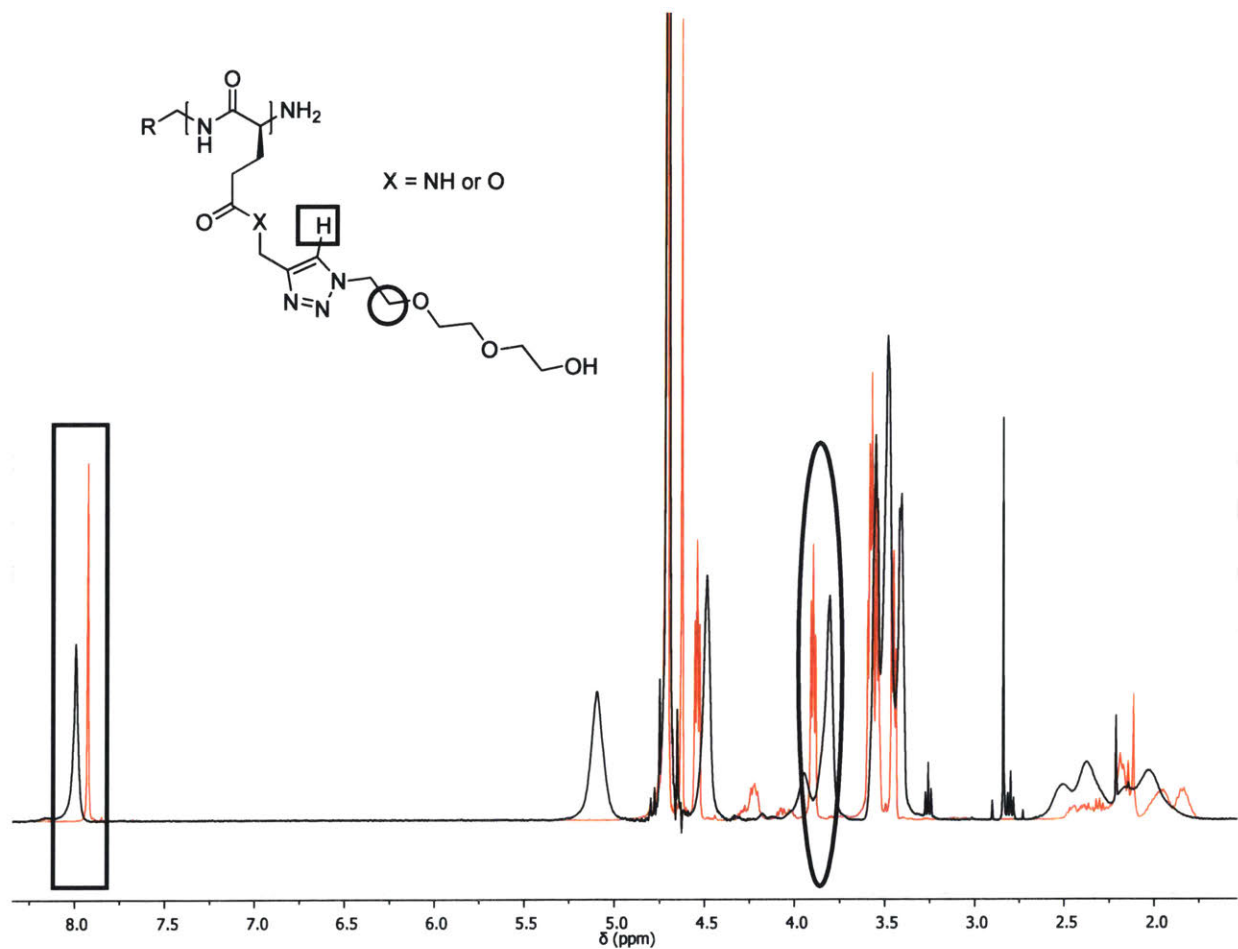
Figure 1.13. Protons monitored by ^{1}H NMR to evaluate hydrolysis. The black trace represents PPLG grafted with an oligomeric ethylene glycol. The red trace represents the polymer sample after complete hydrolysis. The protons are highlighted on the structure and spectrum by corresponding shapes.
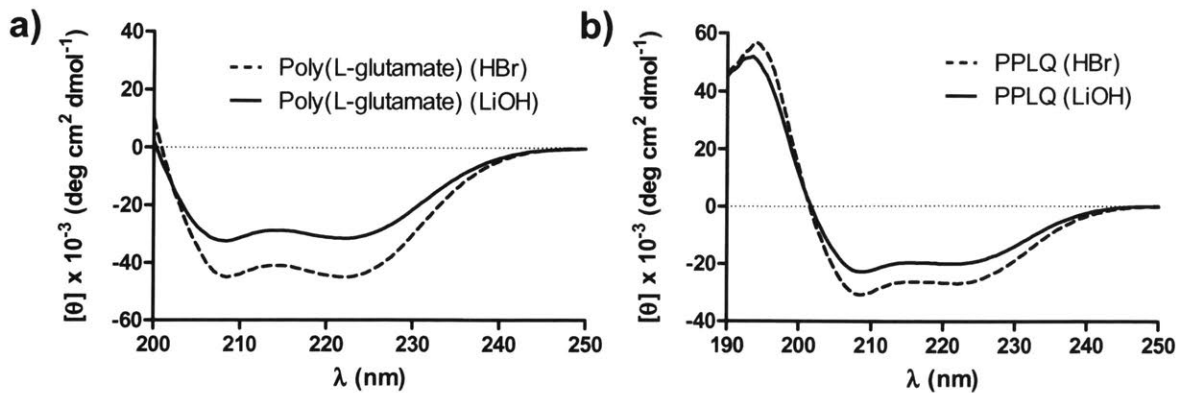
Figure 1.14. (a) Circular dichroism of poly(L-glutamate) obtained through deprotection by either HBr or LiOH as denoted in legend. Spectrum was taken at 0.5 mg/mL in 100 mM sodium acetate pH 4.5. (b) Circular dichroism of PPLQ obtained through deprotection by either HBr or LiOH as denoted in legend. Spectrum was taken at 0.5 mg/mL in hexafluoroisopropanol.
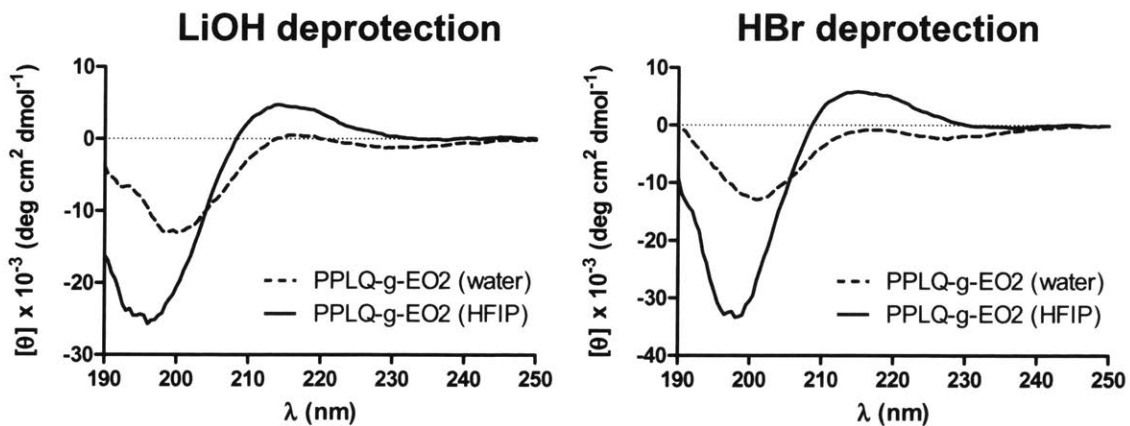

Figure 1.15. Circular dichroism of PPLQ-g-EO2 obtained through deprotection by LiOH or HBr. Spectra were taken at 0.5 mg/mL in either water or hexafluoroisopropanol as denoted in legend.
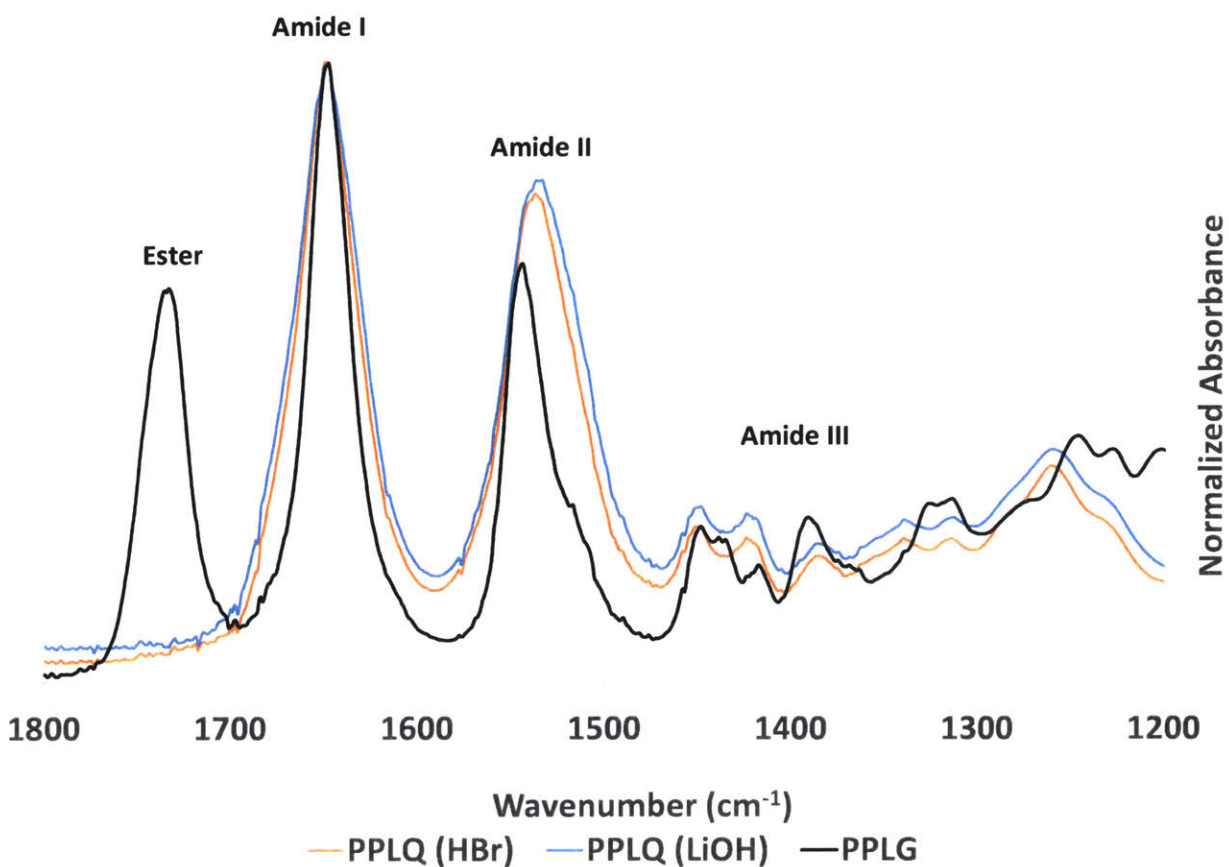
Figure 1.16. Overlaid FTIR spectra of ester PPLG as well as amide PPLQ synthesized through PBLG deprotection by either HBr or LiOH. Though the spectrum of PPLQ and PPLG differ, likely due to the differences of the side chain ester or amide, PPLQ synthesized through acidic and basic deprotection are similar. Spectra are normalized to peak amide I absorbance.
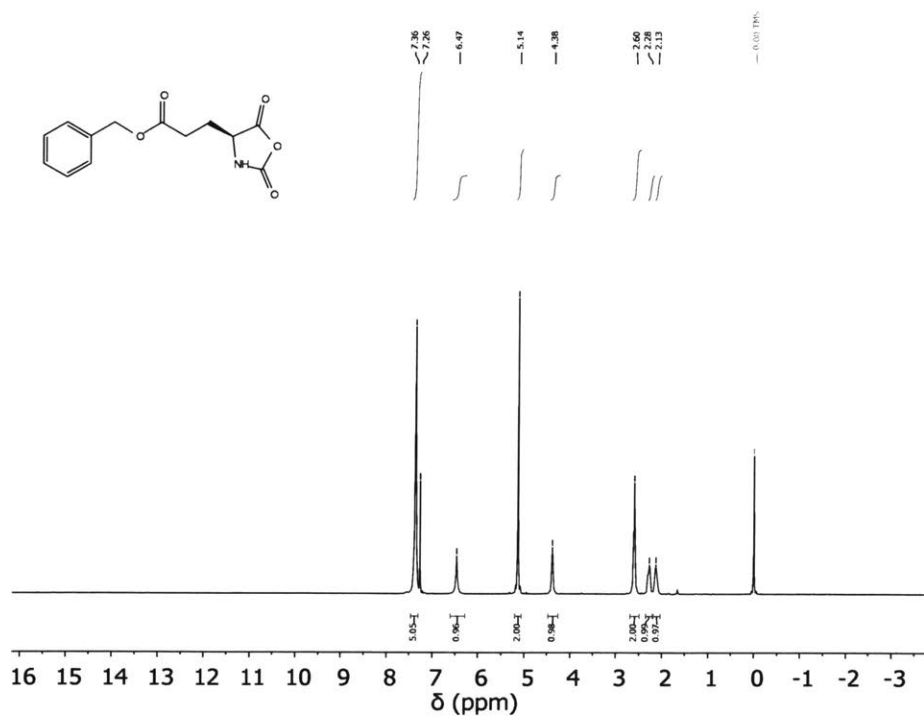
Figure 1.17. ¹H NMR spectrum of γ-Benzyl-L-glutamate N-carboxyanhydride in CDCl₃
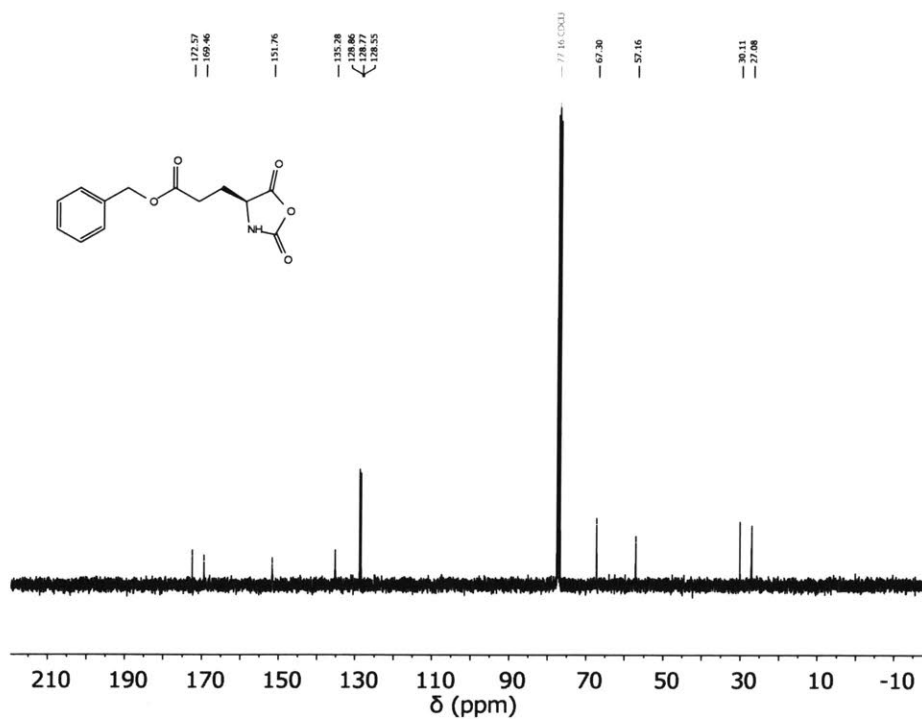

Figure 1.18. ¹³C NMR spectrum of γ-Benzyl-L-glutamate N-carboxyanhydride in CDCl₃

40
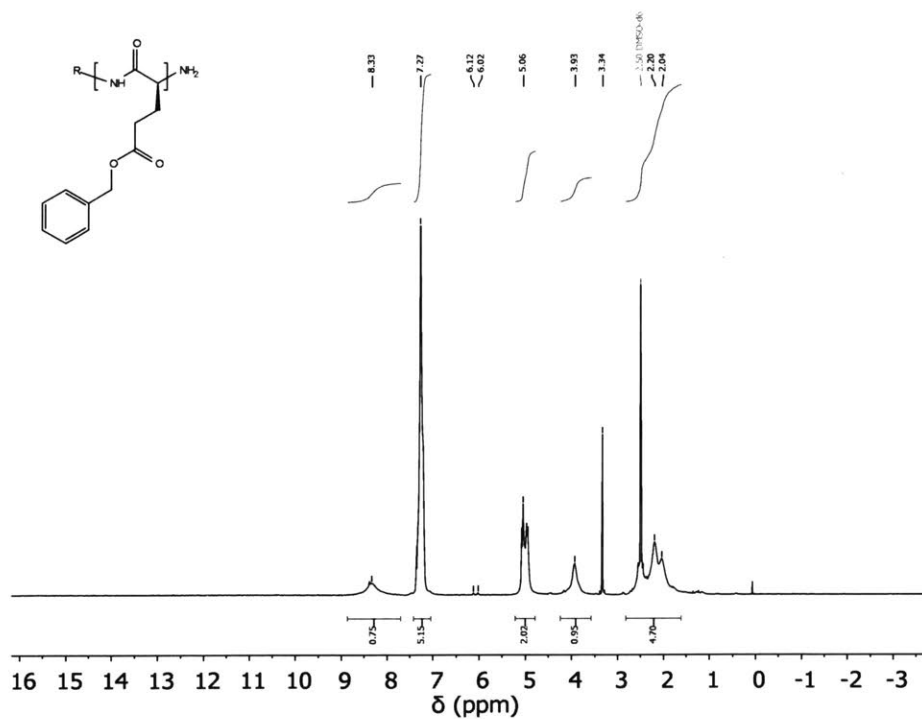
Figure 1.19. ^{1}H NMR spectrum of poly(γ-benzyl-L-glutamate) in $(CD_3)_2SO$. Integration around δ 2.20 is artificially high due to peak from DMSO. Peak at δ 3.34 is from water. Peaks at δ 6.12 and 6.02 are from vinyl protons on a norbornene based initiator.
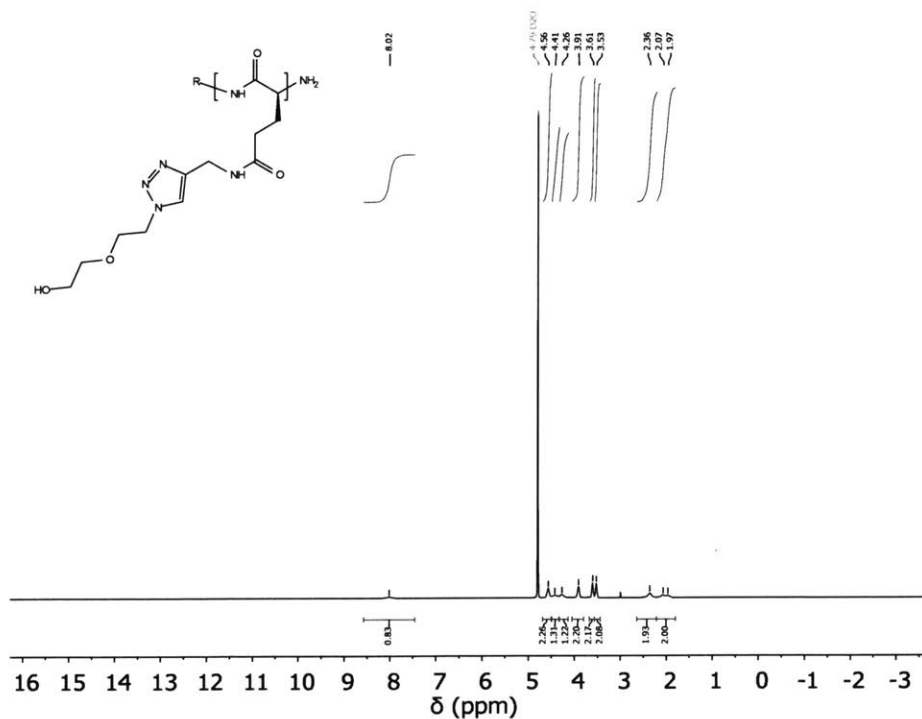

Figure 1.20. ^{1}H NMR spectrum of poly(γ-((1-(2-(hydroxymethoxy)ethyl)-1H-1,2,3-triazol-4-yl)methyl)-L-glutamine) in D_2O.

41
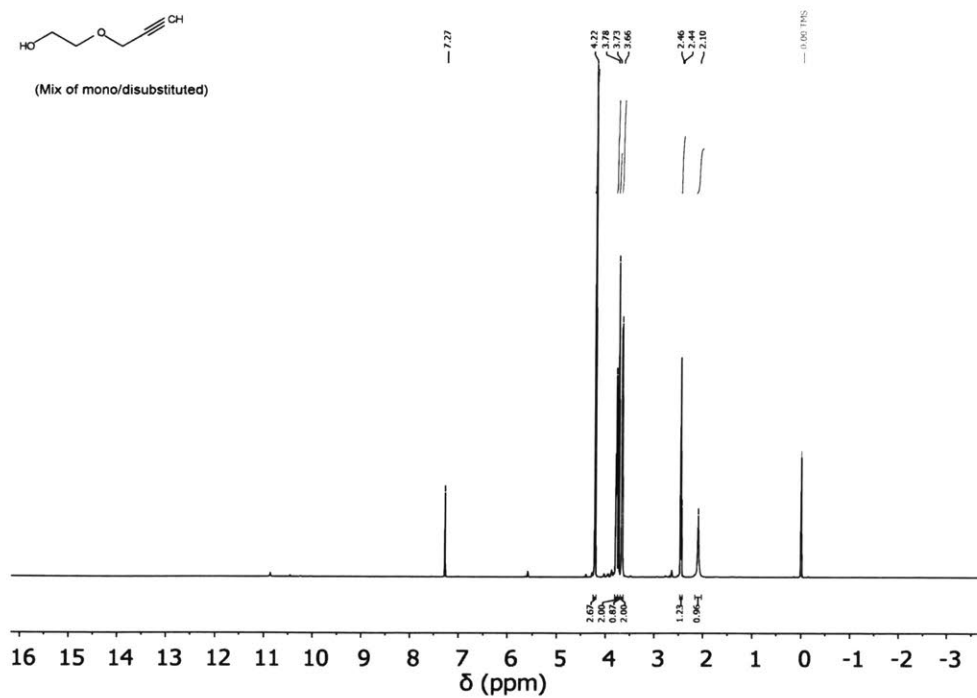
Figure 1.21. ^{1}H NMR spectrum of 2-(prop-2-yn-1-yloxy)ethan-1-ol in CDCl$_3$
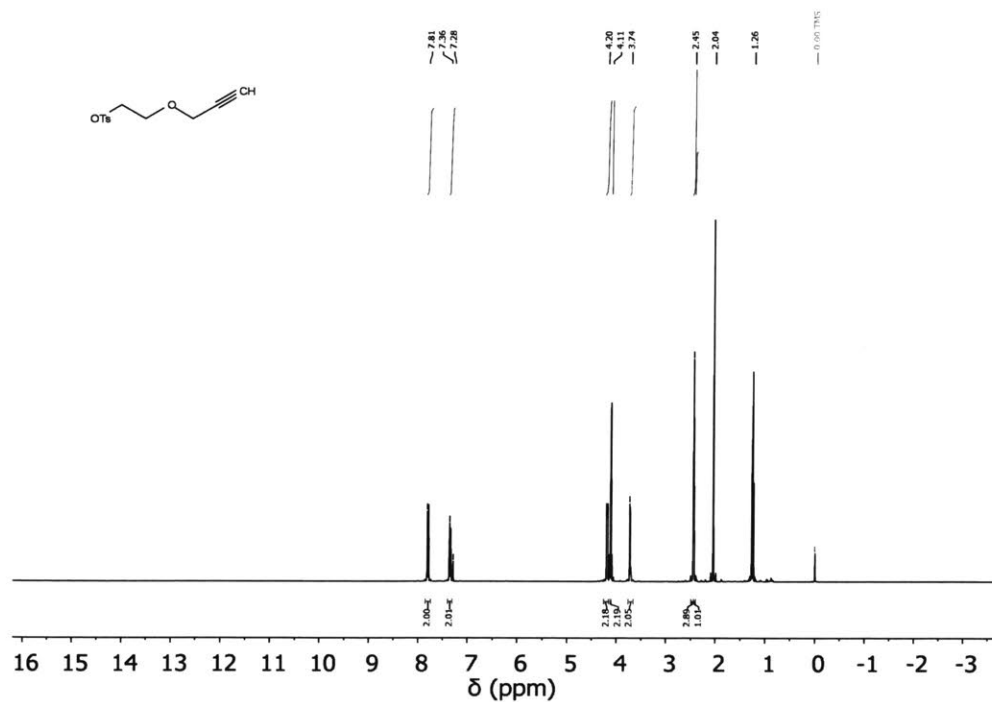
Figure 1.22. ^{1}H NMR spectrum of 2-(prop-2-yn-1-yloxy)ethyl 4-methylbenzenesulfonate in CDCl$_3$. Peaks at δ 4.11, 2.04, and 1.26 are from ethyl acetate.
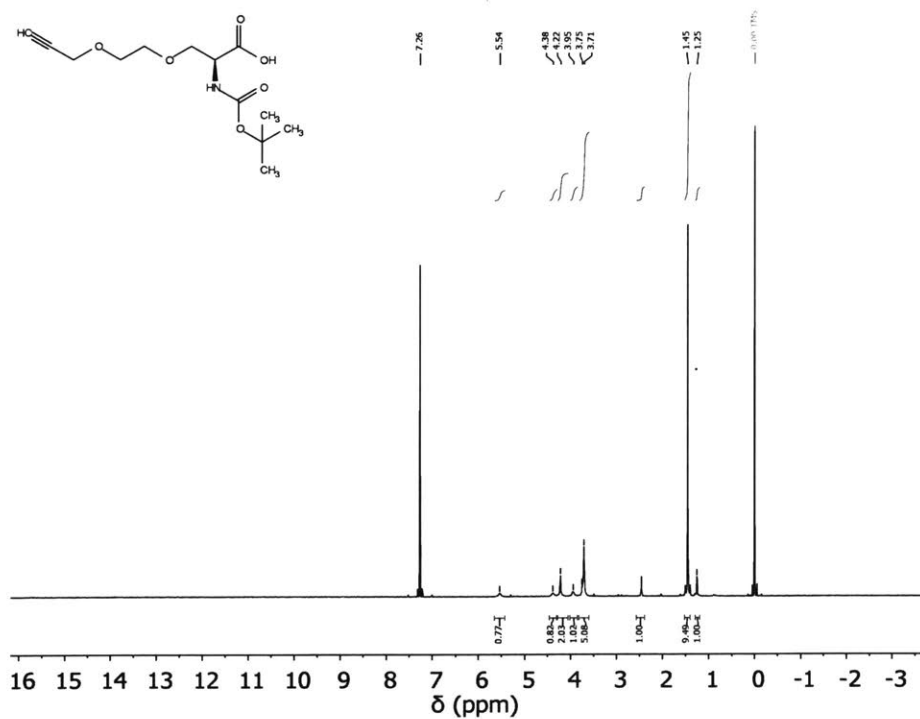
Figure 1.23. ¹H NMR spectrum of N-(*tert*-butoxycarbonyl)-O-(2-(prop-2-yn-1-yloxy)ethyl)-L-serine in CDCl₃.
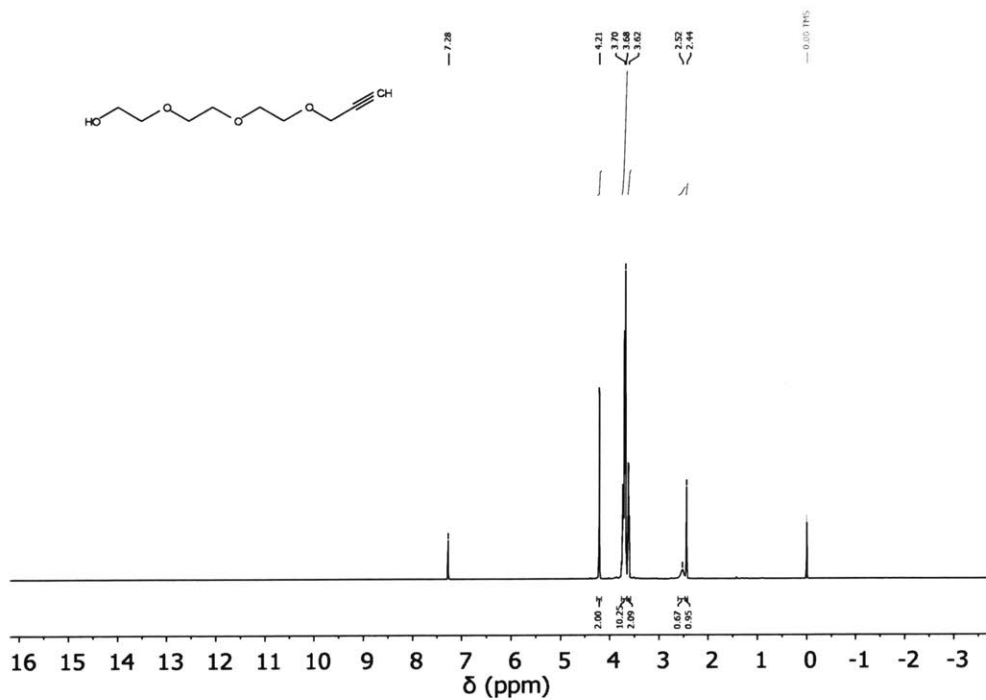
Figure 1.24. ¹H NMR spectrum of 2-(2-(2-(prop-2-yn-1-yloxy)ethoxy)ethoxy)ethan-1-ol in CDCl₃.
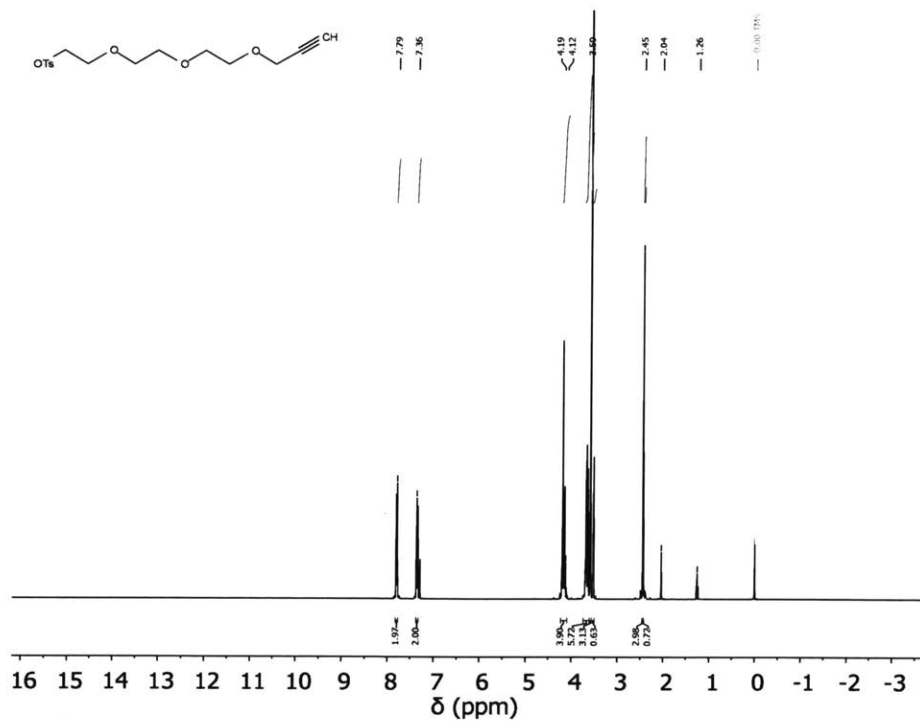
Figure 1.25. ^{1}H NMR spectrum of 2-(2-(2-(prop-2-yn-1-yloxy)ethoxy)ethoxy)ethyl 4-methylbenzenesulfonate in CDCl$_3$. Peaks at δ 4.11, 2.04, and 1.26 are from ethyl acetate.
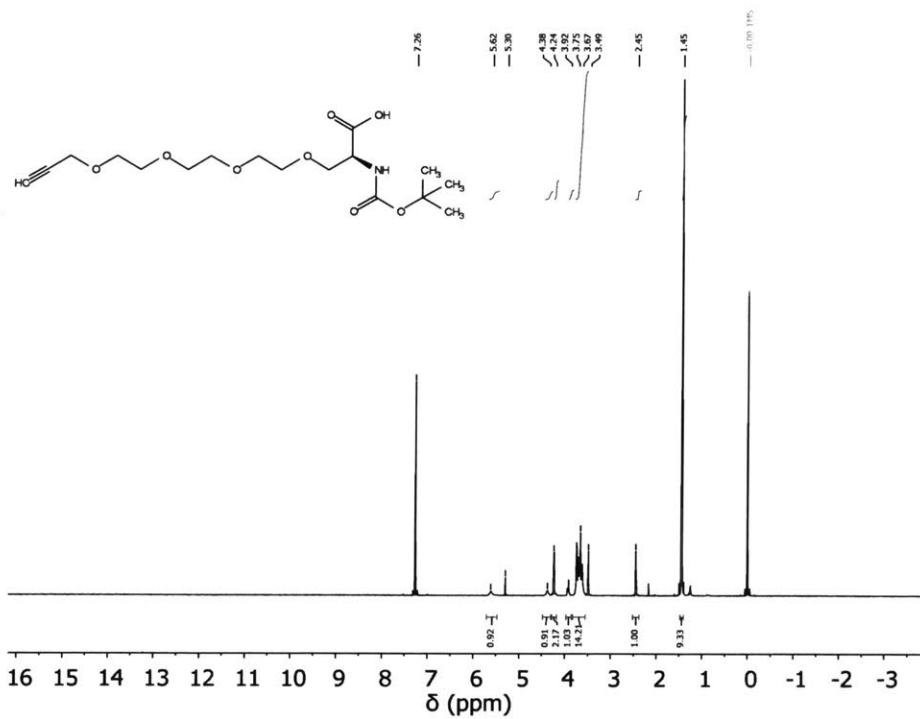
Figure 1.26. ¹H NMR spectrum of (S)-2-((*tert*-butoxycarbonyl)amino)-4,7,10,13-tetraoxahexadec-15-ynoic acid in CDCl₃. Peak at δ 5.30 is from dichloromethane. Peak at δ 3.49 is from methanol.
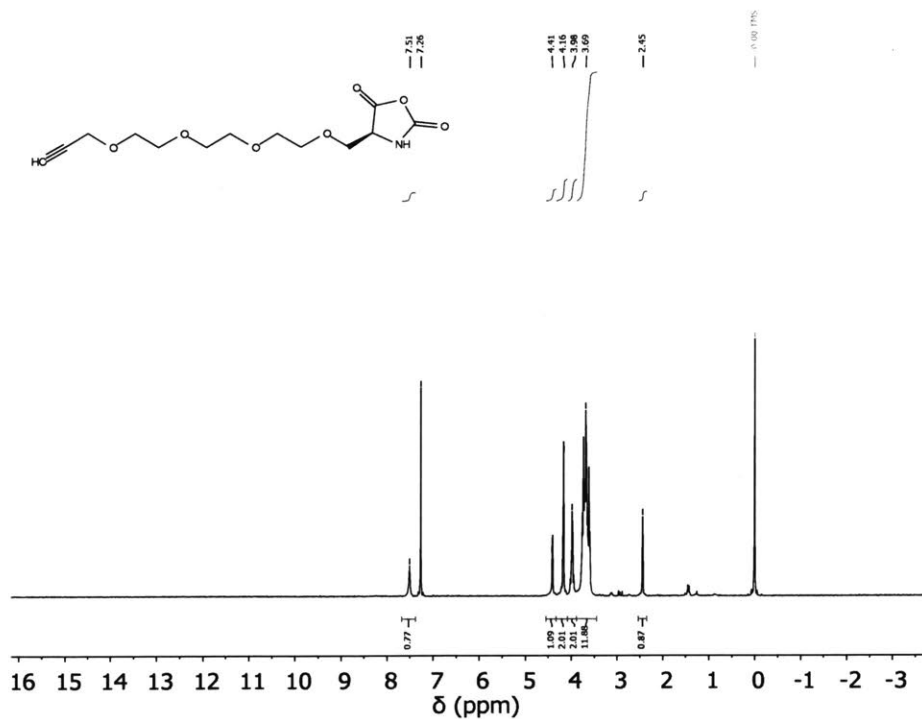
Figure 1.27. ¹H NMR spectrum of (S)-4-(2,5,8,11-tetraoxatetradec-13-yn-1-yl)oxazolidine-2,5-dione in CDCl₃.
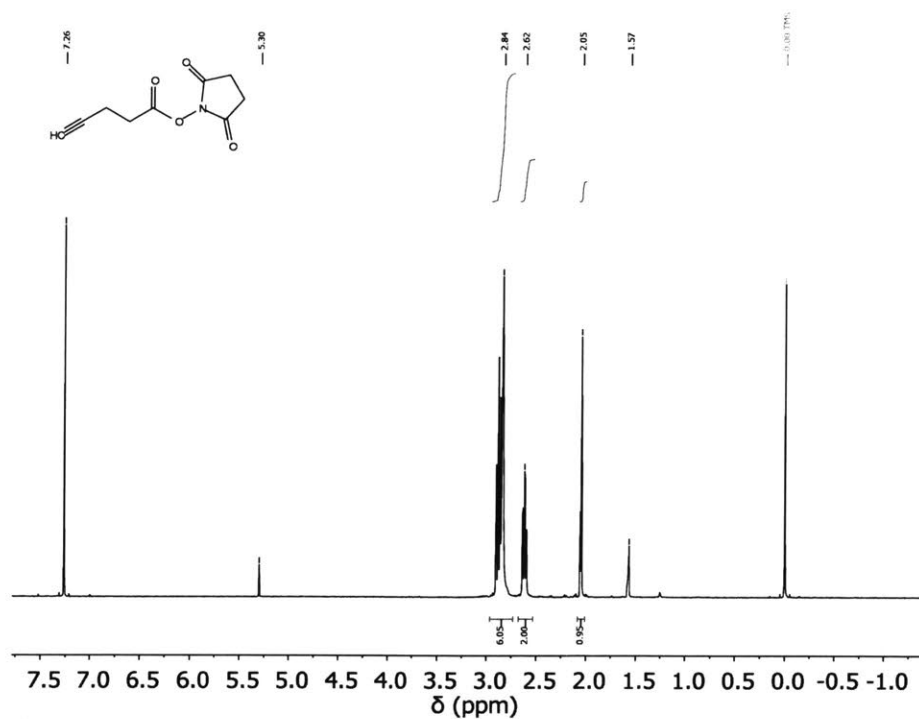
Figure 1.28. ^{1}H NMR spectrum of 4-Pentynoic acid N-hydroxysuccinimide ester in CDCl$_3$. Peak at δ 5.30 is from dichloromethane. Peak at δ 1.57 is from water.
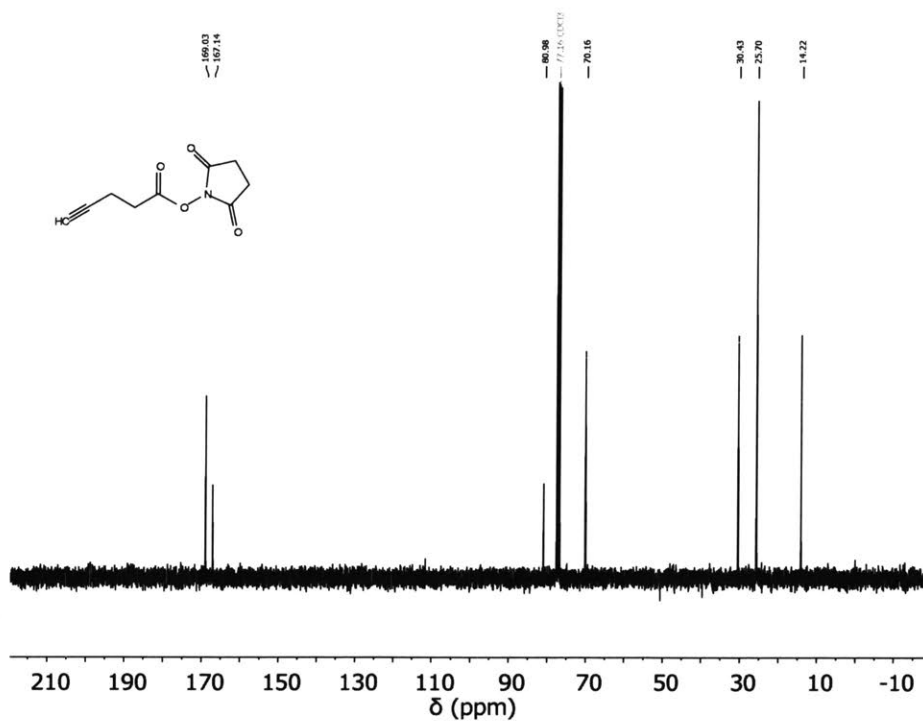
Figure 1.29. ^{13}C NMR spectrum of 4-Pentynoic acid N-hydroxysuccinimide ester in CDCl$_3$.

46
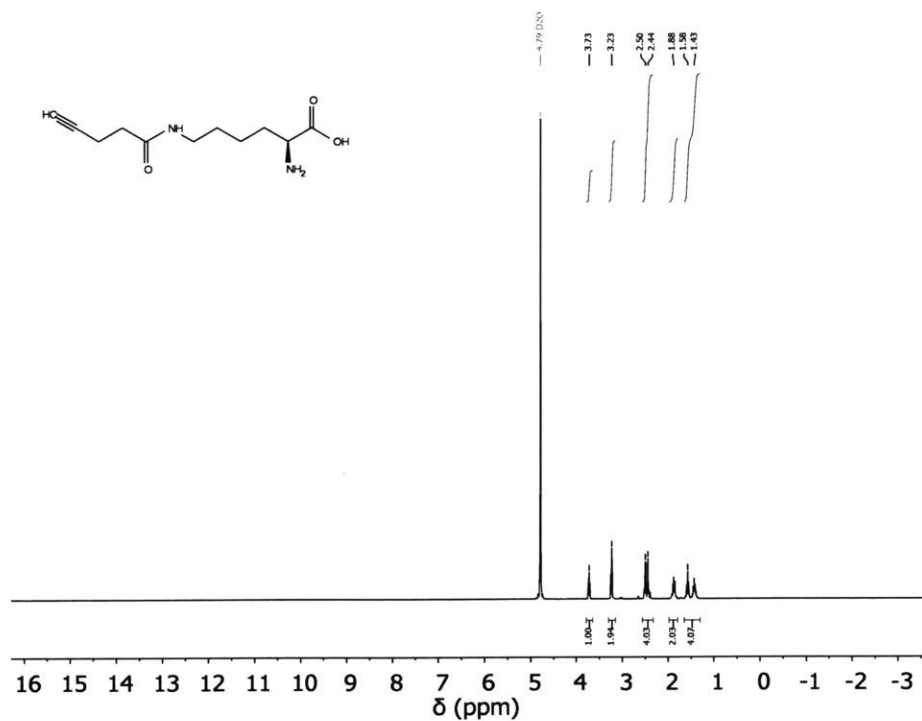
Figure 1.30. ^{1}H NMR spectrum of ε-6-Pentynoic-L-lysine in D$_2$O.
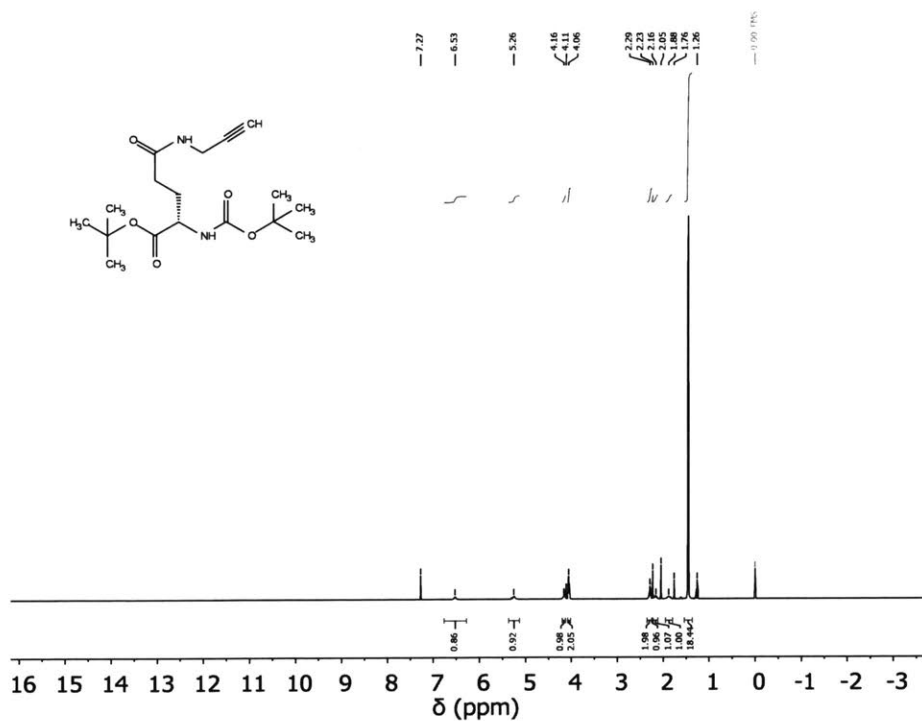
Figure 1.31. ^{1}H NMR spectrum of γ-Propargyl-Boc-L-Gln-OtBu in CDCl$_3$. Peaks at δ 4.11, 2.04, and 1.26 are from ethyl acetate.

47
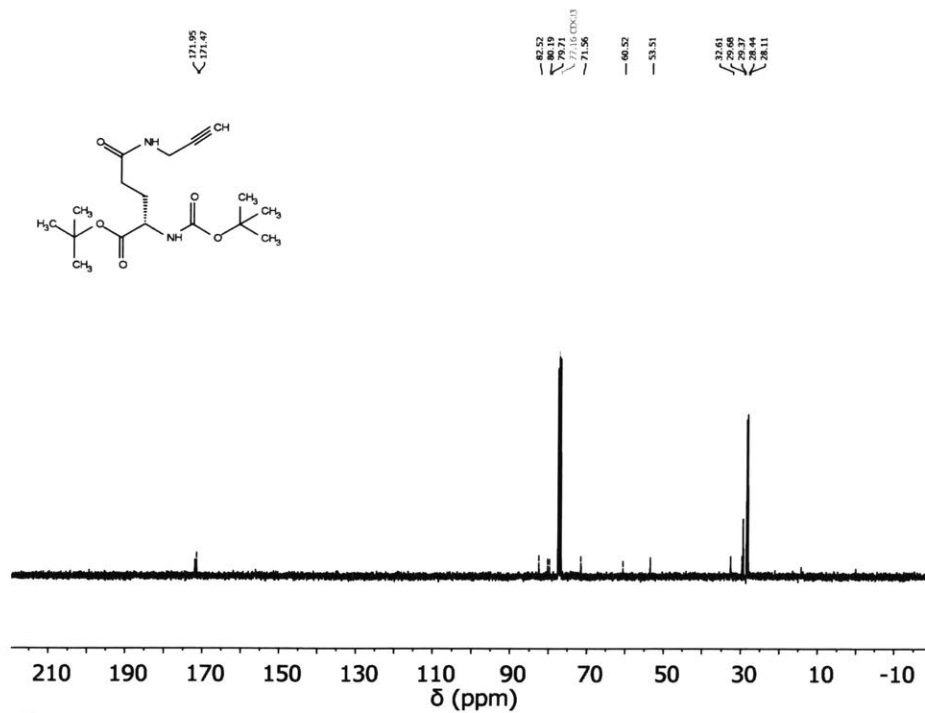
Figure 1.32. ^{13}C NMR spectrum of γ-Propargyl-Boc-L-Gln-OtBu CDCl₃.
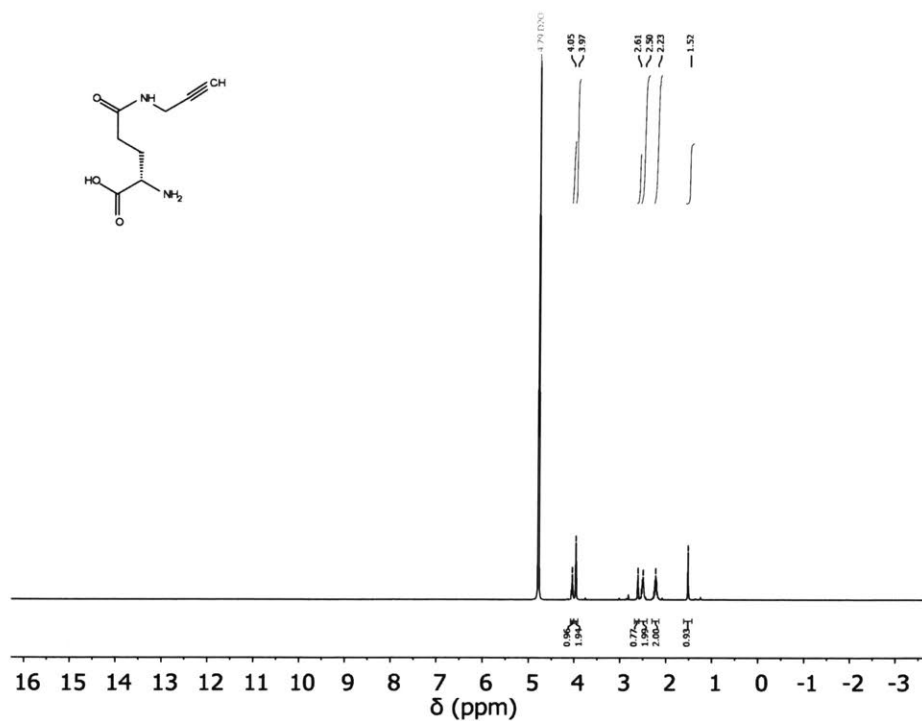
Figure 1.33. ^{1}H NMR spectrum of γ-Propargyl-L-glutamine in D₂O.

48
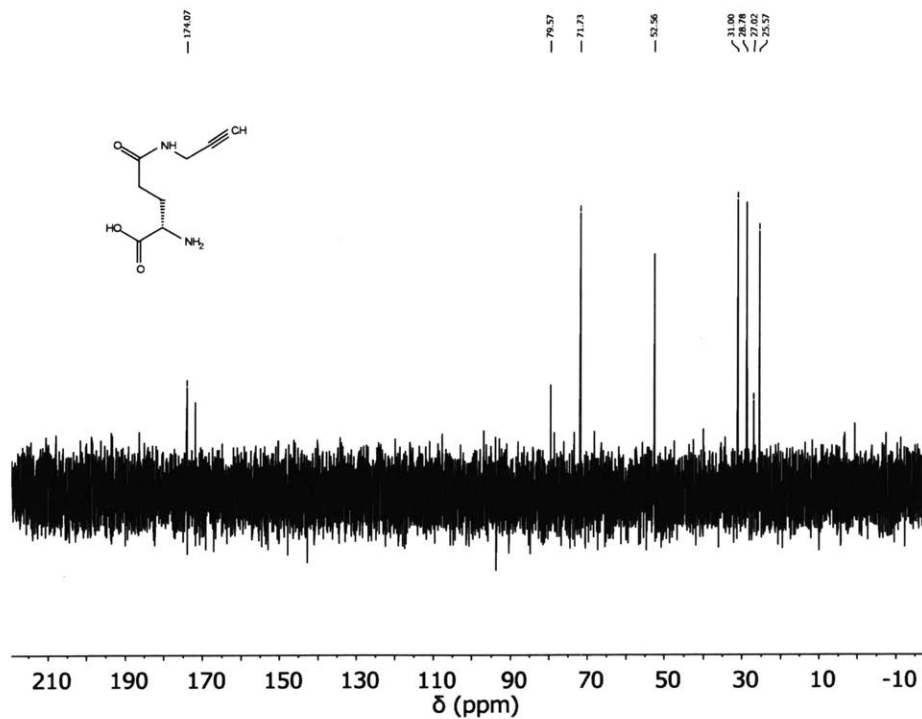
Figure 1.34. ^{13}C NMR spectrum of γ-Propargyl-L-glutamine in D$_2$O.
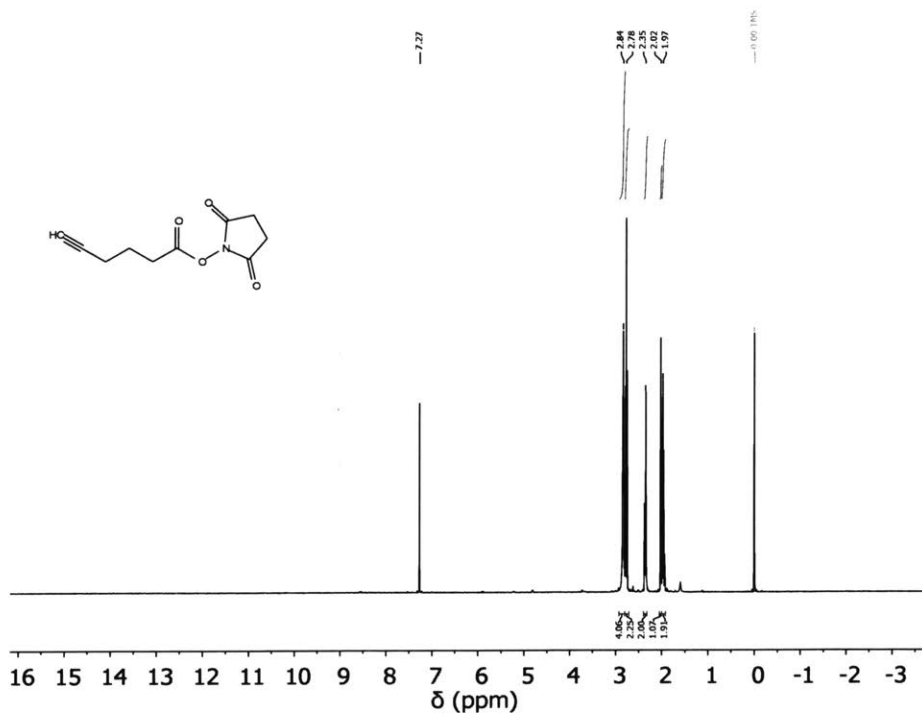
Figure 1.35. ^{1}H NMR spectrum of 5-Hexynoic acid N-hydroxysuccinimide ester in CDCl$_3$.

49
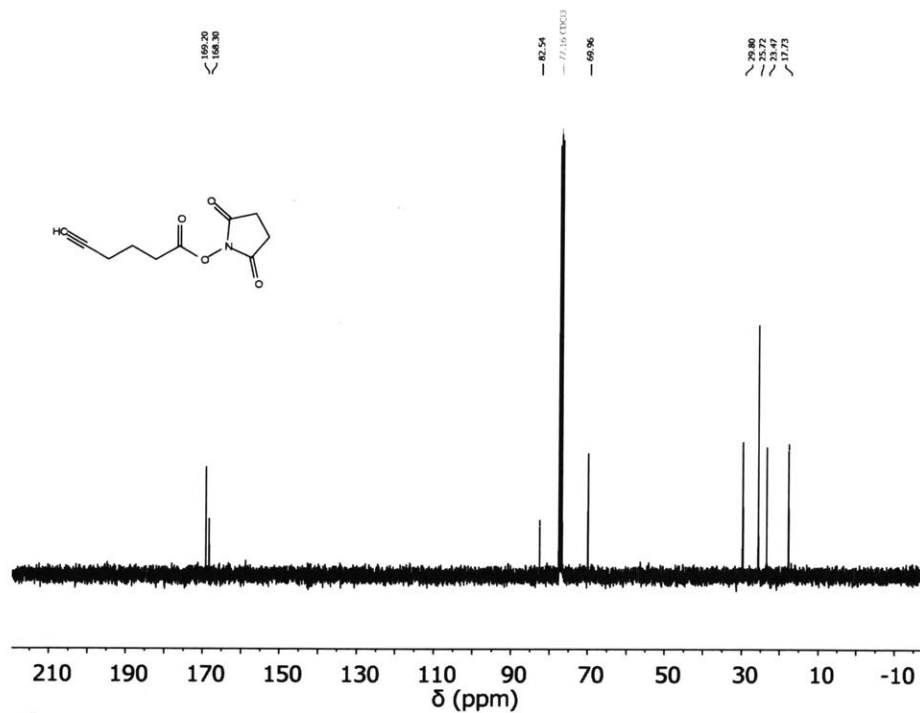
Figure 1.36. ^{13}C NMR spectrum of 5-Hexynoic acid N-hydroxysuccinimide ester in CDCl$_3$.
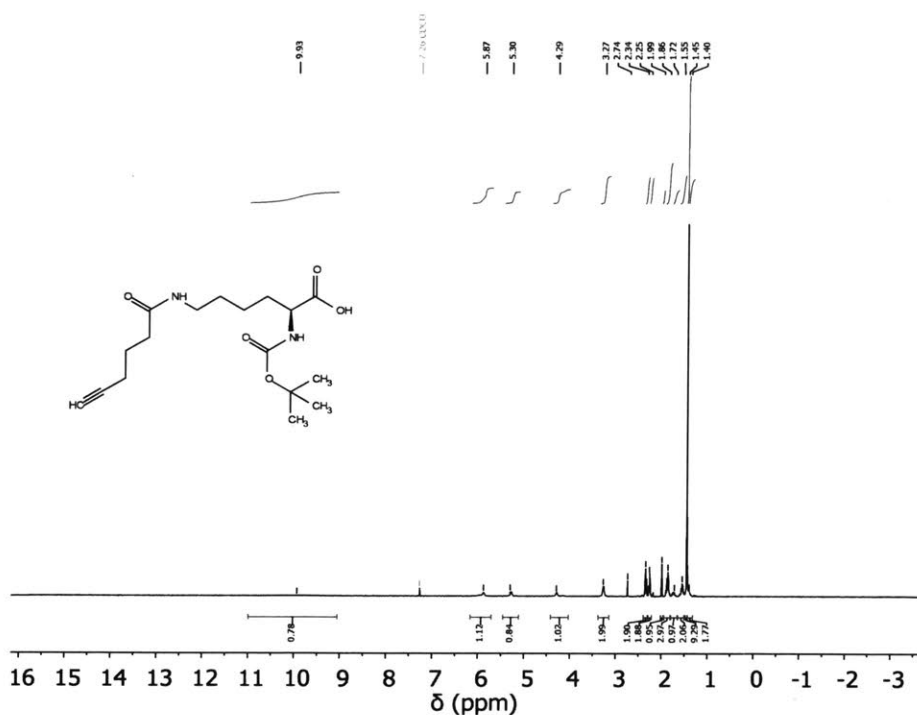
Figure 1.37. ^{1}H NMR spectrum of N$_\alpha$-Boc-N$_\epsilon$-5-hexynoic-L-lysine in CDCl$_3$. Peak at δ 2.74 is from hydroxysuccinimide.
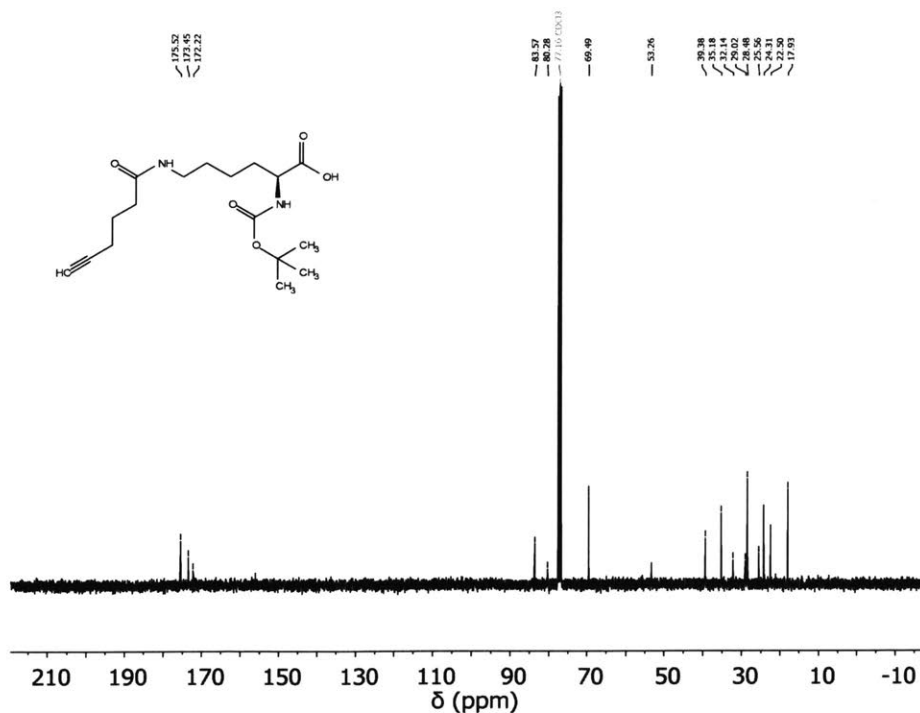
Figure 1.38. ^{13}C NMR spectrum of N_α-Boc-N_ε-5-hexynoic-L-lysine in CDCl$_3$. Peak at δ 25.56 is from hydroxysuccinimide.

3.5 References

(1) M. Vert, Y. Doi, K.-H. Hellwich, M. Hess, P. Hodge, P. Kubisa, M. Rinaudo, F. Schué, *Pure Appl. Chem.* **2012**, *84*, 377–410.

(2) Y. Liang, L. Li, R. A. Scott, K. L. Kiick, *Macromolecules* **2017**, *50*, 483–502.

(3) J. . Mano, G. . Silva, H. . Azevedo, P. . Malafaya, R. . Sousa, S. . Silva, L. . Boesel, J. . Oliveira, T. . Santos, A. . Marques, et al., *J. R. Soc. Interface* **2007**, *4*, 999–1030.

(4) C. K. S. Pillai, *Des. Monomers Polym.* **2010**, *13*, 87–121.

(5) T. J. Deming, *Chem. Rev.* **2016**, *116*, 786–808.

(6) M. A. Quadir, M. Martin, P. T. Hammond, *Chem. Mater.* **2014**, *26*, 461–476.

(7) M. A. Quadir, S. W. Morton, Z. J. Deng, K. E. Shopsowitz, R. P. Murphy, T. H. Epps, P. T. Hammond, *Mol. Pharm.* **2014**, *11*, 2420–2430.

(8) C. C. Ahrens, M. E. Welch, L. G. Griffith, P. T. Hammond, *Biomacromolecules* **2015**, *16*, 3774–3783.

(9) A. C. Engler, H. Lee, P. T. Hammond, *Angew. Chem. Int. Ed.* **2009**, *48*, 9334–9338.

(10) T. Borase, T. Ninjbadgar, A. Kapetanakis, S. Roche, R. O'Connor, C. Kerskens, A. Heise, D. F. Brougham, *Angew. Chem. Int. Ed.* **2013**, *52*, 3164–3167.

(11) J. Cao, P. Hu, L. Lu, B. A. Chan, B.-H. Luo, D. Zhang, *Polym. Chem.* **2015**, *6*, 1226–1229.

(12) P. Chen, C. Li, D. Liu, Z. Li, *Macromolecules* **2012**, *45*, 9579–9584.

(13) M. Nguyen, J.-L. Stigliani, G. Pratviel, C. Bonduelle, *Chem. Commun.* **2017**, *53*, 7501–7504.

(14) A. De Marre, H. Soyez, E. Schacht, J. Pytela, *Polymer* **1994**, *35*, 2443–2446.

(15) K. Ishikawa, T. Endo, *J. Am. Chem. Soc.* **1988**, *110*, 2016–2017.

(16) K. Ishikawa, T. Endo, *J. Polym. Sci. Part C Polym. Lett.* **1989**, *27*, 339–342.

(17) M. Barz, A. Duro-Castano, M. J. Vicent, *Polym. Chem.* **2013**, *4*, 2989–2994.

(18) F. Du, H. Meng, K. Xu, Y. Xu, P. Luo, Y. Luo, W. Lu, J. Huang, S. Liu, J. Yu, *Colloids Surf. B Biointerfaces* **2014**, *113*, 230–236.

(19) C. H. Kim, M. Kang, H. J. Kim, A. Chatterjee, P. G. Schultz, *Angew. Chem. Int. Ed.* **2012**, *51*, 7246–7249.

(20) W. H. Daly, D. Poché, *Tetrahedron Lett.* **1988**, *29*, 5859–5862.

(21) S. Mobashery, M. Johnston, *J. Org. Chem.* **1985**, *50*, 2200–2202.

(22) K.-S. Krannig, H. Schlaad, *J. Am. Chem. Soc.* **2012**, *134*, 18542–18545.

(23) M. F. Jung, M. A. Lyster, *J. Am. Chem. Soc.* **1977**, *99*, 968–969.

(24) G. Subramanian, R. P. Hjelm, T. J. Deming, G. S. Smith, Y. Li, C. R. Safinya, *J. Am. Chem. Soc.* **2000**, *122*, 26–34.

(25) G. J. M. Habraken, K. H. R. M. Wilsens, C. E. Koning, A. Heise, *Polym. Chem.* **2011**, *2*, 1322.

(26) T. P. Creamer, M. N. Campbell, in *Adv. Protein Chem.*, Academic Press, **2002**, pp. 263–282.

(27) B. D. Fairbanks, M. P. Schwartz, C. N. Bowman, K. S. Anseth, *Biomaterials* **2009**, *30*, 6702–6707.

(28) B. J. J. Timmer, M. A. Flos, L. M. Jørgensen, D. Proverbio, S. Altun, O. Ramström, T. Aastrup, S. P. Vincent, *Chem. Commun.* **2016**, *52*, 12326–12329.

Chapter 2: Biological activity of synthetic polypeptide-hyaluronan conjugates

2.1 Introduction

Proteoglycans, proteins grafted with glycans, are prevalent in biological systems. These molecules have diverse functionalities ranging from inert space filling matrix to signaling molecules.[1] Due to the ubiquitous nature of these materials they continue to garner interest in a variety of fields from applications within tissue engineering to understanding their impact and role in a biological system. Despite this interest, research on proteoglycans has been hampered by inadequate supplies of purified proteoglycans, which are notoriously difficult to isolate while maintaining their natural form and activity.[2] One potential alternative to isolating proteoglycans is the production of synthetic analogues. Some synthetic analogs of these glycopeptides aim to recapitulate the physiochemical properties of their natural analogues by incorporating a high density of charged functional groups on a polymer backbone. While this approach has generated interesting materials with useful applications in biomedical engineering[3], these materials are limited in their interaction with biological systems and often only play the role of inert fillers. A more versatile mimic of the natural proteoglycans would also illicit biological responses by binding to cell surface receptors or other molecules through a faithful presentation of native structures.

Natural proteoglycans contain a protein core grafted with glycosaminoglycans. Synthesis of a proteoglycan mimic has been accomplished by polymerization of a glycan modified N-carboxyanhydride monomer[4,5] and by a grafting-to strategy.[6-10] However, current approaches suffer from two main limitations: 1) they are limited in the molecular weight of the glycan, commonly employing mono or di-saccharides, representing only a fraction of natural proteoglycans. Grafting polymer backbones with higher molecular weight glycans is more challenging and the applications and behavior of such synthetic conjugates are not well explored. 2) The core of these polymers are rarely peptides or proteins and may not reproduce the conformation range and biocompatibility of their natural counterparts. To make a more faithful synthetic analogue, an easily modified and well-defined polypeptide is necessary. One promising backbone is poly(γ-propargyl-L-glutamine) (PPLQ), a polypeptide with side chain propargyl groups enabling modification by azide alkyne cycloaddition "click" chemistry.[11] PPLQ is synthesized by N-carboxyanhydride polymerization followed by post polymerization modification, enabling access to a wide range of tightly controlled molecular weights.

Hyaluronic acid (HA) is a ubiquitous and biologically relevant negatively charged glycan that forms a common component of the extracellular matrix (ECM). Beyond its structural contributions, HA also binds cells directly and can associate with growth factors to regulate cellular activity. The nature of these interactions are largely dependent on the molecular weight of HA. High molecular weight HA is known to be antimitogenic and play the role of a matrix that can bind and retain growth factors generated by cells. Low molecular weight HA has been shown to provoke inflammatory responses that release cytokines which induce angiogenesis, and cell proliferation.[12,13] Cellular response to HA is dependent on the interaction of HA with a multitude of cell surface receptors, the two most extensively studied being CD44, which is involved in adhesive interactions and migration, and CD168 also known as RHAMM, a receptor that modulates wound healing and cell migration. Both receptors are commonly studied on cancer and endothelial cells.[14] Though the influence of HA CD168 binding on signaling pathways is still unclear, it has been established that high molecular weight HA binds to CD44, resulting in the receptor clustering that is necessary to induce signaling and upregulation of associated pathways for cell adhesion and migration.[14] On the other hand, low molecular weight or oligomeric HA binds to the receptors but is too small to induce clustering and actively interferes with receptor clustering by blocking interactions with other matrix molecules.[13,15] Given the multivalent nature of a densely-grafted polymer backbone, grafting HA to PPLQ may change the cellular response to the HA.

Here we create synthetic glycopeptides from a PPLQ based polypeptide scaffold and characterize the biological activity of synthetic HA glycopeptides made by this method against HA of various molecular weights. To better control the synthesis and aid characterization of the conjugates, we sacrifice sheer size for more defined architectures in this first study. Thus, the conjugates presented are not intended to exactly emulate very high molecular weight proteoglycans such as aggrecan, though crosslinking of these conjugates is a potential method to generate higher molecular weight but less defined variants.

2.2 Results and discussion

To evaluate the biological activity of PPLQ-g-HA, we sought to compare the performance of PPLQ-HA conjugates to unmodified high and low molecular weight HA in various assays where the influence of HA has been previously studied. Oligomeric as well as high molecular weight HA is known to play an important role in cancer progression and angiogenesis. Therefore, we focused our characterization of PPLQ-HA conjugates on these characteristics as observed in endothelial and cancer cell lines. As a final proof of concept study we also incorporated the conjugates into a synthetic ECM for tissue engineering applications.

Synthesis and Characterization

PPLQ-HA conjugates were synthesized by a grafting-to strategy. The appropriately sized glycans were obtained by enzymatic digestion of high molecular weight HA with bovine testicular hyaluronidase. Oligomeric HA obtained by this method is not monodisperse but elicits a biological response similar to more defined samples.[16] Afterwards, the glycans were functionalized with an azide by reductive amination of the reducing end. This approach avoids altering the natural structure of HA which may decrease its binding to cell surface receptors and diminish its biological activity.[17] Moreover, the presence of only one reducing end per polysaccharide, as well as uniform placement of the azide group on each glycan, enables greater control over the architecture of the final conjugate.

The azide modified HA was grafted to PPLQ using standard copper catalyzed azide alkyne cycloaddition protocols (Figure S1). Any unreacted glycans or other small molecules were removed by dialysis against deionized water across a 50 kDa regenerated cellulose membrane. After screening a range of solvents as well as copper ligands, the maximum grafting density of low molecular weight HA on PPLQ was determined to be approximately 25% by NMR analysis (Figure S2,3). For comparison, uncharged polymers such as poly(ethylene glycol) may be grafted on PPLQ at a density of over 90%.[11] This difference is likely caused by both steric and electrostatic repulsion of free negatively charged HA from the polypeptide core by the grafted HA brush. Depending on the secondary structure of PPLQ, the grafting density may be translated to one HA graft per 0.4 – 3.0 nm of peptide. Despite incomplete grafting, the grafting density is similar to or surpasses what is observed in natural proteoglycans such as aggrecan, where there is one glycosaminoglycan side chain per 2.5-5.0 nm of core protein.[18]

To survey the design landscape, we focused on testing four distinct PPLQ-glycan conjugates of different architecture, each one near the limit of synthetic accessibility. These conjugates were synthesized by grafting either high ("P") or low ("p") molecular weight PPLQ with either high ("G") or low ("g") molecular weight glycans and may be enumerated as "PG", "Pg", "pG", or "pg". The molecular weight of PPLQ was constrained by what was readily obtainable through standard, uncatalyzed N-carboxyanhydride polymerization initiated by a primary amine. In this initial study, "p" is 7 kDa and "P" is 29 kDa. These molecular weights were selected to maximize control over the polymers while maintaining simplicity in the synthesis, and while these polymers are smaller than common biological proteoglycans, higher molecular weight PPLQ may be synthesized by other N-carboxyanhydride polymerization methods such as use of transition metal catalysts[19] or different initiators.[20,21] The molecular weight of "G" is 8 kDa, which is approximately the upper bound. Higher molecular weight HA is difficult to graft to PPLQ due to solubility issues, decreased concentration of the reducing end, and increased steric bulk of the polymer. On the other hand, digestion time limits the lower bound as exponentially more cleavage reactions must occur to produce lower and lower molecular weight HA. Lower molecular weight polymers are also more difficult to isolate by common purification methods such as precipitation or dialysis. For these reasons, HA of 1 kDa was selected as "g". HA of this molecular weight may not occupy the entire binding pocket of certain HA receptors.[22] For 25% grafting of PPLQ, the theoretical molecular weights for these polymers are as follows: "PG" 379 kDa, "Pg" 73 kDa, "pG" 87 kDa, and "pg" 17 kDa (Figure 2.1).
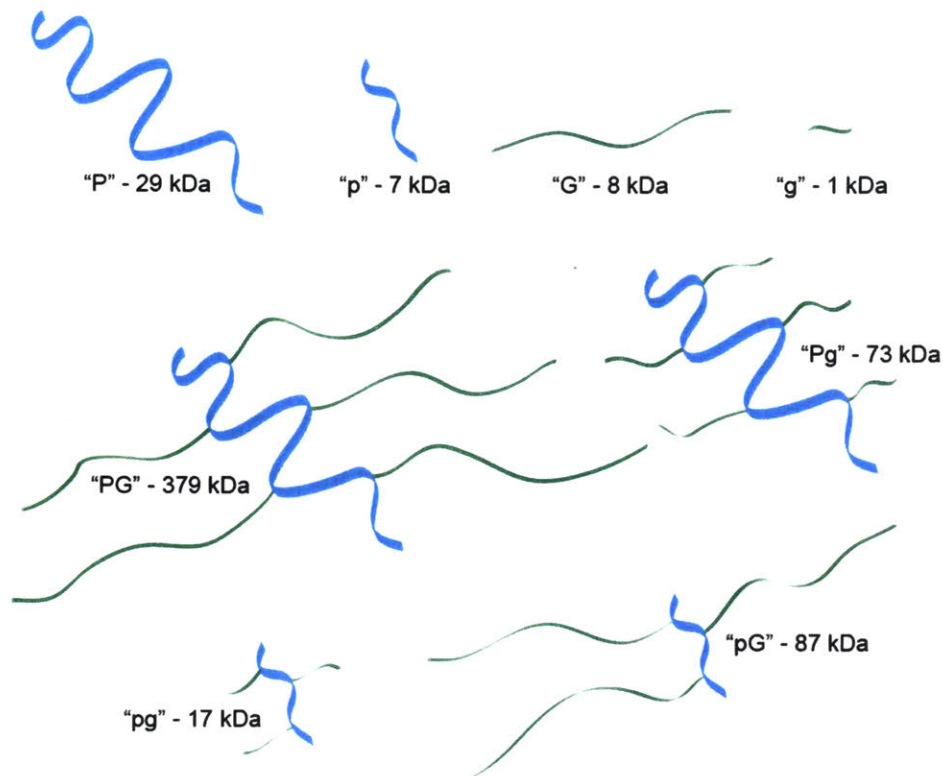
Figure 2.1. Cartoon representation of different architectures of PPLQ-HA conjugates.

Interaction with anchorage independent cancer cells

Normal epithelial cells are dependent upon attachment to the ECM for survival, but many tumor cells lose this dependence and become anchorage independent. HA is known to influence tumor cell anchorage independence in complex ways. Detachment of tumor cells results in inappropriate or inadequate cell-matrix interactions and results in apoptosis. Some cancer cells are surrounded by self-secreted HA, compensating for otherwise lost interactions, and manipulation of HA synthesis or receptor binding affects the ability of cancer cells to grow under anchorage independent conditions.[23–25] Alternatively, oligomeric HA has been shown to induce cell death by apoptosis through disruption of signaling. To parse the differential effects of PPLQ-HA conjugates and compare them with native HA of various molecular weights, we began by testing the apoptotic response of anchorage independent HCT116 human colorectal carcinoma cells. Previously, oligomeric HA has been shown to induce apoptosis in HCT116 (human colorectal carcinoma) cells growing in soft agar or suspension culture.[26,27]

Apoptosis was assessed by phosphatidylserine translocation across the cell membrane as measured by a fluorescent Annexin V conjugate and Caspase 3 activation as measured by cleavage of a fluorescently labeled substrate. While these events are related and both are commonly used as markers for apoptosis, they may indicate a different stage of apoptosis. Furthermore, apoptosis can occur independent of caspase activation and the degree of phosphatidylserine membrane asymmetry may be confounded by other factors.[28-32] Thus measurement of both markers may give further insight into the interaction of PPLQ-HA conjugates with cells.

Low and high molecular weight PPLQ grafted with low molecular weight HA (Pg & pg) elicited a greater degree of Annexin V binding in live cells (Figure 2.2a) with no differences in dead cells (Figure 2.10), suggesting that these conjugates promote a late-stage apoptosis phenotype or initiate apoptosis by a different mechanism. PPLQ-HA conjugates showed similar activation of caspase 3 with the exception of the smallest conjugate (pg) (Figure 2.2b). There is a significant difference in the molecular weight of the smallest conjugate relative to the molecular weight differential between the other conjugates, which may explain the large difference in caspase 3 activation. Likewise, the lowest molecular weight HA showed low caspase 3 activity, possibly due to being too small to interact with the required receptors.[22] Similarly, a short glycan grafted to low molecular weight PPLQ (pg) may not be recognized by cell surface receptors. The relatively weaker interaction of shorter glycans with HA receptors may be rescued by the multivalent display of a higher molecular weight polymer (Pg). This effect is less apparent for higher molecular weight HA that is independently capable of eliciting a response (pG and PG).
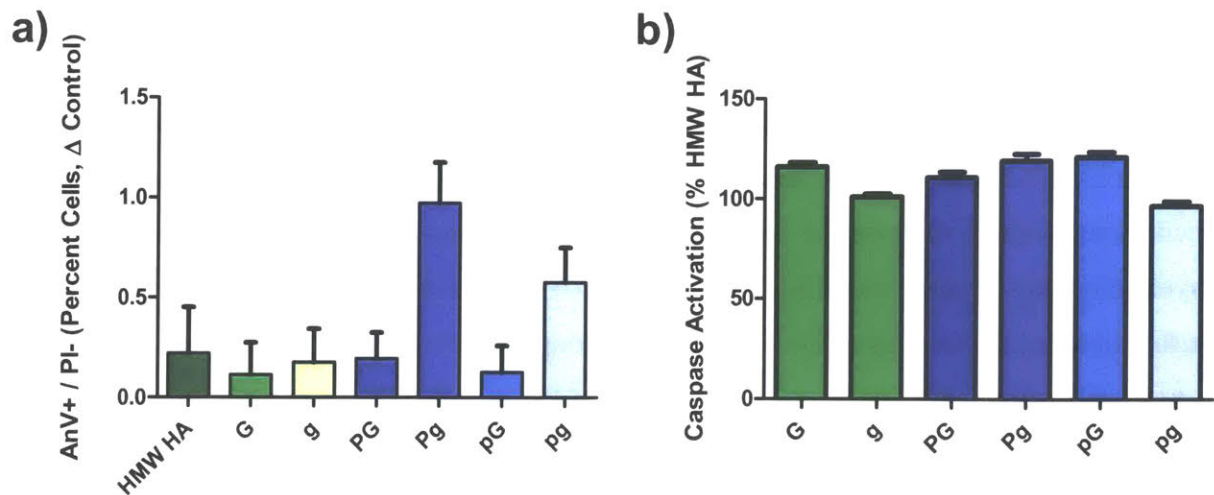
Figure 2.2 (a) Annexin V positive, propidium iodide negative cells as determined by flow cytometry expressed as difference from no treatment control. P < 0.05 for Pg vs. all treatments except pg (b) Caspase 3 response to HA or PPLQ-HA conjugates in HCT116 cells under anchorage independent conditions expressed as a percentage of HMW HA. P < 0.05 for G vs. g, g vs. Pg/pG, pg vs. G/PG/Pg/pG.

To further compare the mechanism of caspase 3 activation by HA and PPLQ-HA conjugates, we probed potential signaling pathways involved in cellular interaction with HA. The activation of caspase 3 in HCT116 cells growing under anchorage independent conditions has been attributed to a decrease in AKT phosphorylation.[26] AKT is involved in signaling pathways that lead to cell survival, growth, and proliferation. Unsurprisingly, AKT is commonly upregulated in cancer. Previously, HA oligomers have been shown to inhibit phosphatidylinositol 3-kinase (PI3K) activity in cancer cells growing under anchorage independent conditions.[26] PI3K generates a secondary messenger, phosphatidylinositol 3,4,5-trisphosphate, resulting in translocation of AKT to the cellular membrane where it is then phosphorylated. Upon activation, AKT protects a cell from apoptosis by influencing many proteins involved in cell death.[33]

Because treatment of anchorage independent HCT116 cells with PPLQ-HA conjugates results in a greater degree of caspase activation, we hypothesized a lesser degree of AKT phosphorylation. Indeed, PPLQ-HA conjugates reduce AKT phosphorylation at Thr308 (Figure 2.3) in these conditions as determined by ELISA. However, PPLQ-HA conjugates reduce phosphorylation to a

greater degree than oligomeric HA despite comparable caspase activation, indicating there may be other signaling pathways at play in the control of caspase 3 dependent apoptosis. Phosphorylation of AKT at Ser473 does not depict the same trend as phosphorylation at Thr308 (Show this in SI). While both phosphorylation events regulate the activity of AKT, they result in different downstream signaling. Literature suggests that phosphorylation of Thr308 correlates well with AKT activity in tumors.[34] The caspase 3 activity is not fully accounted for by the attenuation of AKT signaling, indicating there may be other pathways involved in the signal transduction of PPLQ-HA conjugates.
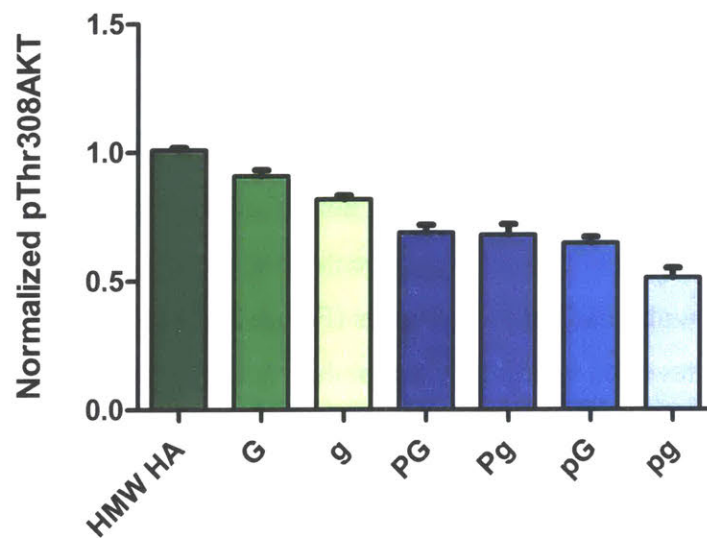
Figure 2.3. AKT activation by phosphorylation at the Thr308 position in response to HA or PPLQ-HA conjugates in HCT116 cells under anchorage independent conditions expressed as a percentage of total AKT relative to a no treatment control. All means are statistically different (P < 0.05) with the exception of PG vs. Pg, PG vs. pG, and Pg vs pG.

Cellular migration

Cellular migration is an important biological process in both cancer and wound healing. High molecular weight HA has been shown to augment integrin signaling[35], which plays a central role in cellular migration.[36] Oligomeric HA is known to weaken high affinity and multivalent interactions between high molecular weight HA and its receptors, and we next wanted to test for any interference by PPLQ-HA conjugates with these interactions. Grafting oligomeric HA onto

PPLQ may increase its interaction with receptors by a multivalent effect, making it a stronger competitor against native HA, but without sufficient receptor clustering to elicit the effects of native HA.

To probe these effects, we utilized a migration assay with of human ovarian adenocarcinoma (SKOV3) and human induced pluripotent stem cell-derived endothelial cells (iPS-ECs). As expected, PPLQ-HA conjugates did impact cellular migration. Migration of SKOV3 cells and iPS-ECs was slowed by PPLQ-HA conjugates relative to both no treatment and treatments with HA. In contrast, the native free HA resulted in small to moderate enhancements in cell migration for endothelial cells, an effect that has been observed in the past in wound healing studies. Native HA results in little or no changes in proliferative behavior for the SKOV3 cancer cells, which may already exhibit highly mitogenic behavior (Figures 2.4, 2.13, 2.14). Likewise, another ovarian cancer cell line, OVCAR8, was not affected by any treatment (Figure 2.14). Migration of iPS-ECs in growth media supplemented with serum or growth factors is not affected by treatment with PPLQ-HA conjugates (Figure 2.15) indicating that the disruption of HA signaling may be reversed by mitogenic stimulus. A similar result was found when examining the proliferation of these cells (Figure 2.16). All PPLQ conjugates yield notably lower cell migration, though there is no clear trend of cellular response among the 4 different PPLQ-HA conjugate architecture for both cell lines.
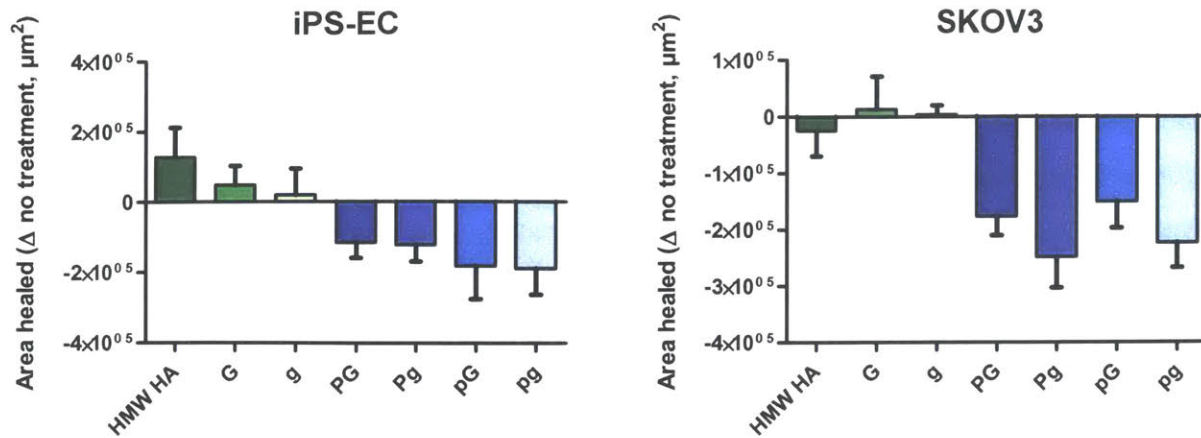
Figure 2.4. Migration of iPS-ECs (endothelial) and SK-OV-3 (cancer) cells in low serum conditions is impaired by PPLQ-g-HA, in contrast to improvements in proliferation found with native HA treatments. In SKOV3, P < 0.05 for HMW HA vs. Pg, G/g vs. Pg/pg. In iPS-EC, P < 0.05 for HMW HA vs. pg/pG.

Synthetic ECM for three-dimensional (3D) vasculogenesis

An important aspect of the synthetic capabilities introduced with the unique backbone of PPLQ-glycan conjugates is the ability to incorporate these modified HA presenting polypeptides directly into crosslinked hydrogels, thus providing a grafted scaffold of fixed matrix molecules, much like what may be presented in the native ECM. Vasculogenesis, defined here as the formation of endothelial networks from isolated endothelial cells, is a complex process resulting from a combination of soluble signals, cell-cell and cell-matrix interactions that drive endothelial cell proliferation, migration, proteolytic degradation, and matrix deposition in the formation of new vascular networks.[37–41] Differences in these fundamental cell behaviors between 2D and 3D culture have been well appreciated across several *in vitro* biological systems.[42,43] Furthermore, altered cell signaling has been observed when comparing growth factors delivered as soluble cues with the same growth factors tethered to an extracellular matrix.[44–46] HA has been suggested to promote vascular morphogenesis by stimulating proliferation and migration, as well as inducing protease activity mediating the invasion of endothelial cells into the surrounding matrix environment.[14,47,48] In addition to active roles in modulating endothelial cell signaling, HA as an ECM component plays a role in regulating vascular network formation through changes in the biophysical environment and sequestration and release of vasculogenic growth factors.[49,50]

To investigate the utility of controlled HA presentation in regulating vasculogenesis, 3D hydrogels were synthesized by combining multi-arm norbornene-functionalized PEG macromers with norbornene-functionalized PPLQ, generating a synthetic matrix in which PPLQ conjugates are covalently incorporated into the ECM structure along with integrin binding motifs. The incorporation of HA-grafted PPLQ conjugate (Pg) within the matrix induced a marked improvement in vasculogenesis, supporting the formation of more extensive tubule structures with larger diameters compared to the PEG-grafted PPLQ control. Notably, the presence of soluble HA (g) at equivalent MW and concentration to the HA presented in "Pg" hydrogels strongly inhibited vasculogenesis in control gels. This effect is not observed for the larger oligomeric HA (G). Larger oligomeric HA grafted PPLQ (PG) did not significantly increase overall network length above control gels, but increased the thickness of individual tubule structures similarly to "Pg" gels. (Figure 2.5).

Context dependency in endothelial cell response to HA conjugates is apparent, as soluble conjugates delivered to cells in traditional 2D assays lead to a reduction in migration. Similarly, small soluble oligomeric HA strongly inhibited endothelial network formation in a 3D matrix. In contrast, it is clear that the tethered presentation of HA fragments at the same MW and concentration enhances endothelial network formation when bound in synthetic 3D environments. This enhancement could be derived from changes in the biophysical environment, HA-mediated cell signaling processes, or a combination of the two. Previous work suggests a role for β_1 integrin interactions with CD44 (a primary HA cell surface receptor) in vascular network formation, and soluble HA has also been shown to interfere with CD44-dependent activation of β_1 integrin.[51-53] It is possible that soluble low MW oligomeric HA (g) leads to receptor internalization of CD44, β_1 integrin, or both, preventing them from performing functions integral to vascular morphogenesis. The multifaceted role of HA in mediating vascular morphogenesis is complex and dependent upon multiple factors including the MW, cell surface receptor interactions, internalization and subsequent metabolism, making it difficult to attribute these results to any specific molecular mechanism. A thorough investigation of HA-mediated signaling in these engineered 3D hydrogel environments is beyond the scope of this work; however, further experiments in this area may

clarify the signal transduction mechanisms that underlie the morphological differences in this initial demonstration.
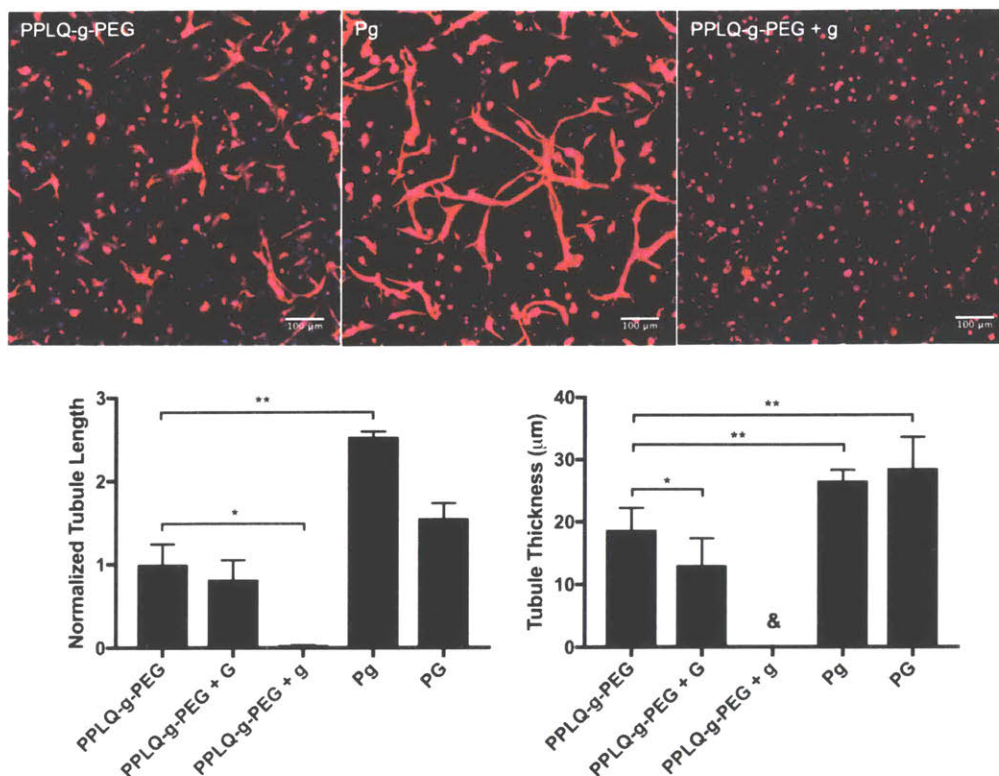

Figure 2.5. Hydrogels containing covalently incorporated PPLQ-HA conjugates and PEG-functionalized with PHSRN-K-RGD promote formation of endothelial networks in 3D, highlighted by nuclei (blue) and f-actin (red) staining after 2 days in culture. In contrast, treatment with an equal concentration of exogenous soluble HA inhibits vascular network formation in control (synKRGD functional PPLQ-g-PEG) gels. Representative maximum intensity projections (400 μm depth) and quantification of length (normalized to control gels) and diameter of tubule structures are shown. (&) PPLQ-g-PEG with soluble 'g' exhibited no quantifiable network formation, so tubule thickness could not be computed. (* $p < 0.05$, ** $p < 0.01$).

2.3 Conclusion

PPLQ-HA conjugates, regardless of size and architecture, are not perceived by cells in the same manner as either high or low molecular weight HA. In addition, linking low molecular weight HA chains through PPLQ does not produce a higher molecular weight HA, but rather a more potent

low molecular HA. This is evident in assays evaluating anchorage independent growth and cellular migration, where PPLQ-HA conjugates appear to block binding of high molecular weight HA much more effectively than oligomeric HA, but yet does not elicit the same effect as high molecular weight HA. The cellular response to PPLQ-HA conjugates is also not similar to literature studies of immobilized HA.[54] When incorporated into a hydrogel, these conjugates continue to exhibit activity differing from soluble low molecular weight HA. PPLQ-HA conjugates may produce a unique profile of receptor clustering and integrin interaction, resulting in cellular responses different from native HA. PPLQ-HA conjugates represent a biopolymer created with natural biological components and while not a mimic of endogenous HA, they have unique biological activity. These conjugates may be applied in cancer treatments or tissue engineering, and the interaction of these conjugates with biological systems may be extrapolated to develop other PPLQ conjugate platforms.

2.4 Experimental

PPLQ was synthesized as previously described by post polymerization functionalization of poly(glutamic acid).[11] High molecular weight HA was obtained from Carbosynth. N-Acetyl-Asp-Glu-Val-Asp p-nitroanilide (Ac-DEVD-pNA) was obtained from Alfa Aesar. Regenerated cellulose dialysis membrane was obtained from Spectrum Labs. All other reagents and materials were purchased from Sigma-Aldrich and used as received.

^{1}H and ^{13}C NMR spectra were obtained in $CDCl_3$, $(CD_3)_2SO$, or D_2O (Cambridge Isotope Laboratories) using a Bruker Avance 400 MHz NMR spectrometer at 25 °C. Gel permeation chromatography (GPC) measurements in DMF with 10 mM LiBr were carried out using a Waters 1525 binary pump system equipped with two Polypore columns operated at 75 °C, series 2414 refractive index detector, and 717plus autosampler. Waters Breeze Chromatography Software Version 3.30 was used for data collection as well as data processing. The instrument was calibrated against narrow molecular weight poly(methyl methacrylate) standards. Aqueous Gel Permeation Chromatography (GPC) was performed with a sample concentration of 1-5 mg/mL and eluted by a 100 mM sodium nitrate, 10 mM phosphate buffer with 20% v/v methanol at 35 °C pH 7.4 on a Viscotek GPCmax VE-2001 system equipped with a PL aquagel-OH column, Smartline 2600 UV detector, and VE-3580 RI detector calibrated with monodisperse poly(ethylene oxide) standards.

General method for HA functionalization

To a solution of HA (4.0 g) in digestion buffer consisting of 150 mM NaCl, 100 mM acetate, 1 mM EDTA, and pH 5.0 (200 mL) was added bovine testicular hyaluronidase 400-1000 U/mg (80 mg). The solution was mixed by shaking and incubated at 37 °C until the desired molecular weight was reached. Afterwards the solution was boiled for 10 minutes, centrifuged to precipitate protein, filtered, dialyzed against deionized water through a 100-500 Da cellulose ester membrane, frozen, and lyophilized. Molecular weight was determined by Reissig assay[55] and NMR. The Reissig assay was performed on aliquots containing a known mass of HA. NMR analysis was done in deuterium oxide following boiling, dialysis, and lyophilization. The acetyl peak was compared to the anomeric hydrogen peak of the α-anomer (δ 5.2 ppm) for molecular weight determination taking into account a 65 to 35 ratio of the β to α anomer.[56]

The digested HA was dissolved in 1 M borate buffer at pH 8.5 (50 mL) with stirring. PEG azide amine (1.5 g, 6.9 mmol) and 1 M HCl (6.9 mL) were added dropwise. Sodium cyanoborohydride (1.2 g, 19 mmol) was added portion wise over 2 minutes. After foaming subsided, the solution was heated to 65 °C and stirred for 24 hours. The reaction was then allowed to cool and the product was precipitated by addition of ethanol and collected by centrifugation. The solid was dissolved in water, dialyzed against deionized water using a 100-500 Da MWCO cellulose ester membrane, frozen, and lyophilized to yield a white solid.

HA was converted to the tetrabutylammonium salt to improve solubility in organic solutions. For this process, HA was dissolved in water and acidified with Amberlite IR120 strongly acidic, hydrogen form resin to pH 1. The resin was removed by filtration and the pH of the solution was adjusted to 7 by dropwise addition of 10 wt% tetrabutylammonium hydroxide with stirring. The solution was frozen and lyophilized to yield a white solid.

General method for synthesis of PPLQ-HA conjugates

A solution of PPLQ (100 mg) in DMF (4 mL) was mixed with a solution of previously functionalized HA (750 mg) and bathophenanthrolinedisulfonic acid disodium salt hydrate (55 mg) in water (4 mL). The turbid solution was sparged for 45 minutes with argon after which copper (I) bromide (10 mg) was added. The reaction vessel was sealed and stirred for 12 hours after which sodium ascorbate (50 mg) and a 50 vol % aqueous solution of DMSO (10 mL) was added. The

reaction vessel was then sealed and stirred for 5 days. Afterwards, the solution was dialyzed against aqueous 5 mM EDTA followed by DI water using a 50 kDa MWCO regenerated cellulose membrane. The remaining solids were removed by centrifugation followed by filtration and the solution was frozen and lyophilized to yield a white solid.

General method for synthesis of PPLQ-HA conjugates with norbornene

To a solution of Norbornene-NHS (35 mg, 0.15 mmol) in *t*-butanol (1 mL) was added the azide amine ethylene glycol linker (25 μL, 0.13 mmol) and DIPEA (44 μL, 0.25 mmol). The reaction was stirred at room temperature for 4 hours and then added to a solution of PPLQ-HA (50 mg), THPTA (12 mg, 0.027 mmol), and copper (II) sulfate pentahydrate (2 mg, 0.008 mmol) in water (8 mL). To this mixture was added sodium ascorbate (50 mg, 25 mmol). The reaction vessel was sealed and left at room temperature for 24 hours. Afterwards, copper was removed by addition of 5 mL of Dowex M4195 resin, the resin was removed by filtration, and the solution was dialyzed against deionized water across a 1 kDa MWCO regenerated cellulose membrane. Lyophilization gave a white solid.

Cell culture

SKOV3 human carcinoma cells were obtained from American Type Culture Collection and cultured in RPMI 1640 (Invitrogen) with 10% fetal bovine serum and 1% penicillin/streptomycin (Thermo Fisher Scientific). OVCAR8 cells were a gift from S. Bhatia (MIT) and cultured in DMEM (Invitrogen) with 10% fetal bovine serum and 1% penicillin/streptomycin (Thermo Fisher Scientific). Human induced pluripotent stem cell-derived endothelial cells (iPS-ECs) were obtained from Cellular Dynamics International and cultured fibronectin (Corning 356008) coated surfaces in VascuLife growth medium purchased through Lifeline Cell Technology (Frederick, MD) and supplemented with iCell endothelial cell media supplement in place of recommended fetal bovine serum purchased through Cellular Dynamics International. The basal media contains recombinant growth factors (VEGF, FGF, EGF, IGF) to support vasculogenesis, and was additionally supplemented with 1% penicillin/streptomycin (Thermo Fisher Scientific). All cells were incubated in a 37C, 5% CO_2 environment.

Anchorage independent growth

HCT116 cells were harvested by trypsinization and 24 million cells were seeded in 100 mm low adhesion petri dishes (Corning 3262) at a density of 4 million cells per milliliter of DMEM + 10% FBS. The cells were incubated for 72 h, after which they were collected by centrifugation, washed with PBS, and resuspended in 6 mL of DMEM + 2% BSA. The cells were incubated for 24 h before addition of HA or PPLQ-HA conjugates in PBS to a final concentration of 50 μg/mL. The treated cells were incubated for another 24 h and harvested by centrifugation. The cell pellet was washed twice with PBS and lysed by addition of lysis buffer with PMSF (Cell Signaling Technologies 9803S, 553S) followed by vortexing for 20 s. The lysate was centrifuged at 6 x g for 5 minutes and the protein content was evaluated by BCA assay (Thermo 23225). The protein concentration of each sample was normalized by addition of lysis buffer for further analysis of caspase 3 and intracellular signaling activity.

Caspase 3 assay

Caspase activity in 50 μL of cell lysate containing approximately 200 μg protein was determined by incubation with Ac-DEVD-pNA (0.2 mM) in 50 μL of assay buffer (20 mM HEPES, pH 7.4, 4 mM EDTA, 20 mM DTT, 0.2% CHAPS) at room temperature overnight in a 96-well clear polystyrene plate. Absorbance at 405 nm was measured by plate reader.

Enzyme Immunoassay

Enzyme immunoassay was performed according to included protocol for sandwich ELISA antibody pairs (Cell Signaling Technologies 7142, 7143, 7144, 7246) with minor modifications. Each well of high binding 96 well plates (Corning 9018) was incubated with 100 μL 1X capture antibody in PBS overnight at 4°C, washed 4 times with 300 μL wash buffer (PBS + 0.05% Tween20), incubated with 150 μL wash buffer + 1% BSA overnight at 4°C, washed 4 times with 300 μL wash buffer, incubated with 100 μL cell lysate at 37°C for 2 hours, washed 4 times with 300 μL wash buffer, incubated with 100 μL 1X detection antibody at 37°C for 1 hour, washed 4 times with 300 μL wash buffer, incubated with 100 μL 1X secondary antibody at 37°C for 30 minutes, washed 4 times with 300 μL wash buffer, and incubated with 100 μL TMB substrate (Cell Signaling Technologies 7004) for 30 minutes. Afterwards 100 μL of 1M HCl was added to each well and the absorbance at 450 nm was read on a plate reader.

Annexin V assay

HCT116 cells were harvested by trypsinization and 24 million cells were seeded in 100 mm low adhesion petri dishes (Corning 3262) at a density of 4 million cells per milliliter of DMEM + 10% FBS. The cells were incubated for 72 h, after which they were collected by centrifugation, washed with PBS, and resuspended in DMEM + 2% BSA. 200,000 cells were seeded into each well of low adhesion 96 well plates (Greiner 655185) at a density of 2 million cells per milliliter and treated with HA or PPLQ-HA conjugates at a concentration of 50 µg/mL. The cells were incubated for 24 hours, after which they were transferred to a 96 well v-bottom assay plate, washed twice with annexin binding buffer (10 mM HEPES, 140 mM NaCl, 2.5 mM $CaCl_2$, pH 7.4), and resuspend in 40 µL annexin binding buffer containing 1 drop/mL Annexin V AlexaFluor488 Ready Flow Conjugate (Thermo R37174) and 0.4 µg/mL propidium iodide (Thermo P3566). The 96 well plates were analyzed by a FACSCelesta instrument (Becton Dickinson, NJ, USA) equipped with a 96 well high throuput sampler, 488 nm and 561 nm lasers, and 530/30 nm and 586/15 nm detectors. The data was processed using FlowJo analysis software (FlowJo, LLC).

Scratch assay

iPS-ECs or SK-OV-3 cells were harvested by trypsinization and seeded in 24 well plates at a density of 79 x 10^3 cells/cm^2 in 0.50 mL of growth media. Multi-well plates for iPS-ECs were coated with fibronectin as previously described. Cells were grown to confluence, after which a sterile 200 µL pipette tip was used to create a gap in the cell monolayer. Afterwards the media was aspirated, each well was washed with PBS, and 0.5 mL of partially supplemented or serum deficient media was added: SK-OV-3 cells were incubated in RPMI + 0.5% FBS, iPS-ECs were incubated in RPMI + 0.5% FBS or DMEM + 10% FBS. Each well was imaged and the image coordinates were recorded. After incubation (10 hours for SK-OV-3 cells, 13 hours for iPS-ECs) the wells were imaged at the same location. Images were analyzed on ImageJ by tracing of the wound edge and recording the total area of the wound.

Synthetic ECM for three-dimensional (3D) vasculogenesis

8-arm 20kDa poly(ethylene glycol) functionalized with norbornene (PEGNB) (JenKem, China) was mixed in a 1:1 weight ratio with custom synthesized PPLG/PPLQ macromers grafted with

70

oligomeric ethylene glycol or HA in addition to norbornene to a total polymer concentration of 3 wt% in MQ water. A solution of 10x PBS 1M HEPES was added at 10% total volume along with thiolated fibronectin-mimetic peptides to promote cell adhesion ((Ac)PHSRNGGGK-GGGERCG(Ac)-GGRGDSPY(Am) custom synthesized by Boston Open Labs (Cambridge, MA)) at a nominal concentration of 2mM. Protease-sensitive dithiol crosslinking peptides ((Ac)GCRD-LPRTG-GPQIWGQ-DRCG(Am) custom synthesized by Boston Open Labs (Cambridge, MA)) were added at a stoichiometric ratio of 0.5 thiol:norbornene along with photoinitiator IRGACURE 2959 (Ciba, Prod. No. 0298913AB) at a final concentration of 0.05 wt%. Solutions were vortex mixed and a concentrated solution of iPS-EC in serum-free media was added to a final cell density of 12 million cells/mL. Hydrogel precursor solution (20uL) was added to 1 mL syringes from which the tips were removed and UV irradiated for 45 seconds at 100 mW/cm^2, and then transferred to a 24 well plate containing 750 uL of culture media.

Cells were cultured in VascuLife growth medium with full supplements as described previously. Media changes took place after 24 hours, and samples were fixed after 48 hours.

Gels were fixed in 4% paraformaldehyde solution in PHEM buffer for 30 minutes, and permeablized in 0.2% Triton X-100 in PBS for 20 minutes at room temperature on an orbital plate shaker set to 60 rpm. Gels were washed twice for 30 minutes at 60 rpm at room temperature in PBS, then blocked for 1 hour in 1% BSA at room temperature. Staining was performed overnight with DAPI (1:1000) and Phalloidin (1:100) at 4°C and 60 rpm in 1% BSA. Following staining, gels were washed three times for 30 minutes at 60 rpm at room temperature in PBS before imaging.

Z-stacks covering a 400 μm hydrogel depth were taken in 3 random fields of view in each hydrogel in 3 hydrogels per condition with a step size of 10 μm using a Zeiss LSM 880 confocal microscope. In FIJI, images were collapsed into maximum intensity z-projections and were modified by despeckling, increasing contrast, and performing a Gaussian blur to better distinguish vessel structures from background. A threshold was applied to produce a binary map of the vascular network, which was segmented and analyzed using the included "skeletonize" and "analyze skeleton" functions. The resulting data were analyzed using MATLAB to determine total network length within a representative image volume, including only segments larger than 100 μm in length

in order to exclude single or aggregated rounded cells from the analysis. To calculate average tubule thickness within each image volume, the total area of the vascular network was divided by the total length of network.

Proliferation assay

Proliferation of iPS-ECs was measured by a 5-bromo-2'-deoxyuridine (BrdU) assay kit (Cell Signaling Technologies 6813S). iPS-ECs were harvested by trypsinization and seeded in 96 well plates at a density of 9.4×10^3 cells/cm^2 in 100 µL of growth media. Multi-well plates were coated with fibronectin as previously described. After a 24 hour incubation, the media was replaced with either fresh growth media or various depleted media and a 5 µL solution of HA or PPLQ-HA conjugate dissolved in PBS was added to each well. The plates were incubated for 36 hours after which 10 µL of a 10x BrdU solution was added to each well. The plates were then incubated for another 3 hours after which the media was aspirated and cells were fixed by addition of 100 µL of the provided fixing solution to each well and incubated for 30 minutes at room temperature. The remaining antibody incubations and assay readout were done in accordance to the instructions provided with the kit.

Cell TiterGlo

Cells were seeded in white, clear bottom 96 well tissue culture plates (Corning 3903) at a density of 9,000 cells/cm^2 in growth media and incubated for 12 hours. Afterwards, the growth media was exchanged for low serum media (0.5% FBS) and a treatment of either HA, PPLQ-HA conjugate, or vehicle was added. The cells were treated for 72h, then assessed for metabolic activity as an indicator of cell viability by CellTiter-Glo (Promega). CellTiter-Glo reagent was reconstituted according to the manufacturer's instructions. Incubation media from the 96-well plates was aspirated, and 40 µL of CellTiter-Glo reagent was added to each well. The plates were sealed with adhesive film and incubated at room temperature in the dark for 30 minutes, after which luminescence in each well was measured using the plate reader (Tecan, 1s integration).

Synthesis

5-Norbornene-2-carboxylic acid succinimidyl ester, mixture of *endo* and *exo*

Synthesis of norbornene-NHS was performed according to a modified literature procedure.[57]

To a stirring solution of 5-Norbornene-2-carboxylic acid, mixture of *endo* and *exo*, predominantly *endo* (15 mL, 96 mmol), N-hydroxysuccinimide (15.5 g, 135 mmol), and DCM (200 mL) was added EDC-HCl (24.0 g, 125 mmol) in one portion. The reaction was stirred for 24 hours after which consumption of starting material was verified by TLC. The crude reaction mixture was washed three times with water (125 mL) followed by a saturated aqueous solution of sodium bicarbonate (125 mL) and brine (125 mL) and dried over sodium sulfate. The solvent was removed *in vacuo* to give a clear oil which solidified upon standing. Recrystallization from ethyl acetate and hexanes yielded a white crystalline solid (16.6 g, 70.7 mmol, 73.5%). ^{1}H NMR (400 MHz, Chloroform-*d*) δ 6.34 – 6.04 (m, 2H), 3.44 – 3.38 (m, 1H), 3.25 (dt, *J* = 9.1, 3.8 Hz, 1H), 3.06 – 2.93 (m, 1H), 2.81 (d, *J* = 1.8 Hz, 4H), 2.13 – 1.91 (m, 1H), 1.55 – 1.47 (m, 2H). ^{13}C NMR (101 MHz, Chloroform-*d*) δ 170.11, 138.28, 132.33, 49.81, 46.60, 42.68, 40.77, 29.74, 25.73. R$_f$ 0.26 (33% EtOAc:Hex, visualized by KMnO$_4$ stain and UV)

2-(2-(2-(2-azidoethoxy)ethoxy)ethoxy)ethan-1-amine

Synthesis of the bifunctional azide amine ethylene glycol linker was performed according to a modified literature procedure.[58]

To a stirred solution of tetraethylene glycol (17.3 g, 100 mmol) and THF (100 mL) cooled by an ice water bath was added methanesulfonyl chloride (17.0 mL, 220 mmol) in one portion followed be dropwise addition of a chilled solution of triethylamine (31 mL, 220 mmol) in THF (25 mL) over 30 minutes. Afterwards, the cooling bath was removed and the reaction was stirred at room temperature for 5 hours. Water (70 mL), sodium bicarbonate (6 g), and sodium azide (15.5 g, 238 mmol) were subsequently added and the reaction was heated to boiling to evaporate THF. Upon completion, a reflux condenser was added and the reaction was stirred under reflux for 3 days. The crude reaction mixture was then extracted three times with diethyl ether (100 mL) and the combined organic extracts were rinsed with brine and dried over magnesium sulfate. Removal of solvent *in vacuo* yielded a yellow oil (20.2 g, 82.7 mmol, 83%). ^{1}H NMR (400 MHz, Chloroform-*d*) δ 3.75 – 3.62 (m, 12H), 3.39 (t, *J* = 5.1 Hz, 4H). ^{13}C NMR (101 MHz, Chloroform-*d*) δ 70.86, 70.18, 50.83.

To a stirred solution of tetraethylene glycol diazide (20.2 g, 82.7 mmol) in 5% HCl (200 mL) was added dropwise over 3 hours a solution of triphenylphosphine (19.9 g, 75.9 mmol) in diethyl ether (150 mL). The reaction was stirred for 24 hours after which the aqueous phase was washed 4 times

with dichloromethane (100 mL), basified to pH 12 with addition of potassium hydroxide (17 g), and extracted 3 times with dichloromethane (100 mL). The combined organic extracts were dried over magnesium sulfate and the solvent was removed *in vacuo* to yield a yellow brown oil (11.2 g, 51.3 mmol). ^{1}H NMR (400 MHz, Chloroform-*d*) δ 3.75 – 3.55 (m, 10H), 3.51 (t, *J* = 5.2 Hz, 2H), 3.39 (t, *J* = 5.1 Hz, 2H), 2.86 (t, *J* = 5.2 Hz, 2H), 1.34 (s, 2H). ^{13}C NMR (101 MHz, Chloroform-*d*) δ 73.24, 70.42, 70.38, 70.37, 70.02, 69.77, 50.40, 41.57.
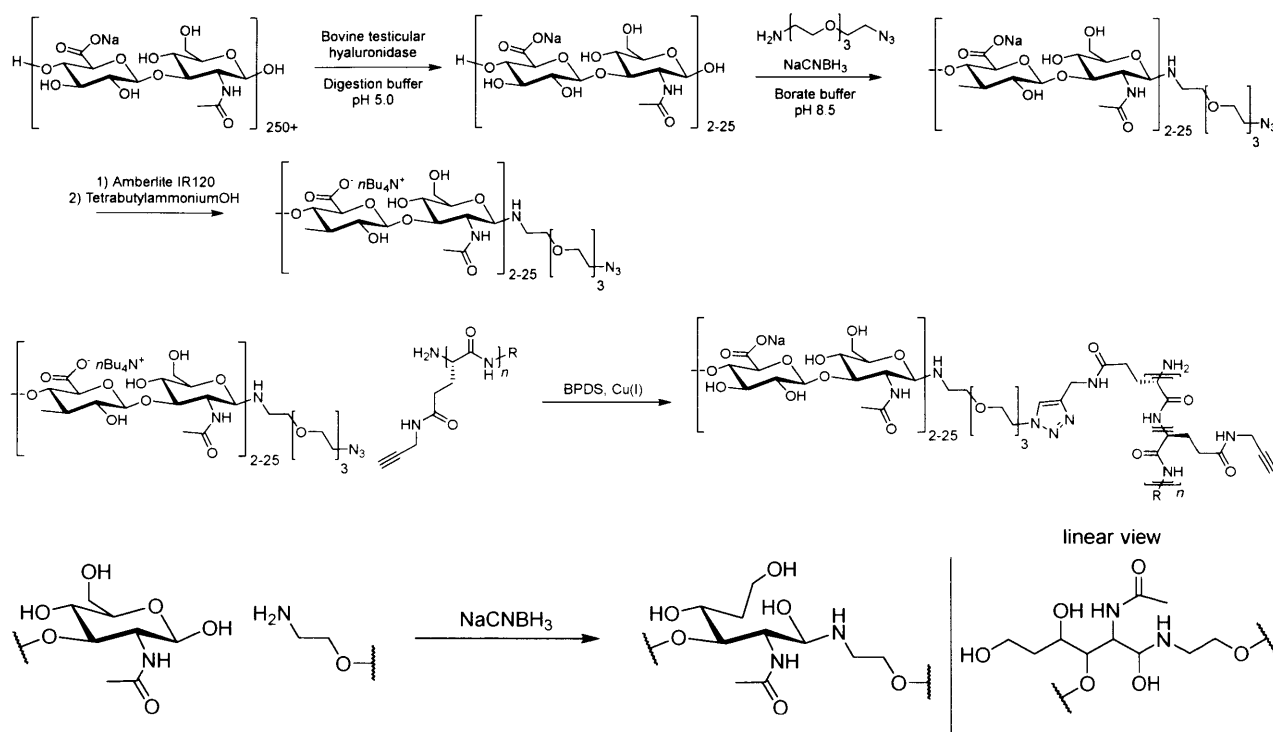
Figure 2.6. Synthetic scheme for modification of HA and conjugation of HA to PPLQ. For simplicity, the glycans have been illustrated as a repeating disaccharide. The reality is that the structure of the reducing end saccharide is modified in process of functionalization. The reaction of the reducing end of a glycan with an amine proceeds via a Schiff base intermediate that is subsequently reduced by sodium cyanoborohydride.

74
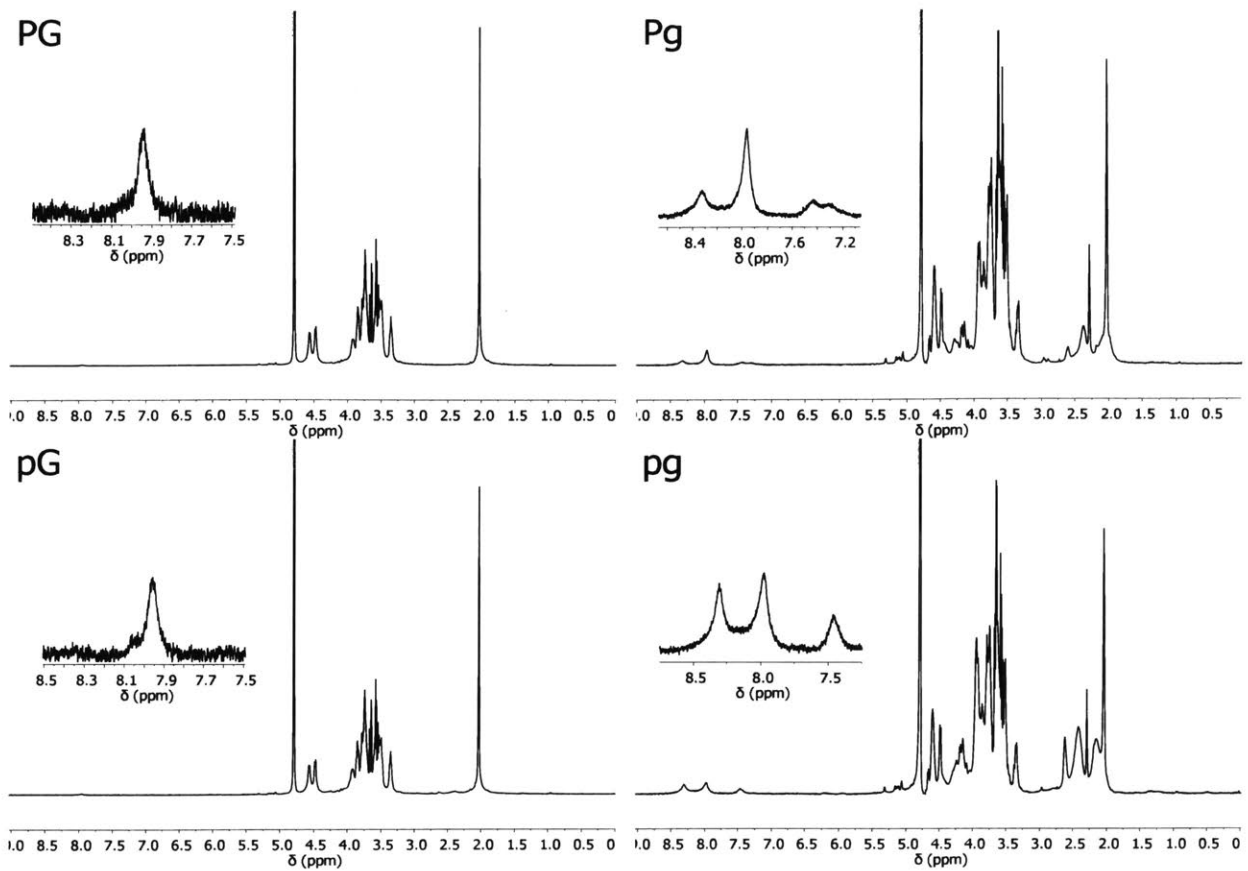
Figure 2.7. ^{1}H NMR spectra of PPLQ-HA conjugates
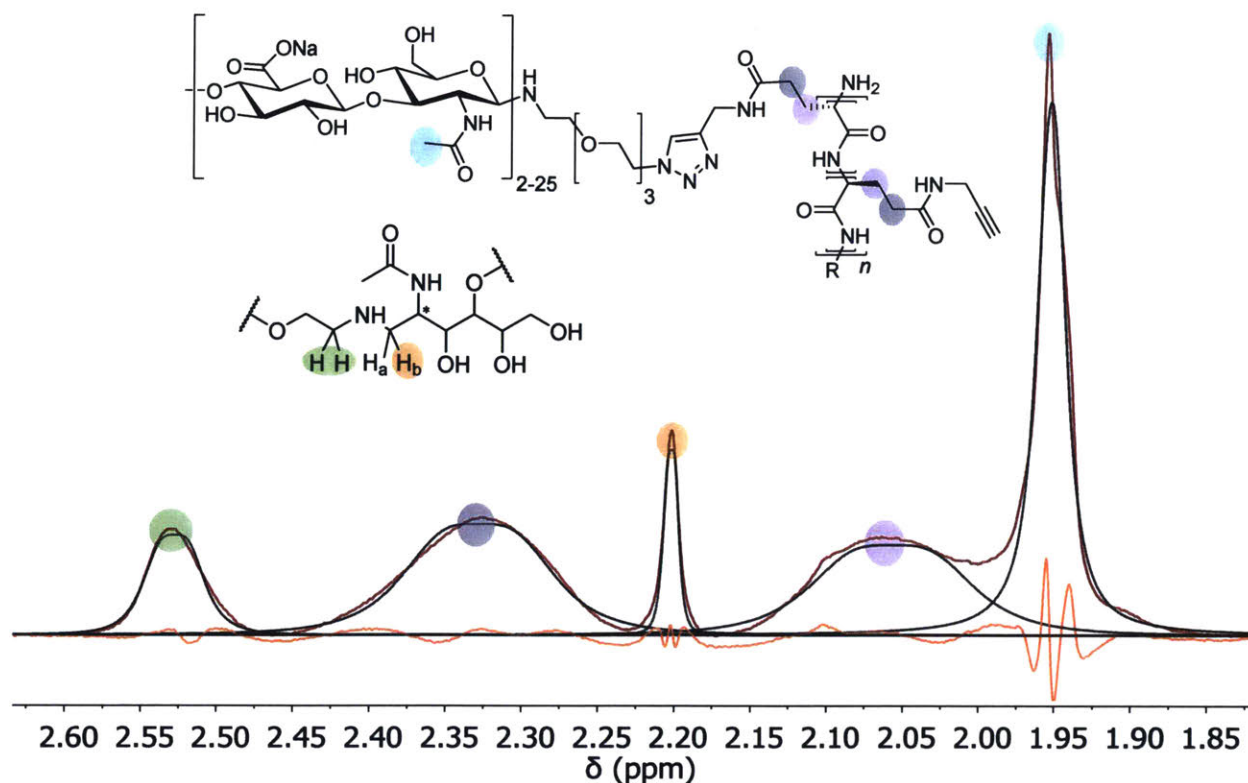
Figure 2.8. ^{1}H NMR spectrum of "pg" and determination of grafting density by peak fitting. The original NMR spectrum is maroon, fit peaks are drawn in black, and the residual error is represented in red. The ring open structure of the first glycan repeat unit is unique from the rest of the glycan and chemical shifts from the identical protons and the diasteromeric proton adjacent to the amine can be seen at δ2.2 ppm and δ2.52 ppm. For Pg and pg, these shifts are visible given the lower molecular weight of the glycan and thus greater abundance of reducing ends relative to repeating disaccharides. However, for PG and pG, the shifts are not visible over the signal of the higher molecular weight HA.

Peak fit: 1.74 ppm - 2.68 ppm				
Residual Error: 1.43E08				
Peak	δ (ppm)	Width (Hz)	Area	Relative %
HA (RE)	2.53	21.2	2.19E07	10
PPLQ (CH$_2$)	2.33	52.4	6.00E07	27
HA (RE)	2.20	5.5	1.08E07	5
PPLQ (CH$_2$)	2.06	56.9	5.30E07	24
HA (Ac)	1.95	11.0	7.73E07	35

RE = reducing end, CH$_2$ = side chain methylene, Ac = acetyl

Figure 2.9. Based on the relative areas, a grafting efficiency is estimated to be 40% substitution and the molecular weight of HA is confirmed to be approximately 1 kDa. The triazole peak has an absolute area of 1.32E07, which is in reasonable agreement with the areas provided by the peak fitting with the discrepancy being attributed to broad peaks, noise, baseline correction, and possibly small amounts of ungrafted hyaluronic acid, though no free hyaluronic acid was detected with gel permeation chromatography.
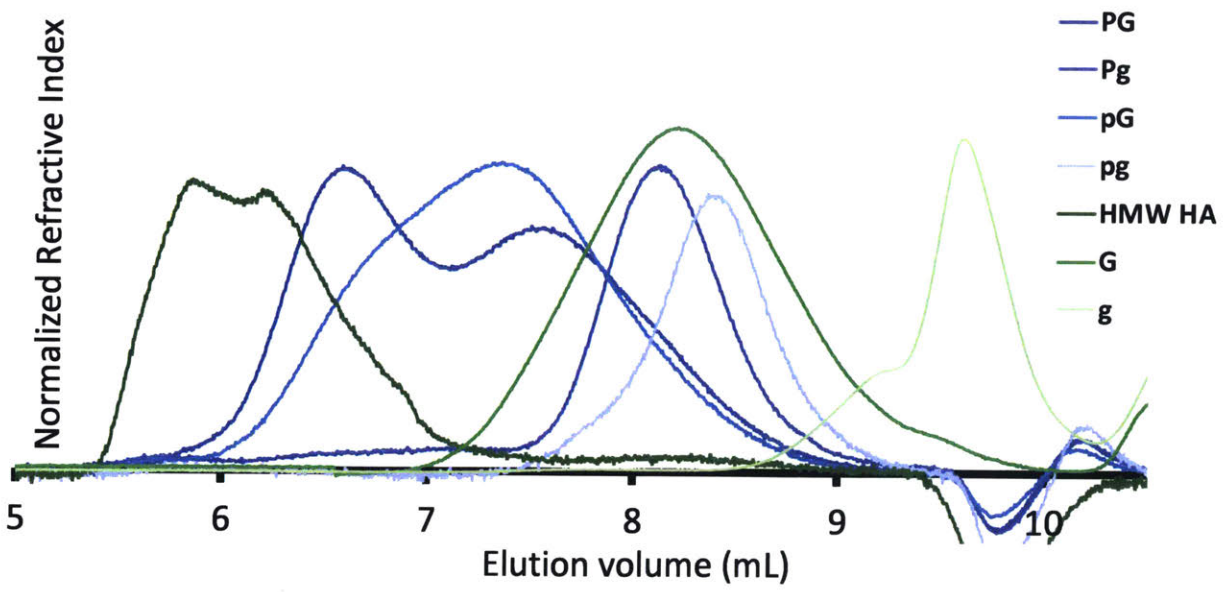
	HMW HA	G	g	PG	Pg	pG	pg
Retention Vol. (mL)	5.86	8.21	9.6	6.59	8.12	7.35	8.39
M_n (Daltons)	360361	8297	1183	39057	12567	39911	8747
M_w (Daltons)	531892	16646	1604	131263	15955	96845	11636
M_w/M_n	1.48	2.01	1.36	3.36	1.27	2.43	1.33

Figure 2.10. Overlaid GPC chromatograms of endogenous HA and PPLQ-HA conjugates studied as well as molecular weights relative to poly(ethylene glycol) standards. Refractive index is normalized to show equal peak heights.
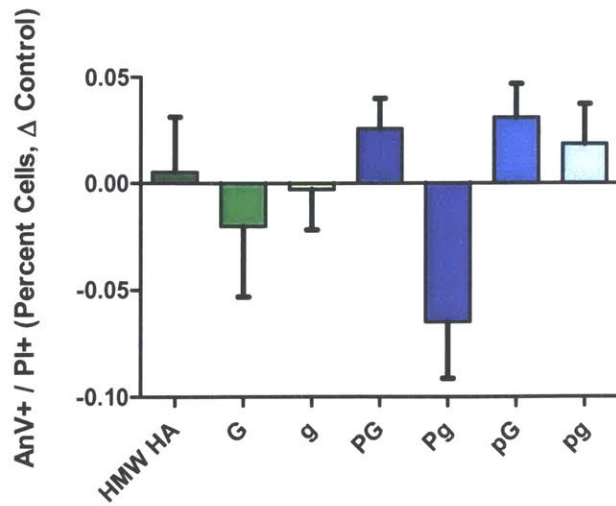
Figure 2.11. No difference in Annexin V binding for dead cells in anchorage independent HCT116 cells treated with HA or PPLQ-HA conjugates as determined by flow cytometry expressed as difference from a no treatment control.
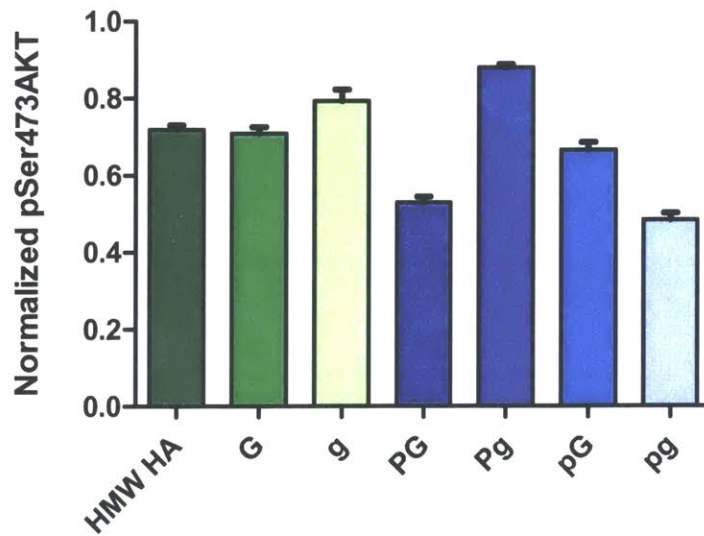
Figure 2.12. No robust trend of AKT activation by phosphorylation of Ser473 in response to HA or PPLQ-HA conjugates in HCT116 cells under anchorage independent conditions expressed as a percentage of total AKT relative to a no treatment control.
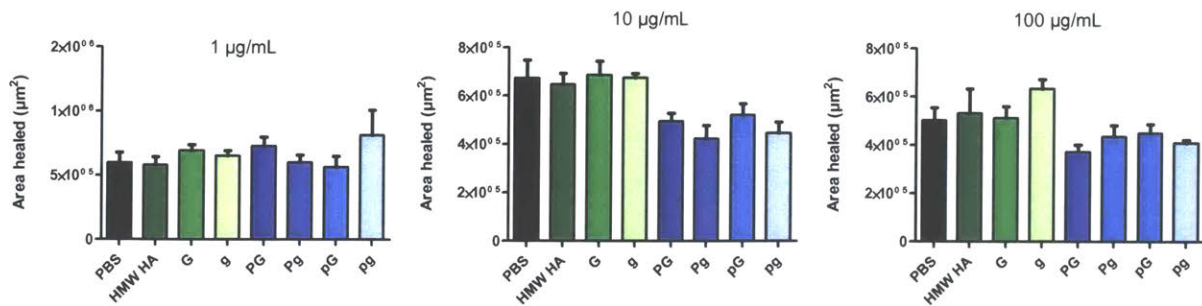
Figure 2.13. Dose dependent migration of SKOV3 cells in RPMI + 0.5% FBS. For 1 µg/mL, P > 0.05. For 10 µg/mL, P < 0.05 for PBS vs. Pg, HMW HA vs. Pg, G/g vs. Pg/pg. For 100 µg/mL, P < 0.05 for g vs. PG.
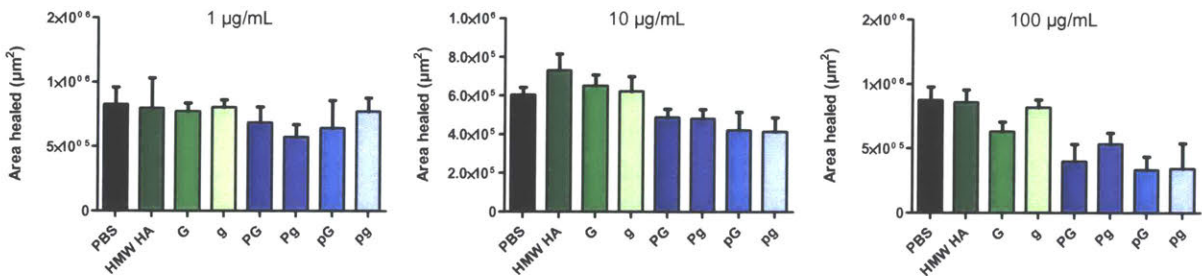
Figure 2.14. Dose dependent migration of iPS-ECs in RPMI + 0.5% FBS. For 1 µg/mL, P > 0.05. For 10 µg/mL, P < 0.05 for HMW HA vs. pg/pG. For 100 µg/mL, P < 0.05 for PBS vs. PG/pG, HMW HA vs. PG/pG, g vs. pG.
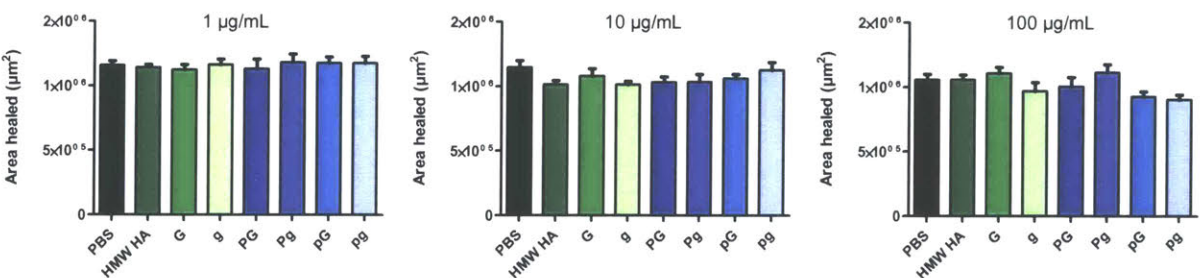
Figure 2.15. Dose dependent migration of OVCAR8 cells in RPMI + 0.5% FBS. P > 0.05
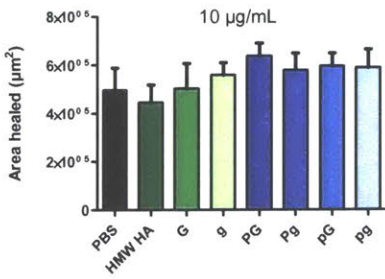
Figure 2.16. Migration of iPS-ECs in DMEM + 10% FBS. P > 0.05
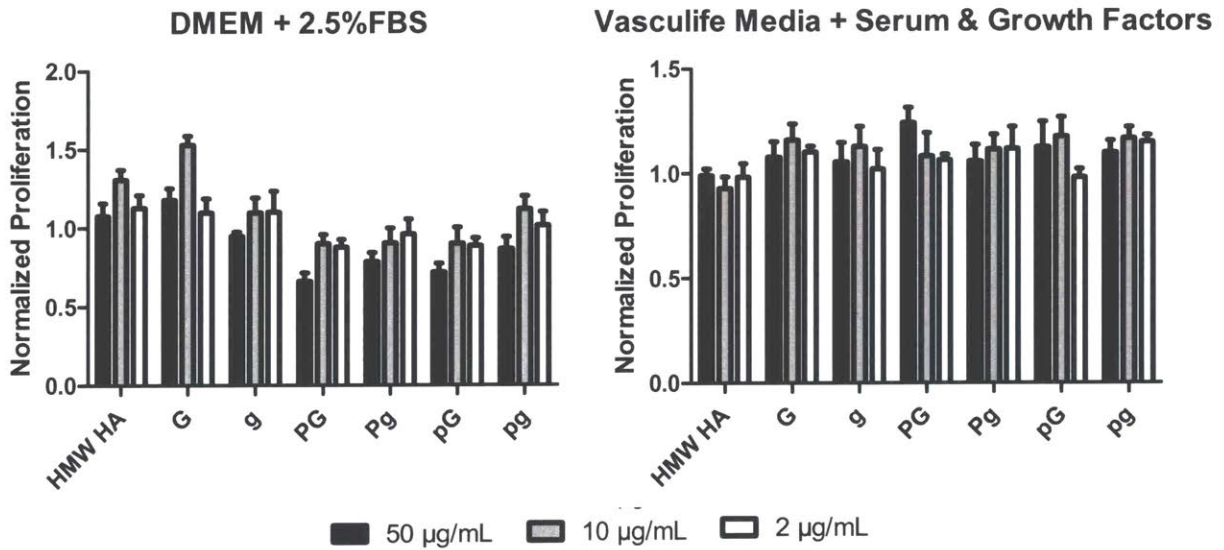
Figure 2.17. BRDU cell proliferation assay of iPS-ECs treated in different growth medium normalized to vehicle control. PPLQ-HA conjugates modestly inhibit cell division in low serum media (2way ANOVA P < 0.05 for dose and treatment), but proliferation of iPS-ECs is unaffected by treatment in media supplemented with growth factors (P > 0.05 for dose and treatment).
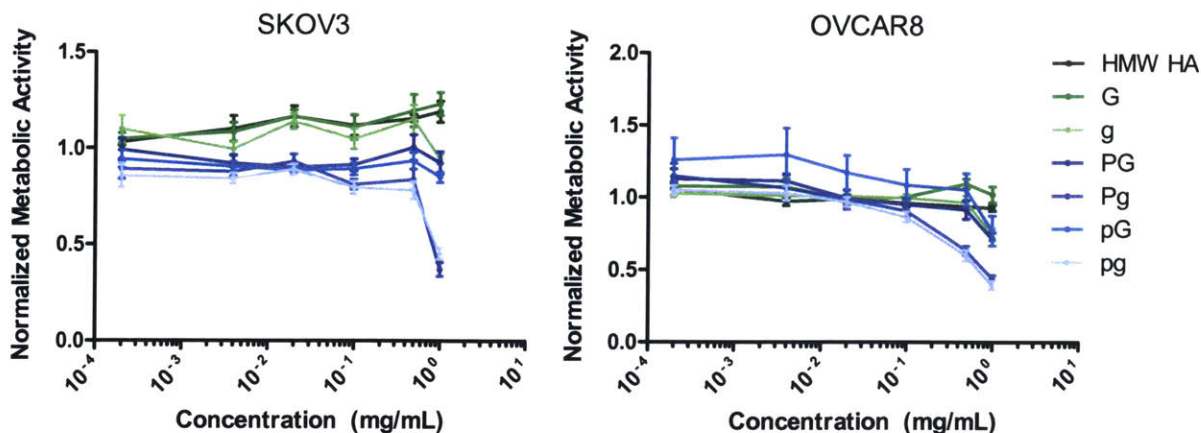
Figure 2.18. Cell Titer Glo assay of SKOV3 and OVCAR8 cells in low serum media (0.5% FBS). Overall, PPLQ-HA conjugates and endogenous HA are not toxic to adherent cells at biologically relevant concentrations. PPLQ-HA conjugates with a larger HA brush are less toxic than PPLQ-HA conjugates with a shorter HA brush at very high concentrations. Different cell lines react differently to endogenous HA and PPLQ-HA conjugates.
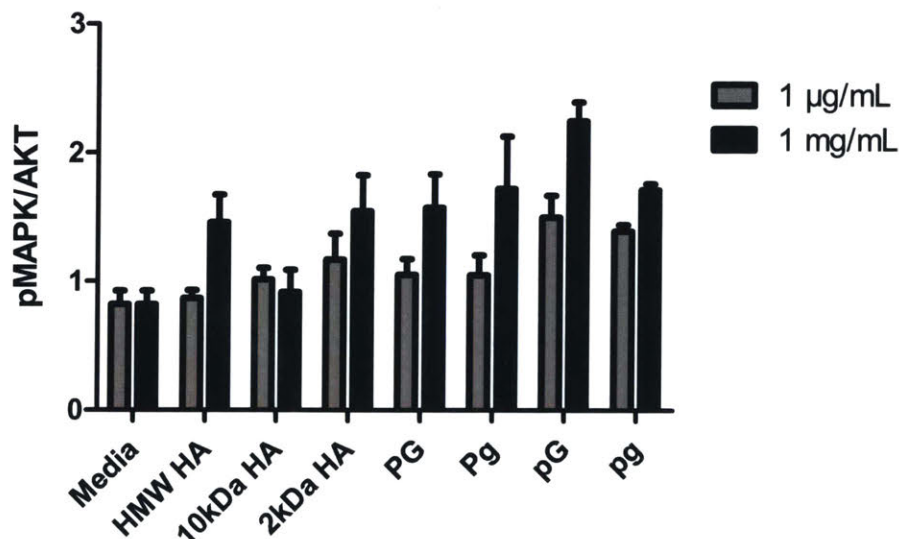

Figure 2.19. After acute treatment following serum starvation, PPLQ-HA conjugates cause activation of p44/42 MAPK similar to oligomeric HA. There is no phosphorylation of AKT (data not shown).

82
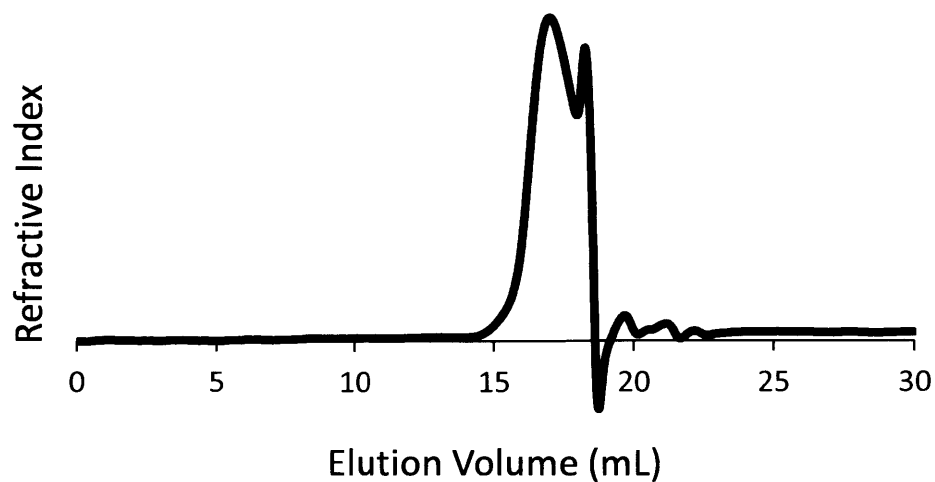
Figure 2.20. Gel permeation chromatogram of PBLG_25. The peak at 18.8 mL corresponds to injected DMF and solvent. Relative to poly(methyl methacrylate) standards: M_n 3846, PDI 1.17
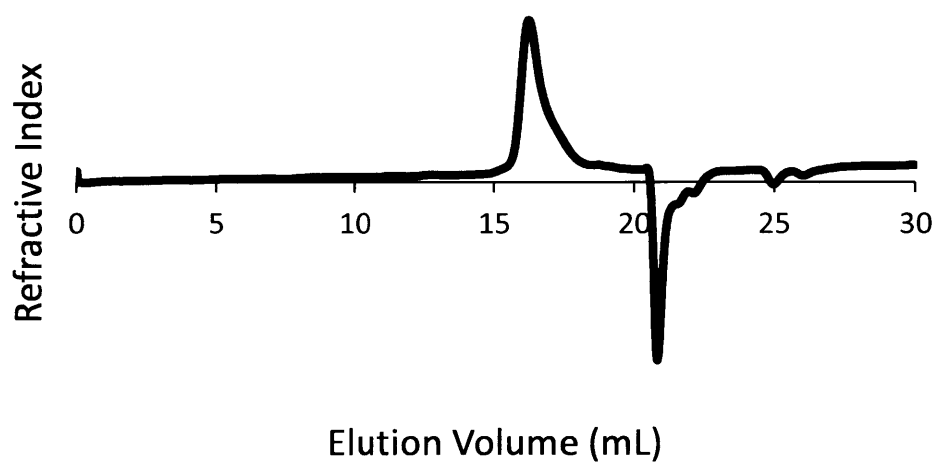

Figure 2.21. Gel permeation chromatogram of PBLG_150. The peak at 20.9mL corresponds to injected DMF and solvent. Relative to poly(methyl methacrylate) standards: M_n 9430, PDI 1.21
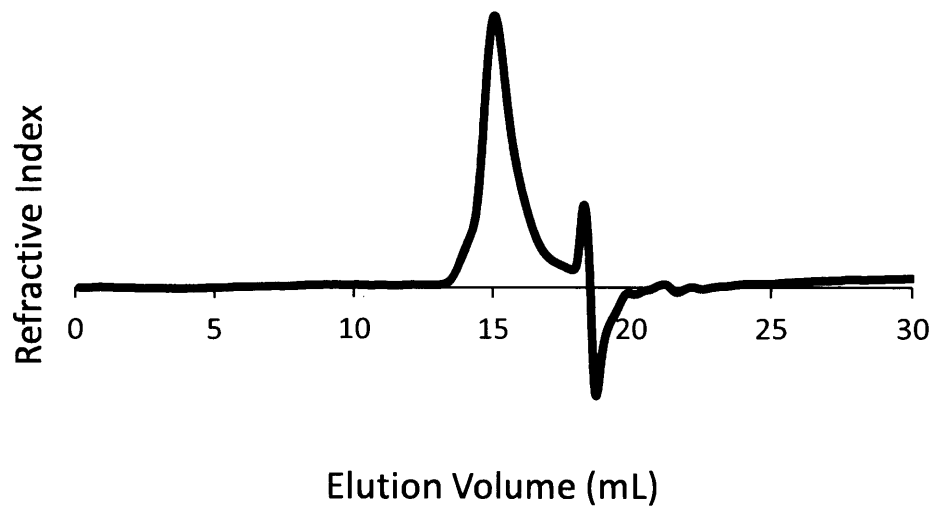
Figure 2.22. Gel permeation chromatogram of PPLQ_25. The peak at 18.8 mL corresponds to injected DMF and solvent. Relative to poly(methyl methacrylate) standards: M_n 17299, PDI 1.38
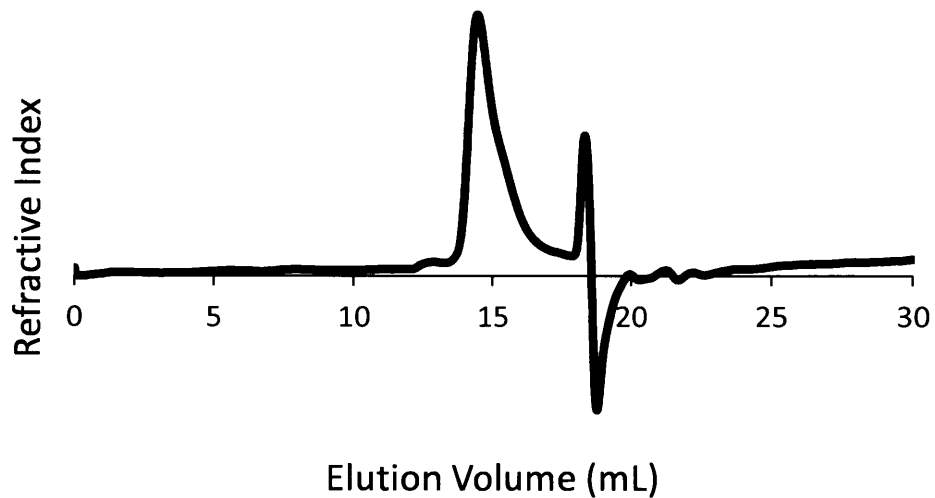

Figure 2.23. Gel permeation chromatogram of PPLQ_150. The peak at 18.8 mL corresponds to injected DMF and solvent. Relative to poly(methyl methacrylate) standards: M_n 26306, PDI 1.30
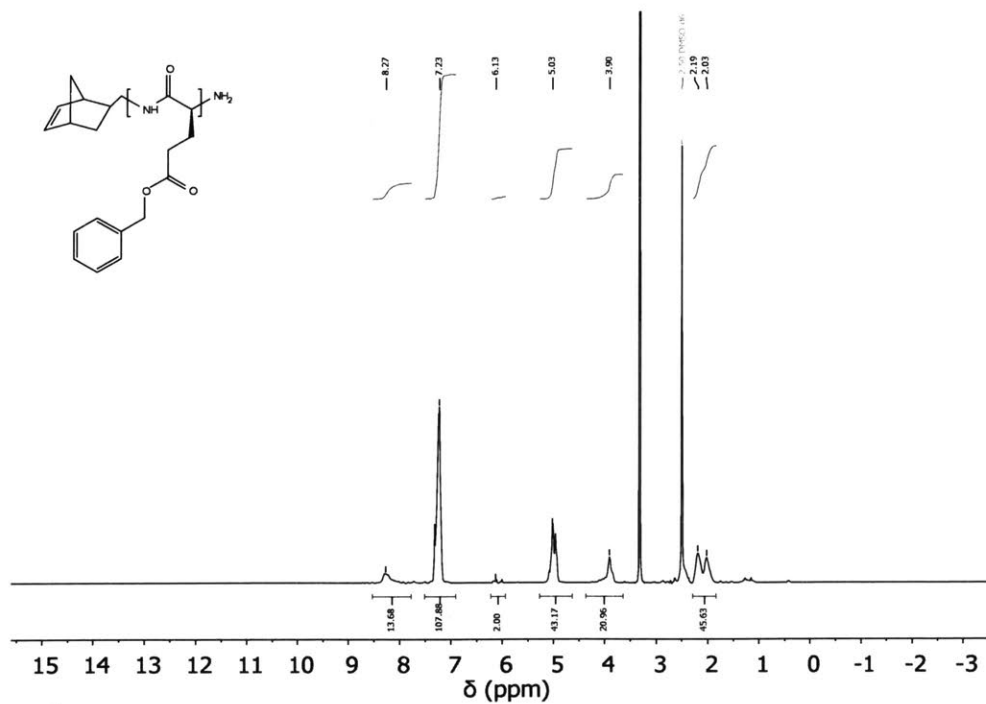
**Figure 2.24.** ^{1}H NMR spectrum of PBLG_25 in $(CD_3)_2SO$. Peak at δ 3.33 is from water.
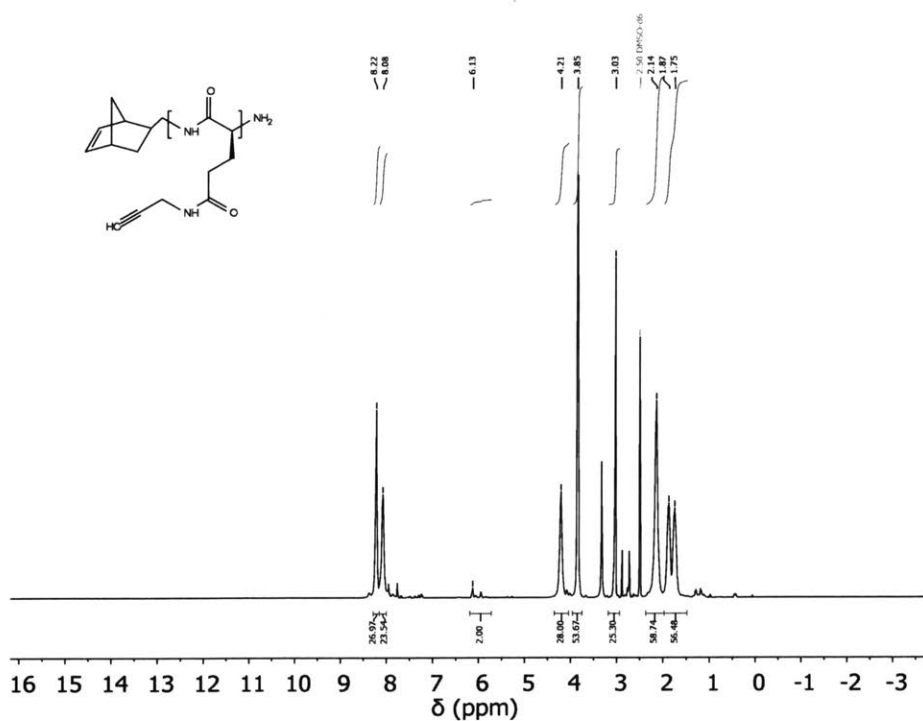
Figure 2.25. ^{1}H NMR spectrum of PPLQ_25 in $(CD_3)_2SO$. Peak at δ 3.33 is from water. Peaks at δ 7.95, 2.89, 2.73 is from DMF. Other peaks at are from small amounts of residual HOBt and EDC from coupling reaction.
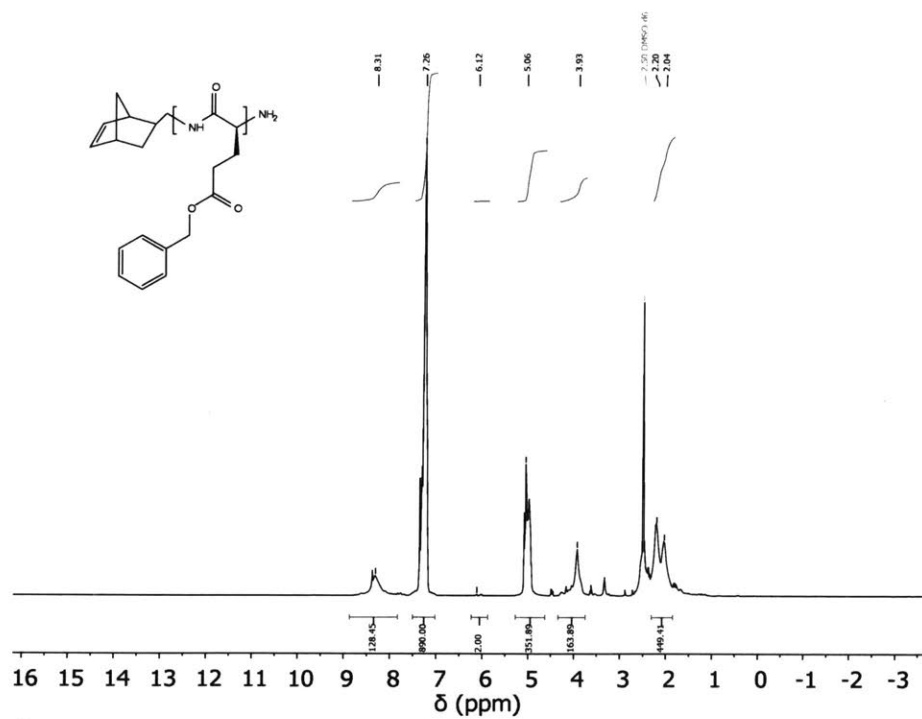
**Figure 2.26.** ^{1}H NMR spectrum of PBLG_175 in $(CD_3)_2SO$. Peak at δ 3.33 is from water.
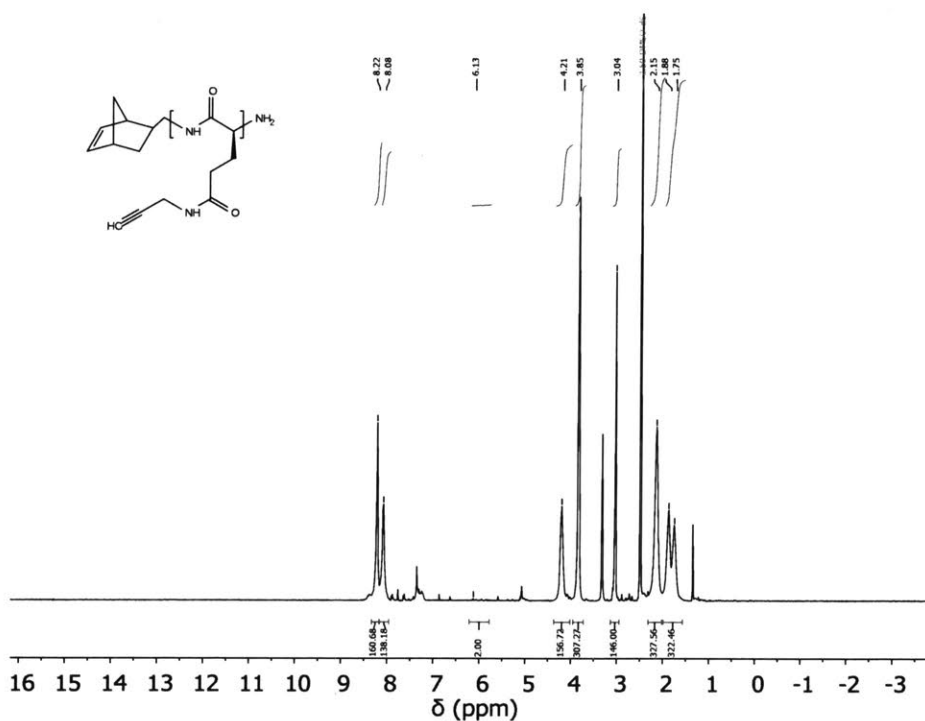
Figure 2.27. ^{1}H NMR spectrum of PPLQ_175 in $(CD_3)_2SO$. Peak at δ 3.32 is from water.

3.5 References

(1) L. Schaefer, R. M. Schaefer, *Cell Tissue Res.* **2010**, *339*, 237.

(2) O. Lieleg, C. Lieleg, J. Bloom, C. B. Buck, K. Ribbeck, *Biomacromolecules* **2012**, *13*, 1724–1732.

(3) M. Wathier, B. A. Lakin, P. N. Bansal, S. S. Stoddart, B. D. Snyder, M. W. Grinstaff, *J. Am. Chem. Soc.* **2013**, *135*, 4930–4933.

(4) K. Aoi, K. Tsutsumiuchi, M. Okada, *Macromolecules* **1994**, *27*, 875–877.

(5) D. Pati, A. Y. Shaikh, S. Das, P. K. Nareddy, M. J. Swamy, S. Hotha, S. S. Gupta, *Biomacromolecules* **2012**, *13*, 1287–1295.

(6) V. Dhaware, A. Y. Shaikh, M. Kar, S. Hotha, S. Sen Gupta, *Langmuir* **2013**, *29*, 5659–5667.

(7) T. Borase, T. Ninjbadgar, A. Kapetanakis, S. Roche, R. O'Connor, C. Kerskens, A. Heise, D. F. Brougham, *Angew. Chem. Int. Ed.* **2013**, *52*, 3164–3167.

(8) J. Huang, G. Habraken, F. Audouin, A. Heise, *Macromolecules* **2010**, *43*, 6050–6057.

(9) H. Tang, D. Zhang, *Biomacromolecules* **2010**, *11*, 1585–1592.

(10) C. Xiao, C. Zhao, P. He, Z. Tang, X. Chen, X. Jing, *Macromol. Rapid Commun.* **2010**, *31*, 991–997.

(11) W. Wang, P. T. Hammond, *Polym. Chem.* **2018**, *9*, 346–351.

(12) F. Gao, M. Cao, C. Yang, Y. He, Y. Liu, *J. Biomed. Mater. Res. B Appl. Biomater.* **2006**, *78*, 385–392.

(13) B. P. Toole, *Nat. Rev. Cancer* **2004**, *4*, 528–539.

(14) R. C. Savani, G. Cao, P. M. Pooler, A. Zaman, Z. Zhou, H. M. DeLisser, *J. Biol. Chem.* **2001**, *276*, 36770–36778.

(15) C. Yang, M. Cao, H. Liu, Y. He, J. Xu, Y. Du, Y. Liu, W. Wang, L. Cui, J. Hu, et al., *J. Biol. Chem.* **2012**, *287*, 43094–43107.

(16) S. Ibrahim, A. Ramamurthi, *J. Tissue Eng. Regen. Med.* **2008**, *2*, 22–32.

(17) J. Kim, K. S. Kim, G. Jiang, H. Kang, S. Kim, B.-S. Kim, M. H. Park, S. K. Hahn, *Biopolymers* **2008**, *89*, 1144–1153.

(18) L. Ng, A. J. Grodzinsky, P. Patwari, J. Sandy, A. Plaas, C. Ortiz, *J. Struct. Biol.* **2003**, *143*, 242–257.

(19) T. J. Deming, *J. Polym. Sci. Part Polym. Chem.* **2000**, *38*, 3011–3018.

(20) E. R. Blout, R. H. Karlson, *J. Am. Chem. Soc.* **1956**, *78*, 941–946.

(21) M. Idelson, E. R. Blout, *J. Am. Chem. Soc.* **1958**, *80*, 4631–4634.

(22) P. Teriete, S. Banerji, M. Noble, C. D. Blundell, A. J. Wright, A. R. Pickford, E. Lowe, D. J. Mahoney, M. I. Tammi, J. D. Kahmann, et al., *Mol. Cell* **2004**, *13*, 483–496.

(23) R. Kosaki, K. Watanabe, Y. Yamaguchi, *Cancer Res.* **1999**, *59*, 1141–1145.

(24) Y. Li, P. Heldin, *Br. J. Cancer* **2001**, *85*, 600–607.

(25) R. M. Peterson, Q. Yu, I. Stamenkovic, B. P. Toole, *Am. J. Pathol.* **2000**, *156*, 2159–2167.

(26) S. Ghatak, S. Misra, B. P. Toole, *J. Biol. Chem.* **2002**, *277*, 38013–38020.

(27) S. Mueller, E. Cadenas, A. H. Schönthal, *Cancer Res.* **2000**, *60*, 156–163.

(28) H. van Genderen, H. Kenis, P. Lux, L. Ungeth, C. Maassen, N. Deckers, J. Narula, L. Hofstra, C. Reutelingsperger, *Nat. Protoc.* **2006**, *1*, 363–367.

(29) K. Segawa, S. Kurata, Y. Yanagihashi, T. R. Brummelkamp, F. Matsuda, S. Nagata, *Science* **2014**, *344*, 1164–1168.

(30) S. Nagata, J. Suzuki, K. Segawa, T. Fujii, *Cell Death Differ.* **2016**, *23*, 952–961.

(31) B. Fadeel, B. Gleiss, K. Högstrand, J. Chandra, T. Wiedmer, P. J. Sims, J. I. Henter, S. Orrenius, A. Samali, *Biochem. Biophys. Res. Commun.* **1999**, *266*, 504–511.

(32) S.-H. Lee, X. W. Meng, K. S. Flatten, D. A. Loegering, S. H. Kaufmann, *Cell Death Differ.* **2013**, *20*, 64–76.

(33) I. Vivanco, C. L. Sawyers, *Nat. Rev. Cancer* **2002**, *2*, 489–501.

(34) E. E. Vincent, D. J. E. Elder, E. C. Thomas, L. Phillips, C. Morgan, J. Pawade, M. Sohail, M. T. May, M. R. Hetzel, J. M. Tavaré, *Br. J. Cancer* **2011**, *104*, 1755–1761.

(35) A. Chopra, M. E. Murray, F. Byfield, M. Mendez, R. Halleluyan, D. Restle, D. R.-B. Aroush, P. A. Galie, K. Pogoda, R. Bucki, et al., *Biomaterials* **2014**, *35*, 71–82.

(36) A. Huttenlocher, A. R. Horwitz, *Cold Spring Harb. Perspect. Biol.* **2011**, *3*, DOI 10.1101/cshperspect.a005074.

(37) H. Gerhardt, M. Golding, M. Fruttiger, C. Ruhrberg, A. Lundkvist, A. Abramsson, M. Jeltsch, C. Mitchell, K. Alitalo, D. Shima, et al., *J. Cell Biol.* **2003**, *161*, 1163–1177.

(38) A. Mettouchi, *Cell Adhes. Migr.* **2012**, *6*, 528–534.

(39) B. Vailhé, D. Vittet, J.-J. Feige, *Lab. Invest.* **2001**, *81*, 439–452.

(40) V. W. M. van Hinsbergh, M. A. Engelse, P. H. A. Quax, *Arterioscler. Thromb. Vasc. Biol.* **2006**, *26*, 716–728.

(41) G. E. Davis, K. J. Bayless, A. Mavila, *Anat. Rec.* **2002**, *268*, 252–275.

(42) K. M. Yamada, E. Cukierman, *Cell* **2007**, *130*, 601–610.

(43) F. Pampaloni, E. G. Reynaud, E. H. K. Stelzer, *Nat. Rev. Mol. Cell Biol.* **2007**, *8*, 839–845.

(44) C. M. Williams, G. Mehta, S. R. Peyton, A. S. Zeiger, K. J. Van Vliet, L. G. Griffith, *Tissue Eng. Part A* **2010**, *17*, 1055–1068.

(45) G. Mehta, C. M. Williams, L. Alvarez, M. Lesniewski, R. D. Kamm, L. G. Griffith, *Biomaterials* **2010**, *31*, 4657–4671.

(46) Y. Zhao, K. Swenson, J. J. Sergio, J. S. Arn, D. H. Sachs, M. Sykes, *Nat. Med.* **1996**, *2*, 1211–1216.

(47) E. L. Pardue, S. Ibrahim, A. Ramamurthi, *Organogenesis* **2008**, *4*, 203–214.

(48) D. Park, Y. Kim, H. Kim, K. Kim, Y.-S. Lee, J. Choe, J.-H. Hahn, H. Lee, J. Jeon, C. Choi, et al., *Mol. Cells* **2012**, *33*, 563–574.

(49) D. Yee, D. Hanjaya-Putra, V. Bose, E. Luong, S. Gerecht, *Tissue Eng. Part A* **2011**, *17*, 1351–1361.

(50) P.-H. Lai, Y. Chang, S.-C. Chen, C.-C. Wang, H.-C. Liang, W.-C. Chang, H.-W. Sung, *Tissue Eng.* **2006**, *12*, 2499–2508.

(51) S. Ouasti, P. J. Kingham, G. Terenghi, N. Tirelli, *Biomaterials* **2012**, *33*, 1120–1134.

(52) M. Martchenko, S.-Y. Jeong, S. N. Cohen, *Proc. Natl. Acad. Sci.* **2010**, *107*, 15583–15588.

(53) R. Racine, M. E. Mummert, *Mol. Regul. Endocytosis* **2012**, DOI 10.5772/45976.

(54) S. Ibrahim, B. Joddar, M. Craps, A. Ramamurthi, *Biomaterials* **2007**, *28*, 825–835.

(55) T. Asteriou, B. Deschrevel, B. Delpech, P. Bertrand, F. Bultelle, C. Merai, J.-C. Vincent, *Anal. Biochem.* **2001**, *293*, 53–59.

(56) F. J. Wende, S. Gohil, H. Mojarradi, T. Gerfaud, L. I. Nord, A. Karlsson, J.-G. Boiteau, A. H. Kenne, C. Sandström, *Carbohydr. Polym.* **2016**, *136*, 1348–1357.

(57) J. K. Pontrello, M. J. Allen, E. S. Underbakke, L. L. Kiessling, *J. Am. Chem. Soc.* **2005**, *127*, 14536–14537.

(58) L. N. Goswami, Z. H. Houston, S. J. Sarma, S. S. Jalisatgi, M. Frederick Hawthorne, *Org. Biomol. Chem.* **2013**, *11*, 1116–1126.

Chapter 3: Exploration of end linked polypeptide scaffold networks

3.1 Introduction

Hydrogels are formed when a hydrophilic polymer network is swollen with water. These hydrated networks can be engineered to exhibit physical properties similar to that of biological tissues. As such, these materials are employed in biological and medical applications. The synthesis of a hydrogel involves cross-linking molecules to form the network. These molecules can be chosen from a range in molecular weights as well as chemical structures, and these choices ultimately affect the physical properties of the gel. Furthermore, the cross-linking method can also have a profound impact on hydrogel properties. Crosslinking poly(ethylene glycol) diacrylate with free radical initiators generates one of the most widely studied hydrogels for biomaterials applications. In this example, the crosslinking chemistry proceeds analogously to a chain growth polymerization where there is a continuity of reactions on a reactive end until a termination event. Much like the polymerization reaction, the crosslinking is difficult to control given the reactive nature of a free radical. Moreover, the hydrogel develops a heterogeneous structure as a consequence of concentrated areas of crosslinks. Alternatively, networks can be formed by crosslinking through the "A+B = C" type of reaction typical of step growth polymerization. These networks are significantly more homogenous, but not immune to defects from dangling ends, loop formation, or incomplete crosslinking. In addition, efficient cross linking reactions are required to reach the high conversions required to form a continuous network in the same way efficient reactions are required for synthesis of a high molecular weight polymer by step growth polymerization (Figure 3.1).
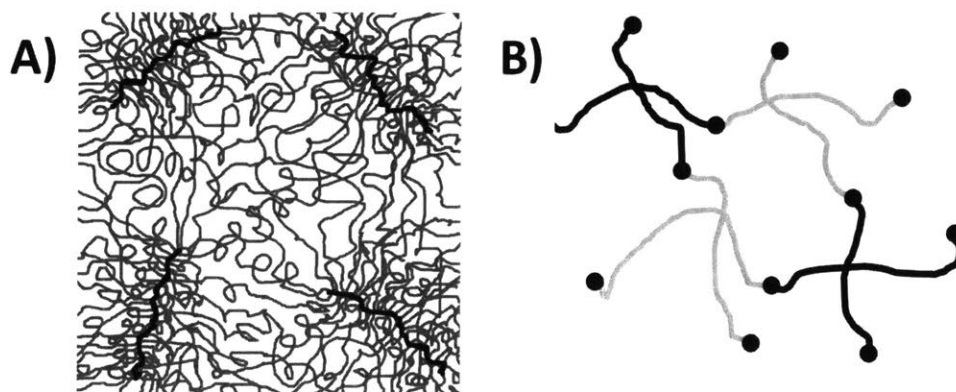
Figure 3.1. Idealized cartoon of network formation by A) chain growth and B) step growth methods.

Hydrogels may also be modified to incorporate functional groups with the ultimate goal of promoting desired responses from biological systems. These modifications can range in complexity: tethering of functional groups for altering physical properties such as hydrophobicity and ionic charge to endowing hydrogels with biological activity by conjugation of proteins, peptides, or glycans. These modifications are conveniently accomplished by reaction with the same functional groups that participate in cross linking because these groups are a readily available reactive chemical handle. However, conjugation by an orthogonal chemistry would enable modification of the polymer network without interfering with the cross linking reaction, removing the competition between network functionalization versus formation.

Poly(γ-propargyl-L-glutamate) is a polymer scaffold that possesses many of the ideal properties for biomaterial hydrogels. PPLG is an α-helical, biocompatible synthetic polypeptide whose side chains may be modified by copper(I) catalyzed azide alkyne cycloaddition. The high density of grafting enabled by this "click" chemistry means incorporation of biologically active molecules or reactive sites for crosslinking is not limited by chemical handles on the polymer. Moreover, the option of quantitative grafting, something not easily achieved in post polymerization modification, expands the spectrum of polymer characteristics that can be assumed by PPLG. The modular nature of this grafting reaction facilitates the synthesis of diverse materials. Additionally, the rigid α-helical structure of PPLG may endow these networks with distinct physical properties with regard to control over mesh size or ligand presentation. Finally, PPLG is synthesized with controlled length and dispersity, enabling fine tuning and probing of structure vs. activity.

PPLG has previously been used as a macromer component in hydrogels for biological applications.[1] These first step to formation of these PPLG networks is to graft reactive sites on the side chain for later crosslinking. By nature, the post polymerization modification process results in a random copolymer with a stochastic distribution of groups along the polymer backbone. Consequently, there can be large variation in both the distance between and number of reactive groups on a polymer backbone, translating to variance in the molecular weight between crosslinks

and number of crosslinks per PPLG macromer. The ultimate result is heterogeneity in the network structure. One method to better control network formation is to link the PPLG macromer by reactive groups on the end of the polymer. The molecular weight between crosslinks is determined by the molecular weight of the polymer and the number of crosslinks is defined by the number of ends on the macromer. Because PPLG is synthesized by a living anionic polymerization resulting in low dispersity, this method could result in macromers that produce a more uniform network (Figure 3.2). For these reasons, the end-linking of PPLG to form a hydrogel was investigated.
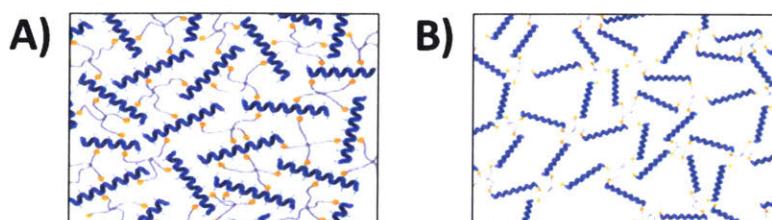

Figure 3.2. Idealized cartoon of PPLG polymer networks cross-linked by a 4-arm polymer through A) random side chain grafting and B) end-linked methods.

3.2 Results/Discussion

There are many important factors for generating an end-linked polymer network from PPLG, the most fundamental of which is that formation of an end linked network involves synthesis of PPLG with appropriate reactive groups on the ends of the polymer chain. The polymer synthesis was planned and optimized to fulfill this requirement.

The anionic ring opening polymerization of N-carboxyanhydrides (NCAs) to form polypeptides may proceed by the activated monomer mechanism or normal amine mechanism. Polymerization by active monomer mechanism begins when a base deprotonates the NCA monomer. This newly formed anion then serves as a nucleophile and initiates polymerization which continues to propagate by either reaction of the α-amine with NCA monomer or by reaction of an activated monomer or amine nucleophile with the NCA on the end of a polymer backbone that was previously initiated with an activated monomer.[2] While this polymerization mechanism can lead to very high molecular weight polymers, end functionality is difficult to control and the polymers

have a large molecular weight distribution (Figure 3.3a). The normal amine mechanism is a form of living polymerization, where a nucleophile, most frequently a primary amine, initiates the polymerization. The polymerization proceeds by reaction of the α-amine with NCA monomer. As such, any functional groups present on the initiator will be presented at one end of the resulting polymer chain (Figure 3.3b). The polymerization may be terminated by consumption of the amine on the end of the polymer chain. This can occur by reaction of the amine with electrophilic groups present in the solvent or polymer side chain, resulting in unwanted termination. If the polymerization conditions are optimized to avoid unwanted termination, introduction of a reagent to the polymerization reaction is one method to incorporate a functional group on the other end of the polymer chain.
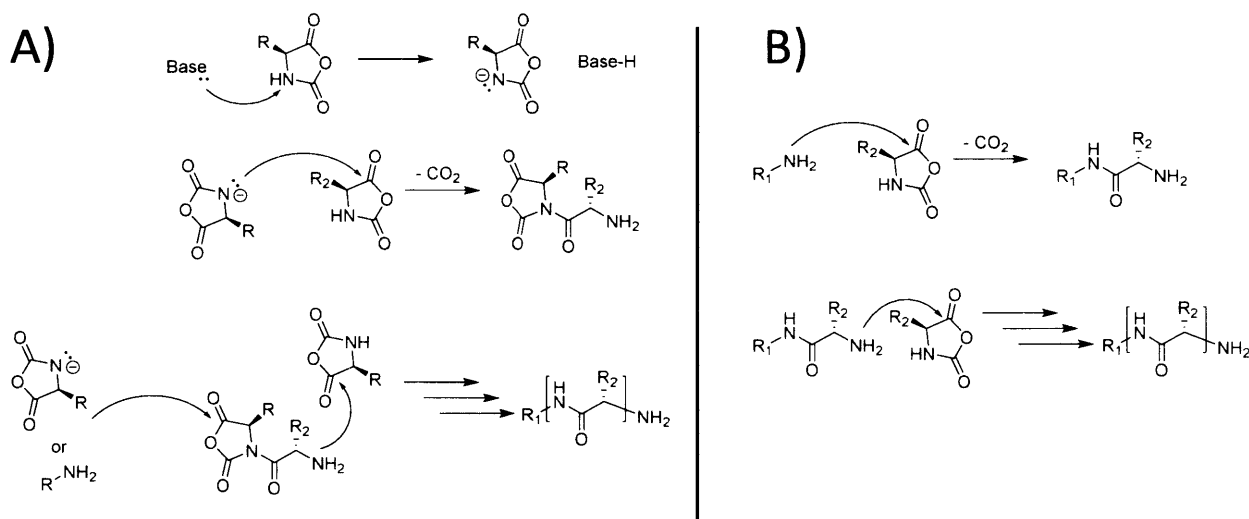

Figure 3.3. Initiation and propagation of NCA ring opening polymerization by A) an activated monomer or B) a nucleophilic amine.

There are many methods to minimize side reactions during NCA polymerization including but not limited to: the use of an amine hydrochloride salt as an initiator[3], TMS protected amines as an inititator[4,5], polymerization under reduced temperature and/or pressure[6,7], purging or sparging the polymerization with inert gas[8], and transition metal catalysts[9]. No individual method is clearly superior to the others, and the relevance of each method is dependent on the size and structure of the target polypeptide.

For the purpose of generating end functionalized PPLG for end linking, all the methods listed above were investigated, but ultimately polymerization under reduced temperature/pressure or sparging with argon at room temperature was chosen for initiator versatility and convenience. These methods yielded PPLG of low dispersity and predictable molecular weights. Moreover, end caps could be installed on PPLG if the polymerization was monitored and the capping reagent was introduced within a short time frame after complete consumption of NCA monomer. Consumption of the monomer was determined by the disappearance of the carbonyl stretch of the anhydride which has a strong and distinct absorbance at 1786 cm^{-1} (Figure 3.4). A delay in end-capping or reaction workup provides opportunities for side reactions to consume the amine on the end of the polymer, resulting in reduced capping efficiency. Purification of polymers with different end functionality is often not possible given the small influence of the end group on the physical properties of the polymer, and polymers without the proper end functionality will not participate in end linking reactions as intended and result in defects in the form of a dangling end in the final end-linked network. Because the primary motivation behind end-linking is to create a more uniform network, these defects would diminish the advantages of generating an end linked network over a randomly cross-linked network.
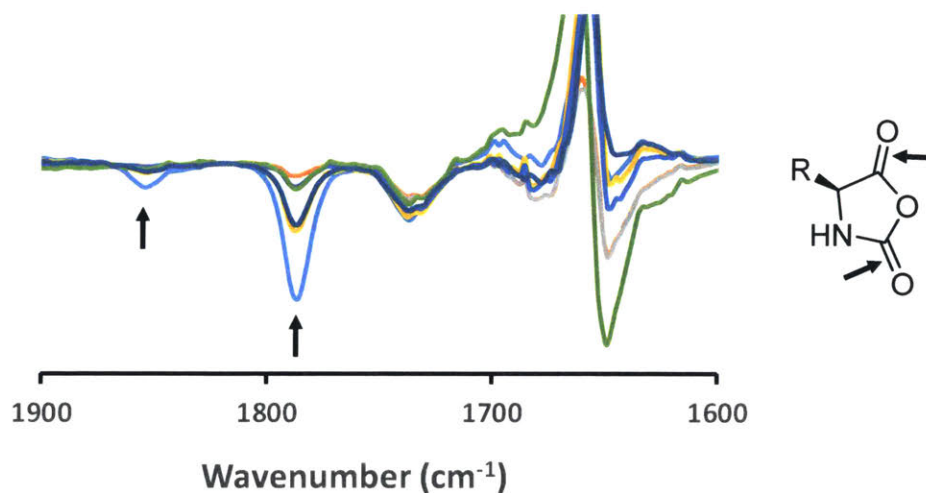

Figure 3.4. FTIR spectra of a NCA polymerizations reaction at various time points during the reaction illustrating the disappearance of the carbonyl stretch from the anhydride at 1786 cm^{-1} and a weaker stretch at 1850 cm^{-1}.

Various chemistries were considered for the end-linking of polymers. The reaction of an amine with a carboxylic acid or activated ester has been previously used to form hydrogels[10] and a N-terminal amine could be used in such a fashion. However, the reaction between stoichiometric amounts of amine and carboxylic acid under the dilute aqueous conditions typical of end-linked hydrogel preparation is slow and often incomplete. Moreover, previous members of the Hammond lab have been unsuccessful when using this tactic. Alternatively, the amine may be used as a chemical handle for attachment of an orthogonal reactive group. This approach enables to use of excess reagent to ensure complete functionalization of the polymer end with a more reactive functional group. Although this approach adds steps to the synthesis, a reactive polymer end group maximizes the chances of forming an ideal network.

After considering a variety of efficient and well characterized reactions, the inverse electron demand Diels Alder reaction between a tetrazine and strained alkene as well as the radical addition of a thiol to an alkene were chosen for end linking (Figure 3.5). These reactions are orthogonal to the copper catalyzed azide alkyne cycloaddition reaction used to graft PPLG. In addition, these reactions are highly efficient, and all components of the reaction are stable in neutral aqueous solutions. Both reactions have previously been used for the formation of end-linked polymeric networks from telechelic star polymers[11], but there is uncertainty regarding the efficacy of the thiol-ene reaction for conjugation of macromolecules.[12] Because both reactions have advantages and disadvantages in the context of network formation, PPLG end functionalized with norbornene was synthesized as a macromer compatible with either end-linking approach. The radical addition of a thiol to norbornene has been difficult to monitor in the context of network formation. Once a thiol radical is generated, it either reacts with norbornene or undergoes side reactions, rarely reverting back to a free thiol. Consequently, the concentration of free thiol, which is easily measured by Ellman's assay, is not related the extent of linking. On the other hand, reaction of tetrazine can be monitored by visible wavelength spectroscopy. Furthermore, the reaction between tetrazine and norbornene is spontaneous and does not require addition radical initiators, but evolution of nitrogen gas as a byproduct of the reaction can disrupt the physical integrity of the gel.[13]
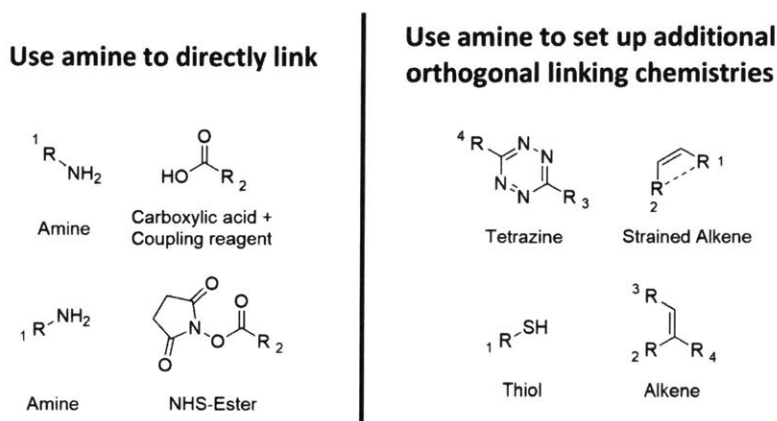
Figure 3.5. Potential reactions for the end linking of polypeptides.

The initial plan to form an end-linked network involved linking difunctional PPLG macromers by a tetra or hexafunctional cross-linker. The difunctional PPLG macromer was synthesized by either initiation with norbornene amine followed by end-capping with a norbornene active ester or by initiation with a diamine followed by end-capping with a norbornene active ester (Figure 3.6). Both approaches are viable for the synthesis norborne end-functionalized PPLG and the presence of norbornene groups on the ends of the polymer was verified by titration with a tetrazine (Figure 3.7). As another test, organogels were formed in DMSO by crosslinking the norbornene end-functionalized PPLG with a tetrazine end-functionalized 8-arm poly(ethylene glycol). Despite these initial results, attempts to form a hydrogel by crosslinking of a the same PPLG grafted with oligo(ethylene glycol) were unsuccessful. The NMR spectrum of the polymer after side chain grafting by copper(I) catalyzed azide alkyne cycloaddition revealed a significantly diminished peak corresponding to the vinyl protons from the norbornene end group (Figure 3.8), possibly due to reaction between norbornene and the azide during grafting[14] and/or dilution of the end groups of the polymer with the oligo(ethylene glycol) side chain.
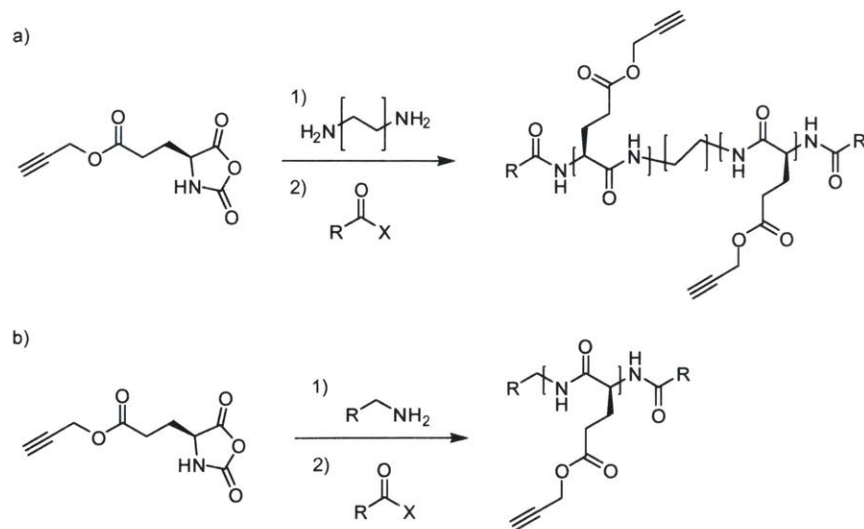
Figure 3.6. Two approaches to difunctional PPLG: A) initiation with a diamine followed by capping or B) initiation with a functionalized amine followed by capping. 1,12-Diaminododecane and 5-norbornene-2-methylamine were chosen as initiators with distinct proton NMR shifts to aid in molecular weight characterization by end group analysis of the polymer.
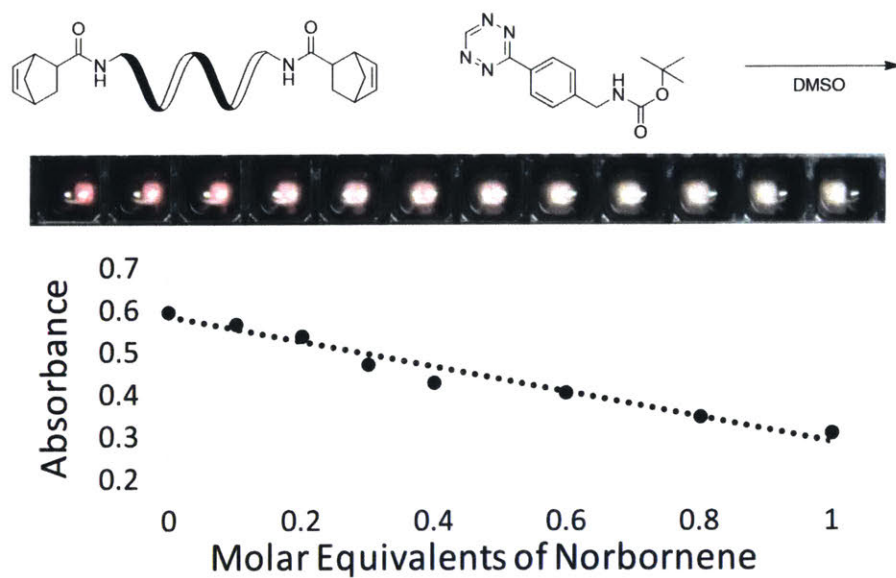

**Figure 3.7.** Titration of norbornene terminated PPLG with tetrazine in DMSO.
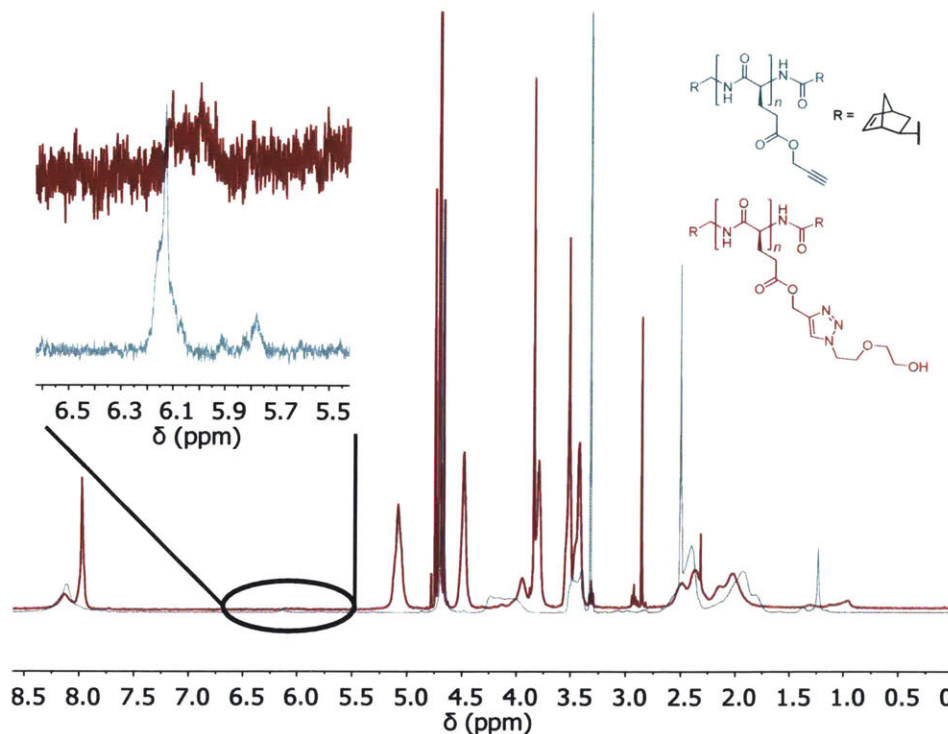
Figure 3.8. ^{1}H NMR spectrum of norbornene terminated PPLG before and after grafting by copper catalyzed cycloaddition with 2-(2-azidoethoxy)ethanol. The insert highlights vinyl protons from the norbornene end groups.

The inability of norbornene terminated PPLG to form hydrogels prompted additional studies of a model system to better understand the reactivity of the norbornene end group. Because the radical initiated reaction between a thiol and norbornene has previously been used to form PPLG hydrogels[1], there may be additional steric or entropic penalties as consequence of installing the norbornene group on the end of the polymer versus on the side chains. Steric penalties may be a result of the proximity of the norbornene group to the polymer backbone where it may be blocked by a dense brush of oligo(ethylene glycol). When norbornene was previously incorporated onto the side chain of PPLG macromers for network formation, it was distanced by a ~500 Da oligo(ethylene glycol) linker. Entropic penalties may result from restricted or slower motion of the polymer backbone relative to a dangling side chain. To test these hypotheses, PPLG terminated with a single norbornene and grafted with oligo(ethylene glycol) was synthesized as a water soluble model polymer. The reaction between this polymer and a thiol crosslinker should not form a network, even at complete conversion, meaning this system may be readily characterized by NMR spectroscopy after reaction. Vinyl protons corresponding to unreacted norbornene are

detected after exposure of a deuterium oxide solution of model PPLG, 8-arm 10kDa PEG-thiol, and a photoinitiator to UV light for 10 minutes (Figure 3.9a). When β-mercaptoethanol is also present in the previously described solution, the signal from norbornene is greatly diminished after illumination (Figure 3.9b). It was hypothesized that the photoreaction involving a small molecule thiol instead of the 8-arm 10kDa PEG-thiol is less sterically and entropically demanding. These results indicate that it may be necessary to reduce the steric and entropic barriers to reaction. One solution is to place the norbornene group on the end of a spacer, such as the case with sidechain-linked PPLG networks, to achieve network formation in the end-linked system.
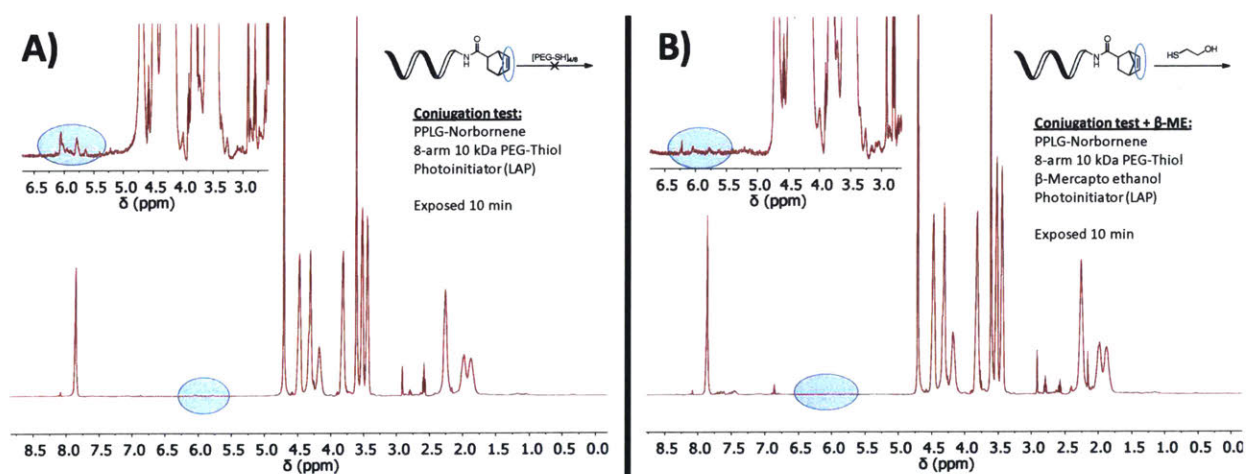
Figure 3.9. A) Photoreaction of a norbornene terminated, oligo(ethylene glycol) grafted PPLG with an 8-arm 10kDa PEG-thiol. The highlighted signals correspond to the vinyl protons on unreacted norbornene. B) A similar photoreaction with the addition of β-mercaptoethanol to the solution prior to illumination. The vinyl proton signal is greatly reduced by addition of a small molecule thiol.

A multi-arm PPLG synthesized by installation of the norbornene end functionality post-grafting would remedy some of the aforementioned problems preventing hydrogel formation. The multiple arms could serve to increase the concentration of norbornene end groups. Moreover, a multi-arm polymer is able to form a gel at lower conversions by Flory-Stockmayer theory. Assuming all functional groups are equally reactive and reactions only occur between the end functional groups of the polymers, the conversion at which a network is formed is inversely proportional to the

average functionality of the polymers (Figure 3.10). Furthermore, a multi-arm PPLG opens the possibility of pure PPLG gels that may be formed without other cross linkers if PPLG is synthesized with complimentary end-groups. The absence of a flexible polymeric crosslinker would amplify attributes of the polymer network endowed by the rigid α-helical structure of PPLG.

For 1 to 1 stoichiometry of reactive end-groups:

$$\pi_c = \frac{2}{f_{avg}}$$

π_c — $conversion\ at\ gel\ point$

f_{avg} — $Average\ functionality\ of\ polymers\ (weighted)$

Figure 3.10. A simplified Flory-Stockmayer equation for 1 to 1 stoichiometry of end groups. Increasing the average functionality of polymers decreases the conversion required to form a gel.

Small molecule compounds with many amines are not readily commercially available and end group analysis by NMR of a multi-arm PPLG synthesized by initiation with a commercially available polymeric amine or poly(amidoamine) dendrimers would be complicated by dispersity of the initiator and lack of distinct NMR shifts.. A six-arm, hexa-amine initiator with a benzene core was designed so that the aromatic protons in the core and the well-defined number of amines per initiator would aid in NMR analysis of PPLG. The synthesis began with protection of the primary amines on N-(3-aminopropyl)propane-1,3-diamine with *tert*-butyloxycarbonyl groups. Three of these molecules were joined by reaction with 1,3,5-benzenetricarbonyl trichloride followed be deprotection with anhydrous hydrochloric acid. Because the final result is a hydrochloride salt, the initiator must first be deprotonated or the polymerization must be reoptimized and run under different conditions. Quantitative deprotonation was determined to be unnecessary as NCA polymerizations have been successful without complete deprotonation of the initiator or in the presence of catalytic acid[15,16]. However, a base much stronger than a primary amine is important to ensure that the acid-base equilibrium favors a deprotonated primary amine, guaranteeing that initiation of polymerization is mostly by the hexa-amine and not by the base. The conjugate acid of the ideal base should not interfere with the polymerization. A variety of bases were considered for this purpose (Figure 3.11), but potassium *t*-butoxide was chosen. It is

approximately seven orders of magnitude more basic than a primary amine but not so basic as to cause side reactions during addition to a solution of the initiator in polar aprotic solvent.

R^{NH_2}

Amine
pK$_a$ ~ 9-10

1,8-Diazabicyclo[5.4.0]undec-7-ene
(DBU)
pK$_a$ ~ 12

KO

Potassium *t*-Butoxide
pK$_a$ ~ 17

Li

butyllithium
pK$_a$ ~ 50
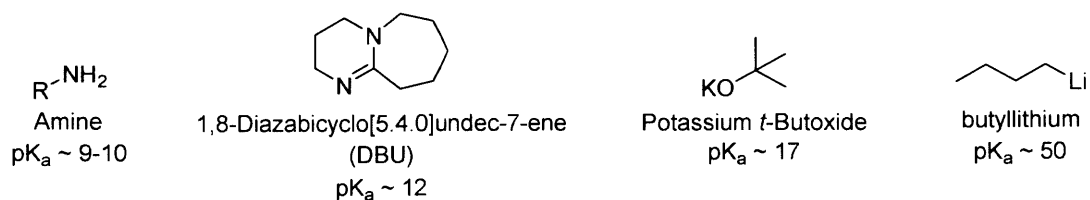
Figure 3.11. Bases considered for deprotonation of hexa-amine initiator annotated with pK$_a$'s of the respective conjugate acid.

To install the norbornene functionality post grafting with the addition of a spacer, the capping strategy was also changed to initiate the polymerization with a multi-functional amine and end cap with excess of a M$_n$ ~600 Da poly(ethylene glycol) bis(carboxymethyl) ether preactivated with the uronium/iminium amide bond coupling reagent, HATU. The resulting carboxylic acid terminated polypeptide can be grafted by azide alkyne cycloaddition to be made water soluble prior to coupling of 5-norbornene-2-methylamie with the carboxylic acid end group for end-linking reactions, thus avoiding any reactions between norbornene and azide (Figure 3.12).
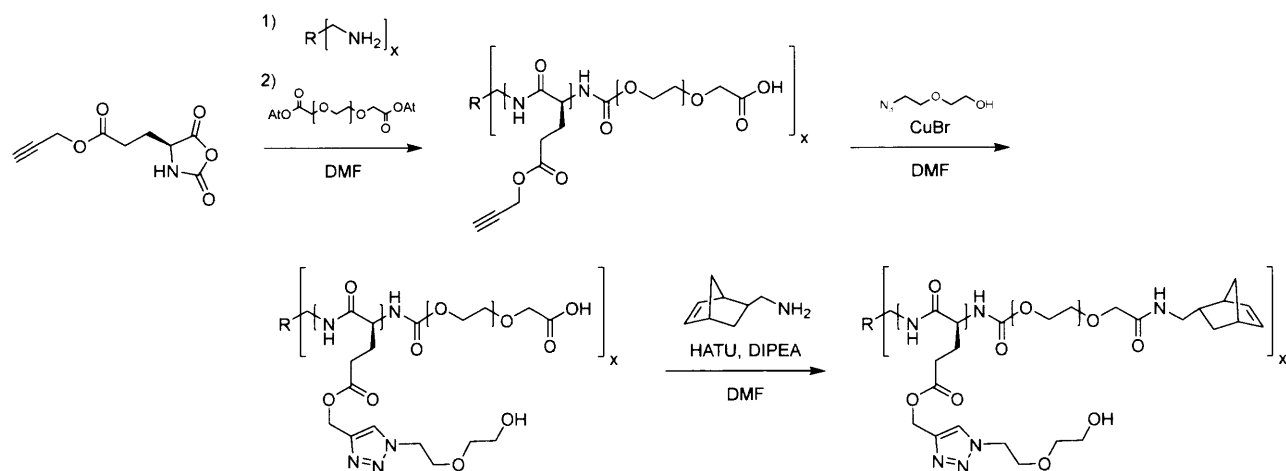
Figure 3.12. Synthetic route for preparation of PPLG with norbornene end groups on a ~500Da PEG spacer after grafting.

End-linked PPLG hydrogels were successfully fabricated with this PPLG by crosslinking with an 8-arm 10kDa PEG-thiol (Figure 3.13). However, the gels were extremely soft with all gels unable to hold their original cylindrical shape without being completely submerged in water. Because of this, further characterization of these gels was not attempted. At this point, the potential benefit of an end-linked gel was reevaluated and it was decided that the gels may possess too many defects to exhibit unique properties. End capping PPLG is complicated by the side reactions during polymerization, which are exacerbated by the difficulties in purifying the γ-propargyl-L-glutamate N-carboxyanhydride monomer. The imperfect nature of the end capping reaction contributes to defects, and this is amplified by any inadequacies in the macromer linking reaction. Too many defects cause the network properties to deviate from ideal and the end-linked network begins to resemble the side chain cross-linked network. Furthermore, the use of linkers on the ends of PPLG as well as a flexible polymeric cross-linker dilutes the portion of the polymer network comprised of rigid α-helical polypeptides. It is unlikely that a small amount of α-helical character would result in a significantly unique hydrogel, and the resulting gels may approximate the many examples of end-linked poly(ethylene glycol) networks in the literature. Ultimately, the uncertainty of any distinct advantages and difficulty in synthesis discouraged further efforts in the formation of end-linked PPLG hydrogel networks.
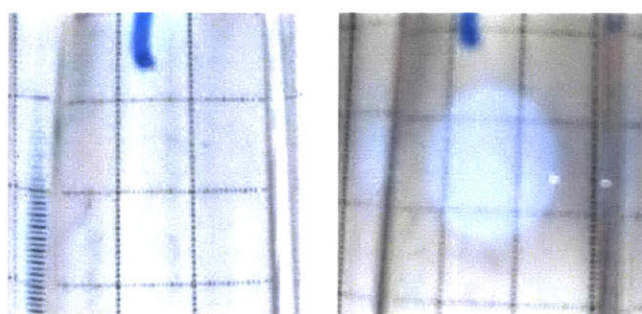

PPLG + 8arm 10kPEG-SH
13.5 wt% polymer hydrogel

Figure 3.13. A 120 µL cylindrical end-linked hydrogel fabricated from PPLG and an 8-arm 10kDa PEG-thiol by photoinitiated thiol norbornene reaction. The hydrogel is extremely faint under ambient light (left), but more apparent under direct illumination (right).

3.3 Conclusion

Formation of end-linked PPLG networks was explored and a synthesis of PPLG was designed to incorporate reactive end groups. While these groups were accessible for formation of naïve PPLG networks in organic solvent, their reactivity was altered by grafting of PPLG, making the initial approach unfeasible for preparation of a hydrogel. After iterations of troubleshooting to optimize the reactivity and density of the end groups, these macromers were incorporated into end-linked PPLG hydrogels. However, the initial assessment of mechanical properties, re-evaluation of potential benefit, and difficult synthesis discouraged further exploration of end-linked PPLG hydrogels.

3.4 Experimental

N₃∼O∼OH
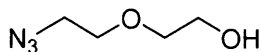
2-(2-azidoethoxy)ethan-1-ol

To a stirring solution of 2-(2-chloroethoxy)ethan-1-ol (32.7 g, 0.263 mol) in water (200 mL) was added sodium azide (39.4 g, 0.606 mol). The reaction was heated to 80°C and stirred at this temperature for 4 days. Afterwards, the reaction was cooled to room temperature and the solution was extracted three times with diethyl ether (600 mL total). The combined organic extracts were rinsed with brine and dried over magnesium sulfate. Removal of solvent *in vacuo* gave a clear oil (28.1 g, 0.214 mol, 82%). ^{1}H NMR (400 MHz, Chloroform-*d*) δ 3.75 (s, 2H), 3.70 (s, 2H), 3.63 (s, 2H), 3.42 (s, 2H), 2.43 (s, 1H). ^{1}H NMR (400 MHz, DMSO-*d₆*) δ 4.60 (t, *J* = 5.2 Hz, 1H), 3.67 – 3.56 (m, 2H), 3.56 – 3.42 (m, 4H), 3.43 – 3.36 (m, 2H). ^{13}C NMR (101 MHz, Chloroform-*d*) δ 72.51, 70.08, 61.79, 50.78.
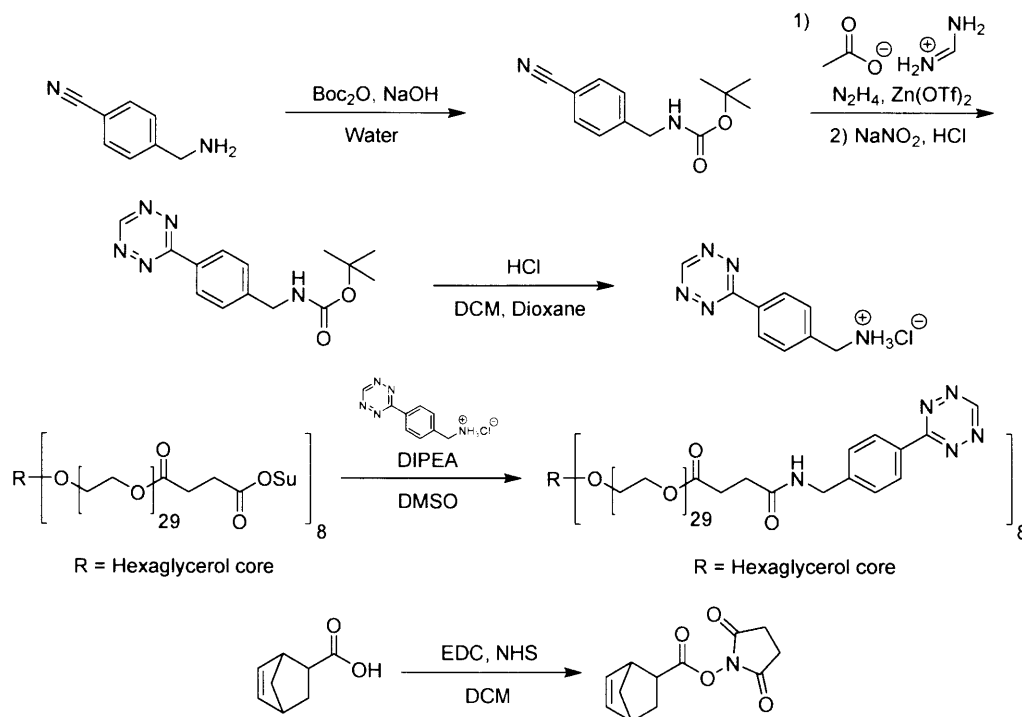

Figure 3.14. Synthetic routes for preparation of linking materials and reagents.
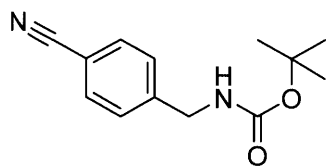
tert-butyl (4-cyanobenzyl)carbamate

tert-butyl (4-cyanobenzyl)carbamate was synthesized according to a modified literature procedure.[17] To a stirring solution of sodium hydroxide (3.6 g, 89 mmol) in water (24 mL) was added di-*tert*-butyl dicarbonate (7.1 g, 33 mmol) followed by 4-(aminomethyl)benzonitrile (5.0 g, 30 mmol). The addition results in an exotherm, evolution of gas, and generation of a white precipitate. The reaction was stirred at room temperature for 6 hours after which the precipitate was isolated by filtration, washed with water, and dried *in vacuo* to give a white powder (5.6 g, 24 mmol, 81%). ^{1}H NMR (400 MHz, Chloroform-*d*) δ 7.62 (d, J = 8.3 Hz, 2H), 7.39 (d, J = 8.4 Hz, 2H), 4.95 (s, 1H), 4.37 (d, J = 6.3 Hz, 2H), 1.46 (s, 9H).
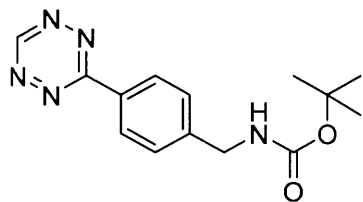

tert-butyl (4-(1,2,4,5-tetrazin-3-yl)benzyl)carbamate

tert-butyl (4-(1,2,4,5-tetrazin-3-yl)benzyl)carbamate was synthesized according to a modified literature procedure.[18] To a stirring solution of *tert*-butyl (4-cyanobenzyl)carbamate (2.0 g, 8.4 mmol), formamidine acetate (8.8 g, 84 mmol), and zinc trifluoromethanesulfonate (1.5 g, 4.2 mmol) in DMF (7 mL) chilled by an ice water bath was added anhydrous hydrazine (13 mL, 0.42 mol) dropwise over 15 minutes. The ice water bath was removed and the reaction was stirred at 30°C for 24 hours. A solution of sodium nitrite (11.6 g, 169 mmol) in water (34 mL) was added dropwise over 4 minutes followed by 1M HCl dropwise until the pH of the reaction was approximately 3. The precipitate was isolated by filtration and purified by silica gel flash chromatography eluted by a solution of 30% ethyl acetate:hexanes to give a pink powder (1.29 g, 4.49 mmol, 53%). ^{1}H NMR (400 MHz, Chloroform-*d*) δ 10.21 (s, 1H), 8.60 (d, J = 8.4 Hz, 2H), 7.53 (d, J = 8.4 Hz, 2H), 5.00 (s, 1H), 4.44 (s, 2H), 1.48 (s, 9H). R$_f$ 0.35 (30% EtOAc:DCM, colored compound).

105
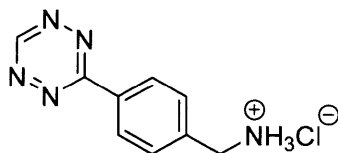
**(4-(1,2,4,5-tetrazin-3-yl)phenyl)methanaminium chloride**

To a stirring solution of *tert*-butyl (4-(1,2,4,5-tetrazin-3-yl)benzyl)carbamate (0.32 g, 1.0 mmol) in dichloromethane (15 mL) was added 4M HCl in dioxane (8 mL) in one portion. The reaction was stirred at room temperature for 5 hours. The solution was sparged with argon for 20 minutes and the solvent was removed *in vacuo* to give a pink powder (0.25 g, 1.0 mmol, 100%). ^{1}H NMR (400 MHz, Deuterium Oxide) δ 10.43 (s, 1H), 8.56 (d, J = 8.1 Hz, 2H), 7.76 (d, J = 8.1 Hz, 2H), 4.36 (s, 2H). ^{1}H NMR (400 MHz, DMSO-d_6) δ 10.63 (s, 1H), 8.55 (d, J = 8.4 Hz, 2H), 8.50 (s, 1H), 7.78 (d, J = 8.4 Hz, 2H), 4.19 (s, 2H).
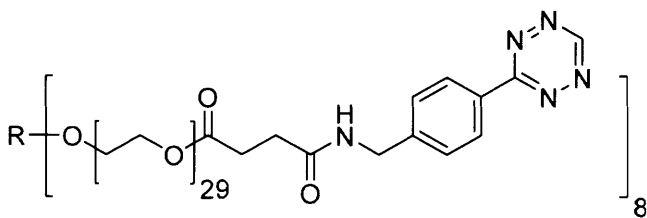
R = Hexaglycerol core

8-arm tetrazine terminated poly(ethyele glycol)

To a solution of 10.3 kDa succinimidyl ester terminated poly(ethylene glycol) (200 mg, 0.0194 mmol) and (4-(1,2,4,5-tetrazin-3-yl)phenyl)methanaminium chloride (39 mg, 0.16 mmol) in DMSO (3 mL) was added diisopropylethylamine (54 µL, 0.31 mmol). The solution was mixed and incubated at room temperature for 26 hours, dialyzed against deionized water across a 3,500 Da MWCO regenerated cellulose membrane, frozen, and lyophilized to give a pink solid (196 mg). NMR analysis indicated approximately 6 tetrazine groups per polymer, equating to 75% substitution. ^{1}H NMR (400 MHz, Chloroform-d) δ 10.22 (s, 6H), 8.59 (d, J = 8.0 Hz, 12H), 7.53 (d, J = 8.1 Hz, 14H), 6.54 (s, 5H), 4.57 (d, J = 6.0 Hz, 11H), 4.25 (t, J = 4.8 Hz, 16H), 3.64 (s, 936H), 2.85 – 2.66 (m, 14H), 2.58 (t, J = 6.7 Hz, 14H), 1.75 (s, 18H), 1.25 (s, 12H).
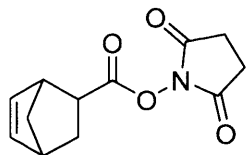
## 5-Norbornene-2-carboxylic acid succinimidyl ester, mixture of *endo* and *exo*

Synthesis of norbornene-NHS was performed according to a modified literature procedure.[19] To a stirring solution of 5-Norbornene-2-carboxylic acid, mixture of *endo* and *exo*, predominantly *endo* (15 mL, 96 mmol), N-hydroxysuccinimide (15.5 g, 135 mmol), and DCM (200 mL) was added EDC-HCl (24.0 g, 125 mmol) in one portion. The reaction was stirred for 24 hours after which consumption of starting material was verified by TLC. The crude reaction mixture was washed three times with water (125 mL) followed by a saturated aqueous solution of sodium bicarbonate (125 mL) and brine (125 mL) and dried over sodium sulfate. The solvent was removed *in vacuo* to give a clear oil which solidified upon standing. Recrystallization from ethyl acetate and hexanes yielded a white crystalline solid (16.6 g, 70.7 mmol, 73.5%). ^{1}H NMR (400 MHz, Chloroform-*d*) δ 6.34 – 6.04 (m, 2H), 3.44 – 3.38 (m, 1H), 3.25 (dt, J = 9.1, 3.8 Hz, 1H), 3.06 – 2.93 (m, 1H), 2.81 (d, J = 1.8 Hz, 4H), 2.13 – 1.91 (m, 1H), 1.55 – 1.47 (m, 2H). ^{13}C NMR (101 MHz, Chloroform-*d*) δ 170.11, 138.28, 132.33, 49.81, 46.60, 42.68, 40.77, 29.74, 25.73. R$_f$ 0.26 (33% EtOAc:Hex, visualized by KMnO$_4$ stain and UV)


lithium phenyl(2,4,6-trimethylbenzoyl)phosphinate

Synthesis of lithium acylphosphinate was performed according to a modified literature procedure.[20] A flame dried Schlenk flask equipped with a magnetic stir bar was charged with dimethyl phenylphosphonite (3.0 g, 18 mmol). 2,4,6-Trimethylbenzoyl chloride (3.2 g, 18 mmol) was added dropwise over 8 minutes with stirring. The reaction was stirred for 20 hours, after which a solution of lithium bromide (6.1 g, 71 mmol) in 2-butanone (100 mL) was added and the reaction was heated to 50°C and stirred for 10 minutes. The reaction was removed from heat and allowed to cool in the dark for 4 hours. The precipitate was isolated by filtration and washed with 2-butanone to give a white powder (4.37 g, 14.9 mmol, 84%). ^{1}H NMR (400 MHz, Deuterium Oxide)

δ 7.86 – 7.64 (m, 2H), 7.61 – 7.52 (m, 1H), 7.47 (td, J = 7.6, 3.2 Hz, 2H), 6.88 (s, 2H), 2.23 (s, 3H), 2.03 (s, 6H).
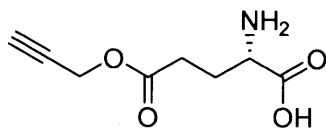

γ-propargyl-L-glutamate

To a stirring suspension of glutamic acid (44.1 g, 0.300 mol) in propargyl alcohol (1.3 L) chilled by an ice water bath was added dropwise trimethylsilyl chloride (94 mL, 0.74 mol) over 1.5 hours. The ice water bath was removed and the suspension was stirred for 36 hours. Diethyl ether (8 L) was added, and the precipitate was isolated by filtration, washed with diethyl ether, and dried *in vacuo* to give a brownish off white solid (52.2 g, 0.282 mol, 94%). ^{1}H NMR (400 MHz, Deuterium Oxide) δ 4.68 (d, J = 2.5 Hz, 2H), 4.02 (t, J = 6.7 Hz, 1H), 2.85 (t, J = 2.5 Hz, 1H), 2.61 (td, J = 7.4, 2.5 Hz, 2H), 2.18 (dp, J = 19.7, 7.3 Hz, 2H). ^{13}C NMR (101 MHz, Deuterium Oxide) δ 173.46, 171.69, 77.61, 76.08, 52.78, 52.14, 29.42, 24.74.
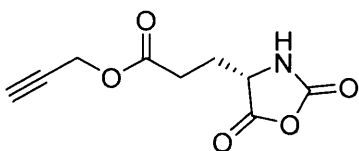
γ-propargyl-L-glutamate N-carboxyanhydride

A 2-neck flask equipped with a magnetic stir bar and reflux condenser continuously cooled to -4°C was charged with γ-propargyl-L-glutamate (10 g, 54 mmol) and ethyl acetate (200 mL). The suspension was stirred and heated to 85°C. A separate flask was charged with triphosgene (40 g, 0.13 mol) and connected to the 2-neck flask by polymer tubing. To the end of the tubing was attached a glass pipette, which was submerged in the ethyl acetate suspension. Aliquat 336 (6 mL, 0.01 mol) was added to the triphosgene and the generated phosgene gas was chased with a steady stream of argon and bubbled through the reaction until solids were no longer visible. The temperature of the reflux condenser was raised to 10°C and the reaction was then sparged with argon for 1 hour to remove excess phosgene gas. The solution was removed from heat and chilled with an ice water bath, washed with cold water, cold 0.5% (w/v) aqueous sodium bicarbonate,

rinsed with cold brine, and dried over magnesium sulfate. Removal of solvent *in vacuo* gave a viscous yellow oil with residual ethyl acetate (10.24 g with 30 mol% EtOAc, 8.71 g based on neat material, 41.3 mmol, 76%). Residual ethyl acetate does not affect the use of this NCA monomer for polymerization. ^{1}H NMR (400 MHz, Chloroform-*d*) δ 6.56 (s, 1H), 4.72 (d, *J* = 2.5 Hz, 2H), 4.43 (t, *J* = 6.1 Hz, 1H), 2.62 (t, *J* = 6.9 Hz, 2H), 2.53 (t, *J* = 2.5 Hz, 1H), 2.38 – 2.23 (m, 1H), 2.25 – 2.08 (m, 1H).
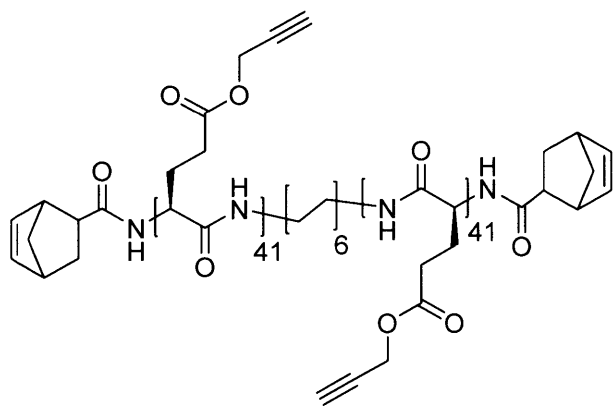
Norbornene terminated PPLG

A flame dried Schlenk flask equipped with a magnetic stir bar was charged with a solution of 1,12-diaminododecane (13.1 mg, 0.0654 mmol) in DMF (1 mL). A solution of γ-propargyl-L-glutamate N-carboxyanhydride (1.0 g, 4.7 mmol) in DMF (10 mL) was added in one portion and the reaction was stirred and sparged with argon for 10 hours. 5-Norbornene-2-carboxylic acid succinimidyl ester, mixture of *endo* and *exo* (0.80 g, 6.8 mmol) followed by diisopropylethylamine (1.8 mL, 10 mmol) were added in one portion and the reaction was stirred for 48 hours with continuous purging of the headspace with argon. The polymer was precipitated by addition to diethyl ether. The precipitate was collected by centrifugation and washed with diethyl ether to give a white powder (0.40 g). End group analysis by NMR indicated a degree of polymerization of 82 and 79% conversion of end-groups to norbornene. ^{1}H NMR (400 MHz, DMSO-*d*₆) δ 8.12 (s, 84H), 6.32 – 5.63 (m, 3.15H), 4.68 (s, 165H), 4.34 – 3.78 (m, 82H), 3.39 (s, 82H), 2.41 (s, 160H), 1.95 (s, 160H), 1.38 (s, 4H), 1.24 (s, 16H), 1.13 (s, 29H). GPC (10mM LiBr in DMF, PMMA standards) M_n 1577, PDI 1.11.
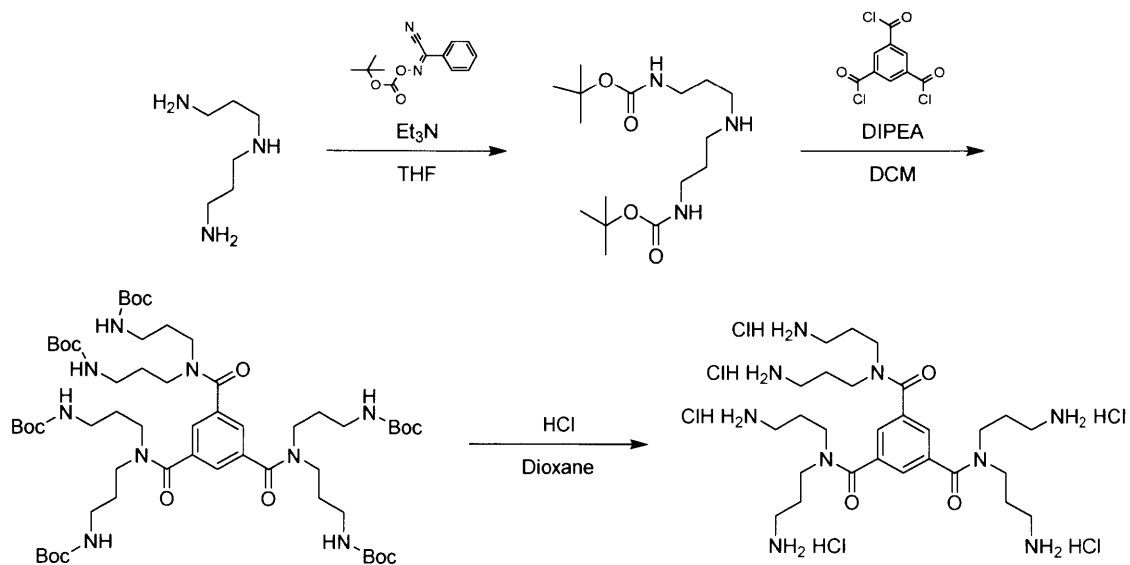
**Figure 3.15.** Synthetic route for preparation of 6-arm amine initiator
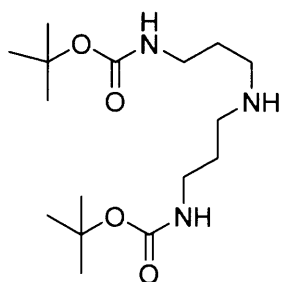
di-*tert*-butyl (azanediylbis(propane-3,1-diyl))dicarbamate

di-*tert*-butyl (azanediylbis(propane-3,1-diyl))dicarbamate was synthesized according to a modified literature procedure[21]. To a stirring, chilled solution of N[1]-(3-aminopropyl)propane-1,3-diamine (6.56 g, 50 mmol) and triethylamine (21 mL, 150 mmol) in THF (250 mL) over an ice water bath was added dropwise a solution of 2-(Boc-oxyimino)-2-phenylacetonitrile (24.6 g , 100 mmol) in THF (250 mL). After addition, the ice water bath was removed and the reaction was stirred at room temperature for 20 hours. The solvent was removed *in* vacuo and the crude reaction mixture was diluted with chloroform, washed twice with 1M HCl, four times with 5 w/v% NaOH, three times with brine, and dried over magnesium sulfate. Removal of the solvent *in vacuo* afforded a white solid (14.1 g, 42.7 mmol, 85%). ^{1}H NMR (400 MHz, Chloroform-*d*) δ 5.19 (s, 1H), 3.22 (s, 4H), 2.65 (s, 4H), 1.65 (s, 4H), 1.44 (s, 18H). ^{13}C NMR (101 MHz, Chloroform-*d*) δ 156.28, 79.14, 47.58, 39.09, 29.92, 28.57.
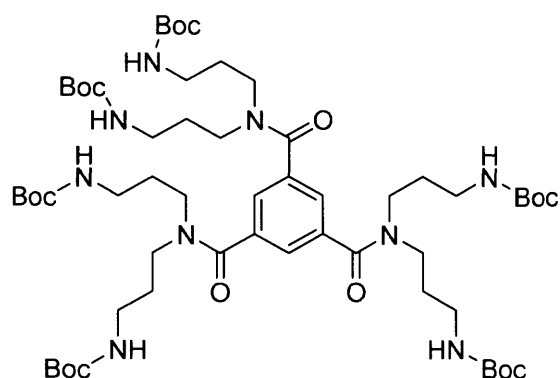
hexa-*tert*-butyl (((benzene-1,3,5-tricarbonyl)tris(azanetriyl))hexakis(propane-3,1-diyl))hexacarbamate

The boc-protected 6-arm initiator was synthesized according to a modified literature procedure.[22] To a flame dried Schleck flask equipped with a magnetic stir bar was added protected amine (4.0 g, 12 mmol), diisopropylethylamine (4.2 mL, 24 mmol), and dichloromethane (25 mL) and the solution was chilled over an ice water bath. 1,3,5-Benzenetricarbonyl trichloride (1.1 g, 4.1 mmol) was a then added dropwise over 1 minute with stirring, after which the ice water bath was removed and the solution was stirred at room temperature overnight. The crude reaction mixture was diluted with chloroform and washed with 1M HCl followed by 1M NaOH, rinsed with brine, and dried over sodium sulfate. Removal of solvent *in vacuo* afforded a brown foamy solid (3.7 g, 3.2 mmol, 78%). ^{1}H NMR (400 MHz, Chloroform-*d*) δ 7.44 (s, 1H), 5.26 (s, 2H), 3.57 (s, 2H), 3.32 – 3.12 (m, 4H), 2.98 (s, 2H), 1.77 (s, 4H), 1.44 (s, 18H). ^{13}C NMR (101 MHz, Chloroform-*d*) δ 170.36, 156.27, 137.46, 125.88, 79.28, 47.20, 42.45, 28.55.
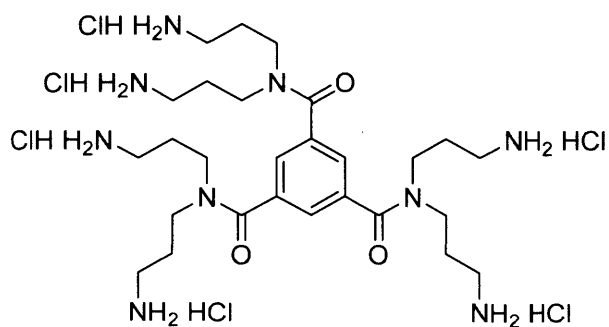

N^1,N^1,N^3,N^3,N^5,N^5-hexakis(3-aminopropyl)benzene-1,3,5-tricarboxamide hexahydrochloride

111

To a stirring solution of boc-protected 6-arm initiator (1.06 g, 0.921 mmol) in dioxane (5 mL) was added dropwise 4M HCl in dioxane (12 mL) over 1 minute. The reaction was stirred for 2 hours, after which diethyl ether was added to form a precipitate. The precipitate was collected by centrifugation, washed with diethyl ether, and dried *in vacuo* to yield a white hygroscopic powder (0.71 g, 0.93 mmol, 100%). ^{1}H NMR (400 MHz, Deuterium Oxide) δ 7.72 (s, 1H), 3.69 (t, J = 7.3 Hz, 2H), 3.43 (t, J = 7.8 Hz, 2H), 3.15 (t, J = 7.5 Hz, 2H), 2.87 (t, J = 8.0 Hz, 2H), 2.13 (p, J = 7.6 Hz, 2H), 1.99 (p, J = 8.3 Hz, 2H). ^{13}C NMR (101 MHz, Deuterium Oxide) δ 172.47, 137.40, 125.87, 47.47, 43.13, 37.76, 37.32, 26.52, 25.57.
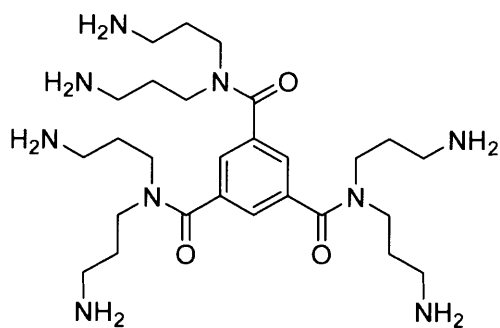

General method for deprotonation of 6-arm amine initiator, N1,N1,N3,N3,N5,N5-hexakis(3-aminopropyl)benzene-1,3,5-tricarboxamide

A flame dried Schlenk flask equipped with a magnetic stir bar was charged with a solution of N^1,N^1,N^3,N^3,N^5,N^5-hexakis(3-aminopropyl)benzene-1,3,5-tricarboxamide hexahydrochloride and fluorene (10 mg) in anhydrous DMSO. A 1M solution of potassium *tert*-butoxide in THF was added dropwise with stirring until a persisting color change of the solution was observed, indicating complete deprotonation of the initiator. The volume of potassium *tert*-butoxide in THF added was recorded. A separate flame dried Schlenk flask equipped with a magnetic stir bar was charged with N^1,N^1,N^3,N^3,N^5,N^5-hexakis(3-aminopropyl)benzene-1,3,5-tricarboxamide hexahydrochloride and formamide. A 1M solution of potassium *tert*-butoxide in THF (95% of the previous volume) was added dropwise with stirring. The THF and *tert*-butanol were removed *in vacuo* and the concentration of initiator in solution was determined by NMR.
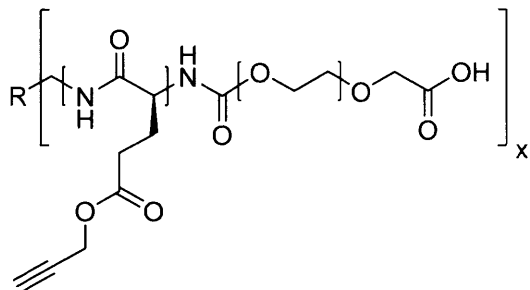
General method for carboxy-PEG terminated PPLG

A flame dried Schlenk flask equipped with a magnetic stir bar was charged with a solution of amine initiator. A solution of γ-propargyl-L-glutamate N-carboxyanhydride in DMF (0.10 g/mL, 0.38 mmol/mL) was added in one portion and the reaction was placed *in vacuo* to remove the carbon dioxide byproduct. The reaction was monitored by FTIR (anhydride stretch at 1786 cm^{-1}). After complete consumption of the monomer, a solution of poly(ethylene glycol) bis(carboxymethyl) ether M_n ~600 Da (10 equivalents per amine on initiator), HATU (10 equivalents per amine on initiator), and DIPEA (20 equivalents per amine on initiator) in DMF (1 mL per mmol PEG/HATU) that was preactivated by mixing for 20 minutes was added in one portion. The reaction was stirred under argon for 24 hours, after which the solution was added dropwise to stirring water. The precipitate was collected by centrifugation, washed with water, and dried *in vacuo* to give a white powder.
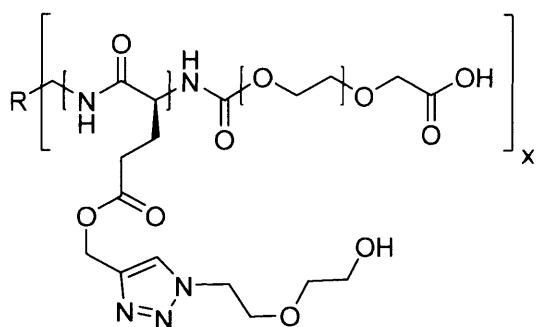
General method for oligo(ethylene glycol) grafted, carboxy-PEG terminated PPLG

To a stirring solution of carboxy-PEG terminated PPLG in DMF (1 g/mL) was added 2-(2-azidoethoxy)ethan-1-ol (1.2 equivalents per alkyne) and PMDETA (0.1 equivalents per alkyne). The solution was sparged with a steady stream of argon gas for 10 minutes, after which copper(I) bromide (0.1 equivalents per alkyne) was added in one portion, and the reaction was sealed in an argon atmosphere and stirred for 24 hours. Diethyl ether was added and the resulting precipitate

113

or oil was isolated by centrifugation. This residue was dissolved in water and copper was removed by portionwise addition of Dowex M4195 resin to the aqueous polymer solution, followed by shaking until the solution no longer appeared blue. The resin was removed by filtration and the solution was exhaustively dialyzed against deionized water across a 1 kDa MWCO regenerated cellulose membrane and lyophilized to give a white powder.
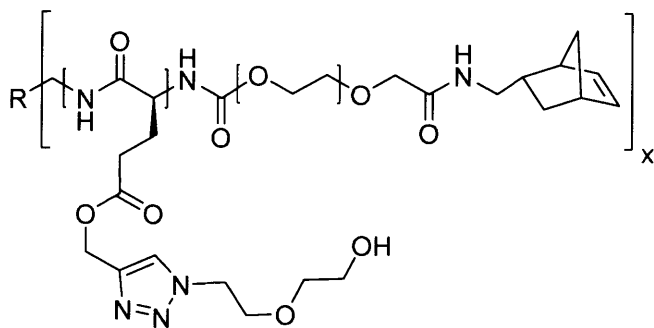
General method for oligo(ethylene glycol) grafted, norbornene-PEG terminated PPLG

To a stirring solution of oligo(ethylene glycol) grafted, carboxy-PEG terminated PPLG in DMF (0.5 g/mL) was added 5-Norbornene-2-methylamine (40 µL/mL) followed by HATU (125 mg/mL) and DIPEA (150 µL/mL). The reaction was sealed and stirred for 24 hours. Diethyl ether was added and the resulting precipitate or oil was isolated by centrifugation. This residue was dissolved in water and the solution was exhaustively dialyzed against deionized water across a 1 kDa MWCO regenerated cellulose membrane and lyophilized to give a white powder.

114
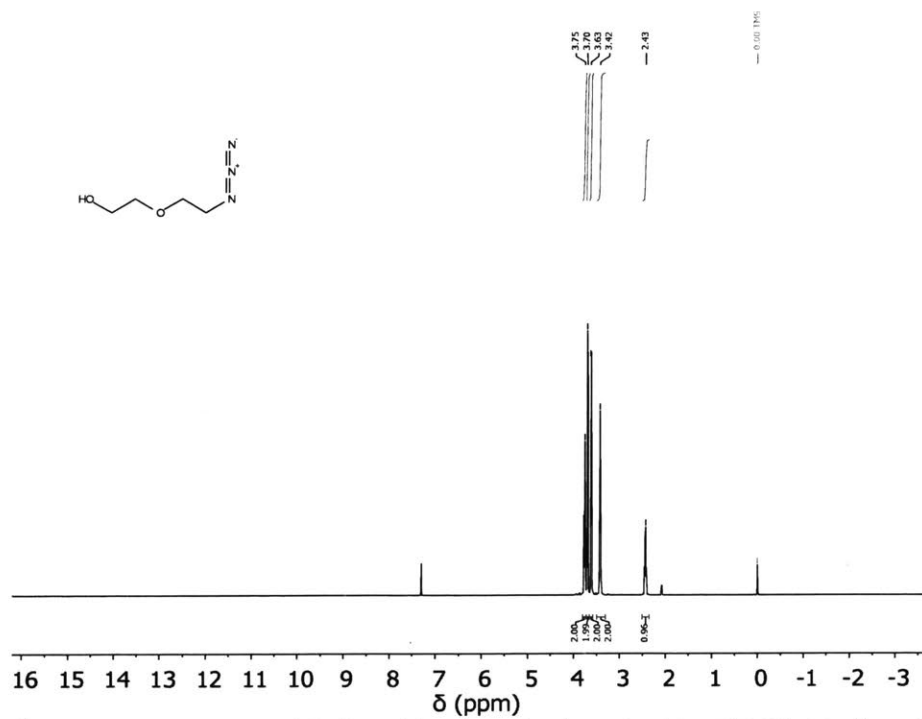
Figure 3.16. ^{1}H NMR spectrum of 2-(2-azidoethoxy)ethan-1-ol in CDCl$_3$. Peak at δ 2.80 is from solvent.
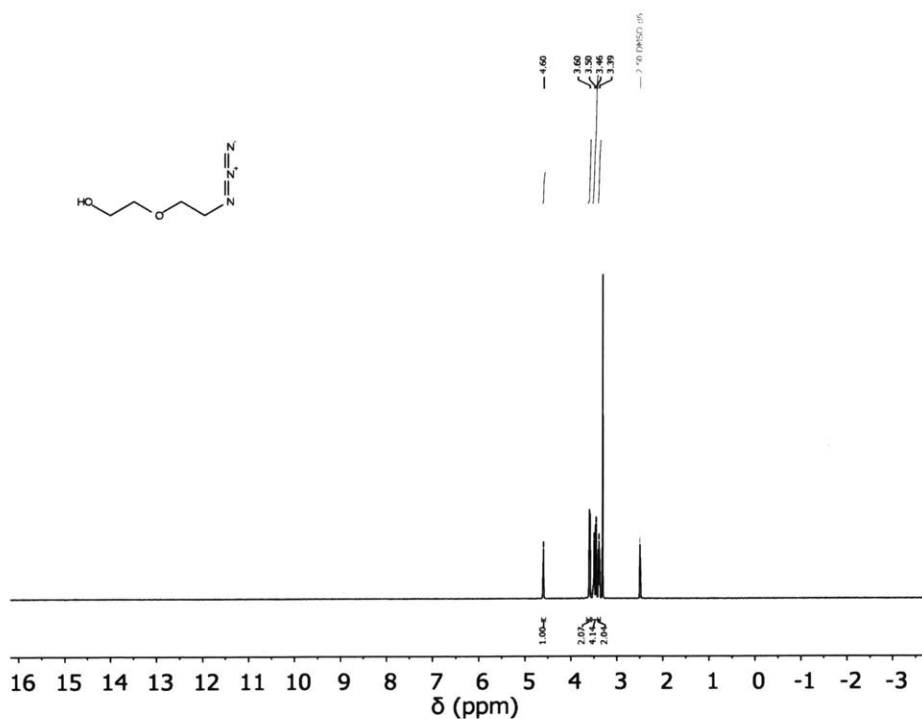

Figure 3.17. ^{1}H NMR spectrum of 2-(2-azidoethoxy)ethan-1-ol in (CD$_3$)$_2$SO. Peak at δ 3.32 is from water.
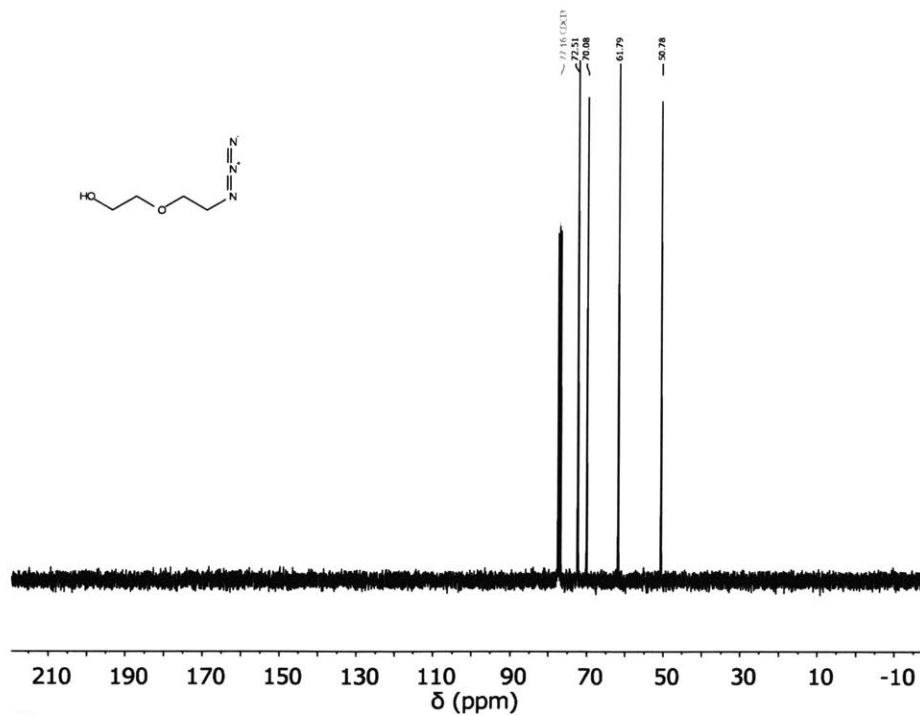
Figure 3.18. ^{13}C NMR spectrum of 2-(2-azidoethoxy)ethan-1-ol in CDCl$_3$
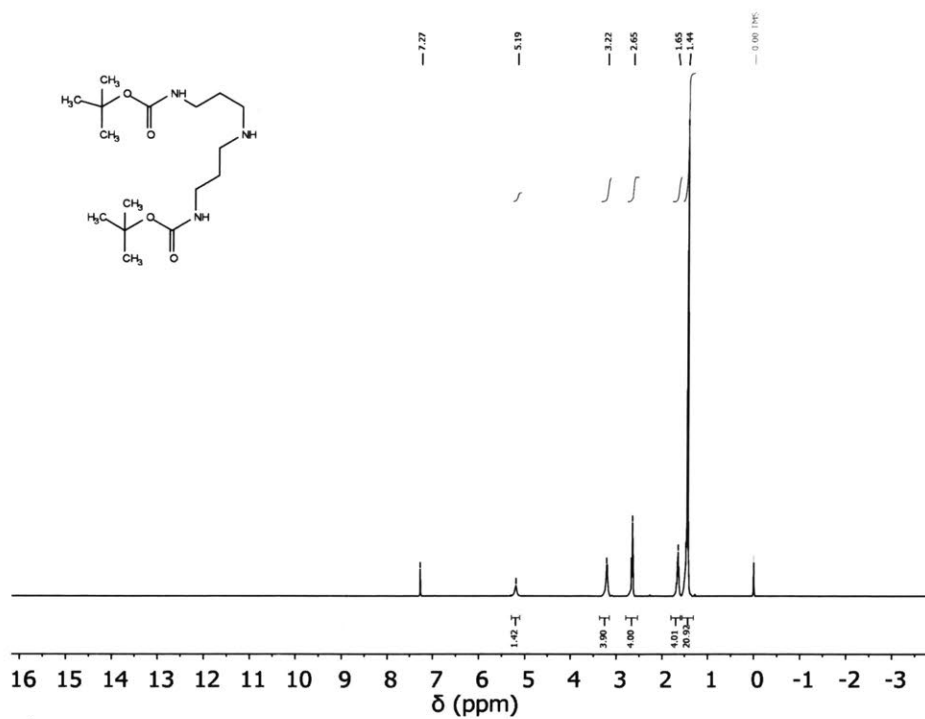

**Figure 3.19.** ^{1}H NMR spectrum of di-*tert*-butyl (azanediylbis(propane-3,1-diyl))dicarbamate in CDCl$_3$
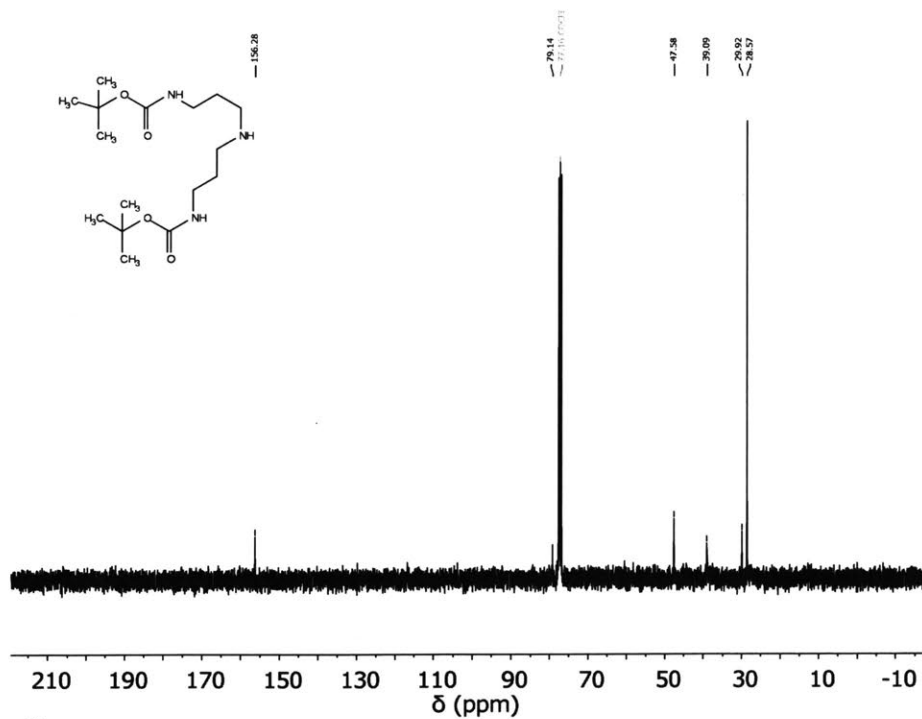
Figure 3.20. ^{13}C NMR spectrum of di-*tert*-butyl (azanediylbis(propane-3,1-diyl))dicarbamate in CDCl$_3$
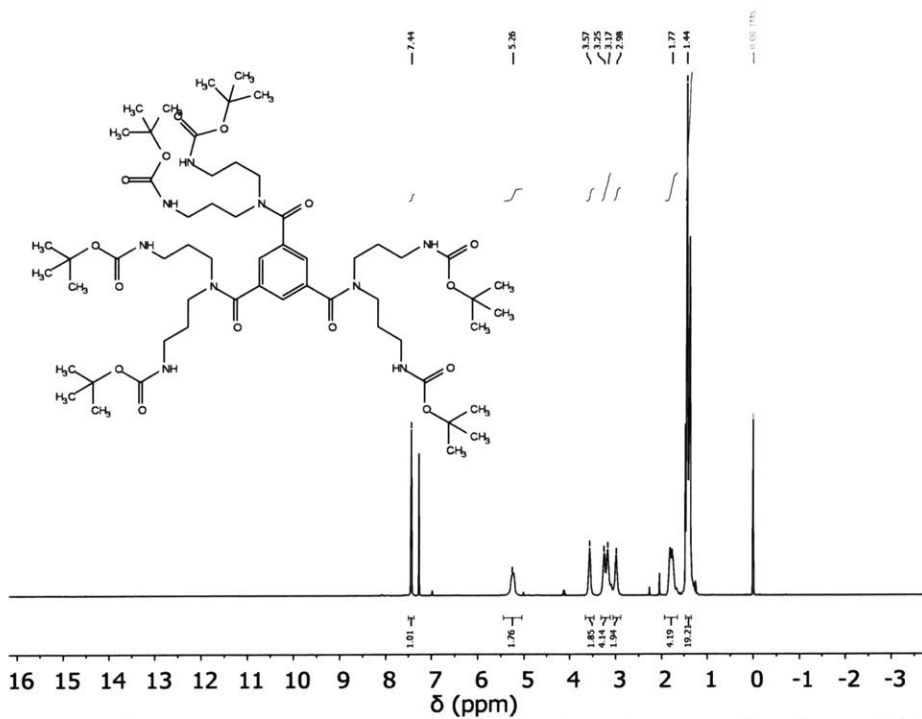

Figure 3.21. ^{1}H NMR spectrum of hexa-*tert*-butyl ((((benzene-1,3,5-tricarbonyl)tris(azanetriyl))hexakis(propane-3,1-diyl))hexacarbamate in CDCl$_3$
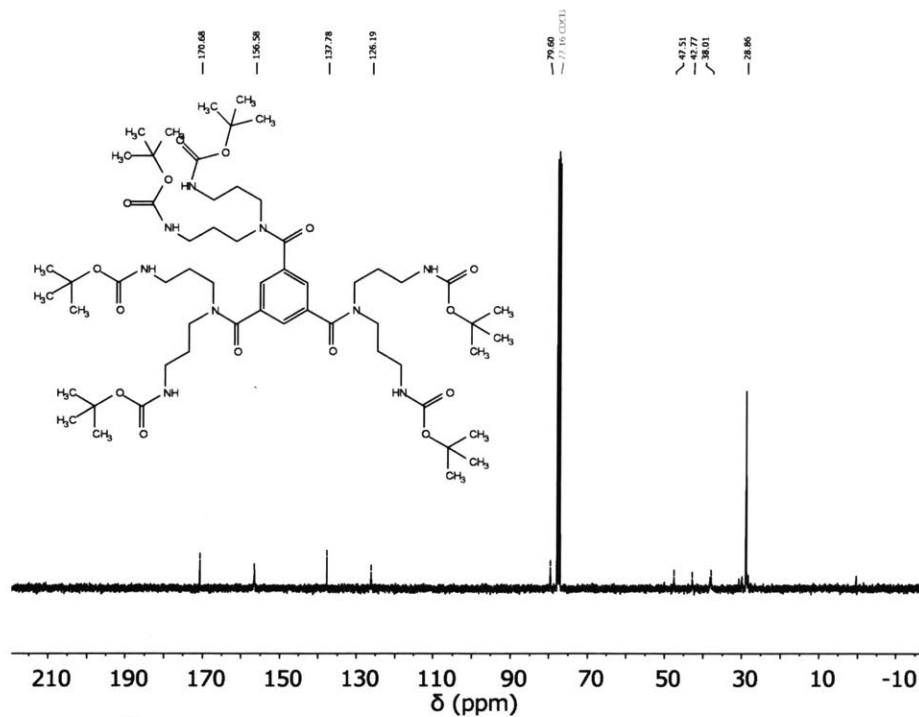
Figure 3.22. ^{13}C NMR spectrum of hexa-*tert*-butyl ((((benzene-1,3,5-tricarbonyl)tris(azanetriyl))hexakis(propane-3,1-diyl))hexacarbamate in CDCl$_3$
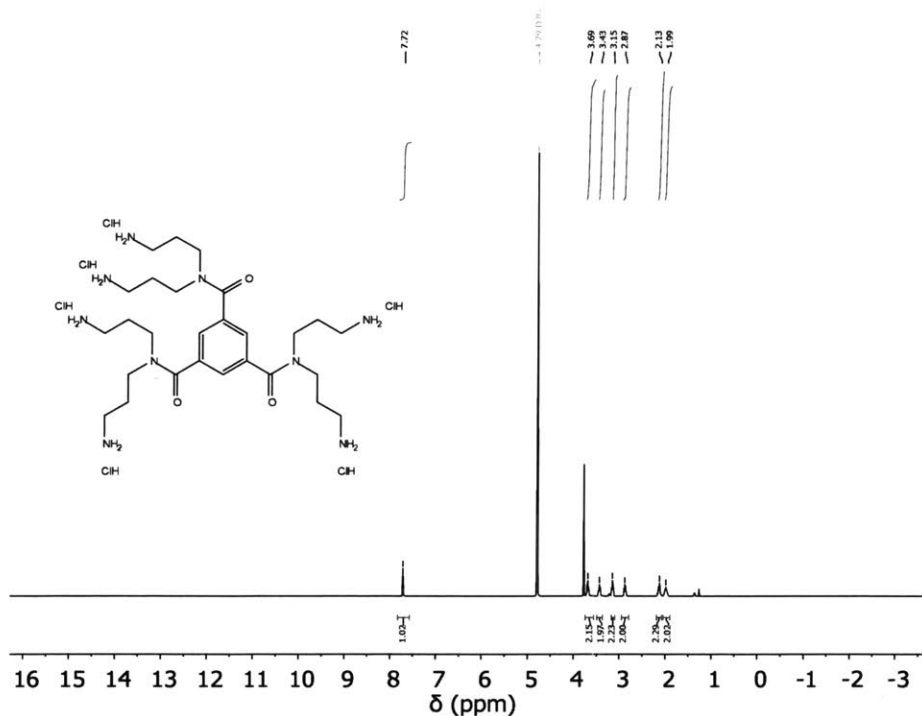
**Figure 3.23.** ^{1}H NMR spectrum of N^1,N^1,N^3,N^3,N^5,N^5-hexakis(3-aminopropyl)benzene-1,3,5-tricarboxamide hexahydrochloride in D$_2$O. Peak at δ 3.77 is from dioxane. Peaks at δ 3.21, 1.35, 1.26 are from residual starting material.
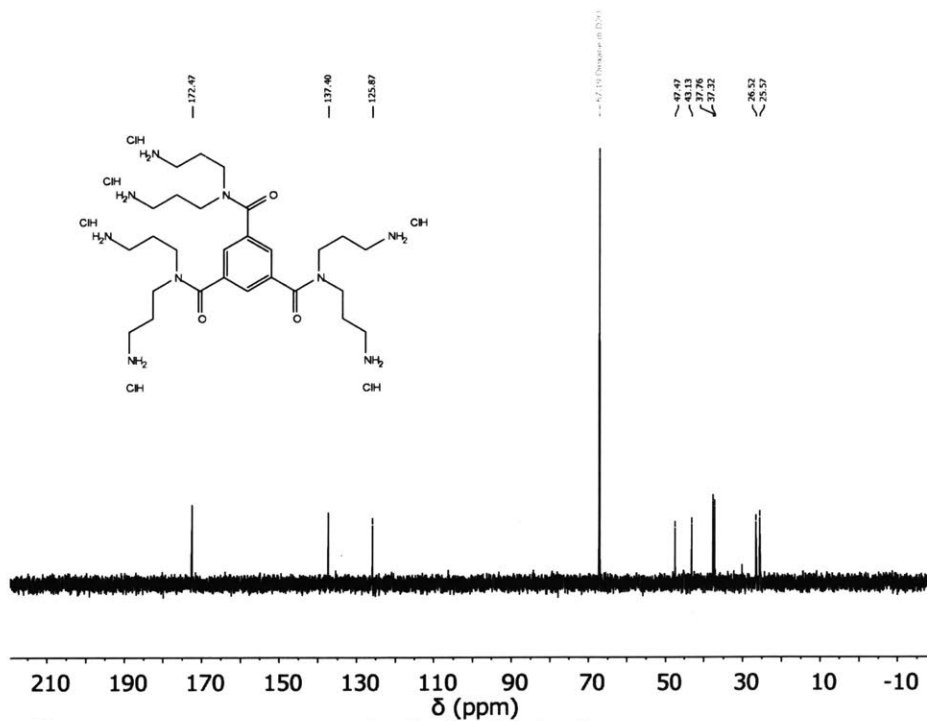
Figure 3.24. ^{13}C NMR spectrum of N^1,N^1,N^3,N^3,N^5,N^5-hexakis(3-aminopropyl)benzene-1,3,5-tricarboxamide hexahydrochloride in D_2O. Peak at δ 67.19 is from dioxane.
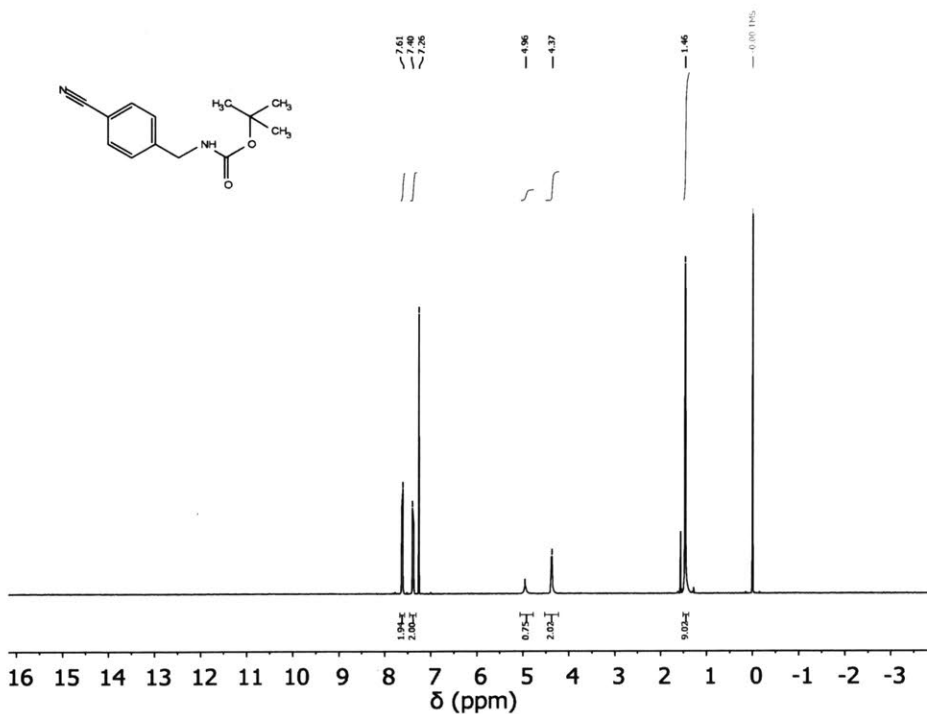
Figure 3.25. ^{1}H NMR spectrum of *tert*-butyl (4-cyanobenzyl)carbamate in CDCl$_3$. Peak at δ 1.56 is from water.
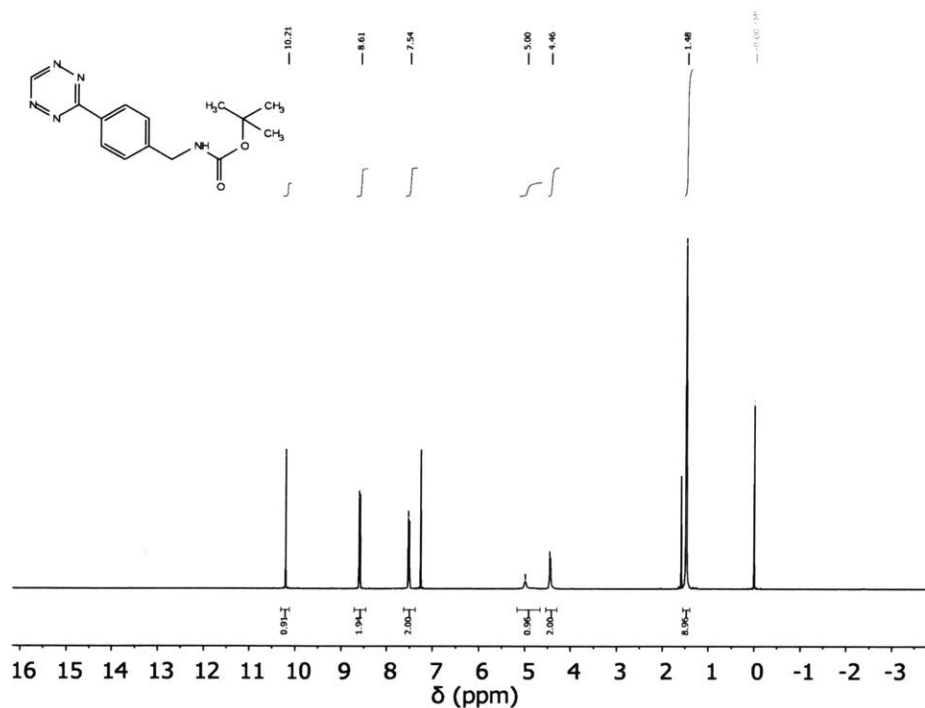
Figure 3.26. ^{1}H NMR spectrum of *tert*-butyl (4-(1,2,4,5-tetrazin-3-yl)benzyl)carbamate in CDCl$_3$. Peak at δ 1.56 is from water.
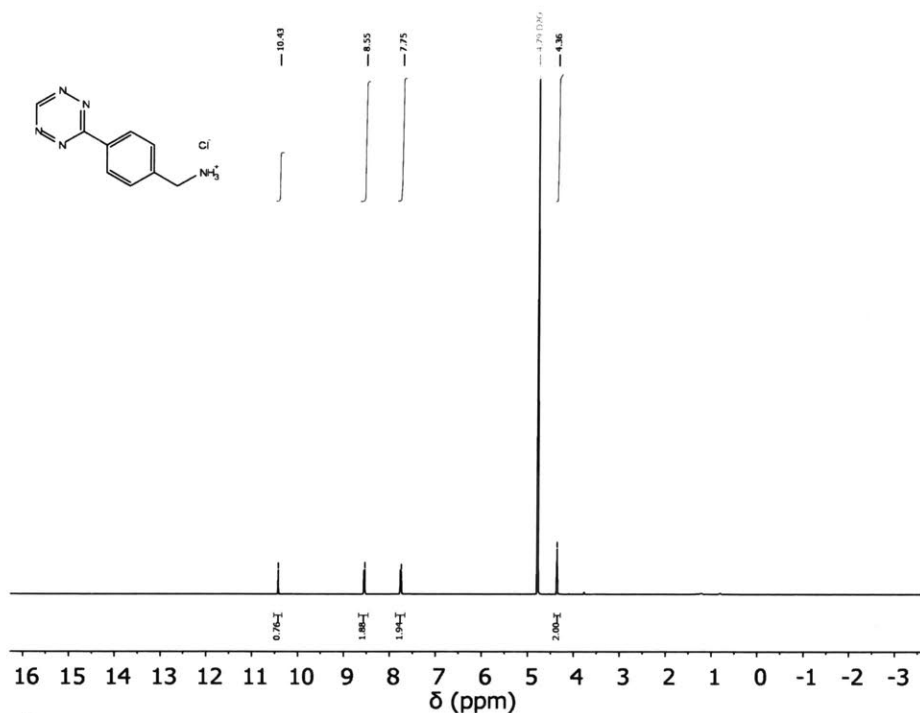
Figure 3.27. ^{1}H NMR spectrum of (4-(1,2,4,5-tetrazin-3-yl)phenyl)methanaminium chloride in D$_2$O.
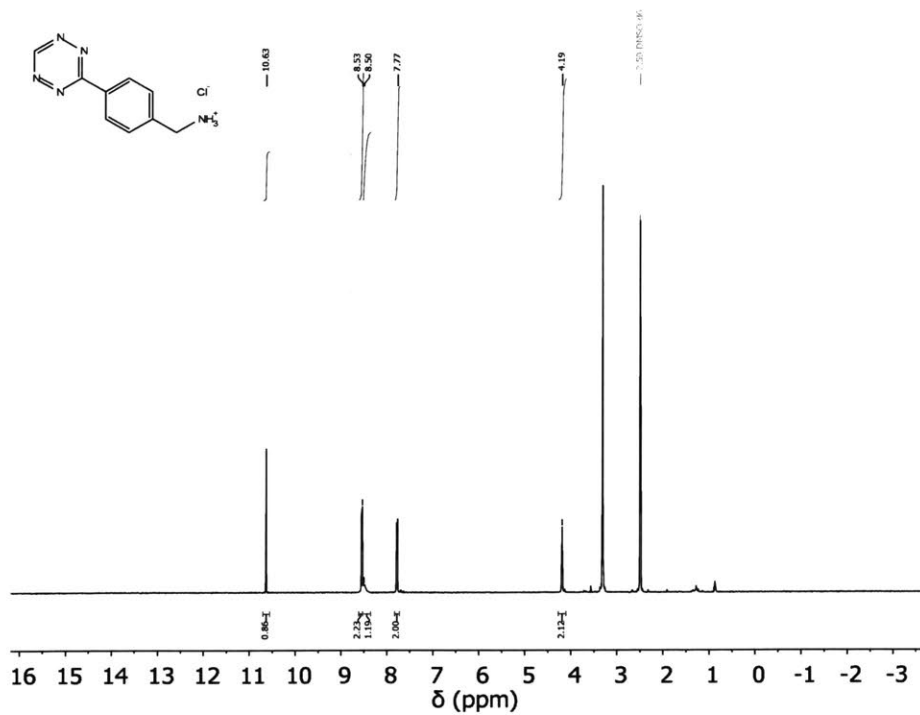
Figure 3.28. ^{1}H NMR spectrum of (4-(1,2,4,5-tetrazin-3-yl)phenyl)methanaminium chloride in (CD$_3$)$_2$SO. Peak at δ 3.33 is from water.
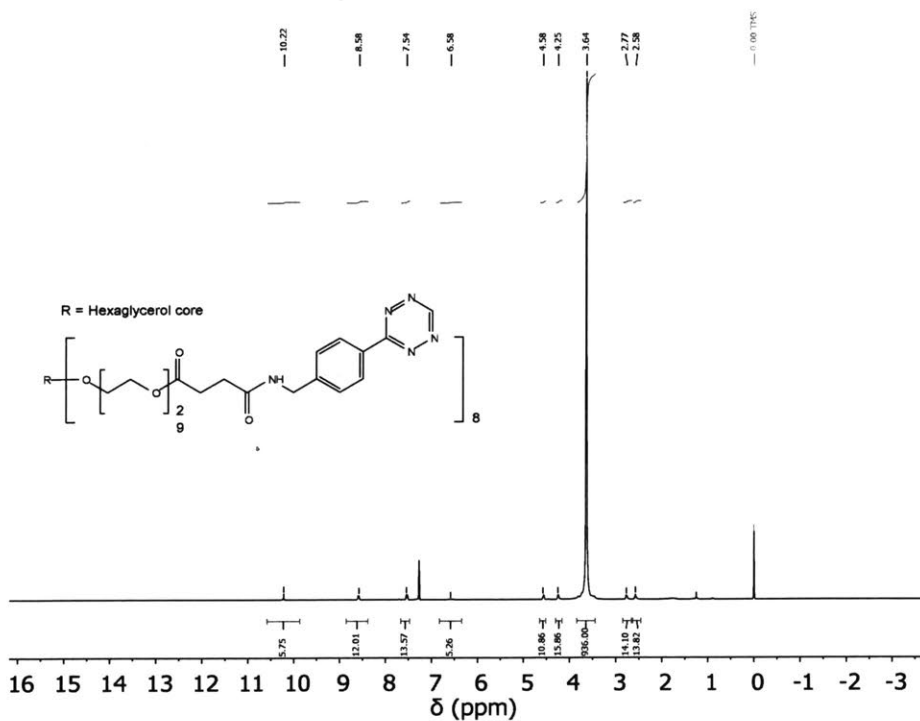
Figure 3.29. ^{1}H NMR spectrum of 8-arm tetrazine terminated poly(ethyele glycol) in CDCl$_3$

121
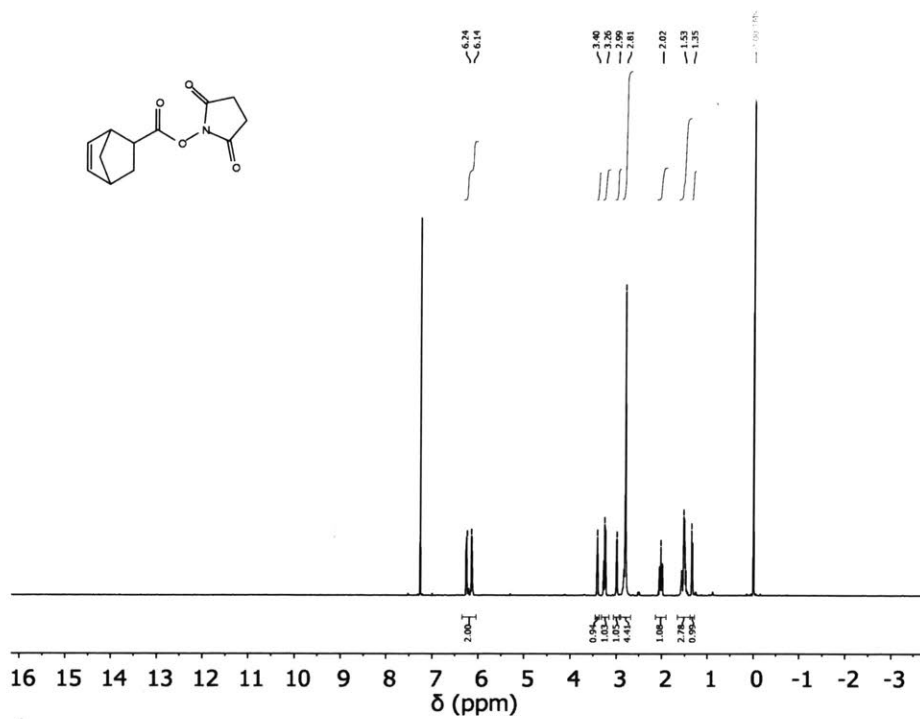
Figure 3.30. ¹H NMR spectrum of 5-Norbornene-2-carboxylic acid succinimidyl ester, mixture of *endo* and *exo* in CDCl₃
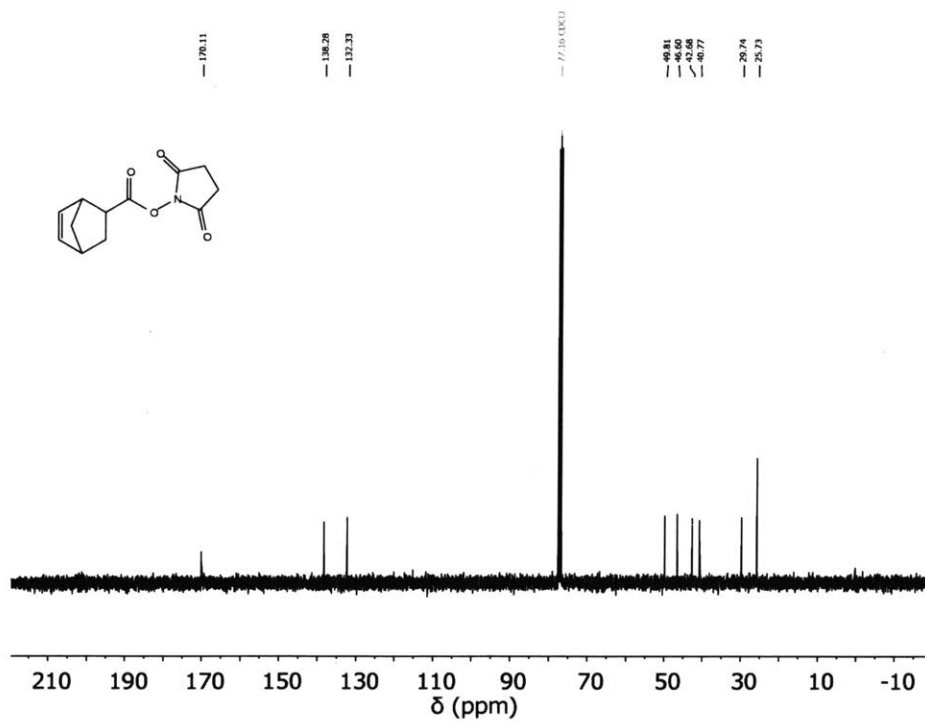
Figure 3.31. ¹³C NMR spectrum of 5-Norbornene-2-carboxylic acid succinimidyl ester, mixture of *endo* and *exo* in CDCl₃
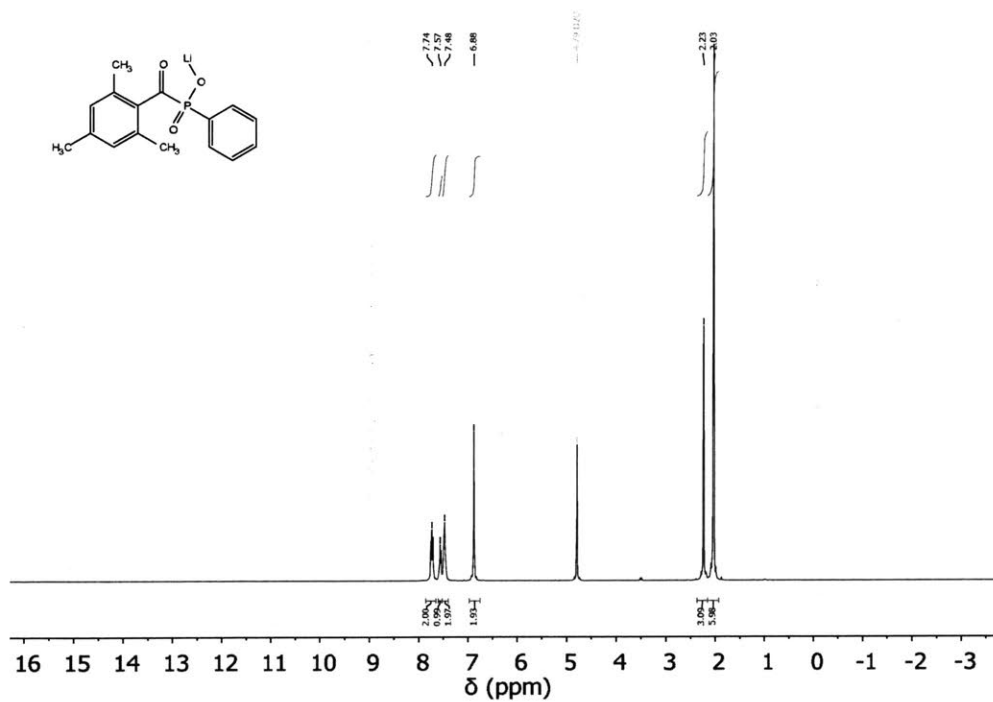
Figure 3.32. ^{1}H NMR spectrum of lithium phenyl(2,4,6-trimethylbenzoyl)phosphinate in D$_2$O
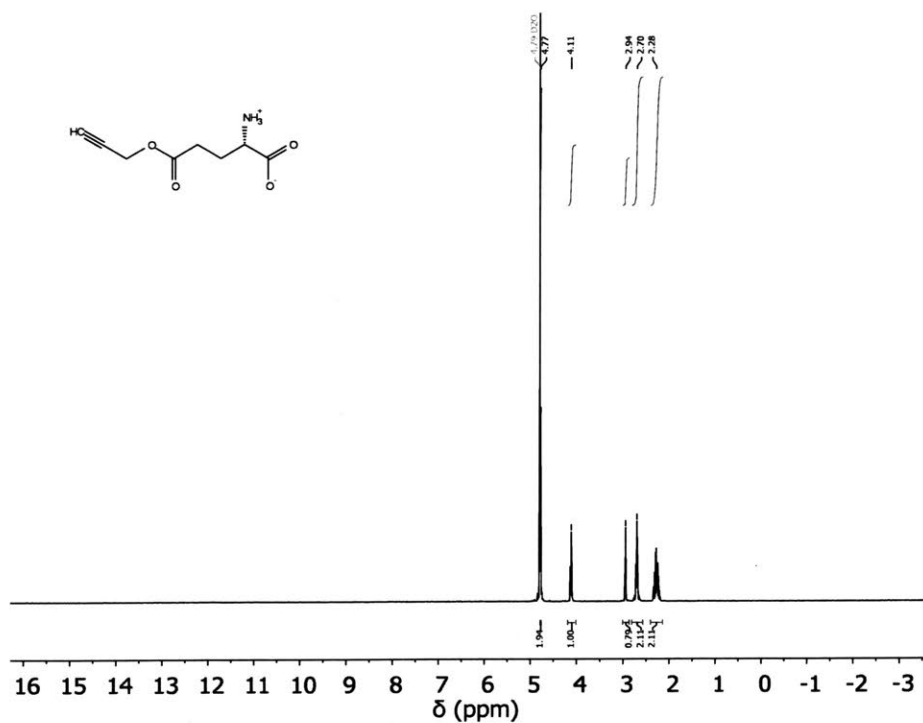
Figure 3.33. ^{1}H NMR spectrum of γ-propargyl-L-glutamate in D$_2$O

123
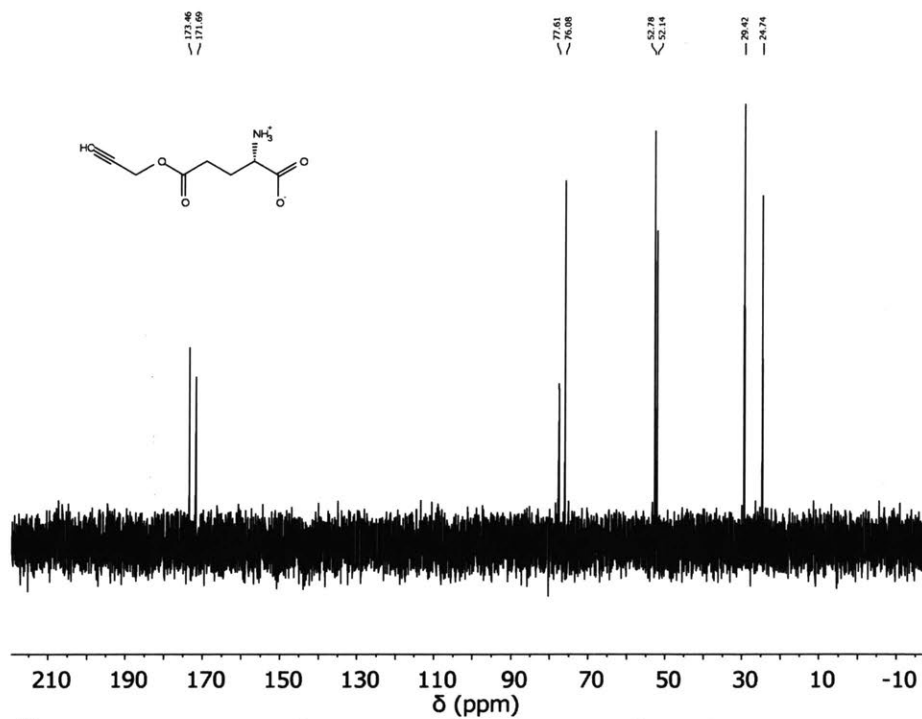
Figure 3.34. ^{13}C NMR spectrum of γ-propargyl-L-glutamate in D_2O
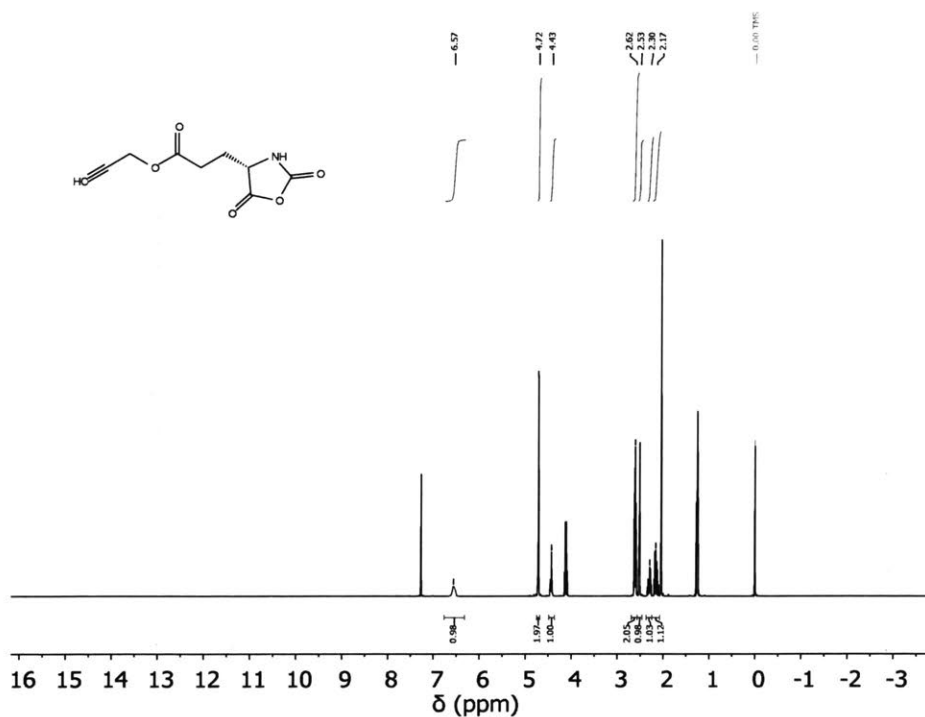
Figure 3.35. ^1H NMR spectrum of γ-propargyl-L-glutamate N-carboxyanhydride in $CDCl_3$. Peaks at δ 4.12, 2.05, and 1.26 are from ethyl acetate.
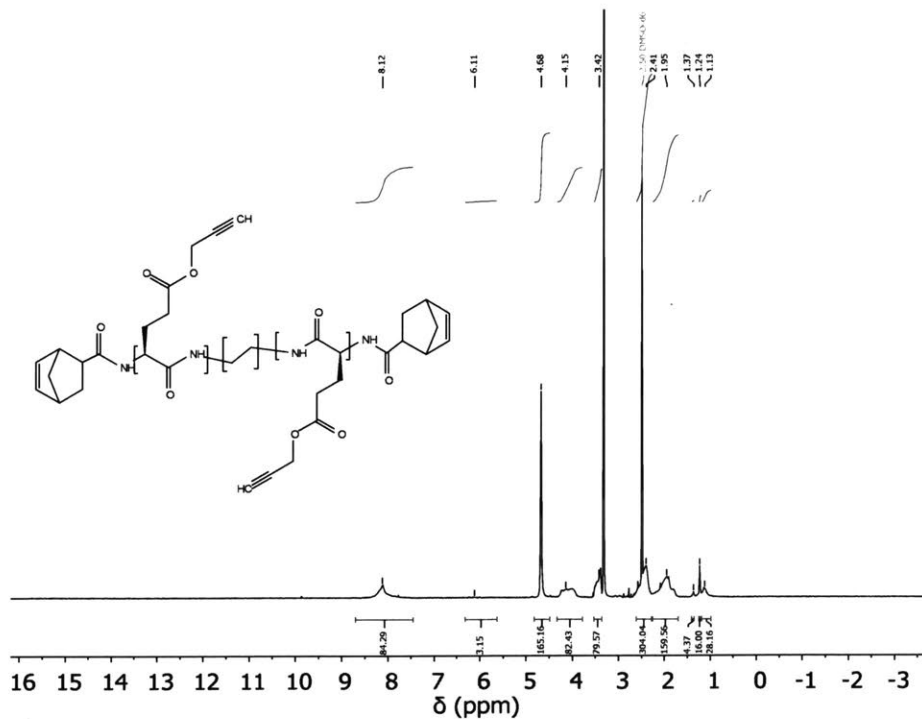
Figure 3.36. ^{1}H NMR spectrum of norbornene terminated PPLG in $(CD_3)_2SO$. Peak at δ 3.32 is from water. End group analysis by NMR indicated a degree of polymerization of 82 and 79% conversion of end-groups to norbornene.
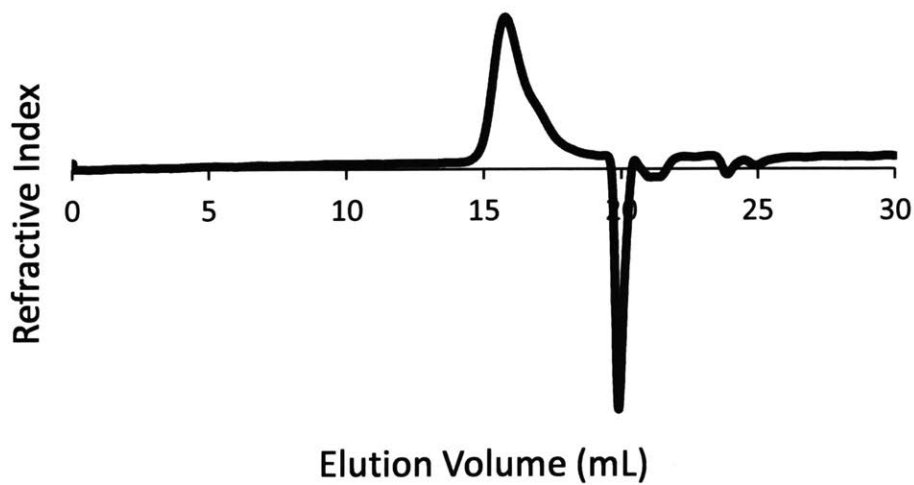
Figure 3.37. Gel permeation chromatogram of norbornene terminated PPLG eluted with DMF + LiBr. The negative peak at 20 mL corresponds to injected DMF. Relative to poly(methyl methacrylate) standards: M_n 1577, PDI 1.11
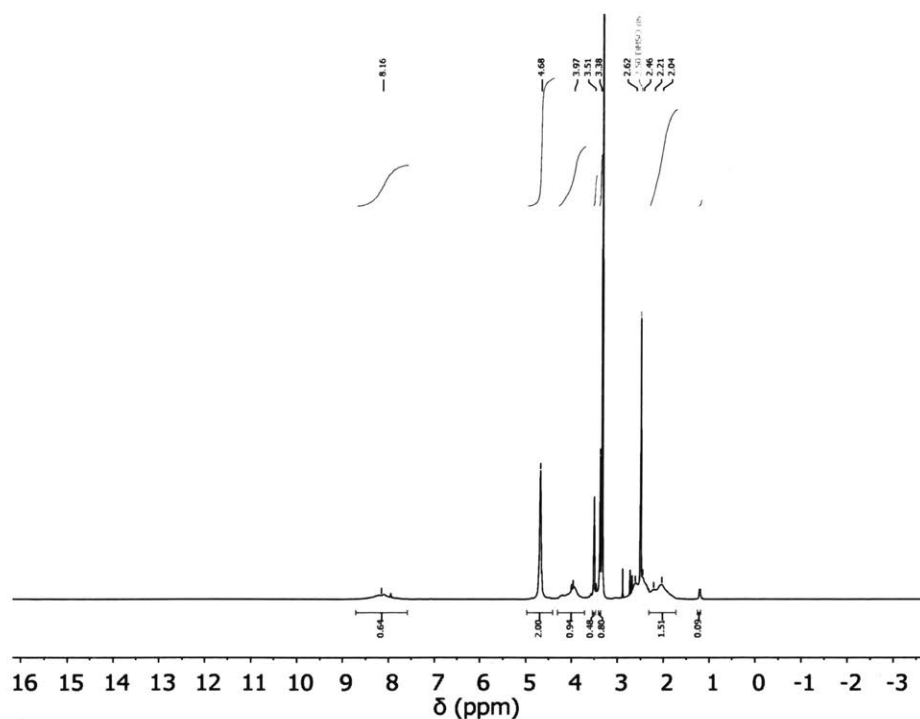
Figure 3.38. ^{1}H NMR spectrum of 6-arm, carboxy-PEG terminated PPLG in (CD$_3$)$_2$SO. Peak at δ 3.33 is from water, peaks at δ 7.95, 2.89, and 2.73 correspond to DMF.
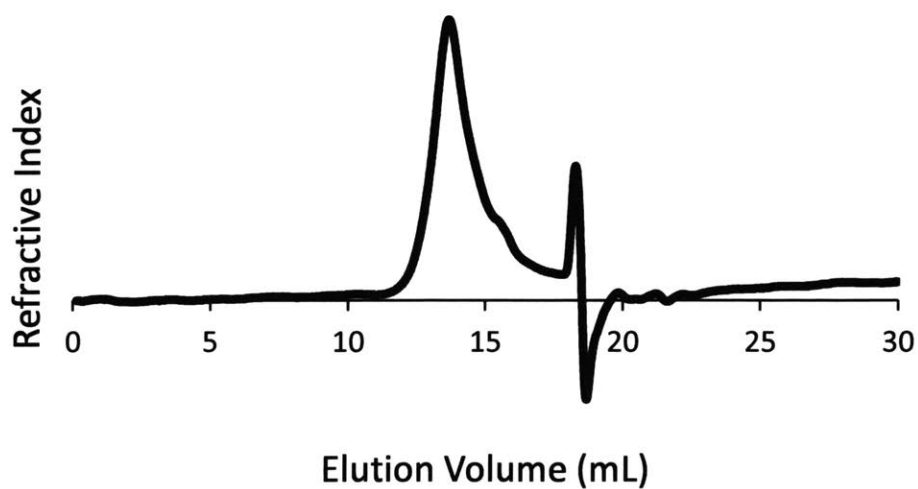
Figure 3.39. Gel permeation chromatogram of 6-arm, carboxy-PEG terminated PPLG eluted with DMF + LiBr. The negative peak at 18 mL corresponds to injected DMF. Relative to poly(methyl methacrylate) standards: M$_n$ 72616, PDI 1.29
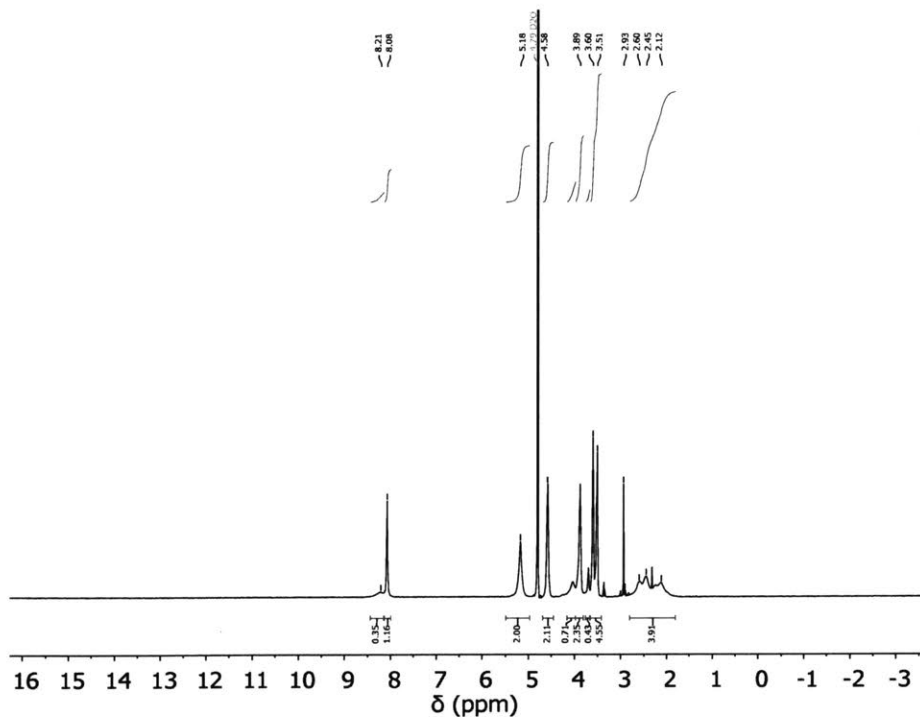
Figure 3.40. ^{1}H NMR spectrum of 6-arm, oligo(ethylene glycol) grafted, carboxy-PEG terminated PPLG in D$_2$O.
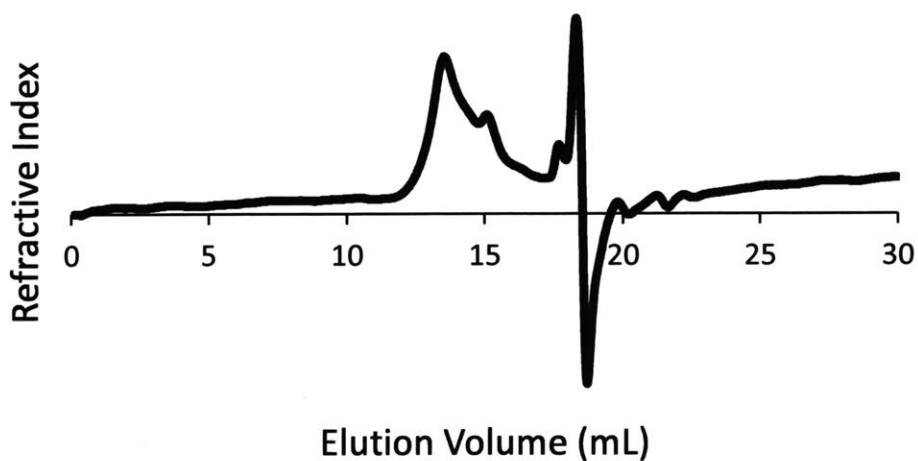
Figure 3.41. Gel permeation chromatogram of 6-arm, oligo(ethylene glycol) grafted, carboxy-PEG terminated PPLG eluted with DMF + LiBr. The negative peak at 18 mL corresponds to injected DMF and solvent. Relative to poly(methyl methacrylate) standards: M$_n$ 58987, PDI 1.49
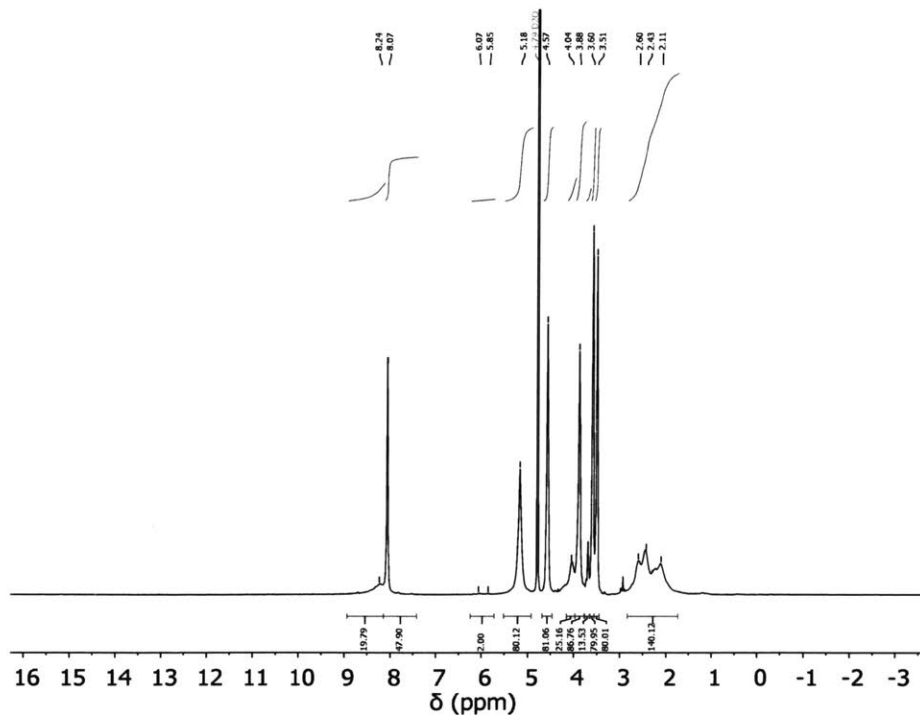
Figure 3.42. ¹H NMR spectrum of 6-arm, oligo(ethylene glycol) grafted, norbornene-PEG terminated PPLG in D₂O.
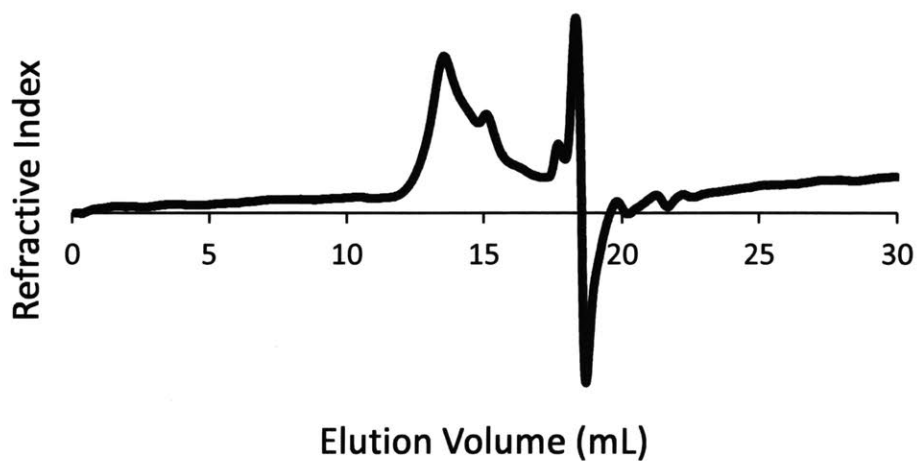
Figure 3.43. Gel permeation chromatogram of 6-arm, oligo(ethylene glycol) grafted, norbornene-PEG terminated PPLG eluted with DMF + LiBr. The negative peak at 18 mL corresponds to injected DMF and solvent. Relative to poly(methyl methacrylate) standards: M_n 58046, PDI 1.48

128

3.5 References

(1)   C. C. Ahrens, M. E. Welch, L. G. Griffith, P. T. Hammond, *Biomacromolecules* **2015**, *16*, 3774–3783.

(2)   D. L. Pickel, N. Politakos, A. Avgeropoulos, J. M. Messman, *Macromolecules* **2009**, *42*, 7781–7788.

(3)   I. Dimitrov, H. Schlaad, *Chemical Communications* **2003**, 2944.

(4)   H. Lu, J. Cheng, *J. Am. Chem. Soc.* **2008**, *130*, 12562–12563.

(5)   H. Lu, J. Cheng, *J. Am. Chem. Soc.* **2007**, *129*, 14114–14115.

(6)   W. Vayaboury, O. Giani, H. Cottet, A. Deratani, F. Schué, *Macromol. Rapid Commun.* **2004**, *25*, 1221–1224.

(7)   G. J. M. Habraken, K. H. R. M. Wilsens, C. E. Koning, A. Heise, *Polymer Chemistry* **2011**, *2*, 1322.

(8)   J. Zou, J. Fan, X. He, S. Zhang, H. Wang, K. L. Wooley, *Macromolecules* **2013**, *46*, 4223–4226.

(9)   T. J. Deming, *J. Polym. Sci. A Polym. Chem.* **2000**, *38*, 3011–3018.

(10)   J. Hua, Z. Li, W. Xia, N. Yang, J. Gong, J. Zhang, C. Qiao, *Mater Sci Eng C Mater Biol Appl* **2016**, *61*, 879–892.

(11)   B. D. Fairbanks, M. P. Schwartz, A. E. Halevi, C. R. Nuttelman, C. N. Bowman, K. S. Anseth, *Adv. Mater.* **2009**, *21*, 5005–5010.

(12)   S. P. S. Koo, M. M. Stamenović, R. A. Prasath, A. J. Inglis, F. E. D. Prez, C. Barner-Kowollik, W. V. Camp, T. Junkers, *Journal of Polymer Science Part A: Polymer Chemistry* **2010**, *48*, 1699–1713.

(13)   A. M. Cok, H. Zhou, J. A. Johnson, *Macromolecular Symposia* **2013**, *329*, 108–112.

(14)   X. Zhang, Q. Zhang, Y. Wu, C. Feng, C. Xie, X. Fan, P. Li, *Macromolecular Rapid Communications* **2016**, *37*, 1311–1317.

(15)   Š. Gradišar, E. Žagar, D. Pahovnik, *ACS Macro Lett.* **2017**, *6*, 637–640.

(16)   C. D. Vacogne, H. Schlaad, *Chemical Communications* **2015**, *51*, 15645–15648.

(17)   K. Lang, L. Davis, S. Wallace, M. Mahesh, D. J. Cox, M. L. Blackman, J. M. Fox, J. W. Chin, *J. Am. Chem. Soc.* **2012**, *134*, 10317–10320.

(18)   J. Yang, M. R. Karver, W. Li, S. Sahu, N. K. Devaraj, *Angewandte Chemie International Edition* **2012**, *51*, 5222–5225.

(19)   J. K. Pontrello, M. J. Allen, E. S. Underbakke, L. L. Kiessling, *J. Am. Chem. Soc.* **2005**, *127*, 14536–14537.

(20)   B. D. Fairbanks, M. P. Schwartz, C. N. Bowman, K. S. Anseth, *Biomaterials* **2009**, *30*, 6702–6707.

(21)   H.-T. Chen, M. F. Neerman, A. R. Parrish, E. E. Simanek, *J. Am. Chem. Soc.* **2004**, *126*, 10044–10048.

(22)   S. Govindaraji, P. Nakache, V. Marks, Z. Pomerantz, A. Zaban, J.-P. Lellouche, *J. Org. Chem.* **2006**, *71*, 9139–9143.

Chapter 4: Secondary Structure Influences Efficacy of Polymer-drug Conjugates Derived from "Clickable" Polypeptide Scaffolds

4.1 Introduction

The efficacy of a cancer treatment is dependent on the potency of the active ingredient and its delivery to tumors; cancer treatments can be improved by maximizing the localization and controlling the release of therapeutics to tumors. Over the past few decades, various nanoparticle-based drug delivery strategies, including polymer micelles,[1-3] liposomes,[4,5] and layer-by-layer technologies[6] have been employed to improve the targeting and release characteristics of small-molecule cancer drugs. Polymer-drug conjugates, in which small-molecule drugs are covalently attached to a polymer backbone,[7] are a complimentary drug delivery method to nanoparticle-based technologies. Polymer-drug conjugates offer several potential advantages to nanoparticles, such as increased functional group density leading to high drug loadings[8] and lower degrees of opsonization in vivo due to the small size of polymer-drug conjugates relative to nanoparticles.[9]

Poly(γ-propargyl-L-glutamate) (PPLG) is a prime candidate for implementation in a polymer-drug conjugate drug delivery platform (Figure 4.1). Each repeat unit of PPLG contains a propargyl group, which can be functionalized by Cu-mediated azide-alkyne cycloaddition. This "click chemistry" is well-described in the literature,[10] and different azide-functionalized moieties may be grafted to the PPLG backbone using similar reaction conditions. The functional group tolerance of click chemistry allows for modular functionalization of PPLG, and previous studies have achieved high grafting densities with PPLG,[11] which is critical to high drug loading on the polymer backbone but unusual for a grafting-to approach.
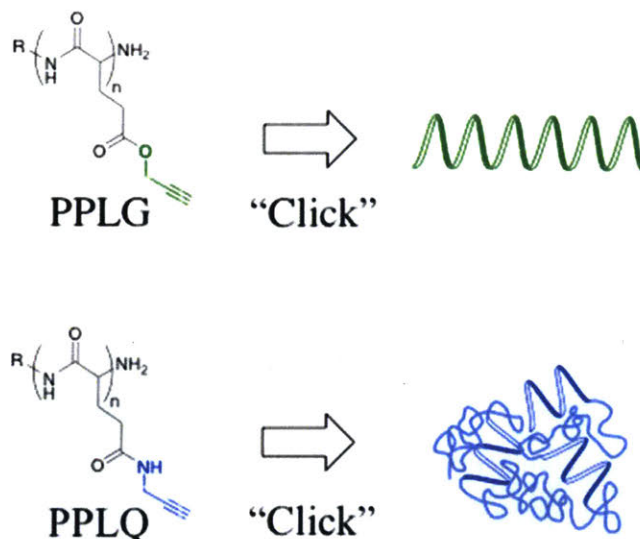
Figure 4.1. Schematic of chemical structures of PPLG and PPLQ and secondary structures of their respective conjugates

Moreover, both unmodified PPLG and PPLG grafted with low or high molecular weight PEG at high density have been shown to adopt α-helical structures in solution,[11] resulting in a rigid-rod conformation that may influence delivery of cargo. Previous in vitro studies investigating the impact of drug delivery vehicle shape on efficacy and internalization have yielded contrasting results.[9,12,13] For particles on the order of 100 nm, Huang et al[14] found that cylindrical nanoparticles were endocytosed to a greater extent than spherical nanoparticles of similar diameter, whereas Chithrani et al[15] demonstrated the opposite for particles of slightly smaller size. Overall, the effect of nanoparticle size, shape, charge, material, etc. have been thoroughly studied and summarized.[16,17] However, the effects of polymer secondary structure on efficacy at the molecular length scales of polymer-drug conjugates is significantly less explored. Consequently, we aim to investigate one aspect of this research area by studying the effects an α-helical secondary structure on polymer-drug conjugate efficacy using the PPLG system.

Here, we report the synthesis and characterization of PPLG polymer-drug conjugates and compare the behavior of PPLG-drug conjugates to polymer-drug conjugates derived from poly(γ-propargyl-L-glutamine) (PPLQ) backbones (Figure 4.1). PPLQ is structurally identical to PPLG, except for the side chain where the ester bond of PPLG is replaced by an amide bond. Conjugates derived

from PPLQ have previously been shown to adopt conformations more similar to random coils than α-helices when grafted with moieties through click chemistry, likely due to competitive hydrogen bonding interactions between the backbone and side chain amide groups.[18] Thus, PPLQ-drug conjugates are globular analogs to PPLG-drug conjugates, enabling similar chemistry for conjugate synthesis but lacking a defined α-helical secondary structure. Dox was chosen as a model drug for conjugation due to its prevalence in cancer treatment regimens and ease of detection through absorbance and fluorescence spectroscopy. Dox was grafted onto PPLG using click chemistry through an azide-functionalized hydrazide linker to enable acid-catalyzed release,[3] which is desirable due to the relatively acidic tumor microenvironment.[19] The remaining alkyne groups were used to graft 750 Da poly(ethylene glycol) (PEG) chains onto the PPLG backbone to improve aqueous solubility and provide a "stealth effect"[20,21] for potential in vivo applications. We characterized the drug loading, release characteristics, and in vitro cytotoxicities of the conjugates. Moreover, we evaluated the association of each polymer with A549 human lung carcinoma cells by flow cytometry. Comparing the characteristics and in vitro behavior of these conjugates will further elucidate the effect of shape and secondary structure on the efficacy of polymer-drug conjugates.

4.2 Results and Discussion

The goal of this research was to interrogate the impact of secondary structure on polymer-drug conjugate behavior using PPLG and PPLQ polypeptide scaffolds. Doxorubicin was conjugated to PPLG and PPLQ backbones grafted with 750 Da PEG chains using an azide-functionalized hydrazide linker (Figure 4.2) to yield PPLG- and PPLQ-Dox conjugates. Drug loading, polymer size and secondary structure, and pH-dependent release were measured for the polymer-drug conjugates. In vitro cytotoxicity of polymer-drug conjugates and association of the fluorescently-labeled PEGylated polymers with A549 cells were assessed as well to determine the effects of differing secondary structure on drug carrier efficacy.

133
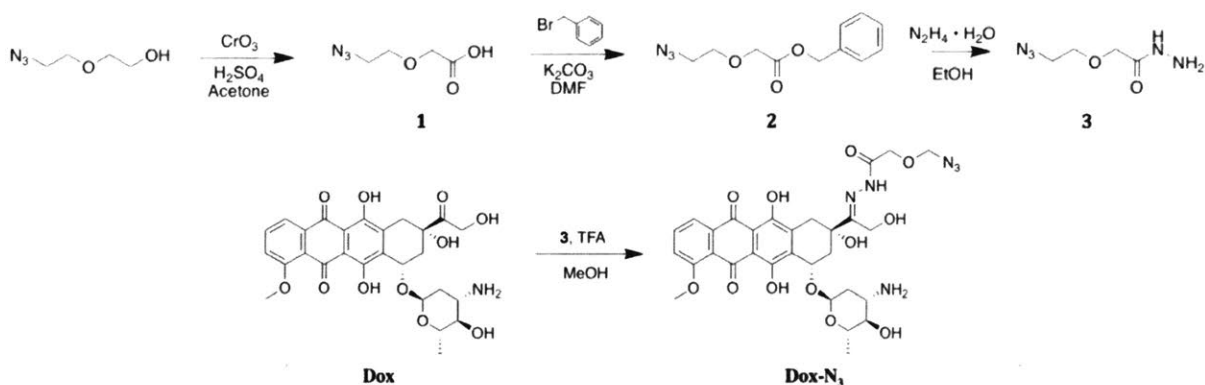
Figure 4.2. Synthesis of azide-functionalized hydrazide linker from 2-(2-azidoethoxy)ethanol and reaction with doxorubicin to generate azide-functionalized Dox

Conjugation Efficiency

Based on the molecular weights of the polymer scaffolds and the grafted moieties, the target for drug loading of the PPLG- and PPLQ-Dox conjugates was 26 wt%, which corresponds to grafting of 40% of repeat unit propargyl groups with Dox-azide and the other 60% with PEG-azide. Absorbance measurements at 480 nm of polymer-Dox conjugates indicate that PPLG-Dox and PPLQ-Dox conjugates have drug loadings of 28 wt% and 19 wt%, respectively. NMR spectra of conjugates revealed high grafting efficiencies of azides to the polymer backbones. Grafting efficiencies were determined by the ratio of the PPLG or PPLQ methylene proton peaks (α and β to the amino acid central carbon) to the triazole proton peak, which appears as an indication of a successful click reaction between a propargyl group and an azide-functionalized moiety (Figure 4.10). 100% efficient grafting results in a 4-to-1 ratio of the methylene peak integration to the triazole peak integration, and the ratios observed in the NMR spectra of conjugates in this study suggest >85% grafting of the polymer backbone for all conjugates. If the grafting density is assumed to be quantitative, PPLG-Dox conjugates contain 43 molecules of dox per 100 repeat units and PPLQ-Dox conjugates contain 29 molecules of dox per 100 repeat units, with the remainder of the repeat units bearing PEG chains. The deviations in drug loadings of PPLG- and PPLQ-Dox conjugates from the targeted drug loading could be a result of differences in reactivity of PEG-azide compared to Dox-azide. Additionally, given the stochastic nature of the grafting reaction, the differences in water solubility of grafted PPLG and PPLQ could result in enrichment of polymers grafted with more PEG by aggregation or precipitation of highly Dox grafted polymers.

134

Conjugate Size and Secondary Structure
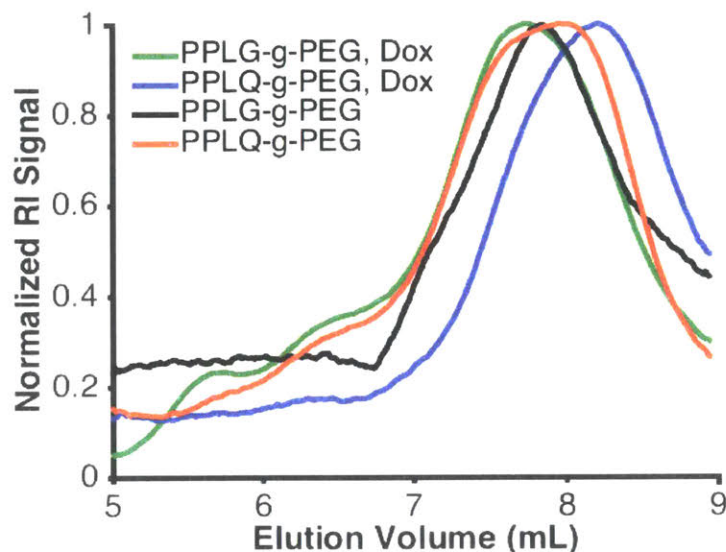
Figure 4.3. Aqueous GPC traces of refractive index for PPLG-g-PEG (black), PPLG-g-PEG conjugated with Dox (green), PPLQ-g-PEG (red), PPLQ-g-PEG conjugated with Dox (blue)

PPLG used in this study had degree of polymerization 62, and PPLQ used in this study had degree of polymerization 153, as determined by end-group analysis using NMR. We compared the hydrodynamic volumes[24,25] of polymer conjugates by elution time on gel-permeation chromatography to determine the relative sizes of the grafted polymers. GPC traces of polymer-Dox conjugates and PEGylated polymers without Dox (Figure 4.3) indicate that each of the conjugates synthesized were of similar size. Although the elution peak of PPLQ grafted with both Dox and PEG is later than the others included in this study, the elution time distribution of this conjugate largely overlapped with the distributions of other conjugates. The key statistics on the relative sizes of the polymer conjugates (Figure 4.15), calculated from regions of the GPC traces from elution volumes of 6-9 mL, corroborate the observation that conjugates synthesized in this study are of similar hydrodynamic volume despite differences in the degree of polymerization as determined by NMR. The comparison of conjugates of similar size may be more applicable than comparisons of polymers of equal molecular weight for probing the influence of polymer secondary structure.
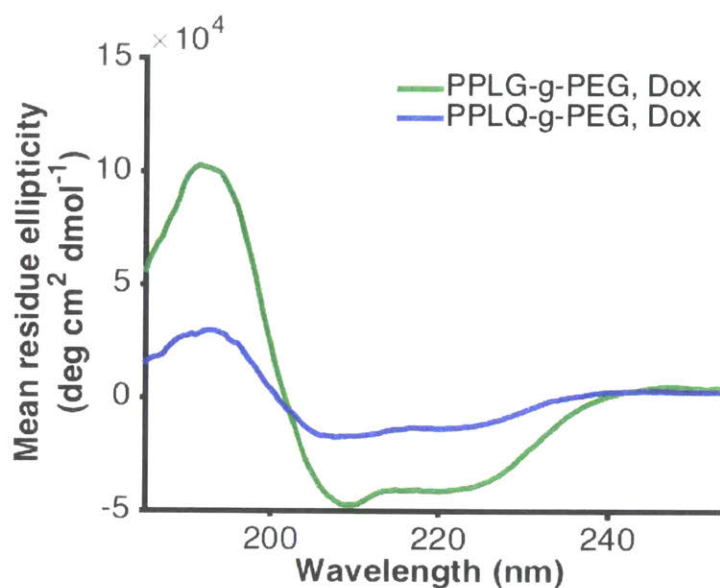
Figure 4.4. CD spectrum of PPLG-g-PEG conjugated with Dox (green) and PPLQ-g-PEG conjugated with Dox (blue) suggest that while both polymer-Dox conjugates exhibit some degree of α-helicity, PPLG conjugates appear to be more α-helical than PPLQ conjugates

Although PPLG and PPLQ differ in structure only by the linkage of the propargyl side chain to the scaffold backbone, the GPC results suggest that conjugates derived from the two backbones may exhibit different physical conformations that contribute to the observed hydrodynamic volumes. PPLG and PPLQ conjugates grafted with the same moieties in this study are roughly the same hydrodynamic volume, but the degree of polymerization and molecular weight of the PPLQ backbone is more than twice that of the PPLG backbone. We performed circular dichroism spectroscopy on PPLG and PPLQ conjugates to gain further insights into the differences in conformations of the conjugates. The CD spectrum of both PPLG- and PPLQ-Dox conjugates depict the typical characteristics of the α-helix secondary structure (Figure 4.4).[26] However, the degrees of helicity, estimated by the mean residue ellipticity at 222 nm, are very different between the two polymers. The mean residue ellipticity of the PPLG-Dox conjugates at 222 nm is roughly -40000 deg cm^2 dmol^{-1}, which is expected for peptides with 100% α-helical character. On the other hand, the PPLQ-Dox analog has a mean residue ellipticity of -13000 deg cm^2 dmol^{-1}. Compared to references of -39500 and -3000 deg cm^2 dmol^{-1} for mean residue ellipticities at 222 nm of 100% and 0% α-helical proteins,[26] respectively, PPLQ-Dox analogs are 27% α-helical. This difference

in secondary structure may account for the observation that conjugates derived from longer PPLQ backbones appear to have the same hydrodynamic volumes as conjugates derived from shorter PPLG backbones. The differences between hydrogen bonding of amide and ester linkages of the propargyl groups in PPLQ and PPLG, respectively, could also mediate the difference in helicity as hydrogen bonding of amides in PPLQ could disrupt the α-helix. The impact of secondary structure on hydrodynamic volume, particularly for α-helices, has previously been observed in other polymer systems,[27] and the greater volume-to-molecular weight ratio of PPLG is consistent with previous studies.

pH-mediated Release of Dox
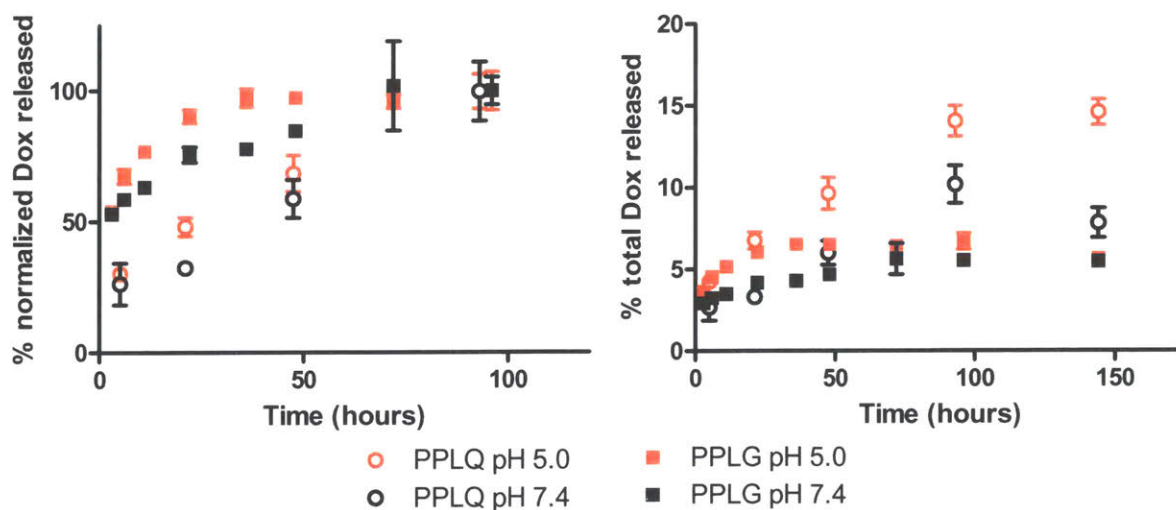
Figure 4.5. Cumulative release profiles of PPLG-Dox (filled squares) and PPLQ-Dox (empty circles) conjugates at pH 5.0 (red) and pH 7.4 (black). Release percentage is normalized to peak release at 100h of release or expressed as a percentage of total dox loading. Error bars represent one standard deviation.

To assess the pH-dependency of Dox release through the hydrazone linkage, we measured the Dox released from PPLQ-Dox conjugates over the course of several days by dialysis. PPLG-Dox conjugates exhibited a faster rate of release than PPLQ-Dox conjugates, but PPLG-Dox conjugates achieved a greater total release (Figure 4.5). The difference in drug release equilibrium and kinetics of PPLG versus PPLQ may be a result of polymer secondary structure or intermolecular

137

interactions of Dox with the amide or ester functional group on the side chain. However, the rate at which drug was released from the conjugates was higher at acidic pH for both PPLG and PPLQ conjugates, which was the intended goal in employing hydrazone chemistry to mediate the release of the drug from the conjugate in order to take advantage of the relatively acidic tumor microenvironment and/or the endosomal pH in tumor cells.[19] These differences in release profiles at acidic and neutral pH are consistent with release profiles from previous studies on hydrazone-mediated release of Dox from polymer drug carriers,[28,29] where a greater proton concentration at acidic pH enables higher and more rapid drug release through increased hydrolysis of the hydrazone. One drawback of the experimental setup is that it may not capture the effective infinite sink conditions of polymer-drug conjugates circulating in the bloodstream. Consequently, an in vivo release study would provide further insights into the release of drug from the conjugates in physiological conditions. Nevertheless, the release profile suggests that differential release rates mediated by pH were achieved using the hydrazone linker chemistry.

In Vitro Cytotoxicity
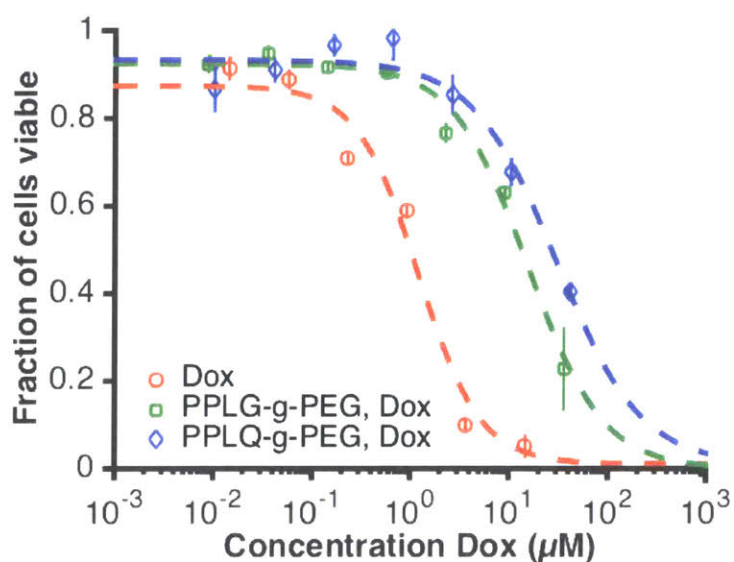
Figure 4.6. Cell viability of A549 cells treated with doxorubicin (red), PPLG-Dox conjugates (green) and PPLQ-Dox conjugates (blue). Concentrations of Dox in polymer-drug conjugate treatments represent the total Dox loaded. Fits to a sigmoidal dose-dependent response curve are depicted in dotted lines of the corresponding color. Error bars represent one standard deviation.

Cell viabilities of A549 cells at various concentrations of Dox and polymer-Dox were evalauted (Figure 4.6). PPLG and PPLQ grafted with PEG alone were found to have minimal cytotoxic effect on A549 cells, even at polymer concentrations corresponding to high doses of polymer-drug conjugate (Figure 4.11). As such, the toxicity of PPLG and PPLQ conjugates is unlikely to be the result of residual copper from the click reaction. In general, polymer-Dox conjugates were less cytotoxic than free Dox. However, PPLG-Dox conjugates appeared to have slightly greater cytotoxicity compared to PPLQ-Dox conjugates. IC50 values for the conjugates were determined by fitting to a sigmoidal dose-dependent response curve (Figure 4.7). The IC50 values of PPLG-Dox conjugates were an order of magnitude greater than those of free Dox, but these IC50 values were still roughly twice as small as the IC50 values for PPLQ-Dox conjugates. The difference in IC50 values of the PPLG-Dox and PPLQ-Dox conjugates was found to be statistically significant by one-way ANOVA ($p < 0.05$).

Treatment	IC50 (µM)
Dox	1.2 ± 0.045
PPLG-g-PEG, Dox[a]	15 ± 3.2
PPLQ-g-PEG, Dox[a]	30 ± 2.5

[a] IC50 values for PPLG- and PPLQ-Dox conjugates were found to be statistically significant from one another.

Figure 4.7. IC50 values for A549 cells treated with doxorubicin and polymer-Dox conjugates

The difference in IC50 between PPLG and PPLQ conjugates may be a result of different release kinetics. The observation of larger IC50 values for polymer-Dox conjugates compared to free Dox has previously been reported in the literature, such as in the case of PEG-Dox conjugates.[30] The gradual release of Dox from polymer-drug conjugates could mitigate the toxicity of the dose administered. While the efficacy of these conjugates was evaluated in this study in vitro, these

results suggest that PPLG- and PPLQ-Dox conjugates may minimize off-target cytotoxicity in vivo by controlled release.

Conjugate Association with A549 Cells
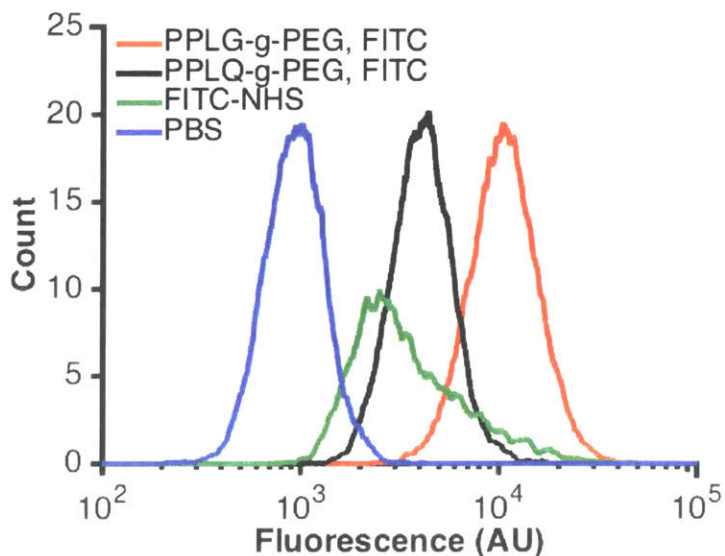
Figure 4.7. Flow cytometry histograms of FITC fluorescence signal for A549 cells treated with FITC-conjugated PPLG-g-PEG (red) and PPLG-g-PEG (black) in reference to those of cells treated with a FITC-NHS positive control (green) and PBS negative control (blue)

In order to better understand the reasons for differences in efficacy of PPLG- and PPLQ-Dox conjugates, we studied the association of FITC-labeled PPLG-g-PEG and PPLQ-g-PEG with A549 cells by flow cytometry. FITC-grafted polymers were of similar hydrodynamic volumes (Figure 4.12) and demonstrated secondary structure features (Figure 4.13) similar to those illustrated in the CD spectra (Figure 4.4). The total amounts of polymer added to the cells were 73 and 80 μg for PPLG and PPLQ conjugates, respectively, and fluorophore loading of polymers were 5.5% and 5% by weight. We standardized the amount of fluorophore administered to A549 cells between the two groups to account for differences in molarity resulting from the differing polymer molecular weights of PPLG and PPLQ used in this study. As such, the differences in FITC signal of the two treatment groups can be seen as a representation of the differences in association with cells between α-helical PPLG conjugates and the more random coil PPLQ analogs.

140

Compared to A549 cells treated with PBS, cells treated with the fluorescent polymers demonstrated higher degrees of FITC fluorescence signal as illustrated in **Figure 6**. Flow cytometry histograms of cells treated with non-fluorescent analogs of both polymers did not record substantial counts of cells with high magnitudes of FITC fluorescence (Figure 4.14). These observations suggest that the polymers are being internalized by the cells during treatment or are otherwise associating with the cells, possibly through interactions with the cell membrane or surface receptors. Moreover, **Figure 6** suggests that PPLG conjugates are associated with cells to a slightly greater degree than PPLQ conjugates, with the center of the PPLG-g-PEG distribution roughly twice that of the PPLQ-g-PEG distribution. In the context of polymer-Dox conjugates, this result suggests that PPLG conjugates may be more effectively internalized by the cells or may localize to the cells to a greater extent than PPLQ conjugates. Internalization of conjugates into the cell could accelerate the liberation of drug from the conjugate due to decreased pH in endosomes after uptake,[7] while enhanced localization of the conjugates at the surface may increase cytotoxicity due to an increased local drug concentration. In either case, the difference in association between the two polymer conjugates could potentially account for the higher cytotoxicity observed with PPLG-Dox conjugates compared to PPLQ-Dox conjugates.

4.3 Conclusions

In this study, we evaluated the effects of secondary structure on polymer-drug conjugate behavior by synthesizing polymer-doxorubicin conjugates through grafting of Dox onto PPLG and PPLQ polypeptide scaffolds using click chemistry. PPLG- and PPLQ-Dox conjugates were shown to have similar hydrodynamic volumes, even though PPLQ scaffolds had a higher degree of polymerization. Additionally, PPLG-derived conjugates adopted conformations with a greater degree of α-helicity than PPLQ-derived conjugates in solution, which may account for the observed difference in hydrodynamic volumes. Dox was grafted through an acid-labile hydrazone linkage, and we observed modestly increased kinetics of drug release at lower pH compared to neutral conditions, as well as a larger amount of total drug released, with 23% of the drug payload released over 700 hours at pH 5. In vitro studies on the cytotoxicity of these conjugates using A549 human lung carcinoma cells yielded IC50s of 15 and 30 μM for PPLG-Dox and PPLQ-Dox, respectively, compared to an IC50 of 1.2 μM for free Dox. The gradual release of Dox from the

conjugates likely contributes to the decrease in cytotoxicity observed in conjugates copared to free Dox. Moreover, PPLG conjugates were found to be associated with cells to a greater degree than PPLQ conjugates in flow cytometric analysis of A549 cells treated with fluorescently-labeled PPLG-g-PEG and PPLQ-g-PEG, which may account for the difference in cytotoxicities of the two conjugates. These in vitro results suggest that PPLG- and PPLQ-drug conjugates could hold promise as a drug carrier capable of gradual, pH-selective release of anticancer therapeutics and that secondary structure may influence the drug carrier abilities of polymer-drug conjugates.

4.4 Experimental

Materials

Doxorubicin hydrochloride was purchased from Combi-Blocks (San Diego, CA, USA). Hydrazine monohydrate, trifluoroacetic acid, benzyl bromide, chromium trioxide, sulfuric acid, methanesulfonyl chloride, and triethylamine were obtained from Alfa Aesar (Haverhill, MA, USA). All other chemical reagents used in the synthesis of polymer-drug conjugates were purchased from Sigma-Aldrich (St. Louis, MO, USA). Deuterated solvents for NMR spectroscopy were acquired from Cambridge Isotope Laboratories (Tewksbury, MA, USA). 5'6-Carboxyfluorescein succinimidyl ester (FITC-NHS) was obtained from Thermo Fisher Scientific (Waltham, MA, USA). A549 human lung carcinoma cells were obtained from American Type Culture Collection (ATCC, Rockville, MD, USA) and cultured in RPMI 1640 (Invitrogen, Grand Island, NY, USA) with 10% fetal bovine serum and 1% penicillin/streptomycin (Thermo Fisher Scientific).

Synthesis of Polymer Backbones

Two types of polymer backbones containing propargyl group side chains, poly(γ-propargyl-L-glutamate) (PPLG) and poly(γ-propargyl-L-glutamine) (PPLQ), were synthesized by previously published procedures[11,18] to serve as scaffolds for polymer-drug conjugates. The chemical structures and degrees of polymerization of each of these polymers were determined through end group analysis by NMR spectroscopy with a Bruker Avance 400 MHz spectrometer.

Synthesis of Azide-functionalized moieties

142

2-(2-azidoethoxy)ethanol was synthesized according to literature protocol.[22] To synthesize an azide-functionalized hydrazide drug linker, 2-(2-azidoethoxy)ethanol was first oxidized to the azide-functionalized carboxylic acid via Jones' oxidation. 2-(2-azidoethoxy)ethanol (5.0 g, 38.1 mmol) in acetone (50 mL) was chilled to 0°C using an ice bath. CrO_3 (11.6 g, 116 mmol) dissolved in 6M sulfuric acid (40 mL) was added dropwise to the acetone solution over the course of 30 minutes. The reaction mixture was then removed from the ice bath and stirred overnight. Afterwards, the mixture was quenched with isopropanol (75 mL), added dropwise, then subject to rotary evaporation. To ensure full oxidation of the starting material, an additional 4.0 g of CrO_3 was dissolved in 50 mL of 4M sulfuric acid and added to the reaction mixture after the rotary evaporation. The mixture was stirred overnight, quenched with isopropanol (30 mL), then subject to rotary evaporation once more. The reaction was extracted 3 times with ethyl acetate (3 x 100 mL). The aqueous layer was discarded, and the ethyl acetate layer was dried with $MgSO_4$, filtered, and evaporated to yield compound 1 (3.4 g, 23.4 mmol, 62% yield). ^{1}H NMR (400 MHz, Chloroform-d) δ 4.12 (s, 2H), 3.70 (t, 2H), 3.41 (t, 2H).

Compound 1 (3.4 g, 23.4 mmol) was mixed with benzyl bromide (4.66 mL, 35.2 mmol) and K_2CO_3 (6.48 g, 46.9 mmol) in DMF (35 mL) to yield the azide-functionalized benzyl ester (compound 2). Compound 2 was isolated using liquid-liquid extraction by washing 3 times with ethyl acetate (3 x 75 mL), followed by 75 mL brine. The ethyl acetate layer was subject to rotary evaporation after drying with $MgSO_4$. The concentrated product was purified by flash chromatography using ethyl acetate (20 vol%) in hexanes to give a slightly yellow, viscous liquid (2.7 g, 11.5 mmol, 49% yield). ^{1}H NMR (400 MHz, Chloroform-d) δ 7.42 – 7.30 (m, 5H), 5.20 (s, 2H), 4.19 (s, 2H), 3.74 (t, 2H), 3.44 (t, 2H).

The benzyl ester was converted to an azide-functionalized hydrazide by reacting compound 2 (2.7 g, 11.5 mmol) with hydrazine monohydrate (1.7 g, 34.5 mmol) in ethanol (15 mL). The reaction mixture was refluxed at 90°C overnight to yield the compound 3. The product was subsequently purified by flash chromatography with methanol (5 vol%) in ethyl acetate to give a yellow, viscous liquid (1.7 g, 10.7 mmol, 93% yield). ^{1}H NMR (400 MHz, Chloroform-d) δ 4.05 (s, 2H), 3.65 (t, 2H), 3.43 (t, 2H).

To synthesize azide-functionalized doxorubicin (Dox-azide), doxorubicin hydrochloride (200 mg, 0.35 mmol) was mixed with compound 3 (164.5 mg, 1.03 mmol) in methanol (15 mL) with a few drops of trifluoroacetic acid and stirred overnight. The reaction mixture was concentrated to 4 mL using rotary evaporation, then precipitated in diethyl ether (40 mL) and centrifuged at 10000 rpm for 10 min. After centrifugation, the ether was decanted, and the precipitate was dried in vacuo to yield a dark red solid (280.8 mg, 0.389 mmol, quantitative). ^{1}H NMR (400 MHz, Deuterium Oxide) δ 7.83 – 7.26 (m, 3H), 5.49 (s, 1H), 4.46 – 4.20 (m, 2H), 4.17 (s, 1H), 4.01 – 3.35 (m, 12H), 2.98 (d, 1H), 2.63 (d, 1H), 2.38 – 2.15 (m, 1H), 2.02 (d, 3H), 1.31 (d, 3H). Excess mass of product may be attributed to potential residual hydrazide linker (compound 3) that could not be readily removed during workup.

Azide-functionalized fluorescein (FITC-azide) was synthesized as previously described[23] to be grafted onto the polymer backbones as a covalently bound fluorophore. Azide-functionalized PEG (PEG-azide) was synthesized from a methoxy-terminated poly(ethylene glycol). To a stirring solution of 750 Da methoxy-terminated poly(ethylene glycol) (13.6 g, 18.1 mmol) in THF (150 mL) was added dropwise methanesulfonyl chloride (3.0 mL, 39.0 mmol) followed by dropwise triethylamine (6.0 mL, 43 mmol). The solution was stirred overnight at room temperature, after which a solution of sodium azide (10.5 g, 162 mmol) and sodium bicarbonate (0.70 g, 8.3 mmol) in water (100 mL) was added. The reaction was stirred under reflux for 2 days and the majority of solvent was removed in vacuo. Toluene (100 mL) and $MgSO_4$ (40 g) was added to the damp solid and stirred at 70°C for 30 minutes. The solids were removed by filtration and the solvent was removed in vacuo to yield a pale yellow liquid that solidifies on standing (9.6 g, 13 mmol, 72%). ^{1}H NMR (400 MHz, Deuterium Oxide) δ 3.61 (s, 70H), 3.45 – 3.37 (m, 2H), 3.29 (s, 3H).

Synthesis of Polymer-drug Conjugates via Click Chemistry

To synthesize PPLG-drug conjugates, PPLG (5.0 mg, 29.9 μmol repeat units) was mixed with PEG-azide (12.9 mg, 17.2 μmol) in DMF (3 mL). N,N,N′,N″,N″-Pentamethyldiethylenetriamine (PMDETA, 1.87 μL, 9.0 μmol) was added to the reaction mixture, and the mixture was stirred and sparged with argon for 30 minutes. After sparging, copper (I) bromide (CuBr, 1.29 mg, 9.0 μmol) was added to the reaction mixture, and the headspace of the reaction vessel was purged with argon for 30 seconds to minimize introduction of oxygen into the system. The mixture was stirred

144

overnight. The reaction mixture was then heated to 40°C, and Dox-azide (8.6 mg, 11.9 μmol) and additional PMDETA (6.23 μL, 29.9 μmol) were added to the reaction mixture. The new mixture was sparged with argon for 30 minutes, and additional CuBr (1.29 mg, 9.0 μmol) was added after sparging. The headspace was purged for 30 seconds, and the mixture was allowed to react at 40°C overnight. The reaction mixture was then precipitated into diethyl ether (40 mL) and centrifuged at 5000 rpm for 10 min. The supernatant was decanted, and the precipitate was dissolved into 50 mM phosphate in water (20 mL). Copper was removed by portionwise addition of Dowex M4195 resin to the aqueous polymer solution, followed by shaking until the solution no longer appeared blue. The resin and any undissolved polymer were filtered using filter paper, and the mixture was dialyzed in water buffered at pH 7 (~5 mL of 1M phosphate buffer in 4L water) using SpectraPor regenerated cellulose dialysis membrane with a molecular weight cutoff of 10 kDa. After dialysis, the product was lyophilized to give a red, gauze-like solid (14.3 mg, 53% yield).

PPLQ-drug conjugates were synthesized in a similar manner as PPLG-drug conjugates. PPLQ (7.5 mg, 45.1 μmol repeat units) was mixed with PEG-azide (19.7 mg, 26.3 μmol) and PMDETA (2.82 μL, 13.5 μmol) in DMF (2.5 mL), and the mixture was stirred and sparged. CuBr (1.95 mg, 13.5 μmol) was quickly added after sparging, the headspace was purged, and the reaction was carried out overnight. The reaction mixture was subsequently heated to 40°C, Dox-azide (13.3 mg, 18.0 μmol) and PMDETA (9.42 μL, 45.0 μmol) were added, and the mixture was sparged. CuBr (1.95 mg, 13.5 μmol) was quickly added, the headspace was purged, and the mixture stirred overnight. The mixture was then precipitated in ether, centrifuged, redissolved in phosphate buffer, purified of copper, dialyzed, and lyophilized as described previously to yield a red solid (17.7 mg, 43% yield).

Additionally, PPLG and PPLQ grafted only with PEG were synthesized as Dox-free polymer-drug conjugate analogs. PPLG-PEG conjugates were synthesized in a two-step procedure. PPLG (5.1 mg, 30.8 μmol repeat units) was mixed with PEG-azide (14.4 mg, 19.2 μmol) and PMDETA (1.87 μL, 9.0 μmol) in DMF (2 mL) and sparged for 30 minutes with argon. After sparging, CuBr (1.29 mg, 9.0 μmol) was quickly added, and the reaction proceeded overnight. Additional PEG-azide (14.9 mg, 19.9 μmol) and PMDETA (1.87 μL, 9.0 μmol) were subsequently added to the reaction mixture, and the mixture was sparged for another 30 minutes with argon. CuBr (1.29 mg, 9.0

μmol) was added after sparging, and the reaction was allowed to proceed overnight. The reaction was worked up in the same manner as the polymer-drug conjugates to yield a sinewy, white solid (9.1 mg, 32% yield).

PPLQ-PEG conjugates were synthesized with a single click reaction. PPLQ (9.7 mg, 58.4 μmol) was mixed with PEG-azide (52.6 mg, 70.1 μmol) and PMDETA (3.77 μL, 18.1 μmol) in DMF (5 mL). The reaction mixture was sparged for 30 minutes with argon, and CuBr (2.59 mg, 18.1 μmol) was subsequently added quickly to the mixture. After reacting overnight, the mixture was worked up as described previously to yield a sinewy, white solid (17 mg, 32% yield).

Synthesis of Fluorescent Polymer Conjugates

PPLG and PPLQ were grafted with FITC in order to synthesize fluorescently-labeled analogs of the polymer-drug conjugates to study the association of the polymers with cancer cells. PPLQ (3.3 mg, 19.9 μmol repeat units) was mixed with FITC-azide (1.26 mg, 2.6 μmol) and PEG-azide (10.5 mg, 14.0 μmol) in DMF (2 mL). PMDETA (1.13 μL, 5.4 μmol) was added to the reaction vessel, and the mixture was stirred and sparged for 30 minutes with argon. CuBr (0.8 mg, 5.4 μmol) was added quickly after sparging, and the reaction was allowed to proceed overnight in the dark. The reaction was then precipitated in ether, centrifuged, redissolved in phosphate buffer, purified of copper, dialyzed in the dark, and lyophilized to yield a yellow gauzelike solid (4.6 mg, 29% yield).

Fluorescent PPLG conjugates were synthesized in a two-step procedure similar to PPLG-PEG conjugates described previously. PPLG (4.3 mg, 25.7 μmol repeat units) was mixed with FITC-azide (1.55 mg, 3.2 μmol) and PEG-azide (11.1 mg, 14.8 μmol) in DMF (2 mL). PMDETA (5.0 μL, 23.9 μmol) was added to the reaction vessel, and the mixture was stirred and sparged for 30 minutes with argon. CuBr (1.29 mg, 9.0 μmol) was added quickly after sparging, and the reaction was allowed to proceed overnight in the dark. Additional PEG-azide (11.9 mg, 15.9 μmol) and PMDETA (5.0 μL, 23.9 μmol) were subsequently added to the reaction. CuBr (1.29 mg, 9.0 μmol) was added quickly after sparging for 30 minutes with argon, and the reaction was allowed to proceed overnight in the dark. The reaction was then precipitated in ether, centrifuged, redissolved in phosphate buffer, purified of copper, dialyzed in the dark, and lyophilized to yield a yellow gauzelike solid (10.0 mg, 44% yield).

Characterization of Polymer Chemical Structure

All polymer-drug conjugates were characterized by ^{1}H-NMR spectroscopy in deuterium oxide to verify the chemical identity and grafting efficiency of polymer-drug conjugates. The sizes of the polymer conjugates were determined relative to PEG standards using aqueous gel permeation chromatography (GPC). GPC was performed with a sample concentration of 1-5 mg mL^{-1} and eluted by a 100 mM sodium nitrate, 10 mM phosphate buffer with 20 vol% methanol at 35°C and pH 7.4 on a Viscotek GPCmax VE-2001 system equipped with a PL aquagel-OH column and VE-3580 RI detector calibrated with monodisperse poly(ethylene oxide) standards. The secondary structures of the conjugates were evaluated using circular dichroism (CD) spectroscopy using an Aviv model 202 CD spectrometer at 25 ± 0.1 °C. Samples were taken every 1 nm from 190 to 260 nm (bandwidth = 1.0 nm) with a 3 s averaging time. Measurements were taken in a quartz cell with 1 mm path length at concentrations between 0.4 and 1.1 mg mL^{-1}.

Measurement of Drug Loading

Drug loading was measured by UV-Vis spectrophotometry by measuring the absorbance of polymer-drug conjugate samples at 480 nm after generating a standard curve with Dox HCl ranging from 5 µg mL^{-1} to 213 µg mL^{-1} (Figure 4.8). UV-Vis was carried out in acidic solution (250 mM HCl).
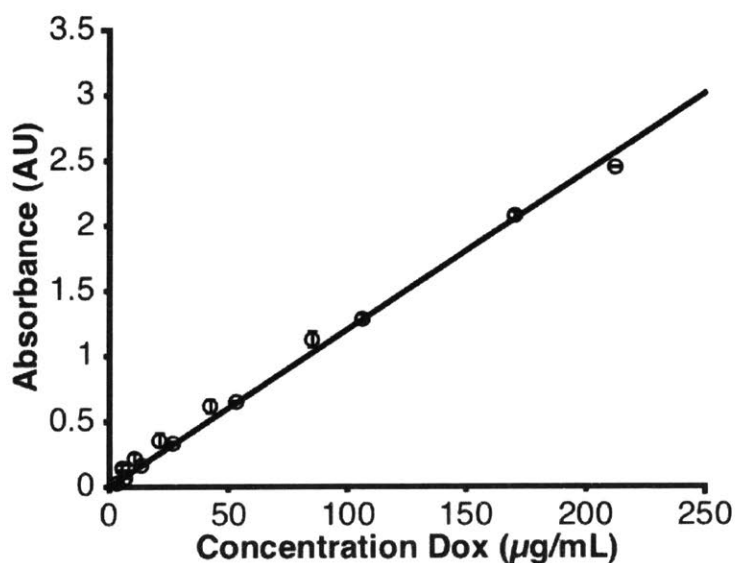
Figure 4.8. Absorbance at 480 nm of doxorubicin HCl standards of known concentrations. Error bars represent one standard deviation.

Characterization of Drug Release Profile

Release of Dox from PPLQ-Dox conjugates in neutral and acidic solution was evaluated to determine the hydrazide-mediated drug release rates. Samples of the PPLQ-Dox conjugate were dissolved in either 10mM phosphate-buffered saline (pH 7.4, 137 mM NaCl) or 10 mM acetate-buffered saline (pH 5, 137 mM NaCl). PPLQ-drug conjugates were first dissolved in water and the concentration of Dox in each sample was measured. 2 mL of PPLQ-Dox conjugate stock solution was placed into 10 kDa regenerated cellulose dialysis membranes along with 200 uL of a 10x solution of the corresponding buffer and sealed using a single dialysis membrane clip to clamp both ends of the membrane. The dialysis membranes containing the samples were subsequently immersed in 13 mL of the corresponding buffered saline solution in a 50 mL conical centrifuge tube. The centrifuge tubes were placed in an incubation bath at 37°C. 300 μL aliquots were withdrawn from the solution in the conical tubes outside of the dialysis membrane at various time points, and 300 μL of fresh buffer was added to the centrifuge tube after each aliquot was withdrawn. The Dox concentration in each aliquot was measured after addition of 100 μL of 1M HCl to determine the amount of Dox released at each time point.

In Vitro Cytotoxicity of Polymer-drug Conjugates

A549 human lung carcinoma cells were cultured in RPMI 1640 media with 10% fetal bovine serum and 1% P/S at 37°C at 5% humidity. Cell treatment solutions of Dox, polymer-Dox conjugates, and polymer-PEG conjugates were prepared by serial dilution in RPMI. A549 cells were seeded in a 96-well plate at 3000 cells per well and cultured for 24 hours prior to treatment with 97.5 μL of each serial dilution. Serial dilutions for each treatment condition were performed at least in triplicate. Cells were grown in 97.5 μL RPMI without any treatment as a control. Cells were treated for 72h, then assessed for cell viability using a CellTiter-Glo assay (Promega) and plate reader (Tecan, 1s integration). CellTiter-Glo reagent was reconstituted according to the manufacturer's instructions and diluted and used as a 2x stock in deionized water. Incubation media from the 96-well plates was aspirated, and 100 μL of 1x CellTiter-Glo reagent was added to each well. The

plates were incubated at room temperature for 30 minutes, after which luminescence in each well was measured using the plate reader.

Determination of Polymer Association via Flow Cytometry

A549 cells were plated in a 12-well plate at a density of 10^6 cells per well in 1 mL RPMI 1640 media with 10% fetal bovine serum and 1% P/S and incubated at 37°C at 5% humidity for 24h. The cells were subsequently treated with each of the FITC-labeled PPLG-g-PEG and PPLQ-g-PEG. Each of the two fluorescent polymers was added to achieve 4 µg of fluorescein in 1 mL of media per well. The amount of fluorescein grafted onto each polymer was quantified using UV-Vis at 440 nm with reference to a fluorescein standard curve (Figure 4.9). Non-fluorescent PPLG-g-PEG and PPLQ-g-PEG were added at concentrations that were similar to the polymer concentrations of the fluorescently-labeled polymers as negative controls. Cells were also cultured in 30 µL PBS diluted to 1 mL with RPMI as another negative control. As a positive control, 4 µg of FITC-NHS was administered to 1 well of cells to calibrate the FITC channels on the flow cytometer. Cells were analyzed by a FACSCelesta instrument (Becton Dickinson, NJ, USA) equipped with a 488 nm laser and 530/30 nm detector. The data was processed using FlowJo analysis software (Becton Dickinson, OR, USA).
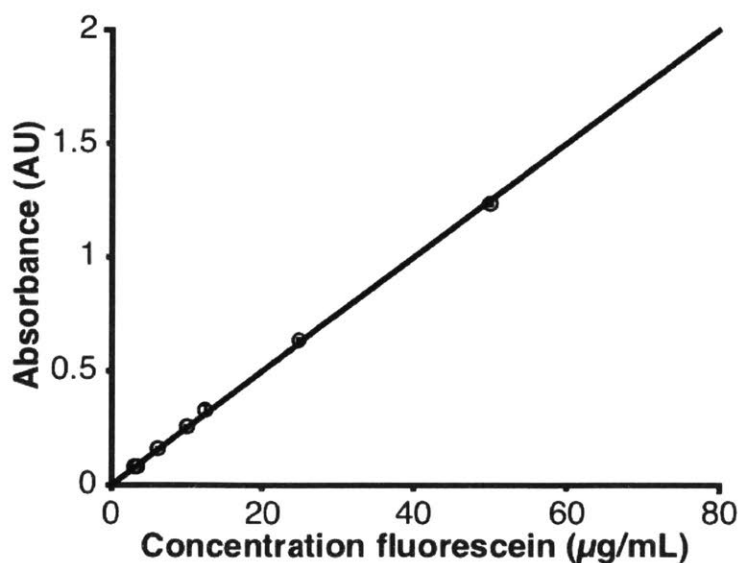
Figure 4.9. Absorbance at 440 nm of fluorescein standards of known concentrations. Error bars represent one standard deviation.
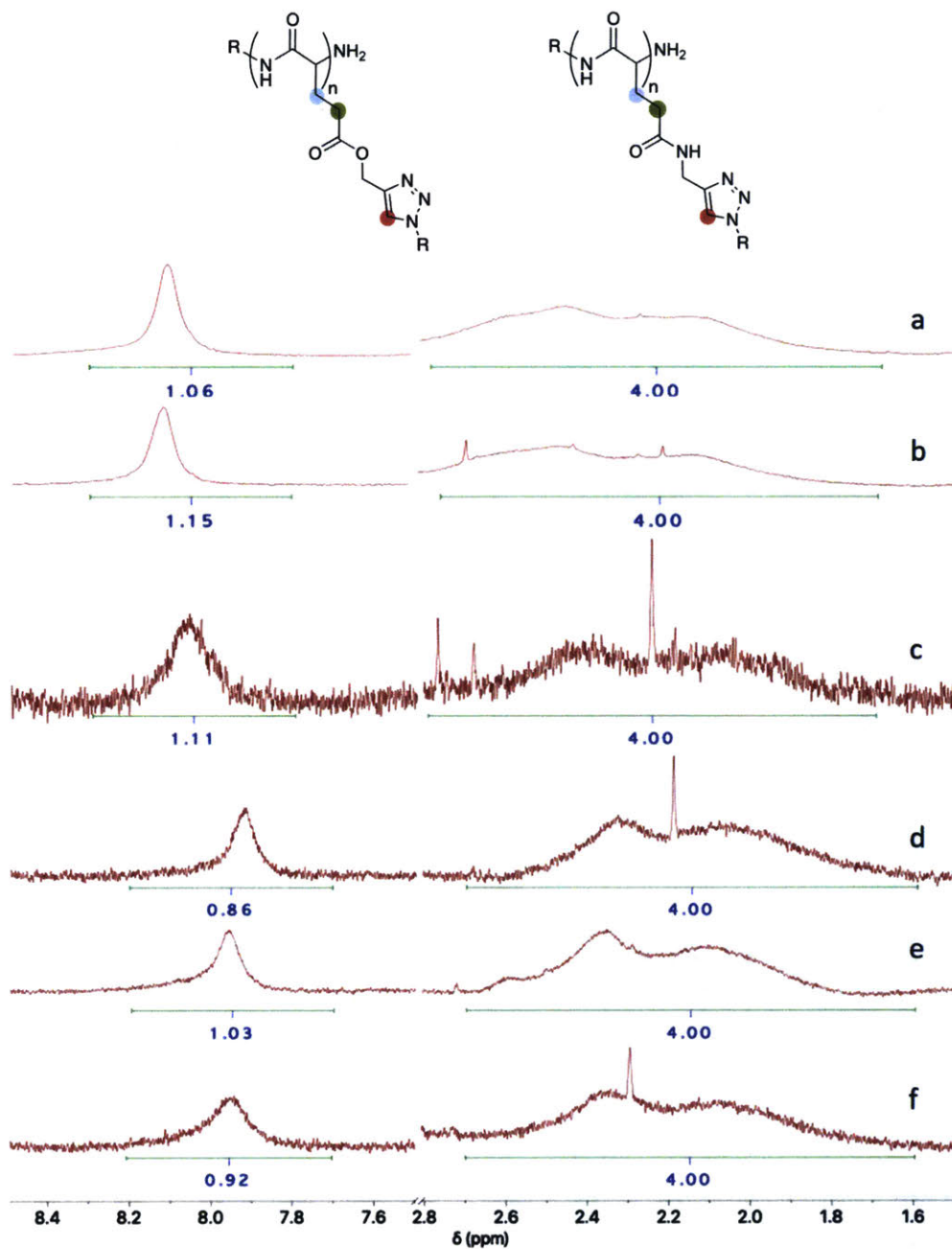

Figure 4.10. Integrations of NMR spectra for PPLG-g-PEG (a), PPLG-g-PEG grafted with Dox (b), PPLG-g-PEG grafted with FITC (c), PPLQ-g-PEG (d), PPLQ-g-PEG grafted with Dox (e), and PPLQ-g-PEG grafted with FITC (f). Integrations from 1.6-2.6 represent the methylene protons

highlighted in blue and green while integrations at ~8.0 ppm represent triazole protons highlighted in red.
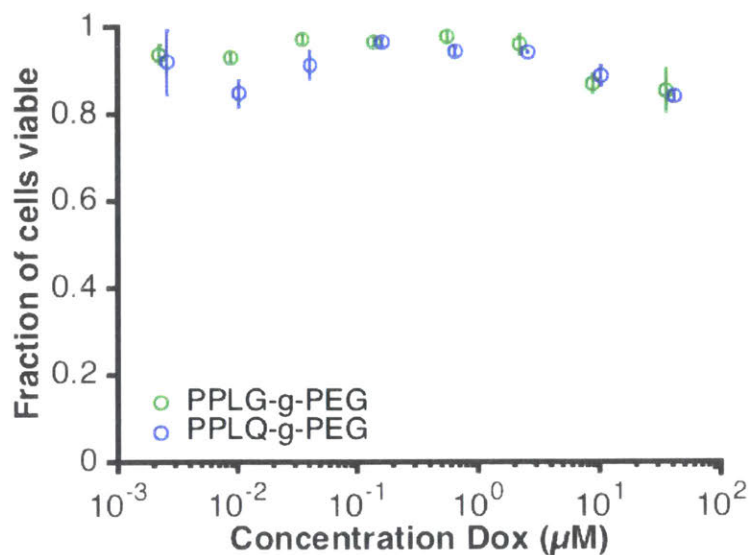
Figure 4.11. Cell viabilities of A549 cells treated with PPLG-g-PEG (green) and PPLQ-g-PEG (blue) indicate that polymers grafted with PEG but without Dox are minimally cytotoxic
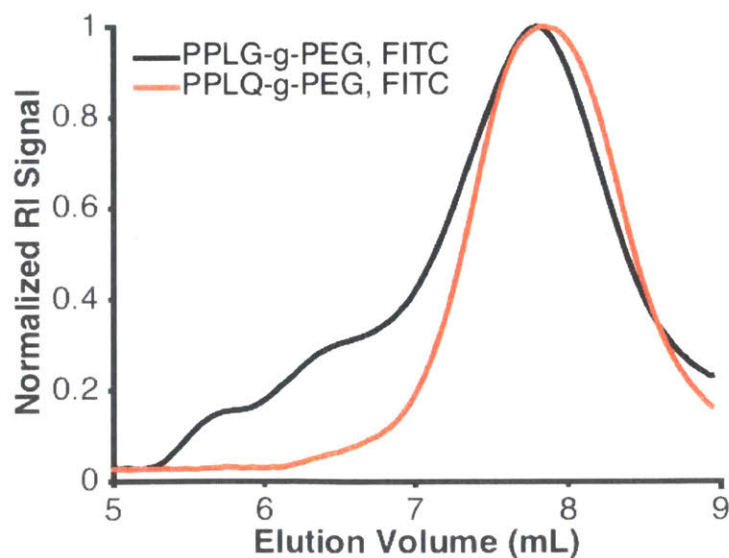

Figure 4.12. Aqueous GPC traces of refractive index for fluoresecent PPLG-g-PEG (black) and PPLQ-g-PEG (red) indicate that the polymer conjugates studied in flow cytometry experiments were of similar hydrodynamic volume. PPLG-g-PEG and PPLQ-g-PEG conjugates grafted with FITC had M_n values of 21.3 and 17.5 kDa, respectively, relative to PEG standards
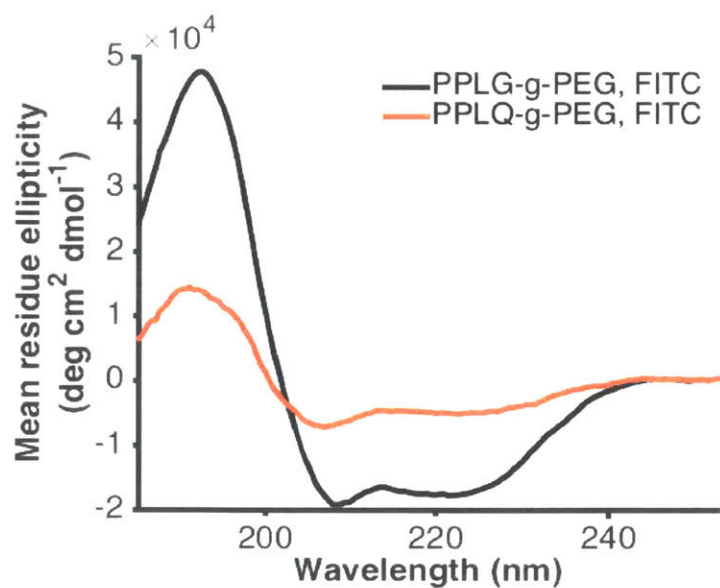
Figure 4.13. CD spectrum of fluorescent PPLG-g-PEG (black) and PPLQ-g-PEG (red) illustrate similar trend as non-fluorescent conjugates, where PPLG conjugates exhibit greater degrees of α-helicity than PPLQ conjugates
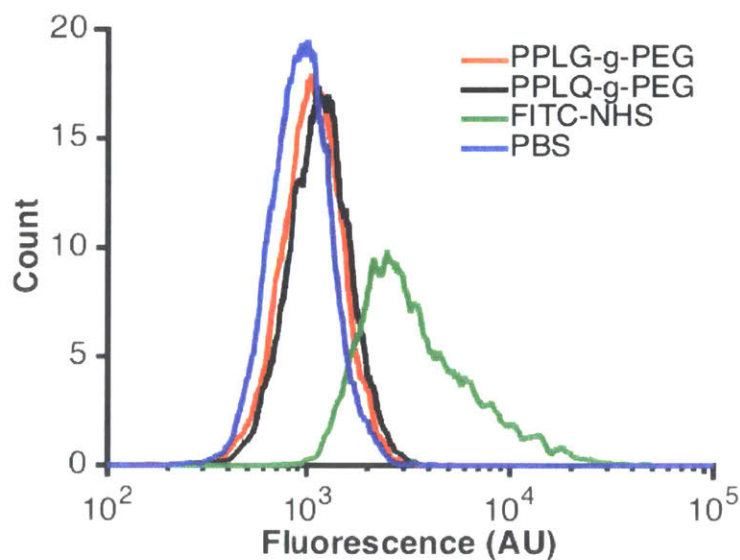


Figure 4.14. FITC signal histograms of A549 cells treated with PPLG-g-PEG and PPLQ-g-PEG suggest that polypeptide scaffolds grafted with PEG without fluorophore do not contribute significantly to fluorescence signal

Polymer Sample	$M_n^{a)}$ (kDa)	M_w/M_n
PPLG-g-PEG, Dox	19.8	3.7
PPLQ-g-PEG, Dox	14.4	3.7
PPLG-g-PEG	16.6	2.5
PPLQ-g-PEG	20.6	2.5

[a)] Molecular weights reported are in reference to PEG standards of corresponding elution times to polymer samples studied

Figure 4.15. Summary statistics for size and dispersity of PPLG and PPLQ conjugates

4.5 References

(1)   Z. Xie, H. Guan, X. Chen, C. Lu, L. Chen, X. Hu, Q. Shi, X. Jing, *J. Control. Release* **2007**, *117*, 210.

(2)   L. Liao, J. Liu, E. C. Dreaden, S. W. Morton, K. E. Shopsowitz, P. T. Hammond, J. A. Johnson, *J. Am. Chem. Soc.* **2014**, *136*, 5896.

(3)   Y. Bae, S. Fukushima, A. Harada, K. Kataoka, *Angew. Chemie - Int. Ed.* **2003**, *42*, 4640.

(4)   H. S. Oberoi, N. V. Nukolova, A. V. Kabanov, T. K. Bronich, *Adv. Drug Deliv. Rev.* **2013**, *65*, 1667.

(5)   Y. Barenholz, *J. Control. Release* **2012**, *160*, 117.

(6)   B. Kim, S. W. Park, P. T. Hammond, *ACS Nano* **2008**, *2*, 386.

(7)   R. Duncan, *Nat. Rev. Cancer* **2006**, *6*, 688.

(8)   P. Kolhe, J. Khandare, O. Pillai, S. Kannan, M. Lieh-Lai, R. Kannan, *Pharm. Res.* **2004**, *21*, 2185.

(9)   M. E. Fox, F. C. Szoka, J. M. J. Fréchet, *Macromolecules* **2010**, *42*, 1141.

(10)   V. V Rostovtsev, L. G. Green, V. V Fokin, K. B. Sharpless, *Angew. Chemie - Int. Ed.* **2002**, *41*, 2596.

(11)   A. C. Engler, H. Lee, P. T. Hammond, **2009**, 9334.

(12)   S. E. A. Gratton, P. A. Ropp, P. D. Pohlhaus, J. C. Luft, V. J. Madden, M. E. Napier, J. M. DeSimone, *Proc. Natl. Acad. Sci. U. S. A.* **2008**, *105*, 11613.

(13)   S. Venkataraman, J. L. Hedrick, Z. Y. Ong, C. Yang, P. L. R. Ee, P. T. Hammond, Y. Y. Yang, *Adv. Drug Deliv. Rev.* **2011**, *63*, 1228.

(14)   X. Huang, X. Teng, D. Chen, F. Tang, J. He, *Biomaterials* **2010**, *31*, 438.

(15)   B. D. Chithrani, A. A. Ghazani, W. C. W. Chan, *Nano Lett.* **2006**, *6*, 662.

(16)   S. Wilhelm, A. J. Tavares, Q. Dai, S. Ohta, J. Audet, H. F. Dvorak, W. C. W. Chan, *Nat. Rev. Mater.* **2016**, *1*, 1.

(17)   J. Williford, J. L. Santos, R. Shyam, H. Mao. *Biomater. Sci.* **2015**, *3*, 894.

(18)   W. Wang, P. T. Hammond, *Polym. Chem.* **2018**, *9*, 346.

(19)   G. L. Zwicke, G. A. Mansoori, C. J. Jeffery, *Nano Rev.* **2012**, *1*, 1.

(20)   J. Khandare, T. Minko, *Prog. Polym. Sci.* **2006**, *31*, 359.

(21)   N. Wiradharma, Y. Zhang, S. Venkataraman, J. L. Hedrick, Y. Y. Yang, *Nano Today* **2009**, *4*, 302.

(22)   B. J. J. Timmer, M. A. Flos, L. M. Jørgensen, D. Proverbio, S. Altun, O. Ramström, T. Aastrup, S. P. Vincent, *Chem. Commun.* **2016**, *52*, 12326.

(23)   B. Huang, J. F. Kukowska-Latallo, S. Tang, H. Zong, K. B. Johnson, A. Desai, C. L. Gordon, P. R. Leroueil, J. R. Baker, *Bioorganic Med. Chem. Lett.* **2012**, *22*, 3152.

(24)   B. Trathnigg, *Prog. Polym. Sci.* **1995**, *20*, 615.

(25)   T. Williams, *J. Mater. Sci.* **1970**, *5*, 811.

(26)   Y. Wei, A. A. Thyparambil, R. A. Latour, *Biochim. Biophys. Acta - Proteins Proteomics* **2014**, *1844*, 2331.

(27)   D. Huesmann, A. Birke, K. Klinker, S. Türk, H. J. Räder, M. Barz, *Macromolecules* **2014**, *47*, 928.

(28)   H. S. Yoo, E. A. Lee, T. G. Park, *J. Control. Release* **2002**, *82*, 17.

(29)   Y. Bae, N. Nishiyama, S. Fukushima, H. Kyoama, M. Yasuhiro, K. Kataoka, *Bioconjug. Chem* **2005**, *16*, 122.

(30)   F. M. Veronese, O. Schiavon, G. Pasut, R. Mendichi, L. Andersson, A. Tsirk, J. Ford, G. F.

Wu, S. Kneller, J. Davies, R. Duncan, *Bioconjug. Chem.* **2005**, *16*, 775.